EPFL

Service Restoration Strategy in Active Distribution Networks

Hossein SEKHAVATMANESH

■ École
polytechnique
fédérale
de Lausanne

2020

In the Name of God

Acknowledgements

This work would have never been completed without the help and support of many kind people, to only some of whom it is possible to give particular mention here.

First of all, I would like to express my deepest gratitude to my thesis director, Dr. Rachid Cherkaoui for giving me the opportunity to pursue my PhD thesis. His inexhaustible kindness, invaluable guidance, scientific enthusiasm, excellent support, and endless encouragement has transformed my PhD from a critical milestone to an exciting journey. Thanks Rachid!

My sincere thanks go to the members of my jury, prof. João Peças Lopes, prof. Janfranco Chicco, prof. Mario Paolone, and Prof. Drazen Dujic for their encouraging and insightful comments. I am in particular grateful to prof. João Peças Lopes for giving me the unique opportunity to collaborate with his lab at INESC TEC on the physical validation of part of my research results. Among the other team members in the hosting lab, I present my special thanks also to my friend, Justino Rodrigues, for his commitment and professional help for the implementation of my test setup.

I would like also to acknowledge the Qatar Environment and Energy Research Institute (QEERI) for funding this dissertation.

I am deeply grateful to Mrs. Andrée Moinat, Mrs. Eulalia Durussel, and Mrs. Sophie Flynn, secretaries of the Laboratory, for all their constant availability, sympathy, and kindness. Merci Andrée, Eulalia, et Sophie!

Abstract

In the last decade, the massive penetration of Distributed Generators (DGs) has brought significant technical challenges to all the aspects related to the planning and operation of distribution networks. Thus, smart grid concept has evolved as a new operating paradigm replacing conventional approaches that were deployed in passive distribution networks. This new operation framework is equipped with intelligent measurement, communication and control infrastructures enabling an efficient electric power transfer from different point of supplies to the end consumers. This modernization and, at the same time, the ever-increasing utilization of sensitive loads in the industrial, commercial and residential distribution networks implies a higher level of requirement regarding the quality of supply. Availability is the most important factor when it comes to power quality. Therefore, the restoration of distribution systems, considering their new active status, is a timely topic that deserves to be revisited.

The restoration problem is widely studied in the literature regarding the passive distribution networks. The ever-increasing penetration of active elements (e.g. DGs) in distribution networks suggests to enable their potentials in better fulfilling the restoration objectives. In this thesis, it is aimed to develop an automatic strategy for the service restoration complying with the requirements of the Distribution Network Automation (DNA) systems.

In this regard, a novel mathematical optimization model of the restoration problem is first proposed for passive distribution networks. The considered self-healing actions besides the switching operation are the tap setting modification of voltage regulation devices including I)

On-Line Tap-Changing (OLTC) transformers, II) Step Voltage Regulators (SVRs), and III) Capacitor Banks (CBs).

Next, the developed formulation is modified and extended such that it is applicable also for active distribution networks. In order to account for the requirements imposed by the start-up process of disconnected DGs, a novel "multi-step restoration" strategy is introduced. For ensuring the feasibility of the obtained solution concerning the technical constraints (e.g. voltage and current limits), a recently published method for the exact and convex relaxation of the Optimal Power Flow (OPF) problem is incorporated into the developed formulation of the restoration problem. The overall restoration problem is in the form of a Mixed-Integer Second-Order Cone Programming (MISOCP) optimization problem. Therefore, it can be solved efficiently by the state-of-the-art commercial solvers for convex optimization problems.

In the next step, we propose a solution strategy making the multi-period restoration problem tractable for analytical solvers in case of a grid of realistic size. According to this strategy, the line switching variables and the AC power flow model are decomposed into master and sub problems, which are solved through successive iterations. At each iteration, the solution of the sub problem is used to augment the constraints of the master problem with the proposed feasibility or optimality cuts. The numerical results indicate that the proposed decomposition algorithm provides, within a short time (after a few iterations), a restoration solution with a quality that is close to the proven optimality, when it can be exhibited.

In this thesis, along with the network security constraints in steady-state, the transient constraints associated with the starting of induction motor loads are also accounted for in the developed restoration problem. In this regard, an mathematical and convex model is derived representing the starting transients of an induction motor in a semi-static fashion. This model is then integrated into a load restoration problem aiming to find the optimal energization sequence of different loads (static and motor loads). This optimization problem includes the optimal control of the converter-based DGs and autotransformers that are used for the induction motor starting. Integrating the AC power flow formulation into the developed optimization problem guarantees that the starting transients of motor loads will not violate the transient operational limits imposed by different protection devices in the distribution network. We validate the feasibility of the optimization results in terms of these transient operational limits using I) off-line time-domain simulations, and II) a Power Hardware-In-the-Loop experiment.

Zusammenfassung

Im letzten Jahrzehnt hat die massive Integration dezentraler Erzeuger (Engl: Distributed Generators, DGs) in Verteilnetze alle Aspekte der Netzplanung und des Netzbetriebes erheblich verkompliziert. Das Smart-Grid-Konzept wurde als neues Betriebsparadigma entwickelt, um herkömmliche Ansätze in passiven Verteilnetze zu ersetzen. Dieses neue Betriebskonzept fußt auf intelligenter Mess-, Kommunikations-, und Netzleittechnik. Diese ermöglichen eine effiziente Übertragung der elektrischen Energie von den verschiedenen Erzeugern zu den Endverbrauchern. Diese Modernisierung und der gleichzeitigen stetigen Zunahme kritischer Lasten in Verteilnetzen erhöhen die Anforderungen an die Stromqualität. Was die Stromqualität betrifft, ist die Stromverfügbarkeit der wichtigste Faktor. Deshalb ist die Netzwiederherstellung in Verteilnetze unter Berücksichtigung ihres neuen Betriebszustands ein aktuelles Thema, das sich zu untersuchen lohnt.

Das Problem der Wiederherstellung von passiven Verteilnetzen wurde bereits eingehend erforscht. Das zunehmende Verfügbarkeit aktiver Komponenten (z.B. DGs) in Verteilnetzen legt es nahe, deren Potentiale dafür zu nutzen, die Netzwiederherstellung besser zu bewältigen. In dieser Doktorarbeit wird eine automatische Strategie für die Netzwiederherstellung entwickelt, die den Anforderungen von Automatisierungssystemen in Verteilnetzen gerecht wird. Zu diesem Zweck schlagen wir zuerst ein neues analytisches Optimierungsmodell für Wiederherstellung von passiven Vertriebsnetzen vor. Die betrachteten Handlungsmöglichkeiten enthalten nebst Schaltvorgängen die Anpassung von Einstellungen der verschiedenen Spannungsregler,

einschließlich Laststufenschaltungstransformer, Schrittspannungsregler, und Kondensatorbänken.

Als Nächstes passen wir die entwickelte mathematische Formulierung an und erweitern sie, so dass sie auch für aktiven Verteilnetze verwendet werden kann. Um die Anforderungen von DGs bezüglich Neustart zu erfüllen, wird ein Mehr-Schritt-Verfahren vorgeschlagen. Wir verwenden eine vor kurzem veröffentliche Methode für die exakte konvexe Relaxation des optimalen Lastflussproblems, um elektrische Grenzwerte (z.B. für Spannung und Strom) beachtet sind. Das gesamte Wiederherstellungsproblem wird als gemischt-ganzzahligen konischen Optimierungsproblems zweiter Ordnung formuliert. Dieses kann mit handelsüblichen Solvern für konvexe Optimierungsprobleme effizient gelöst werden.

Des Weiteren schlagen wir eine Lösungsmethode vor, die es ermöglicht, das Wiederherstellungsproblem mit analytischen Solvern zu behandeln. In diese Strategie werden die Schaltgrößen und das Lastflussmodell in ein Über- und ein Unterproblem aufgespalten. Diese Teilprobleme werden durch aufeinanderfolgende Iterationen gelöst. In jeder Iteration wird das Resultat des Unterproblems als zusätzliche Randbedingung in das Überproblem integriert. Damit sorgen wir für Optimalität und Existenz der Lösung. Die Resultate zeigen, dass die vorgeschlagene Zerlegungsmethode binnen kurzer Zeit (d.h. nach einigen wenigen Iterationen) eine Lösung findet, die nahe am theoretischen Optimum liegt.

In dieser Doktorarbeit werden, zusätzlich zu Sicherheitskriterien für den statischen Betrieb, solche für dynamische Lasten wie Induktionsmotoren berücksichtigt. Zur Darstellung von deren Einschaltströmen entwickeln wir ein analytisches, konvexes Modell unter halb-statischen Bedingungen. Dieses Modell wird dann in einem Wiederherstellungsproblem eingefügt, um die optimale Zuschaltsequenz der verschiedenen Lasten (statische oder dynamische) zu finden. Dieses Optimierungsproblem enthält die optimale Leitung der Konverter-basierten DGs und Spartransformatoren, die für Start der Induktionsmotoren benutzt werden. Dank der Einfügung des Lastflussmodells, werden die transienten Sicherheitskriterien, welche durch verschiedene Schutzvorrichtungen vorgegeben sind, durch die Anlaufströme der Induktionsmotoren nicht verletzt. Wir validieren die erhaltenen Resultate der Optimierung gegen die transienten Sicherheitskriterien. Dazu benutzen wir i) Offline-Simulation im Zeitbereich und ii) einen Power Hardware-In-the-Loop Versuch.

Stichworte- aktive Verteilnetze, Spartransformator, kombinatorische Benders-Zerlegung, konvexe Optimierung, konvexe Relaxation, dezentrale Erzeuger, Netzrekonfiguration, Starten von Induktionsmotoren, Lasttrennschalter, Lastzuschaltsequenz, mehrstufige Netzwiederherstellung, optimale Spannungsreglung, optimaler Lastfluss, Trennschalter, Koppelschalter, Netzwiederherstellung.

Contents

List of Figures

List of Tables

Notation

In the following, all the notations used in this dissertation are listed. In this regard, first, the notations common with all the chapters are presented. Afterwards, the additional notations that are specifically used in a given chapter are provided in separated groups. Unless mentioned, all the parameters and variables are expressed in [p.u.].

Abbreviations:

ADN	Active Distribution Network
CLPU	Cold Load Pickup
DG	Distributed Generator
DNA	Distribution Network Automation
DSO	Distribution System Operator
ENS	Energy Not Supplied
MV	Medium Voltage
MIQCP	Mixed-Integer Quadratic Constraint Programming
MISOCP	Mixed-Integer Second Order Cone Programming
MAS	Multi-Agent System
OPF	Optimal Power Flow
SOCP	Second Order Cone Programming
SOS1	Special Ordered Set-1

Parameters:

$P_{i,max}^{inj}$	Active power capacity of resource at node i (p.u.)
$S_{i,max}^{inj}$	Apparent power capacity of resource at node i (p.u.)

f_{ij}^{thr}	Current threshold level at line ij beyond which the current deviation will be minimized
D_i	Importance factor of the load at bus i
$A_{ij,p}$	Indicator specifying if line ij is totally in zone p (1/0)
$A_{i,p}$	Indicator specifying if node i is in zone p (1/0)
M	Large multiplier
f_{ij}^{max}	Maximum current flow rating of line ij
v^{max}/v^{min}	Maximum(/Minimum) limits of voltage magnitude
$Q_{i,max}^{inj}$ $(Q_{i,min}^{inj})$	Maximum (Minimum) reactive power allowed to inject/extract from resource at node i (p.u.).
$r(/x)_{ij}$	Resistance(/Reactance) of line ij
λ_i	Weighting factor of the load breaker at bus i depending on its operational priority
w_{re}, w_{sw}, w_{op}	Weighting factors of the objective function terms
λ_{ij}	Weighting factor of the switch on line ij depending on its operational priority

Variables:

$P_{i,t}^{inj}$	Active power injection from a DG at bus i, at time t (p.u)
$P(/Q)_{i,t}^{Sub}$	Active(/Reactive) power injection from the substation node i, at time t
$p(/q)_{ij,t}$	Active(/Reactive) power flow in line ij, starting from node i, at time t
$\Psi_{ij,s}$	Auxiliary flow that is travelling at step s in line ij from node i to node j.
L_i	Binary decision variable indicating if the load at node i is supplied or rejected (1/0)
Y_{ij}	Binary decision variable indicating if the switched line ij is energized or not (1/0)
Z_{ij}	Continuous variable indicating if line ij is oriented from node i to node j or not.
B_i	Continuous variable indicating if load breaker at bus i will be operated or not (1/0)
S_{ij}	Continuous variable indicating if sectionalizing switch on line ij will be operated or not (1/0)
$F_{ij,t}^*$	Deviation of squared current flow magnitude in line ij, at time t
X_{ij}	Indicator of line ij, being energized or not (1/0)
X_i	Indicator of node i, being energized or not (1/0)
E_p	Indicator of zone p, being energized or not (1/0)
$Q_{i,t}^{inj}$	Reactive power injected by a CB/DG at bus i, at time t (p.u)
$F_{ij,t}$	Square of current flow magnitude in line ij, at time t
$V_{i,t}$	Square of voltage magnitude at bus i, at time t

Indices and sets:

ij	Index of branches
i, j, k	Index of nodes
t	Index of time
p	Index of zones
W	Set of healthy lines in the faulted and available feeders
N	Set of healthy nodes in the faulted feeder and available neighboring feeders
Ω_{Res}	Set of injection nodes including substations (Ω_{Sub}) and DGs (Ω_{DG})
W_{ava}^S	Set of lines hosting available tie-switches
W_{sec}^S	Set of lines hosting internal sectionalizing switches
W_{int}^S	Set of lines hosting internal tie-switches
$W_{tie}^S = W_{ava}^S \cup W_{int}^S$	Set of lines hosting tie-switches.
W^*	Set of lines (plus tie-lines) in the off-outage area
N^*	Set of nodes in the off-outage area
Z^*	Set of zones in the off-outage area

Notation:

$\lvert . \rvert$	Absolute value of a real number or magnitude value of a complex number
$j := \sqrt{-1}$	Imaginary unit
$\max\{a, b\}$	Maximum value of a and b
$\Re(.)$	Real part of a complex number

Chapter 2: Restoration Problem in Passive Distribution Networks

Abbreviations:

CB	Capacitor Bank
OLTC	On-Load Tap Changer
SVR	Step Voltage Regulator

Parameters:

$(kp/kq)_i$	Active (/Reactive) load voltage sensitivity for the load at bus i.
$P(/Q)_{i,t,s}^0$	Active (/Reactive) power demand when voltage is 1 p.u. at bus i, at time t
$n_i(/n_{ij})$	Number of tap steps at each positive/negative side of the OLTC/SVR/CB installed at bus i/line ij
ΔQ_i	Reactive power change at each tap step in the CB installed at bus i
$\Delta r0_i(/\Delta r0_{ij})$	The pre-fault tap position of CB/SVR at bus i/line ij
$\alpha0_i$	The pre-fault transformer ratio setting of OLTC/SVR at bus i

σ_i/σ_{ij}	Transformer ratio change at each tap step in the OLTC/SVR installed at bus i/line ij.
w_1, w_2	Weighting factors of different sub terms of the operational objective term.

Variables:

$P(/Q)_{i,t}^{cur}$	Active(/Reactive) load curtailment at bus i, at time t
$P(/Q)_{i,t}^{D}$	Active (/Reactive) power demand at bus i, at time t
α_i	Continuous decision variable relaxing the post-fault transformer ratio setting of OLTC at bus i.
$\beta_{ij,t}$	Continuous decision variable used in the linearization of nodal voltage equation for each SVR on line ij, at time t.
$\gamma_{ij,t}$	Continuous variable approximating the tap position of each SVR on line ij, at time t
$T_i(/T_{ij})$	Continuous variable accounting for the tap changing of OLTC/CB/SVR at bus i/ line ij
$\Delta r_i(/\Delta r_{ij})$	Integer decision variable indicating the post-fault tap position of each CB/SVR at bus i/line ij.
δr_k	The k$^{\text{th}}$-element of Δr_{ij} binary representation
b_k	The k$^{\text{th}}$-element of $\beta_{ij,t}$ binary representation

Indices and sets:

Ω_{SVR}	Set of lines in the faulted and available feeders that are hosting an SVR
Ω_{CB}	Set of nodes in the faulted and available feeders that are hosting a CB
Ω_{Sub}	Set of substation nodes in available feeders that are hosting an OLTC

Chapter 3: Service Restoration in DG-Integrated Distribution Networks

Abbreviations:

AR-OPF	Augmented Relaxed Optimal Power Flow
R-OPF	Relaxed Optimal Power Flow
SOE	State of Energy

Parameters:

$P_{i,t}^{D}(Q_{i,t}^{D})$	Active (Reactive) power demand at bus i, at time t
Δ_i	The energization time constant of DG at node i (hour).
Δt	Time step length (hour)
b_{ij}	Susceptance of line ij.

Variables:

$\hat{S}_{ij,t} = \hat{p}_{ij,t} + j\hat{q}_{ij,t}$	Auxiliary variable representing a lower bound on the complex power flow in line ij, starting from node i, at time t.
$\hat{V}_{i,t}$	Auxiliary variable representing a lower bound on the square of voltage magnitude at bus i, at time t.
$\bar{S}_{ij,t} = \bar{p}_{ij,t} + j\bar{q}_{ij,t}$	Auxiliary variable representing an upper bound on the complex power flow in line ij, starting from node i, at time t.
$\bar{F}_{ij,t}$	Auxiliary variable representing an upper bound on the square of current flow magnitude in line ij, at time t.
$Y_{ij,s}$	Binary decision variable indicating if at step s the line ij equipped with a switch is energized or not (1/0)
$Z_{ij,s}$	Continuous variable indicating if at step s the line ij is oriented from node i to node j or not.
$S_{ij,s}$	Continuous variable indicating if at step s sectionalizing switch on line ij will be operated or not (1/0).
$K_{t,s}$	Continuous variable indicating if at time t the network is under the configuration at step s or not (1/0).
$X_{i,s}$	Indicator of node i at step s, being energized or not (1/0).
$X_{ij,s}$	Indicator of line ij at step s, being energized or not (1/0)
T_s	The starting time instant of reconfiguration step s (hour).

Indices and sets:

s	Index of reconfiguration step

Chapter 4: A Novel Solution Algorithm for the Restoration Problem in Distribution Networks

Abbreviations:

CB	Combinatorial Benders
ILP	Integer Linear Programming
MIS	Minimal Infeasible Subset
MIP	Mixed Integer Programming
MILP	Mixed Integer Linear Programming
MCB	Modified Combinatorial Benders
IAO	The Integrated Analytical Optimization

Parameters:

$P^D_{i,t}(Q^D_{i,t})$	Active (Reactive) power demand at bus i, at time t (p.u.)
$A, B, C, D, E, F, G, \bar{G}, H, \bar{H}, J$	Matrices of parameters used in the compact form of the optimization problem
v_{max}	Number of clusters

σ_{max}	Number of conditional constraints
$\bar{h}_i$	Relaxed apparent power limit of the DG at node i in the DistFlow formulation
$\bar{s}_{ij}$	Relaxed ampacity limit of line ij in the DistFlow formulation
ε	The convergence tolerance setting of the decomposition algorithm
$LB^{(q)}$	The lower bound obtained at the qth iteration in the decomposition algorithm
$\mathbb{S}_v(Y^{(k)})$	The obtained value of the objective function in the sub problem at iteration k and for cluster v.
$Y^{(k)}$	The obtained value of Y variables in the master problem at iteration k
$UB^{(q)}$	The upper bound obtained at the qth iteration in the decomposition algorithm
$\eta_\sigma(Y^{(k)})$	The value of the logical expression under configuration $Y^{(k)}$ in the σth conditional constraint.
$a, b, c, d, e,$ $f, g, \bar{g}, h$	Vectors of parameters used in the compact form of the optimization problem

Variables:

α	Vector of auxiliary variables for the feasibility validation in the sub problem
Y	Vector of complicating binary variables
ϕ, u	Vector of continuous variables
L	Vector of floating binary variables

Indices and sets:

v	Index of clusters
σ	Index of conditional constraints
q	Index of current iteration
k	Index of iteration
$\Upsilon^{(k)}$	The minimal infeasible subset corresponding to the obtained solution at iteration k
$\mathbb{C}_1(L, Y)$	The set of constraints of the restoration problem only on the binary variables
$\mathbb{E}(v, Y^{(q)})$	The set of lines in cluster v under configuration $Y^{(k)}$
$\varphi(v, Y^{(k)})$	The set of nodes in cluster v under configuration $Y^{(k)}$
Γ	The set of radial network configurations
$\mathbb{C}_2(L, Y, \phi, u)$	The set of relaxed AC power flow constraints integrated into the restoration problem
$\mathbb{E}_s(v, Y^{(q)})$	The set of source lines in cluster v under configuration $Y^{(k)}$
$\Psi(v, Y^{(k)})$	The set of Y-solutions obtained at iteration k that makes the cluster v infeasible
$\overline{\mathbb{C}_2}(L, Y, \phi, u)$	The set of DistFlow constraints integrated into the restoration problem

Chapter 5: Optimal Load Restoration in Active Distribution Networks Complying with Starting Transients of Induction Motors

Abbreviations:

LVRT	Low-Voltage Ride Through
PHIL	Power Hardware In the Loop

Parameters:

$kp_i(kq_i)$	Active (Reactive) load voltage sensitivity at bus i.
$P_{i,t}^0(Q_{i,t}^0)$	Active (Reactive) nominal load at bus i at time t.
$f_{max,i}^{DG}$	Ampacity limit of the DG converter at node i.
Kd_m	Coefficient of the friction and windage loss in the motor m.
H_m	Inertia constant of the motor m (s)
$L_{i,t}^0$	Load energization status at node i and time t according to the steady-state analysis (1/0).
k_{max}	Number of steps assigned to each starting motor
ΔS_m	Slip interval between two successive steps for the motor m.
$S_{k,m}$	Slip value of the motor m at step k.

Variables:

$P_{i,k,m}^D$ $(Q_{i,k,m}^D)$	Active (Reactive) load power at bus i, at step k, in case of the motor load starting at node m.
$p_{ij,k,m}$ $(q_{ij,k,m})$	Active (Reactive) power flowing in line ij, at step k, in case of the motor load starting at node m.
$P_{i,k,m}^{Sub}$ $(Q_{i,k,m}^{Sub})$	Active (Reactive) power from the substation node i, at step k, in case of the motor load starting at node m.
$P_{i,k,m}^{DG}$ $(Q_{i,k,m}^{DG})$	Active (Reactive) power injection from the DG node i, at step k, in case of the motor load starting at node m.
$\tilde{t}_{k,m}$	An approximation for the acceleration time of the motor m until step k (s).
$\widetilde{\Delta t}_{k,m}$	An approximation for the time lengths of the step k , in case of the motor load starting at node m (s).
$T_{k,m}^{ele}$	Electrical torque of the motor m, at step k.
Δr_m	Integer variable representing the tap position of the autotransformer at the motor m.
$T_{k,m}^{mec}$	Mechanical torque of the motor m, at step k.

$F_{ij,k,m}$	Square of current flow magnitude in line ij, at step k, in case of the motor load starting at node m.
$Fp_{i,m}^{DG}$ $(Fq_{i,m}^{DG})$	Square of the active/reactive current references of the DG converter at node i for the starting of the motor m.
$V_{i,k,m}$	Square of voltage magnitude at bus i, at step k, in case of the motor load starting at node m.

Indices and sets:

m	Index of nodes hosting motor loads in the off-outage area
k	Index of slip step
T	Set of all the time samples in the restorative period
N_m	Set of nodes hosting motor loads
N_m^*	Set of nodes hosting motor loads in the off-outage area
N_s	Set of nodes hosting static loads
W_p	Set of protected lines
N_p	Set of protected nodes

1 Introduction

1.1 Service Restoration after Blackout in Power Systems

In the last decade, a great number of blackouts has been reported around the world. Among the most severe ones, we can mention the huge blackout in the North America on August 14, 2003 which lasted two weeks [1]. Another example is the blackout in northern India on July 30, 2012, which cut 50 GW load and affected 670 million people for two days [2]. The Italy blackout on September 28, 2003 cut the power throughout the whole Italy for 12 hours and part of the Switzerland near Geneva for 3 hours affecting about 56 million people [3]. Although a great amount of work has been conducted to make power systems safe against these outages, the risk of wide-spread black-outs still exist.

A proper plan for restoring the power system can effectively reduce the negative impacts of the network failures on the public, economy, and the power system itself. For many years, the attention of power system engineers was directed to devise restoration plans more for power plants and transmission systems than for distribution networks [4]. This was due to the very high outage costs of sensitive equipment in power plants and transmission systems. In addition, since traditional power systems were operated in a vertical fashion (generating power only at large power plants, then transmitting and distributing power to the customers), the outage in power plants and transmission systems could cut the power to a huge number of customers and leave them without any alternative supply. In this regard, the standards achieved for the restoration of generation and transmission networks are drastically higher than the ones for the distribution networks. For example, according to the statistics in China, on average, 80% of the annual outage

time per customer in the whole system is due to the faults in distribution networks [5]. This percentage is approximately equal to 90% according to the UK statistics [6].

1.2 Motivation of the Thesis

In recent years, the growing penetration of Distributed Generators (DGs) in distribution networks has brought significant technical challenges to all aspects related to the network planning and operation [1,2]. In this respect, the power research community has defined the term "Active Distribution Networks (ADNs)" to distinguish this new shape of distribution networks from the passive distribution networks in the past. These ADNs are equipped with new generation of communication, automation, and protection infrastructures. This modernization implies a higher level of requirement regarding the quality of supply. When it comes to power quality, availability is the most important factor. As mentioned in section 1.1, faults occurring in distribution networks are the main source of reducing the availability of electricity, nowadays. Therefore, the target domain for improving the power system reliability is in distribution networks.

The stable and reliable operation of the distribution networks has become a challenge now more than ever for utilities. There are many reasons contributing to this. The penetration of renewable generation resources is increasing in distribution networks. Due to the stochasticity of these resources, it is difficult to predict or control their generated power. In addition, it is usually difficult to expand the distribution grids in adequacy with the load increase due to economic, environmental, or practical reasons. The resulting postponed grid reinforcement leads to increase the complexity of the distribution network operation.

The other factor that contributes to the operational complexity of the current distribution networks is the advent of electricity market deregulation. Nowadays, electricity markets load the grid in a less predictable and more dynamic way, while the decisions of DG owners do not consider network security constraints [9]. As a result, the security and stability margins are narrowing. In the following, two possible scenarios are introduced, as examples, where the dispatch of DGs pushes the distribution network close to its critical operating limits:

- Overload of feeders and transformers could occur due to the large amounts of DG power production during periods of low power consumption.
- The risk of over-voltage and/or under-voltage violations increase due to production at remote parts of a distribution feeder.

The latter scenario is of particular importance regarding the restoration service at the distribution level. According to the restoration strategy, the configuration of the distribution network changes with respect to the one in normal state. Loads in the faulted feeder are transferred to the adjacent healthy feeders. In the resulting new configuration of the system, the electrical distance between the DG injection nodes in the adjacent feeders and the consumption nodes in the faulted feeder could be significant. In this regard, the possibility of violating the upper voltage limit at the DG nodes and/or the lower voltage limit at the consumption nodes (especially at the leaf nodes of the faulted feeder) increases. If these possible violations are not properly prevented, the restoration solution may cause further outages during its implementation.

In order to handle these complexities brought to the distribution network operation, Distribution Network Automation (DNA) evolved as a new operating paradigm replacing conventional approaches that were deployed in distribution networks. DNA is based on smart grid technologies for grid state identification and subsequent control functions in critical situations. Among these control functions, we can mention the DG power set points or Demand Side Management (DSM) [10]–[12]. In this regard, all the new monitoring, communication and control facilities pertaining to smart grids are deployed resulting in automatic and efficient control and operation services. These services include among others fault detection, fault isolation, and fault restoration [8]. In this thesis, we aim to develop automatic service restoration strategies for ADNs complying with the requirements of the DNA systems. In the following, we present an introduction and a brief literature-review on the restoration problem in distribution networks.

1.3 Problem Statement

In spite of a meshed structure, distribution systems are operated radially. Accordingly, each node is fed from the substation transformer only through one path. This is due to advantages concerning substantial saving in the number and sizing of the protection devices and circuit breakers.

In case of a failure within a distribution network, the globally agreed procedure is to, first, diagnose the fault and then locate its place. Afterwards, the faulted element is isolated from the rest of the network in order to be repaired and also in order to allow the surrounding elements to be restored [13]. Once the faulted element is isolated, the disconnected breaker at the top point of the feeder is re-connected to resupply the area upstream to the fault place (node 1 in Fig. 1-1).
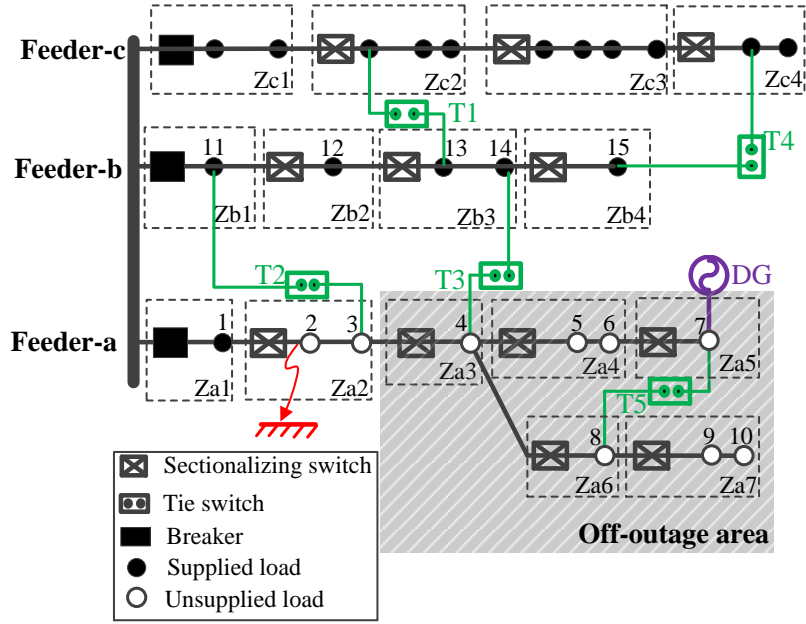
Fig. 1-1. A simple distribution network under fault conditions

Due to the radial operation of the distribution network, the area downstream to the fault location is left unsupplied (see Fig. 1-1). This area is referred as *off-outage area* in the literature. It is the case even for Active Distribution Networks (ADNs). Actually, following a severe disturbance, according to the IEEE standard 1547 [14], every DG in the network should be automatically disconnected. This off-outage area constitutes the main concern for the restoration service, which is the next step of the fault management procedure. In this regard, the emergency service is supposed to find and apply the optimal restoration solution. This optimality is defined as maximizing the energy of restored loads in the off-outage area while minimizing the switching operation time. In the case of passive distribution systems, the restoration process counts only on topological reconfiguration. It consists of load transfer from the off-outage to the neighboring feeders (Feeder-b in Fig. 1-1) using tie-lines equipped with tie-switches (T3 in Fig. 1-1) [4, 5]. These feeders and switches are called *available feeders* (Feeder-b in Fig. 1-1) and *available tie-switches* (T3 in Fig. 1-1), respectively. The resulting new configuration of the network remains for a so-called *restorative period* starting from the fault isolation instant until the time when the faulted element is repaired. After the restorative period, the original configuration of the network is restored.

Solving the restoration problem yields the switching operations for implementing the optimal configuration. Regarding the sequence of these operations in practice, first, the sectionalizing switches (to be open) are operated in order to structure the off-outage area according to the

optimal configuration. Then, the switching operation of tie-switches (to be on) is deployed in order to energize the off-outage area through neighboring feeders.

Following an emergency situation in a distribution network, the control operators have a very stressful and demanding task to deploy the restoration service very quickly while respecting all the security and reliability standards. Concerning the restoration strategy, to support the decision of the system operator, in the past, the distribution utilities used to devise in-advance restoration solutions for a large set of predefined fault scenarios. In this regard, most of the companies in the past were developing their own restoration plans. The authors of [15] present a review of different restoration guidelines taken by different companies in US from year 1981 to 1994. Such a completely pre-planned restoration approach has two major disadvantages making it inappropriate for current distribution networks. First, it is impractical to consider all the possible fault scenarios beforehand in an off-line study. Second, all these prepared scenarios rely on certain assumed fixed input data related to the network infrastructures/topologies (operating schemes) and to the load consumptions. However, in distribution networks, the loads are continuously varying and the actual network topologies can change more frequently than in the past. In addition, in the context of the ongoing distribution network modernization, the infrastructure in these networks can change frequently for example, replacing old components with newer and more reliable ones [13].

In order to tackle the above mentioned problems, the authors in [16] and [17] propose to update the pre-planned restoration solutions in real-time according to the actual operational conditions. However, these "*quasi-automated*" methods cannot be considered as an efficient solution approach due to the ever-increasing complexities within the modern distribution networks. Achieving a completely automatic restoration strategy (i.e. without relying on preplanned solutions) is an attractive but difficult mission to fulfill. It requires an automatic decision-making and an automatic implementation. In this thesis, we focus on deriving an automatic decision-making approach for the restoration service in distribution networks.

Various approaches have so far been proposed to automatically obtain the restoration solution. The authors in [18] present a brief description of different methodologies used for distribution network restoration and their advantages and disadvantages. Among these methodologies, heuristic, meta-heuristic, and mathematical programming approaches are used more frequently.

Unlike the two other approaches, the mathematical programming approach is able to obtain the global optimal solution [19]–[21].

In order to formulate the restoration problem in a form that can be handled using mathematical programming, a profound scientific knowledge is needed in both mathematics and power system engineering. The restoration problem is inherently a combinatorial and multi-disciplinary problem relying simultaneously on the knowledge from graph theory and from electrical power system discipline. From mathematical programming viewpoint, the restoration problem is a mixed-integer and non-linear non-convex optimization problem. It is due to, respectively, the switching status decision making and the power flow equations that are integrated into the restoration problem. In order to cope with the non-polynomial hardness of such optimization problem, we need to develop efficient mathematical formulations and solution strategies such that we find the target restoration solution within a short time even in case of large-scale outages.

As explained above, the restoration problem is widely studied in the literature regarding the passive distribution networks. The ever-increasing penetration of active elements (e.g. DGs) in distribution networks suggests to enable their potentials in better fulfilling the restoration objectives. For this aim, it would be worth to integrate the analytical model of the DG re-dispatch into the restoration problem. Regarding the DGs located in the off-outage area, specific requirements imposed by their start-up process should be carefully addressed.

As mentioned earlier, the voltage magnitude margins with respect to the lower and/or upper voltage limits might be very small in the restored configuration of the network. This shows that the optimal setting of voltage regulation devices installed in distribution networks should be integrated into the developed optimization model of the restoration problem. Therefore, the voltage profile in the distribution network will be improved by the voltage regulation devices and consequently more loads can be restored.

The power flow formulation should be integrated into the restoration problem in order to ensure that the electrical constraints are all respected during the whole restorative period. In this regard, the relaxation methods used for the branch flow model need to be updated such that their exactness can be ensured particularly in presence of high DG penetrations.

The restoration problem is by nature an NP-hard combinatorial optimization problem. Integrating the above-mentioned features into this problem leads to a huge and intractable optimization problem, especially in case of a grid of realistic size. The significance of this

challenge is more highlighted considering that the target restoration strategy should provide a fast decision-making tool compatible with the specific requirement of DNA systems in smart grids. A potential approach for tackling this challenge is to use an appropriate decomposition technique.

Another important issue needed to be addressed is related to the restoration of dynamic loads. For example, the large and reactive current driven by induction motor loads during the starting period can impose high risks both in the motor side and in the network side [22]. The restoration problem formulation containing only static models for loads and DGs cannot guarantee that the obtained solution respects transient operational constraints (e.g. voltage-dip and over-current transient acceptability limits) during the starting of induction motor loads. This restoration problem formulation needs to be modified incorporating the dynamic model of induction motor loads and DGs.

In order to show the advantages of tackling the above-mentioned challenges, they will be addressed progressively through the different chapters proposed in this thesis dissertation.

1.4 Assumptions

In this thesis, we aim to propose a network operation tool in order to support the operators specifically for the service restoration. In this regard, the fault location and the fault isolation procedures are not treated in this thesis. We assume that the fault place is already located and isolated and the statuses of all switches in the off-outage area are known. We also assume that the load and generation forecast profiles during the restorative period are available as inputs to the service restoration tool. We target in this thesis to develop a deterministic approach, meaning that the reliability of the solution regarding the feasibility and optimality is dependent on the accuracy of the input data.

In the following, we present the other challenges pertaining to the service restoration in distribution networks that we are not tackling specifically in this thesis. Among these untreated challenges is the uncertainty analysis that should be integrated into the restoration problem. Actually, the forecast load and generation data used as the input of the restoration problem is subject to uncertainty. Since the planning time window of the restoration problem (restorative period) is rather short, the uncertainty of loads and generation data will not be accounted for in

this thesis. We use the worst realization of load and generation profiles as the input data of the restoration problem.

Another untreated challenge is the modeling and integrating Cold Load Pickup (CLPU) effect in the restoration problem at the distribution level. Loss of diversity in thermostatically-controlled loads makes an increase in the consumption level at the starting of the restorative period. Such a high loading condition, which is called Cold Load Pickup (CLPU), disappears once the normal diversity of loads is restored. The extent of CLPU condition depends on different factors such as the outage duration, connected loads, local weather conditions and thermal characteristics of the user. The consideration of CLPU in the restoration problem while accounting for the special features of CLPU at the distribution network level will be presented in Chapter 6 as a future work.

In this thesis, we study service restoration, assuming that the distribution network is operated radially. In practice, some distribution network utilities might decide to operate their networks in a meshed topology due to the advantages mainly on the network reliability, and also on power losses and voltage regulation [23]. Especially in case of high penetration of DGs, it is beneficial to use meshed topologies in order to exploit more efficiently the capacity of lines and substations.

The restoration problem is solved in this thesis using a centralized solution approach. Many decentralized restoration algorithms are proposed in the literature (see chapter 2, section 2.3). In all these studies, the decision maker entity lacks a global vision of the network. Therefore, the accurate checking of the solution feasibility concerning all the technical constraints (e.g., voltage and current limits) is either ignored or checked in the last stage using load flow simulations. It should be mentioned that the fact that the restoration problem is developed in this thesis based on a centralized solution algorithm does not infer that it is only compatible with centralized operational frameworks. Further insights in this regard are provided in chapter 6 (conclusion).

In this thesis, we assume that the distribution network is operated in a balanced fashion. In this respect, the power flow formulation is integrated into the restoration problem considering the single-phase equivalent model of the distribution network. We also assume that the protection relays (e.g. under voltage or over-current relays) in the distribution network are perfectly reliable. In this regard, the nodal voltage and line current limits are considered as fixed and deterministic values.

The supporting discussion regarding these untreated challenges will be presented in Chapter 6. There, we provide insights about possible extension of the restoration approach proposed in this thesis such that these challenges can be addressed.

1.5 Objectives and contributions of the thesis

The aim of this thesis is to address the above-mentioned challenges regarding the service restoration problem in distribution networks. In this respect, first, we provide a mathematical optimization model for the restoration problem in passive distribution networks. This model is then modified and extended such that it is applicable also for active distribution networks. Further, a novel decomposition strategy is proposed that makes the restoration formulation tractable for analytical solvers in case of a grid of realistic size in a multi-period optimization problem. Finally, we integrate a semi-static model of induction motor loads and the control of converter-based DGs in saturation mode into the restoration problem formulation in order to account for the transient security constraints during the starting period of large motor loads.

In what follows, the main contributions of the thesis are summarized referring to the challenges expressed in section 1.3.

1.5.1 Restoration Problem Formulation in Passive Distribution Networks

1.5.1.1 **Development of a mathematical optimization model for the network reconfiguration complying with service restoration requirements**

The thesis, first, proposes a linear formulation for the radiality constraints during the reconfiguration of passive distribution networks. Unlike the existing formulations in the literature, the proposed formulation covers real scenarios that could occur during the service restoration, such as partial restoration scenarios.

1.5.1.2 **Incorporation of the optimal voltage regulation into the restoration problem**

The derived optimization model for the restoration problem is augmented with the analytical models of voltage regulation devices. The aim is to enhance the quality of the obtained restoration solution using the optimal setting of voltage regulation devices in distribution networks. In this regard, the considered self-healing actions besides the network reconfiguration are the tap setting modification of voltage regulation devices including I) On-Line Tap-Changing (OLTC) transformers, II) Step Voltage Regulators (SVRs), and III) Capacitor Banks (CBs). In

order to account for the voltage dependency of active and reactive load powers, their models are integrated into the optimization problem using a linear approximation method.

1.6 Restoration Problem Formulation in Active Distribution Networks

1.6.1.1 Development of a novel operational strategy for the restoration of ADNs: multi-step restoration

The multi-step restoration is proposed as a novel operational strategy in order to handle in the most efficient fashion a time-dependent process in the reconfiguration of distribution networks. In particular, regarding the restoration problem in ADNs, the start-up process of disconnected DGs is handled in the proposed restoration strategy through successive steps. Since in this thesis we focus on the permanent fault cases, it is assumed that once the fault occurs, all the DGs in the off-outage area are automatically disconnected. In this regard, two types of DGs are studied, namely dispatchable and non-dispatchable DGs. The dispatchable DGs (e.g. PV and Wind generations not equipped with batteries) are modeled as negative power constant loads. The power injections of these DGs are defined as parameters and determined according to their forecast profiles. The other types of DGs are dispatchable with finite active and apparent power capacities. It is assumed that the islanded operation of these DGs (the grid-forming mode for converter-based DGs) is not allowed. It means that these DGs may inject power only once their hosting nodes are already energized (through paths) from the substation. This operation mode is refereed in this thesis as *grid-connected mode*. In this regard, the start-up requirements of these DGs, including the energization of their hosting nodes and their start-up durations are accurately modeled and integrated into the proposed restoration model.

1.6.1.2 Integration of an exact power flow formulation into the restoration problem in ADNs

The developed multi-step restoration model is augmented with an exact power flow formulation called, Augmented Relaxed Optimal Power Flow (AR-OPF). The aim is to ensure the feasibility of the obtained restoration solution concerning the technical constraints (e.g. voltage and current limits). Unlike the other relaxation methods, the AR-OPF is exact even in presence of high DG penetrations in the distribution network. The overall restoration problem is in the form of a Mixed-Integer Second-Order Cone Programming (MISOCP) optimization

problem. Therefore, it can be solved efficiently by the state-of-the-art commercial solvers for convex optimization problems.

1.6.2 The Solution Algorithm of the Restoration Problem

1.6.2.1 Development of a novel decomposition approach for the restoration problem named, *Modified Combinatorial Benders (MCB)*

The thesis proposes a novel solution strategy that makes the restoration formulation tractable for analytical solvers in case of a grid of realistic size in a multi-period optimization problem. The link between the line switching variables and the AC power flow model inhibits the use of classical Benders algorithm in decomposing the restoration problem. Therefore, we present a modification to the combinatorial Benders method so that it can be used for the multi-period restoration problem. In this regard, the derived model for the network reconfiguration and the AC power flow formulation are decomposed into master and sub problems, which are solved through successive iterations. At each iteration, the solution of the sub problem is used to augment the feasibility or optimality cuts of the master problem, which is solved in the next iterations. The results indicate that the proposed decomposition algorithm provides, within a short time (after a few iterations), a restoration solution with a quality that is close to the proven optimality, when it can be exhibited.

1.6.3 The Optimal Restoration of Dynamic Loads

1.6.3.1 Development of an optimization model for the optimal restoration of induction motor loads complying with their starting transients

In this thesis, a mathematical and convex optimization model is derived for the induction motor representing its starting transients in a semi-static fashion. This model is used to find the optimal energization sequence of different loads (static and motor loads) following an outage in a distribution network. In addition to the induction motors, a convex optimization model is derived for the converter-based DGs according to their control mode during transient voltage dips in the network. In this regard, along with the optimal load energization sequence, the optimal set point of the converter-based DGs during the motor starting transients are derived from the developed optimization problem. The proposed optimization problem provides also the optimal tap setting of the autotransformers that are used for the starting of the induction motors. The transient operational limits are imbedded in this optimization problem ensuring that the starting of

induction motors will not trigger any protection device either in the motor side or in network side. The optimization problem is formulated as a MISOCP.

1.7 Thesis outline

The rest of this thesis dissertation is structured as follows.

Chapter 2 presents a description of the state-of-the-art methodologies used for the restoration problem along with their weaknesses. Then, the restoration problem is defined and its particular requirements are expressed with reference to passive distribution networks. According to these requirements, a mathematical optimization formulation is proposed for the restoration problem in passive distribution networks. Further in this chapter, we augment the optimization problem with the optimal voltage regulation in distribution networks. In this regard, first, mathematical optimization models are derived for three types of voltage regulation devices, namely, OLTCs, SVRs, and CBs. Then, the voltage dependency of active and reactive load powers is formulated and integrated into the proposed optimization problem. Finally, different test studies are used to illustrate the effectiveness of the developed mathematical programming method for the restoration problem in passive distribution networks.

Chapter 3 is assigned to the modifications that are required for the restoration problem such that it is applicable also for active distribution networks. In the first part of this chapter, the modifications related to the strategy of the restoration problem are presented. In this regard, after a literature review on the existing approaches, a novel "multi-step restoration" strategy is introduced and formulated. The second part of this chapter is dedicated to the modifications related to the formulation of the restoration problem. More specifically, we focus on the integration of AC power flow formulation into the restoration problem in presence of high DG penetrations. In this respect, first, a literature review is presented. Then, an exact relaxation method for the OPF problem is integrated into the developed formulation of the multi-step restoration problem. The main contributions of this chapter are verified in the last part using different test studies.

Chapter 4 presents a novel solution algorithm for the restoration problem in active distribution networks. In this regard, first, the state-of-the-art algorithms are reviewed while highlighting their weaknesses. Then, the standard combinatorial benders method is explained as the basis for the proposed decomposition strategy. Further, the proposed decomposition algorithm, named,

Modified Combinatorial Bender (MCB) method is described and applied to the multi-period restoration problem. Finally, the effectiveness of this new algorithm is illustrated using different test studies.

Chapter 5 is devoted to model the starting transients of induction motor loads and their effects on the optimal restoration solution. First, a literature review is presented describing the previous studies on the dynamic analysis of motor starting. Then, a mathematical and convex optimization model is derived representing the starting transients of the induction motor in a semi-static fashion. Then, this model is used to find the optimal energization sequence of different loads (static and motor loads) following an outage in a distribution network. In this chapter, we provide mathematical optimization models also for I) the converter-based DGs according to their control mode during transient voltage dips and II) for the autotransformers that are used for the induction motor starting. Further, we illustrate the functionality of the proposed optimization problem in the case of a large-scale test study and under different simulation scenarios. In the last part of this chapter, the feasibility and accuracy of the optimization solution obtained from the proposed semi-static model are validated using I) off-line time-domain simulations, and II) a Power Hardware-In-the-Loop experiment.

Chapter 6 concludes the dissertation by summarizing the main contributions of this research. Moreover, it provides an outlook on the potential future works.

2 Restoration Problem in Passive Distribution Networks

Chapter Highlights:

In this chapter, we provide a novel optimization model for the restoration problem in passive distribution networks. The restoration problem is by nature in the form of a mixed integer and non-linear problem, respectively due to the switching decisions and power flow constraints (e.g. voltage and current limits). In this regard, first, a novel mathematical formulation is presented modeling the switching actions in distribution networks. In comparison to the existing formulations, the proposed one incorporates fewer numbers of binary variables and covers more practical scenarios such as *partial restoration*.

Further, we aim to incorporate any voltage regulation device installed in a distribution network into the proposed restoration problem in order to achieve enhanced solutions. In this regard, mathematical optimization models are derived for three types of voltage regulation devices, namely, I) On-Line Tap-Changing (OLTC) transformers, II) Step Voltage Regulators (SVRs), and III) Capacitor Banks (CBs). Then, the voltage-dependent model of static load powers is in turn integrated into the updated optimization formulation using a linear approximation method. Consequently, the voltage dependency of active/reactive load consumptions is considered in finding the optimal set point of those voltage regulation devices. The overall resulting restoration problem is expressed as a MISOCP optimization model. This formulation will be regarded as the basis of the next chapters for modeling specific aspects of the restoration problem in distribution networks.

Related Publication:

H. **Sekhavatmanesh** and R. Cherkaoui, "Analytical Approach for Active Distribution Network Restoration Including Optimal Voltage Regulation," *IEEE Transactions on Power Systems*, pp. 1–1, 2018, doi: 10.1109/TPWRS.2018.2889241.

2.1 Chapter Organization

The motivation of presenting this chapter is illustrated in section 2.2 according to the context of the whole thesis. Section 2.3 is devoted to the literature review on the restoration problem methodologies applied to passive distribution networks. The restoration problem is defined in section 2.4. Afterwards, the proposed mathematical formulation for the restoration problem is presented in section 2.5. Section 2.6 is assigned to integrate voltage regulation modeling into the developed restoration problem. In this section, first, mathematical optimization models are derived for three types of voltage regulation devices, namely, OLTCs, SVRs, and CBs. Then, the voltage dependency of active/reactive load consumptions is formulated and integrated into the proposed optimization problem. Section 2.7 provides different test studies illustrating the main contributions of this chapter. The conclusion and summary of this chapter are provided in section 2.8.

2.2 Motivation

In recent years, smart grid concept has evolved as a new operating paradigm for distribution network management. This new operation framework is equipped with intelligent measurement, communication and control infrastructures enabling an efficient electric power transfer from different point of supplies to the end consumers [1,4]. This modernization and, at the same time, the ever-increasing complexities of distribution system operation suggest to investigate self-healing features pertaining to the smart-grid concept [8]. According to this feature, all the new automation facilities pertaining to smart grids should be deployed resulting in an automatic and efficient restoration strategy [8]. Under the pressure of an actual emergency, DSOs are usually faced with a challenging task in taking the best decision for the restoration service. The need for an operator decision support is becoming more crucial with the ever-increasing load demand and reliability requirements in distribution networks. Therefore, the main motivation of this chapter is to develop a mathematical formulation for the restoration problem such that an optimal and feasible solution can be found autonomously and in a short time.

In most of the restoration processes provided in the literature (e.g. in [25] and [26]), it is assumed that all the nodes are energized at the final step. Consequently, each load without breaker (non-detachable loads) is automatically restored. This assumption could not be valid in practice. For example, it might be possible that a set of non-detachable loads cannot be restored while respecting all the electrical constraints. In these cases, a part of the network may be needed

to be left without any supply. These cases are referred as *partial restoration* scenarios. In section 2.5, a new convex formulation of the restoration problem is presented while addressing the above-mentioned weakness of the existing formulations.

Regarding the electrical constraints in passive distribution networks, usually the under voltage limit is the most challenging constraint for the restoration problem. As it will be illustrated in section 2.7, the obtained optimal solutions for the restoration problem usually have very small margins of the voltage magnitude with respect to the under voltage limit. This shows that the quality of the restoration solution in terms of the amount of the restored loads is very sensitive to the under-voltage limit. As the next contribution of this chapter, *the optimal setting of voltage regulation devices* is integrated into the developed optimization model of the restoration problem. Therefore, the voltage profile in the distribution network will be improved by the voltage regulation devices and consequently more loads can be restored. The presented formulation in this chapter will be regarded as the main building block for modeling specific aspects of the restoration problem through the next chapters.

2.3 State-of-the-art of the methodologies applied to the restoration problem

With the advent of smart grids concept, the monitoring, control, and communication technologies should be deployed in restoration plans resulting in an autonomous framework known as self-healing structure [27]. As an important potentiality of smart grids, self-healing feature has attracted a lot of attention among researchers. The most frequently used methodologies in the literature for solving the restoration problem considering self-healing approach can be categorized in two general groups, namely heuristic approaches and global optimization methods.

The restoration problem is a combinatorial and multi-disciplinary problem embedding simultaneously knowledge from graph theory and electrical power system discipline. Due to these complexities, heuristic approaches based on expert systems are proposed for the restoration problem to achieve a near-optimal solution in a short time. Expert systems are defined as algorithms that tend to reproduce the procedures and rules that control operators apply for finding the restoration solution in practice. [19], [28]–[31]. These procedures and rules are derived from the experiences and knowledge acquired by the control operators.

All these strategies are based on operational research [1-4]. In this regard, a guided search (not an exhaustive search) is performed through the topology of the distribution network in order to determine a number of feasible combination of loads that can be restored [3]. In [32], an expert system including approximately 180 rules have been developed for maximizing the loads that can be restored through neighboring feeders. In [33], a new restoration methodology is developed by combining an expert system and a mathematical programming method. In that work, specific operational weight costs are assigned to each switch in the network. In this regard, an optimal configuration is found which is characterized by a lowest total switching cost. Other examples of heuristic approaches applied to the restoration problem include an improved multi objective harmony search algorithm [19], Multi Objective Molecular Differential Evolution (MOMDE) method [20], and Shuffled Frog Leaping Algorithm (SFLA) [21].

In general, all these heuristic approaches are based on the graph search methodologies and are applicable in some specific conditions only. Therefore, they cannot be generalized for any network topology [3], [6-7].

In global optimization methods, all the technical constraints (e.g., voltage and current limits) are modeled and gathered along with an objective function into one set handled by an optimization solver. From the mathematical formulation viewpoint, the restoration problem is a mixed-integer (due to the status of switches) and non-linear (due to the power flow formulation) optimization problem. In order to deal with the non-polynomial hardness of such an OPF-based optimization problem, some papers apply fuzzy algorithms [9–11] or meta-heuristic methods such as Genetic Algorithm, Particle Swarm Optimization, Multi Objective Molecular Differential Evolution method [20], Shuffled Frog Leaping Algorithm [21], and Tabu Search [9].

In [37], the functionality of four meta-heuristic algorithms are compared in solving the restoration problem for a distribution system. These algorithms include Reactive Tabu Search, Tabu Search, Parallel Simulated Annealing and Genetic Algorithm. It is illustrated that the Reactive Tabu Search algorithm performs better than the others in terms of the computation time and the quality of the obtained optimal solution. However, the meta-heuristic methods are in general time-consuming and could fail to give a feasible solution in a reasonable time complying with online operation requirements.

The heuristic and meta-heuristic methodologies are widely employed in the literature to solve the restoration problem in distribution networks with decentralized operational architectures.

Thanks to the booming computer science and communication technologies, Multi-Agent Systems (MAS) is introduced as means for the development of such decentralized operational architectures [38]. MAS is a network of distributed agents that are intelligent enough to sense and react to the environment changes. These agents have the ability to interpret data, interact with each other and make autonomous decisions in order to achieve specific goals.

The authors in [39] proposed a MAS consisting of software agents that cooperate with each other to solve the multi-objective restoration problem in a coordinated fashion. The authors of that paper assigned one individual agent to deal with each objective term. Accordingly, three hierarchical levels of agents were considered. The aim in the primary level is to maximize restored loads using an improved GA. In the secondary level, the total switching operation time and active power loss is minimized. Finally, the third level analyses the solutions obtained from the two other levels and makes a trade-off between different terms of the objective function using Pareto Principle and Analytical Hierarchy Process. A resembling MAS is introduced in [40] considering three layers of agents called response, coordination and organization agents. A two-stage optimization problem is proposed in [41] solved by multiple software agents. In that paper, the network is decomposed into subnetworks, where the reconfiguration of each subnetwork is assigned to one individual software agent. The MAS proposed in all the above-mentioned studies is introduced as a computational aid at the operation center. The main functionality of MAS in those papers is to help accelerating the process of automatic restoration algorithm. Therefore, these approaches still have the weaknesses that are subject to the centralized approaches.

A multi-agent based restoration strategy is proposed in [42], assigning three types of agents to switches, loads, and generators, respectively. According to the proposed strategy, when a fault occurs, the agents of unsupplied loads find and apply the best restoration solution in a stepwise fashion. At each step, a given unsupplied load agent is interacting with the neighboring agents so that it finds a supply path that provides the largest remaining capacity. At the next step, the free capacity of the corresponding supply path is updated and passed through the next unsupplied load agent. A Similar approach is proposed in [43] highlighting the information exchange protocols to be used between different agents. A distributed restoration strategy is proposed in [44], considering one individual agent for each switch in a BDI (believe–desire–intention) architecture. The switch agent nearby the fault place solves the whole restoration problem based on a decision tree approach. The information is aggregated by a peer-to-peer communication

between the agents and the final decision is made using the decision tree methodology. The authors in [45] apply another heuristic strategy, based on the expert systems, taking into account for the load priorities and DG incorporation. The authors in [46] assign two agent types to the loads and feeders. The authors of that paper proposed a novel MAS-based restoration strategy using the prim's minimum spanning tree method. The main contribution provided by that paper is that it reduces the number of interaction rounds that are required between different agents. However, the loads are modeled as current constant types using the pre-fault load values, not accounting for their variation along the restorative period. In addition, the minimization of the switching operation time is not considered.

In all the above-mentioned studies and many others in the context of MAS-based restoration problem, the decision maker agent lacks a global vision of the network. Therefore, the accurate checking of the solution feasibility concerning all the technical constraints (e.g., voltage and current limits) is either ignored or checked in the last stage using load flow simulations. In the latter case, if the obtained solution is not feasible according to the post power flow simulation, it is removed from the search space and the process is repeated to find a new solution [45]. This approach can be very time consuming and/or lead to a solution very far from the optimal one.

In order to solve this problem, a decentralized restoration strategy is proposed in [30] while considering one agent for each zone. A zone is defined as an area in a feeder surrounded by sectionalizing switches. According to that strategy, similar restoration strategies are run in parallel on all the zone agents in the unsupplied area. A communication law is designed for the information exchange between the neighboring agents based on the Average-Consensus theorem so that the global information can be discovered and made available for the agents. The restoration problem is modeled as a 0-1 knapsack problem solved by dynamic programming method for small-scale and by greedy algorithms for large-scale networks. In the proposed model, only the active power capacity of each generator is considered as the knapsack size. The reactive and apparent capacities of generators along with the power losses are disregarded in that approach. Furthermore, the voltage and current limits are not considered. In addition, this strategy relies on the exchange of large amount of data between the agents. This requires low-latency communication links to transfer the data and powerful processors to process them at each agent, which results in a huge capital cost.

The authors of [47] present a hierarchical and decentralized MAS architecture where the restoration problem is solved again by zone agents. The contribution of that paper is to use a coordinating agent that modifies continuously the local parameters of all the zone agents participating to the solution algorithm. This enables these zone agents to act cooperatively and quickly in real operation in case of any fault in an autonomous way. A multi-step expert-based decision making approach is used to solve the restoration problem. However, the proposed restoration algorithm cannot be generalized to address all the possible contingencies. Another hierarchical structure of MAS is proposed in [48] for the restoration problem, assigning three types of agents to the switching devices, feeders, and substations. The decision maker is the faulted feeder agent. The restoration problem is modeled as a 1-0 knapsack problem and solved using Genetic Algorithm. In both algorithm proposed in [47] and [48], the available remaining capacities of neighboring feeders are approximated and simply compared with the summation of loads in the unsupplied area. This assumption is very conservative and limits the number of unsupplied loads that can be restored.

In order to address the weaknesses corresponding to the heuristic and meta-heuristic methodologies, mathematical formulations were proposed for the restoration problem. However, these formulations fail to represent *partial restoration* scenarios accurately. Partial restoration scenarios refer to the cases where the whole outage area cannot be restored while respecting all the electrical constraints (such as voltage and current limits). For dealing with this situation, the authors in [18, 19] propose to leave a part of the outage area without any supply (no voltage) which is called *isolated area*. In that work, in addition to the binary variables considered for the switch status, another set of binary variables is assumed to indicate if the corresponding nodes belong to the isolated area or not. Adding this auxiliary set of binary variables increases the complexity of the problem. Another approach for partial restoration scenarios is proposed in [51]. According to this method, the loads can be rejected in partial restoration scenarios but all the nodes in the off-outage area must be re-energized in any case. This could result in no feasible solution if all the loads are not detachable. Even in the case that all the loads are detachable, this approach could lead to increase uselessly the number of required switching operation.

2.4 Restoration problem statement

Although distribution networks have a meshed structure, most of them are operated radially to ensure economic savings in terms of required number and size of protection devices. A simple
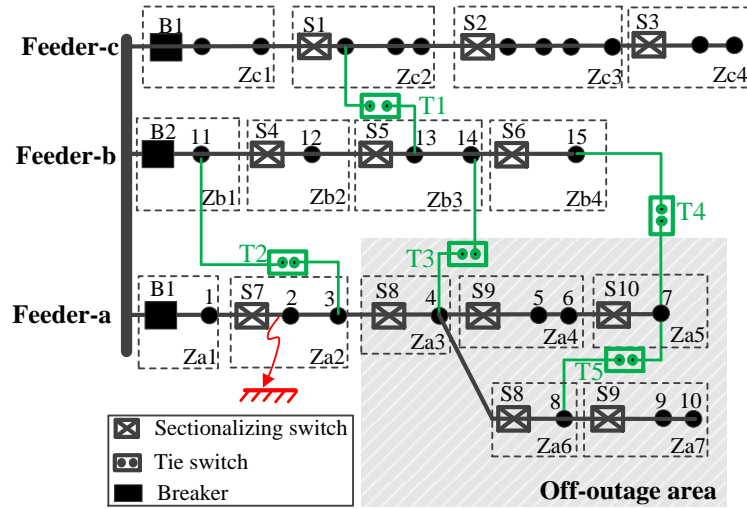
Fig. 2-1. A Simple schematic of a distribution network under a fault condition

schematic of a distribution network under faulted conditions is shown in Fig. 2-1. It is assumed that the MV network that is under study is balanced and can be represented by a single-phase equivalent. When a fault occurs in a distribution network feeder, immediately the breaker located at the top of the feeder (e.g. breaker B1 in Fig. 2-1) trips out thanks to the protective relay. The whole faulted feeder (Feeder-a in Fig. 2-1) is then out of service. Once the faulted element is isolated (opening S7 and S8 in Fig. 2-1), the breaker is reconnected to resupply the area upstream to the fault location. The area downstream to the fault location (shaded area in Fig. 2-1) remains unsupplied. It is referred as *off-outage area*. This area is the target of the restoration service to be re-energized in the most optimal fashion. The objective is to restore rapidly as many customers as possible with a minimum number of switching operations [4]. In the case of passive distribution networks, the restoration solution counts only on the switching operations. According to this strategy, the loads in the off-outage area are transferred to the healthy neighboring feeders through changing the status of normally-closed (sectionalizing) and normally-open (tie) switches. The new configuration of the network remains for a so-called *restorative period* until the faulted element is repaired.

It is preferred for DSO to provide a network configuration for the restoration strategy closer to the pre-fault one. In this way, it will be easier to return to the topology of the normal state, once the fault is cleared. Therefore, in this work, only those healthy feeders that can be directly connected to the off-outage area through tie-switches are involved in the restoration process. These feeders and switches are called *available feeders* (Feeder-b in Fig. 2-1) and *available tie-switches* (T3 and T4 in Fig. 2-1), respectively. From here after, the network part including the

off-outage area, available tie-switches and available feeders is referred to as *reduced network*. Including this reduced network instead of the entire network into the optimization problem helps to significantly decrease the computation time and burden. The tie-switches and sectionalizing switches with both ending nodes inside the off-outage area are referred to as *internal tie-switches* (T5 in Fig. 2-1) and *internal sectionalizing switches*, respectively.

With this assumption, it could happen that the available feeders do not have enough capacity altogether to restore the whole off-outage area. These cases are called *partial restoration scenarios* and are tackled in the literature proposing two different approaches. The authors in [22, 23] propose to leave a part of the off-outage area without any supply which is called *isolated area*. In that work, in addition to binary variables that are considered for switch status, another set of binary variables is assumed designating if a node belongs to the isolated area or not. Adding this auxiliary set of binary variables increases the complexity of the problem. Another drawback of [22, 23] is that the load rejection possibility is not considered for an energized node. In other words, if a bus is decided to be energized, its load will be automatically energized as well.

The load rejection possibility is considered in [51], assigning a binary variable to each bus indicating if its load is left connected or it must be disconnected from the bus. However, the authors propose to re-energize all the nodes in the off-outage area in any case independently from the load energization status. This assumption leads to increase the number of required switching operations (i.e. load breaker switching). In order to clarify this weakness, consider the fault shown in the system of Fig. 2-1, as an example. Assume that *Feeder-b* has a certain spare capacity that is enough to restore only the loads on buses 5, 6, and 7. With the assumption made in [51], restoring these loads needs five switching operations, namely disconnecting the loads on buses 4, 8, 9, and 10 first and closing T4 afterwards. However, in practice, for restoring the load on buses 5, 6, and 7 it is enough to open the sectionalizing switch on line 4-5 and then to close T4, without the need to energize all the buses. Therefore, in the modeling of the restoration problem it is mandatory to consider the cases with isolated areas. The isolated areas are identified in the proposed formulation using only the decision that is made concerning the energization status of line switches, without further needs of additional binary variables as in [22, 23]. In addition, for an energized bus in the presented approach, there will be an option to reject its load or to keep it connected, adding more flexibility to the restoration strategy.

The other technical aspects that must be considered in the restoration problem are listed below:

- Operational constraints (e.g., voltage and current limits) regarding the new configuration of the network. According to ANSI standard, the technical limits in the restorative state (as an emergency state) are slightly relaxed with respect to those in normal state [52].

- The radial topology of the network.

- Variation in consumption and generation values during the restorative period. This concern is tackled in this paper, using a multi-period optimization for the restoration problem.

- The optimal tap position of voltage regulation transformers (OLTCs and SVRs) and CBs regarding the new configuration of the network. This optimal setting is identified in this study without increasing significantly the complexity of the optimization problem.

- Accurate load modeling. In order to find the optimal set point of the voltage regulations devices in the reconfigured network, it is necessary to model the voltage dependency of load consumptions.

2.5 Formulation of the restoration problem in passive distribution networks

In this section, it is aimed to provide a mixed-integer convex optimization model for the restoration problem while accounting for the operational limits using the full constraints of an AC-OPF problem. The number of discrete decision variables has the most weight in the computation burden of mixed-integer optimization problems. In the proposed model for the restoration problem (without incorporating optimal voltage regulation), the binary-or-integer decision variables are limited to I) the load rejection status at each node in the off-outage area, and II) the energization status of available tie-switches, internal tie-switches, and internal sectionalizing switches. The foundation of the optimization problem is formulated as follows:

Minimize:
$$F^{obj} = w_{re}.F^{re} + w_{sw}.F^{sw} + w_{op}.F^{op} \tag{2.1}$$

$$F^{re} = \sum_{t}\sum_{i \in N} D_i.P_{i,t}^{cur} \tag{2.2}$$

$$F^{sw} = \sum_{(i,j) \in W_{ava}^S \cup W_{int}^S} Y_{ij}.\lambda_{ij} + \sum_{(i,j) \in W_{sec}^S} S_{ij}.\lambda_{ij} + \sum_{i \in N^*} B_i.\lambda_i \tag{2.3}$$

$$F^{Op} = \sum_{t} \sum_{(i,j)\in W} F^*_{ij,t} \tag{2.4}$$

Subject to:

$$0 \le Z_{ij} \le 1 \qquad\qquad \forall(i,j) \in W^S \tag{2.5}$$

$$Z_{ij} = Y_{ij} \;\;,\;\; Z_{ji} = 0 \qquad\qquad \forall(i,j) \in W^S_{ava} \tag{2.6}$$

$$Z_{ij} + Z_{ji} = Y_{ij} \qquad\qquad \forall(i,j) \in W^S \tag{2.7}$$

$$\sum_{i\in N^*}\left(A_{i,p}.\sum_{j:(i,j)\in W^*} Z_{ji}\right) = E_p \le 1 \qquad\qquad \forall p \in Z^* \tag{2.8}$$

$$0 \le Y_{ij} \le M.F_{ij,t} \qquad\qquad \forall(i,j) \in W^S, \forall t \tag{2.9}$$

$$\begin{cases} X_i = \displaystyle\sum_{p\in Z^*}\left(A_{i,p}.E_p\right), & i \in N^* \\ X_i = 1, & i \in N\backslash N^* \end{cases} \tag{2.10}$$

$$\begin{cases} L_i \le X_i, & i \in N^* \\ L_i = 1, & i \in N\backslash N^* \end{cases} \tag{2.11}$$

$$X_{ij} = \begin{cases} \displaystyle\sum_{p\in Z^*}\left(A_{ij,p}.E_p\right), & (i,j) \in W^*\backslash W^S \\ Y_{ij}, & (i,j) \in W^S \\ 1, & (i,j) \in W\backslash W^* \end{cases} \tag{2.12}$$

Switching operation constraints $\qquad\qquad$ (2.13)

OPF constraints $\qquad\qquad$ (2.14)

The objective function given in (2.1) consists of reliability (F^{re}), switching (F^{sw}), and operational (F^{op}) terms, in decreasing order of priority. It should be noted that the way different objective terms are illustrated in (2.1) is just for the sake of presentation. In practice, the aforementioned hierarchical priority among those three objective terms is enabled according to the $\epsilon-constraint$ method [53]. The reliability objective term expressed in (2.2) tends to minimize the total active and reactive curtailed loads, while accounting for their importance factors. The constraints related to these curtailed powers are formulated in section 2.5.2. The second objective term (2.3) corresponds to the switching criteria. It includes three sub-terms associated, respectively, to the operation of available and internal tie-switches, sectionalizing switches, and load breakers at each node in the off-outage area. With coefficient λ_{ij} in (2.3), remotely controlled switches are prioritized for being operated over manually controlled ones.

The operation of all these switches and breakers are determined using the constraints given in section 2.5.1. The operational objective term is formulated in (2.4) as the total deviation of squared magnitude of current flows beyond a certain threshold. This squared current flow deviation ($F_{ij,t}^*$) is formulated in the form of the following constraints [54].

$$F_{ij,t}^* \geq 0 \qquad\qquad \forall(i,j) \in W, \forall t \qquad (2.15)$$

$$F_{ij,t}^* \geq F_{ij,t} - \left(f_{ij}^{thr}\right)^2 \qquad\qquad \forall(i,j) \in W, \forall t \qquad (2.16)$$

All the weighting factors are applied on the normalized terms of expressions defined in (2.2)-(2.4). In order to make the reliability and switching terms in the same scales (per unit), they are divided by their maximum possible values. The importance factors of loads and switches are taken into account to determine these maximum values.

Constraints (2.5)-(2.9) model the network reconfiguration ensuring the radial topology of the network [55]. A binary decision variable Y_{ij} [1]is associated with each line in the off-outage area that is equipped with a switch indicating if it is energized or not. To each of these switched lines, is also assigned two continuous variables Z_{ij} and Z_{ji} indicating the orientation of the line with respect to the virtual source nodes. These nodes refer to the nodes outside the off-outage area that are connected to the available tie-switches (e.g. nodes 14 and 15 in Fig. 2-2). The presented constraints seem identical to those introduced in [26], which were already benchmarked on standard IEEE test systems. However, the formulation presented here accounts for the possible isolated areas in partial restoration scenarios. Based on a general example network, an empirical discussion is provided in the following to show that the proposed constraint set ensures a radial configuration accounting for partial restoration solutions.

Claim 1: in the feasible solution space, Z variables must take only binary values, and, $Y_{ij} = 1$ shows that line ij is an edge of a connected spanning tree.

Discussion: Let $W^y = \{(i,j) \in W^S | Y_{ij} = 1\}$ is the set of energized switched lines corresponding to a specific solution for $\boldsymbol{Y}$, according to (2.5)-(2.9). Consider the system shown in Fig. 2-2. In this network, bus 0 is assumed a virtual source node. If line $(0,1)$ belongs to W^y, then $Z_{0-1} = 1$ according to (2.6). It means that we have one entering flow to zone[2] p_1 hosting

---

[1] In this thesis, the indices of Y and Z are used exclusively for reconfiguration variables and should not be interpreted as grid impedances and admittances.

[2] In this chapter, a zone is referring to each segment of the feeder that is surrounded by two or more sectionalizing switches (Fig. 2-2).

node 1. Thus, by (2.8), there should not be any other entering flow[3] to zone p_1. Therefore, if line (n, m) is a switched line and node n is inside zone p_1, then Z_{mn} must be zero. It means that if line $(n, m \in W^y$, then $Z_{n-m} = 1$. This is formulated in (2.7) . In other words, zone p_2 that is hosting node m is not feeding zone p_1 but is supplied from zone p_1. The same analysis made for zone p_1 can be applied for zone p_2 and other zones in the paths originating from bus 0. From such a recursive analysis it can be concluded that each line through W^y is oriented such that its Z variable toward the source node is 0, and the one outgoing from the source node is 1. Therefore, all the branches of W^y that are in a path connected to bus 0 takes the form of a connected tree without forming any loop. If one part of the network does not contain any path connected to a source node, it means that its buses are not receiving any supply. Consequently, the current flow variables must be 0 ($F_{ij,t} = 0$). This enforces Y_{ij} variables for the lines in such an isolated area to be 0, according to (2.9), M being a large multiplier. We conclude that W^y is composed of spanning trees, each originated from one source node. Thus, the set of variables Y results in a radial configuration of the network with the possibility of having isolated areas in the network.

According to (2.10), a node in the off-outage area is energized ($X_i = 1$) if it is inside an energized zone ($E_p = 1$). For such an energized node in the off-outage area, a decision is made in (2.11) with binary variable L_i, indicating if its load will be restored or rejected (1/0). Outside the off-outage area, all the nodes are kept energized ($X_i = 1$) and all the loads are kept connected ($L_i = 1$) all the time. According to (2.12) in the off-outage area, energized switched lines are identified directly with variable Y, while the other lines will be energized if their hosting zones are energized. Outside the off-outage area, all the lines (equipped with switches or not) are kept energized ($X_{ij} = 1$).
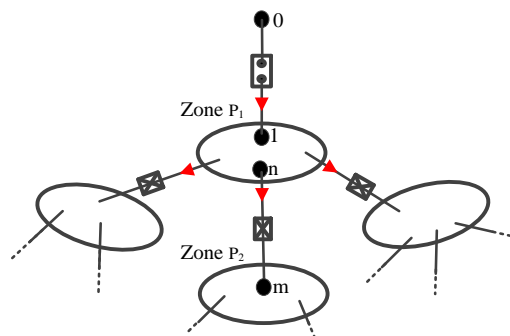
Fig. 2-2. Switched line orientation in the reconfigured network.

[3] It is meant directional flow with regard to the graph theory

2.5.1 Switching operation constraints

As expressed in (2.4) normally open switches including available and internal tie-switches are operated when they are energized ($Y_{ij} = 1$). However, for sectionalizing switches, energization status does not necessarily imply that they should be operated or not. For example, in case of a partial restoration scenario, sectionalizing switches that are entirely in the isolated part are de-energized, but do not need to be opened. As formulated in (2.13.a), the sectionalizing switch on line ij must be operated (opened) only if it is de-energized ($Y_{ij} = 0$) and at least one of its ending buses are energized ($X_i = 1$ or $X_j = 1$). According to (2.13.a), S_{ij} for other sectionalizing switches can get a value between 0 and 1. However, since minimization of S_{ij} is included in the objective function, S_{ij} for these switches will be zero, meaning that they should not be opened. As given in (2.13.b), the load breaker at each MV/LV substation node should be operated only if the node is energized ($X_i = 1$) and the load is to be rejected ($L_i = 0$). Otherwise, the breaker will not be operated ($B_i = 0$) according to the problem solution, since its value is to be minimized as a term in the objective function (2.4).

$$\begin{cases} \left(1 - Y_{ij}\right) + X_i - 1 \leq S_{ij} \leq 1 \\ \left(1 - Y_{ij}\right) + X_j - 1 \leq S_{ij} \leq 1 \\ 0 \leq S_{ij} \end{cases} \qquad \forall (i,j) \in W_{sec}^S \quad (2.13.a)$$

$$\left(1 - L_i\right) + X_i - 1 \leq B_i \leq 1 \qquad \forall i \in N^* \quad (2.13.b)$$

2.5.2 Relaxed AC-OPF constraints

In the following, a relaxed formulation of the AC-OPF problem is presented, incorporating the derived model of the restoration problem. The aim is to ensure that all the security constraints are respected in the reconfigured network.

$$0 \leq P_{i,t}^D - P_{i,t}^{cur} \leq M.L_i$$
$$\qquad \qquad \qquad \qquad \forall i \in N, \forall t \qquad (2.14.a)$$
$$0 \leq Q_{i,t}^D - Q_{i,t}^{cur} \leq M.L_i$$

$$0 \leq P_{i,t}^{cur} \leq M.(1 - L_i)$$
$$\qquad \qquad \qquad \qquad \forall i \in N, \forall t$$
$$\qquad \qquad \qquad \qquad \qquad \qquad \qquad (2.14.b)$$
$$0 \leq Q_{i,t}^{cur} \leq M.(1 - L_i)$$

$$0 \leq F_{ij,t} \leq X_{ij}.f_{ij}^{max2} \qquad \forall (i,j) \in W, \forall t \qquad (2.14.c)$$

$$-M.X_{ij} \le p_{ij,t} \le M.X_{ij}$$
$$-M.X_{ij} \le q_{ij,t} \le M.X_{ij}$$
$$\forall (i,j) \in W, \forall t \quad (2.14.\text{d})$$

$$v_i^{min^2}.X_i \le V_{i,t} \le v^{max^2}.X_i \qquad \forall i \in N, \forall t \quad (2.14.\text{e})$$

$$-M.\left(1 - X_{ij}\right) \le V_{i,t} - V_{j,t} - 2\left(r_{ij}.p_{ij,t} + x_{ij}.q_{ij,t}\right) \le M.\left(1 - X_{ij}\right)$$
$$\forall (i,j) \in W, \forall t \quad (2.14.\text{f})$$

$$p_{ij,t} = \Big(\sum_{\substack{i^* \ne i \\ (i^*,j) \in W}} p_{ji^*,t} \Big) + r_{ij}.F_{ij,t} + P_{j,t}^D - P_{j,t}^{cur} - P_{j,t}^{Sub} \qquad \forall t, (i,j) \in W \quad (2.14.\text{g})$$

$$q_{ij,t} = \Big(\sum_{\substack{i^* \ne i \\ (i^*,j) \in W}} q_{ji^*,t} \Big) + x_{ij}.F_{ij,t} + Q_{j,t}^D - Q_{j,t}^{cur} - Q_{j,t}^{Sub} \qquad \forall t, (i,j) \in W \quad (2.14.\text{h})$$

$$\left\| \begin{matrix} 2p_{ij,t} \\ 2q_{ij,t} \\ F_{ij,t} - V_{i,t} \end{matrix} \right\|_2 \le F_{ij,t} + V_{i,t} \qquad \forall (i,j) \in W, \forall t \quad (2.14.\text{i})$$

The discrete switching variables (L_i, X_i, X_{ij}) are linked to the corresponding continuous variables of the OPF problem using constraints (2.14.a)-(2.14.f), where M is a large multiplier. Constraints (2.14.a) and (2.14.b) enforce active/reactive load curtailment variables $(P_{i,t,s}^{cur}/Q_{i,t,s}^{cur})$ being equal to the active/reactive load powers for de-energized loads ($L_i = 0$) and zero for energized ones ($L_i = 1$). Constraints (2.14.c) and (2.14.d) enforce, respectively, current and active/reactive power flows to be zero for each de-energized line. The squared voltage magnitude is set to zero, in (2.14.e), for de-energized nodes ($X_i = 0$), and kept within the feasible region for energized nodes ($X_i = 1$). The nodal voltage constraint in [26] is revised in (2.14.f) to exclude unrestored lines. Constraints (2.14.g) and (2.14.h), respectively, concern with the active-/reactive power balances at the end buses of each line, taking into account the active/reactive load curtailments. Constraint (2.14.i) is the relaxed version of the current flow equation in each line as proposed in [26].

2.6 Restoration problem incorporating voltage regulation

In most of practical situations, the amount of loads that can be restored is limited in order to mainly respect the under-voltage limit. In the obtained restoration results reported in section 2.7, it is illustrated that the margin of the voltage magnitude with respect to the under voltage limit

is very small. This shows that regarding the electrical constraints, usually, the under voltage limit is the most challenging constraint for the restoration problem. In distribution networks, different types of voltage regulation devices could be installed in order to improve the local voltage profiles in the network. Therefore, it may be possible to increase the quality of the restoration problem if the setting of these voltage regulation devices is optimally determined. In this section, it is aimed to formulate the problem of finding these optimal set points and integrate this formulation into to the developed formulation of the restoration problem.

Three types of voltage regulation devices in distribution networks are studied in this work, namely OLTCs at the HV/MV substation nodes (Ω_{Sub}), SVRs on certain branches (Ω_{SVR}), and CBs at some nodes at some nodes (Ω_{CB}). In this section, a linear modeling is proposed for these devices considering a limited number of discrete decision variables. The aim is to find their optimal set points regarding the voltage control objectives while minimizing the number of required tap changes for the restorative period. It is assumed that the tap setting of each voltage regulator remains unchanged for the whole restorative period.

To account for the voltage regulation models described in the subsequent sections, the original mathematical formulation presented in the previous one (from (2.1) to (2.14)) will be modified and extended according to the following considerations:

- The set W is supposed to include the sets Ω_{Sub} and Ω_{SVR}. Consequently (2.14.f) is valid only for W\Ω_{SVR}.
- (2.4) will be gradually extended to account for the setting changes of OLTCs (2.19), then SVRs (2.22) and finally CBs (2.31).
- (2.14h) will be extended as (2.30) to account for the reactive power injections from CBs.
- Each type of regulation devices will be characterized by specific constraints to be added to the original mathematical formulation.

2.6.1 On-Load Tap Changing Transformers (OLTCs)[4]

The voltage at the HV side of OLTC is assumed to be constant (1 p.u.), while the voltage at the MV side is regarded as the slack voltage in the OPF constraints formulated in section 2.5.2. The OLTC transformer ratio changes a little between two consecutive tap positions (e.g., $\sigma = 0.625\%$ as reported in [51]). Therefore, in order to relax the problem complexity, we represent

---

[4] OLTC and SVR are modeled as ideal transformers in series with virtual lines representing their impedances.

the step-wise values of tap ratio $\sigma.\Delta r$ ($\Delta r \in \{-n, \dots, -1, 0, 1, \dots, n\}$) with a continuous variable $\alpha \in [-n.\sigma, n.\sigma]$. Finally, the optimal value obtained for α will be rounded to the closest $\sigma.\Delta r$ value in the original discrete set. With this assumption, the constraints related to each OLTC installed at a HV/MV substation are formulated as follows:

$$V_{i,t} = 1.(1 + \alpha_i)^2 \approx 1 + 2\alpha_i \qquad\qquad \forall i \in \Omega_{Sub}, \forall t \quad (2.17)$$

$$-n_i.\sigma_i \leq \alpha_i \leq n_i.\sigma_i \qquad\qquad \forall i \in \Omega_{Sub} \quad (2.18)$$

$$F^{Op} = w_1.\sum_{t}\sum_{(i,j)\in W} F^*_{ij,t} + w_2.\sum_{i\in\Omega_{Sub}} T_i \qquad\qquad (2.19)$$

$$\begin{cases} T_i \geq \dfrac{\alpha_i - \alpha 0_i}{\sigma_i} \\[2mm] T_i \geq -\dfrac{\alpha_i - \alpha 0_i}{\sigma_i} \\[2mm] T_i \geq 0 \end{cases} \qquad\qquad \forall i \in \Omega_{Sub} \quad (2.20)$$

Regarding the small positive values of α_i, squared voltage relationship in (2.17) is linearized using binomial approximation. It is aimed for each OLTC to minimize the change of its tap position with respect to the tap position prior the fault occurrence ($\alpha 0_i$). In this regard, the operational objective term (F^{Op}) under (2.4) is replaced by (2.19). In (2.19), w_1 and w_2 represent the relative importance of two sub-terms of the operational objective term. These coefficients are determined depending on the operational policies of DSO during the restorative period. The tap position will be changed only if the deviation of relaxed transformer ratio (α_i) from the initial one ($\alpha 0_i$) is higher than the ratio step size (σ_i). This condition is linearized in (2.20) defining a set of auxiliary continuous variables (T_i) showing quantitatively the extent of tap change.

2.6.2 Step Voltage Regulator (SVR)

Fig. 2-3(b) shows the equivalent model of the SVR shown in Fig. 2-3(a), where, $Z_{p,ij} = r_{p,ij} + jx_{p,ij}$ and $Z_{s,ij} = r_{s,ij} + jx_{s,ij}$ denote the impedances at the primary and secondary sides, respectively. $S_{i'j'}$ is the apparent power flowing from the auxiliary node i' to the auxiliary node j'. Similar to OLTCs, the granularity of tap positions in SVRs allows using the binomial approximation. However, since the voltage at the starting node cannot be assumed 1 p.u. as for OLTCS, tap ratio setting cannot be represented by continuous variables. In this regard, the squared voltage relationship is approximated as the following.

$$V_{j',t} = V_{i',t}.\left(1 + \sigma_{ij}.\Delta r_{ij}\right)^2 \approx V_{i',t}.\left(1 + 2\sigma_{ij}.\Delta r_{ij}\right) = V_{i',t} + 2\sigma_{ij}.\beta_{ij,t}$$

Considering the equivalent model shown in Fig. 2-3(c), the nodal voltage equation (2.14.f) and the operational objective function (F^{Op}) are modified and extended as follow.

$$-M.\left(1 - X_{ij}\right) \leq V_{i,t} - V_{j,t} + 2\sigma_{ij}.\beta_{ij,t} - 2\left((r_{p,ij} + r_{s,ij}).p_{ij,t} + (x_{p,ij} + x_{s,ij}).q_{ij,t}\right)$$

$$\leq M.\left(1 - X_{ij}\right) \qquad \forall(i,j) \in \Omega_{SVR}, \forall t \quad (2.21)$$

$$F^{Op} = w_1.\sum_t \sum_{(i,j)\in W} F_{ij,t}^* + w_2.\left(\sum_{i\in\Omega_{Sub}} T_i + \sum_{ij\in\Omega_{SVR}} T_{ij}\right) \qquad (2.22)$$

$$\begin{cases} T_{ij} \geq \Delta r_{ij} - \Delta r0_{ij} \\ T_{ij} \geq \Delta r0_{ij} - \Delta r_{ij} \\ T_{ij} \geq 0 \end{cases} \qquad \forall(i,j) \in \Omega_{SVR} \quad (2.23)$$

An auxiliary set of continuous variables ($\beta_{ij,t}$) is introduced to linearize the product of $\Delta r_{ij}.V_{i,t}$. For this aim, the integer variable $\Delta r \in \{-n, n\}$ is represented by 2n+1 binary variables denoted by δr_k, as given in (2.24) and (2.25). The indices i, j and t are omitted for sake of clarity. Constraint (2.26) enforces continuous variables b_k to take the value of $\delta r_k.V$, M being a large multiplier. Accordingly, the value of $\Delta r.V$ denoted by β is retrieved from weighted summation of b_k variables (2.27).
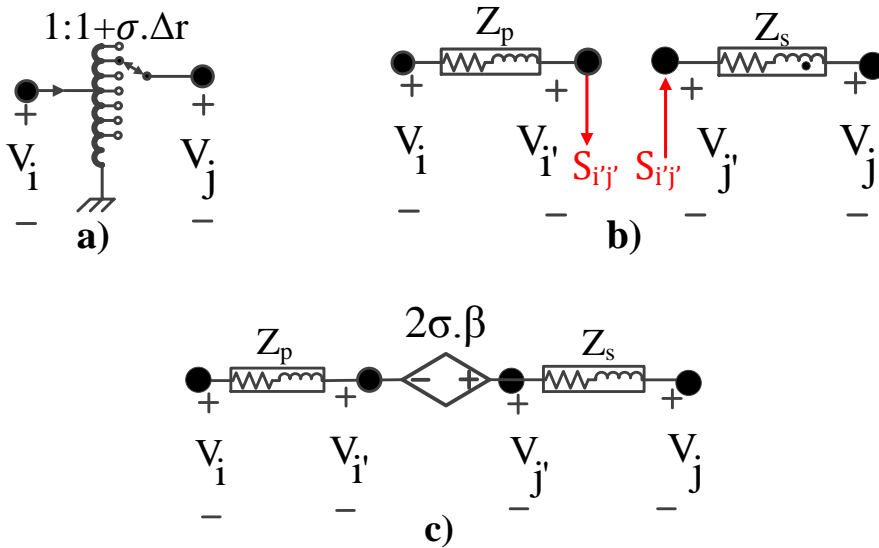
Fig. 2-3. Modeling of SVR in the restoration problem. a) SVR schematic b) standard equivalent model c) linearized equivalent model.

$$\Delta r = \sum_k k . \delta r_k \quad : \quad k \in \{-n, \ldots, -1, 1, \ldots, n\} \tag{2.24}$$

$$\sum_k \delta r_k = \delta r_0 \quad : \quad k \in \{-n, \ldots, -1, 1, \ldots, n\} \tag{2.25}$$

$$\begin{cases} b_k \leq M . \delta r_k \\ b_k \leq V \\ b_k \geq V - M . (1 - \delta r_k) \\ b_k \geq 0 \end{cases} \qquad \forall k^{`} \in \{-n, \ldots, -1, 1, \ldots, n\} \tag{2.26}$$

$$\beta = \sum_k k . b_k \quad : \quad k \in \{-n, \ldots, -1, 1, \ldots, n\} \tag{2.27}$$

Adding binary variables (δr_k) does not increase the computation cost too much, since the above-mentioned constraints are in the form of the Special Ordered Set-1 (SOS1) constraints [56]. With these types of constraints, the number of nodes to be searched in the underlying branch and bound process will be reduced significantly. Finally, the model shown in Fig. 2-3(c) will be the linearized model of each SVR that can be incorporated into the OPF constraints presented in section 2.5.2. As for the OLTC, it is aimed also for the SVR to minimize the change of its tap position with respect to the tap position prior the fault occurrence ($\Delta r0_{ij}$). In this regard, the operation objective term F^{op} under (2.19) is extended according to (2.22). In this model, the tap changing amount will be obtained according to (2.23), in the same way as formulated for the OLTC.

2.6.3 Capacitor Banks (CB)

Regarding the CBs, the amount of reactive power change at each step (ΔQ_i) is not small. Therefore, unlike OLTCs and SVRs, the step changes of CBs should be modeled with integer variable Δr_i. Therefore, the model of CBs participating in the restoration process can be expressed as given in (2.28)-(2.32).

$$Q_{i,t}^{inj} = \Delta Q_i . \Delta r_i \qquad\qquad \forall i \in \Omega_{CB}, \forall t \tag{2.28}$$

$$\Delta r_i \in \{0, 1, 2, \ldots, n_i\} \qquad\qquad \forall i \in \Omega_{CB} \tag{2.29}$$

$$q_{ij,t} = \left(\sum_{\substack{i^* \neq i \\ (i^*, j) \in W}} q_{ji^*,t} \right) + x_{ij} . F_{ij,t} + Q_{j,t}^{D} - Q_{j,t}^{cur} - Q_{j,t}^{Sub} - (Q_{j,t}^{inj} : j \in \Omega_{CB}) \tag{2.30}$$

$$F^{Op} = w_1 . \sum_t \sum_{(i,j)\in W} F^*_{ij,t} + w_2 . \left(\sum_{i\in\Omega_{Sub}\cup\Omega_{CB}} T_i + \sum_{ij\in\Omega_{SVR}} T_{ij} \right) \tag{2.31}$$

$$\begin{cases} T_i \geq \Delta r_i - \Delta r0_i \\ T_i \geq \Delta r0_i - \Delta r_i \\ \quad T_i \geq 0 \end{cases} \qquad \forall i \in \Omega_{CB} \tag{2.32}$$

Since CBs inject reactive power to the network, the reactive power balance of the OPF formulation, given already in (2.14.h), should be modified according to (2.30). Likewise OLTCs and SVRs, the operational objective term (F^{Op}) under (2.22) is further extended as in (2.31) in order to minimize the tap changing of CBs. This tap changing is modeled in (2.32) using the auxiliary set of continuous variables T_i.

2.6.4 Modeling load-voltage dependency

In order to find the optimal set point for the regulation devices during the restorative period, it is important to consider the voltage dependency of load consumption. In this paper, the models shown in the following are used in order to express the voltage dependency of active and reactive load powers, respectively.

$$P^D_{i,t} = P^0_{i,t} \left(\frac{v_{i,t}}{v_0} \right)^{kp_i}$$

$$Q^D_{i,t} = Q^0_{i,t} \left(\frac{v_{i,t}}{v_0} \right)^{kq_i}$$

This model is linearized assuming that $v_0 = 1\ p.u.$ and $V_{i,t,s}$ is close to $1\ p.u.$, so that the binomial approximation can be applied according to the followings.

$$P^D_{i,t} = P^0_{i,t} \left(1 + (V_{i,t} - 1) \right)^{kp_i/2} \approx P^0_{i,t} \left(1 + \frac{kp_i}{2} (V_{i,t} - 1) \right) \qquad \forall i \in N, \forall t \tag{2.33}$$

$$Q^D_{i,t} = Q^0_{i,t} \left(1 + (V_{i,t} - 1) \right)^{kq_i/2} \approx Q^0_{i,t,s} \left(1 + \frac{kq_i}{2} (V_{i,t} - 1) \right) \qquad \forall i \in N, \forall t, s \tag{2.34}$$

To summarize, the overall developed restoration problem is in the form of a MISOCP optimization problem. It is structured as follows:

$$\text{Minimize:} \quad F^{obj} = w_{re} . F^{re} + w_{sw} . F^{sw} + w_{op} . F^{op}$$

$$\text{with:} \quad (2.2), (2.3), (2.31)$$

subject to:

Network reconfiguration constraints:	(2.5)-(2.12)
Switching operation constraints:	(2.13.a), (2.13.b)
Relaxed AC-OPF constraints:	(2.14.a)-(2.14.i)
Current deviation constraints:	(2.15), (2.16)
OLTC constraints:	(2.17)-(2.20)
SVR constraints:	(2.21)-(2.27)
CB constraints:	(2.28)-(2.32)
Load-voltage dependency constraints:	(2.33), (2.34)

2.7 Numerical analysis

The proposed optimization model of the restoration problem is tested on a 11.4 kV distribution network shown in Fig. 2-4. This test system is based on a practical distribution network in Taiwan with 2 substations, 4 feeders, 83 nodes, and 96 branches (incl. tie-branches) [57]. The detailed nodal and branch data is given in [57]. The base power and energy are chosen as 1 MVA and 1 MWh, respectively. The network is updated adding two OLTCs at the both substations, one SVR on line 52-53, and one CB at bus 80. The set points of these devices are determined by DSO a day ahead, which might be subject to further tuning for the restoration strategy. The current threshold for each line (f_{ij}^{thr} in (2.4)) is assumed to be 50% of its current capacity limit. According to ANSI C84.1 standard, the minimum and maximum voltage magnitude limits for the restorative period are set, respectively, to 0.917 and 1.050 p.u. [52].
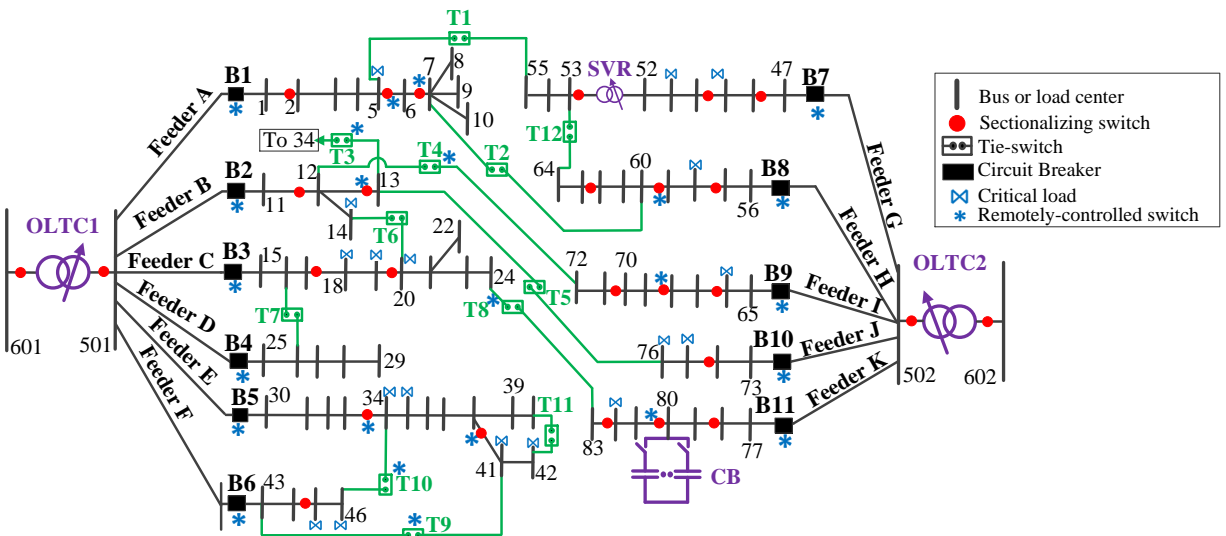
Fig. 2-4. Test distribution network in normal state configuration [58].
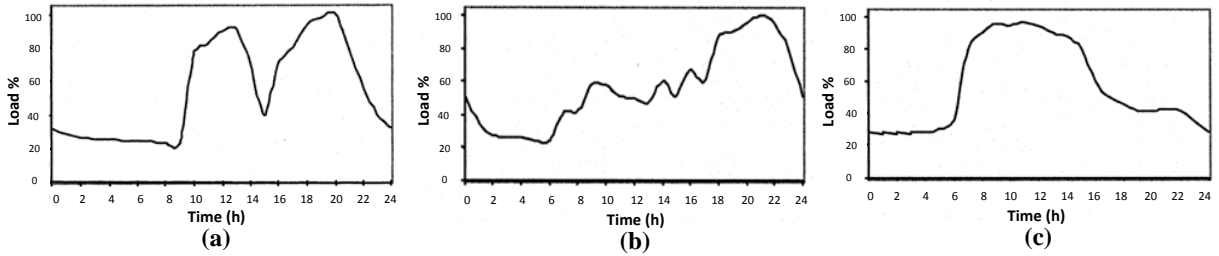
Fig. 2-5. The hourly profile of residential, commercial, and industrial loads according to the original data reported in [58].

The majority of nodes along feeders A, B and E in Fig. 2-4 are assigned, respectively, to rural, light and high industrial load types. Most of the nodes in feeders C, F, H, J have load characteristics close to residential loads and most of the nodes along feeders D, G, I, and K supply commercial loads. There is also 10-30% of public light loads considered at each node. The hourly profile for each of these load patterns are shown in Fig. 2-5 according to the original data reported in [58]. The switches shown with '*' in Fig. 2-4 are remotely controlled. All the load breakers are assumed to be manually-controlled. It is assumed that the average time needed for the operation of each remotely- and manually-controlled switch is 0.8 and 22.5 minutes, respectively [59]. The loads shown with '⋈' in Fig. 2-4 are critical loads. The priority factors of these critical loads are assumed to be 10 while the one of the other loads are assumed to be 1. The coefficients $w_{re}, w_{sw}, w_{op}, w_1,$ and w_2 are the weighting factors in the formulation of the objective function in 2.5, which are tuned, respectively, to 100, 10, 1, 0.5, and 0.5, according to the criteria explained in section 2.5. The algorithm is implemented on a PC with an Intel(R) Xeon(R) CPU and 6 GB RAM; and solved in Matlab/Yalmip environment, using Gurobi solver. This commercial solver uses Branch-and-Bound method handling mixed-integer convex optimization problems. It terminates when the gap between the lower and upper bounds is either less than 1e-10 (absolute gap limit) or less than 1e-4 (relative gap limit) times the absolute value of the upper bound. Therefore, it can be said that the global optimality of the solution is up to a good accuracy certified. The proposed restoration strategy is applied on the test system shown in Fig. 2-4 according to different case studies. Through these scenarios, voltage regulation devices are incorporated independently one by one into the optimization problem in order to evaluate the effect of each on the quality of the restoration solution. The optimal solution of the restoration strategy in each case study is reported in Table 2-1 and Table 2-2. In all the cases, the

Table 2-1. Optimal restoration results in case of fault scenarios 1-4.

Scenario	Fault location	Sequence of switching	F^{re}(p.u.)	t^{sw} (min.)	Optimal tap settings	Computation time (s)
1	Line 1-2	- Open switches 5-6 and 6-7 - Close T1 and T2	13.17	46.6	-	2.84
2a	Line 1-2	- Open switch 6-7 - Open load breaker 2 - Close T1 and T2	1.35	68.3	$\dfrac{v_{502}}{v_{602}} = 1.025$	2.89
2b	Line 1-2	- Open switch 6-7 - Open load breaker 3 - Close T1 and T2	3.61	68.3	$\dfrac{v_{502}}{v_{602}} = 1.019$	3.30
3	Line 1-2	- Open switch 6-7 - Close T1 and T2	0	45.8	$\dfrac{v_{502}}{v_{602}} = 1.019$ $\dfrac{v_{53}}{v_{52}} = 1.0125$	7.18
4a	Line 16-17	- Close T6	0	22.5	$\dfrac{v_{501}}{v_{601}} = 1.006$ $\dfrac{v_{502}}{v_{602}} = 1.006$	1.98
4b	Line 16-17	- Close T8	0	0.8	$\dfrac{v_{501}}{v_{601}} = 1.006$ $\dfrac{v_{502}}{v_{602}} = 1.025$ $Q_{80}^{inj} = 3.6\,p.u.$	0.90

restorative period is assumed from 10:00 A.M. to 8:00 P.M., during which most of the loads experience their peak values. The load voltage sensitivity coefficients ($K_p \ and \ K_q$ in (2.33) and (2.34)) are assumed the same for all the loads. The default values of K_p and K_q are equal to 0.6 and 0.3, respectively.

2.7.1 Scenario 1: a partial restoration scenario

Scenario 1 is defined where a fault occurs at bus 1 in the test network shown in Fig. 2-4. In this scenario, it is assumed that none of the voltage regulation devices are controllable, fixing their tap positions at zero. The fault will be isolated, opening the closest upstream and downstream sectionalizing switches to the fault place (B1 and switch on line 1-2, respectively). These operations are not considered as part of service restoration. The required switching operations for the obtained optimal restoration solution are displayed in Table 2-1.

As it can be noticed, while most of the off-outage area is resupplied through tie-switches T1 and T2, node 6 is left unrestored. This type of maneuver is missing in all the mathematical formulations proposed in the literature for the restoration problem. Actually, according to those

strategies, instead of opening the remotely-controlled switch on line 6-7, the load breaker at node 6 must be disconnected. This leads to increase uselessly the deployment time of the restoration strategy. It is also worth to mention that in this scenario, instead of load at node 6, loads at buses 3, 4 and 5 could have been rejected, decreasing the total F^{re} value from 13.22 p.u. to 11.19 p.u. However, regarding the higher priority factor of the load at node 5, it is preferred to be restored. In addition, instead of opening the switch on line 5-6, the load breaker at bus 6 could have been opened. However, operating the switch 5-6, which is remotely controlled helps to accelerate the restoration solution deployment. The value of F^{re} shown in Table 2-1 and Table 2-2 accounts for the resulting value of the reliability objective term formulated in (2.2) which is actually the ENS value weighted by the load priority factors. This ENS does not refer to the total energy that is not supplied during the entire outage time but only to the unsupplied energy during the restorative period. The effect of the second objective term formulated in (2.3) is shown in Table 2-1 and Table 2-2 in terms of t^{sw} which is the time that is taken to deploy the switching actions.

2.7.2   Scenario 2: effects of OLTC optimal tap setting

In scenario 2a, the restoration strategy in case of the fault on line 1-2 is studied while incorporating the tap control of the OLTC in line 601-501. This OLTC enables $\pm 5\%$ voltage regulating range, in 8 steps ($\sigma = 0.625\%, n = 4$). The results of this scenario are shown in Table 2-1. With the optimal setting of OLTC-2, instead of isolating node 6 as in scenario 1, node 2 is rejected, decreasing the F^{re} value by one order of magnitude. The optimal voltage ratio of OLTC-2 in terms of the continuous variable $1 + \alpha_i$ in (2.17) is obtained 1.024. This value is corresponding to a tap position equal to +4 (the closest discrete value to $\frac{\alpha_i}{\sigma_i}$). As it can be seen, the computation time remains very small, thanks to the continuous representation of OLTC tap positions.

In order to see the effect of load voltage sensitivity coefficients (K_p and K_q in (2.33) and (2.34)), the scenario 2.b is studied without accounting for K_p and K_q. According to the results shown in Table 2-1, the optimal restoration strategy in scenario 2.b is to reject the load at bus 3 leading to a larger value of F^{re} compared to scenario 2a. As it can be seen, the optimal tap position of OLTC is changed from 4 in scenario 2.a to 3 (2.75 which is rounded to 3) in scenario 2.b. Comparing the results of these two scenarios highlights a trade-off between keeping the voltage profile at the feeder extremities (leaf nodes) above the minimum limit and limiting the increase of the load consumption level.

2.7.3 Scenario 3: effects of SVR optimal tap setting

In scenario 3, it is assumed that the fault occurs on line 1-2 and the SVR on line 52-53 is controllable besides the OLTC-2. This SVR enables $\pm 5\%$ voltage regulation range in 8 steps ($\sigma = 0.625\%, n = 4$). According to the results shown in Table 2-1, incorporating optimal tap setting of SVR in the restoration strategy helps to restore all the nodes. The optimal tap position of SVR is obtained as +2. As it can be seen, the computation time still remains reasonable.

2.7.4 Scenario 4: effects of CB optimal tap setting

In this part, the effects of incorporating optimal tap setting of CB in the restoration strategy is studied. First of all, scenario 4.a is considered, where the restoration problem in case of a fault on line 18-19 is studied under default test conditions. As reported in Table 2-1, the manually-controlled tie-switch T6 is closed to restore the whole off-outage area. The effect of optimal CB tap setting is illustrated in scenario 4b. In this scenario, the fault on line 18-19 is considered again while incorporating the CB at node 80, with 3.6 Mvar injection capacity in 6 steps. As it can be seen in Table 2-1, putting the tap of this CB on +6 enables to restore the whole off-outage area through the manually-controlled T8 decreasing the deployment time (t_{sw}) significantly. The detailed results of scenario 4b is reported in Table 2-1.

2.7.5 Scenario 5. Scale up the off-outage area

In order to show how the proposed algorithm would scale up, it is applied on the test network in case of a fault on substation 601 (see Fig. 2-4). In this case, feeders A, B, C, D, E, and F build the off-outage area which is connected to feeders F, H, I, J, and K through tie-switches T1, T2, T4, T5, and T8, respectively. Therefore, in this case study, the whole system with no reduction must be involved in the optimization problem. The results corresponding to the obtained optimal restoration solution are given in Table 2-1. As it can be seen, the computation time for this scenario is largely more than the previous scenarios. Considering a large number of binary decision variables associated with the status of all 46 load breakers, 16 sectionalizing switches and 10 tie-switches in the off-outage area is the main reason behind this larger computation time. However, even with such a huge outage area and with so many switches, the computation time is still reasonable (around 13 minutes). It means the proposed strategy can be applied in practice to find the optimal restoration solution in case of large-scale outages in distribution networks.

In order to show the case where voltage regulation devices are installed in the off-outage area, scenario 5b is studied. In this scenario, a fault occurs on substation 602. In this case, the whole

Table 2-2. Optimal restoration results in case of fault scenarios 5 and 6.

Scenario	Fault location	Sequence of switching	F^{re} (p.u.)	t^{sw} (min.)	Optimal tap settings	Computation time (s)
5a	Bus 601	- Open circuit breakers B1 and B5. - Open switches on lines 12-13, 17-18, and 44-45. - Open load breakers at nodes 6,7,28,29 and 31. - Close T1 , T3, T4, T5, T8, and T10.	60.34	208.1	$\frac{v_{502}}{v_{602}} = 1.019$ $\frac{v_{53}}{v_{52}} = 1.0125$ $Q_{80}^{inj} = 3.6\,p.u$	811.2
5b	Bus 602	- Open circuit breaker B10. - Open switch on line 52-53, 62-63, 70-71 and 80-81. - Open load breakers at nodes 54,62,63,66,68,71,78,79,80 and 83. - Close T1, T2, T4, T5, T8, and T12.	71.28	385.7	$\frac{v_{502}}{v_{602}} = 0.9750$ $\frac{v_{53}}{v_{52}} = 1.000$ $Q_{80}^{inj} = 3.6\,p.u$	610.2
6a	Bus 601	- Open circuit breakers B2, B4, and B5. - Open switches on lines 5-6, 6-7, 12-13, 17-18, 33-34, 38-41, 44-45. - Close T1,T2, T3, T4, T5, T6, T9, and T10.	73.35	144.6	$\frac{v_{502}}{v_{602}} = 1.025$ $\frac{v_{53}}{v_{52}} = 1.019$ $Q_{80}^{inj} = 0\,p.u$	102.3
6b	Bus 601	- Open circuit breakers B2, B4, and B5. - Open switches on lines 5-6, 6-7, 17-18, 19-20, and 44-45. - Close T1,T2, T5, and T8.	406.43	139.8	$\frac{v_{502}}{v_{602}} = 1.025$ $\frac{v_{53}}{v_{52}} = 1.019$ $Q_{80}^{inj} = 0\,p.u$	43.8

right part of the test network shown in Fig. 2-4 is within the off-outage area, including the installed voltage regulation devices. The optimal restoration solution is given in Table 2-2. Since all the hosting nodes and lines are energized, the voltage regulation devices in the off-outage area can be operated with the optimal settings reported in Table 2-2. This scenario shows that SVRs and CBs can help to improve the restoration solution even when they are in the off-outage area.
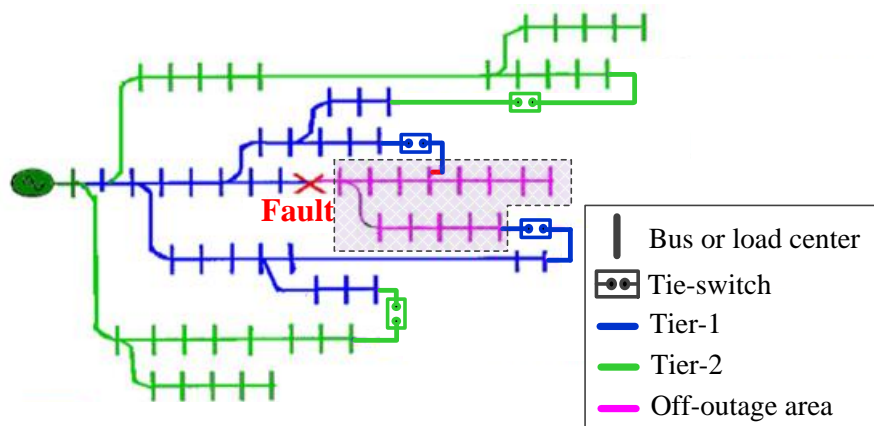
Fig. 2-6. A test distribution network illustrating the notion of Tier_1 and Tier_2 defined in [60].

2.7.6 Scenario 6. Comparing with a heuristic algorithm

In order to show the efficiency and superiority of the presented restoration methodology, it is compared with a heuristic algorithm proposed in [60] for the restoration. Since the operation of load breakers is not considered in [60] and in order to make a fair comparison, first, the proposed strategy is applied in case of a fault on bus 601 without considering load breakers. The optimal configuration obtained for this scenario is shown in Fig. 2-7, where the group of nodes supplied by each available tie-switch is illustrated with a specific color.

The detailed numerical results are reported in Table 2-2 under scenario 6a. As it is shown, the computation time is significantly reduced with respect to scenario 5, where load breakers were considered. In addition, it can be seen that the deployment time is reduced and the reliability objective term is increased. The solution obtained in scenario 6a could be chosen by operators who accept this trade-off to accelerate the process of finding and deploying the restoration solution at the cost of losing the efficiency of the solution to some extent.

In scenario 6b, the process presented in [60] is exactly followed for a fault occurred on the substation 601 of the test network shown in Fig. 2-4. All the test conditions are the same as the ones assumed for scenario 6a. The algorithm is implemented in Matlab, where MATPOWER toolbox is used for power flow simulations. In order to present the obtained result, we introduce in the following the notations that are defined in [60] (see Fig. 2-6).

- Switch pair: the pair of sectionalizing and tie switches that should be operated jointly to respect the radiality constraint.
- Tier_1: tie-switches, switch pairs and feeders that are incident to the off-outage area.

- Tier_2: tie-switches, switch pairs and feeders that are incident to Tier_1.

- …
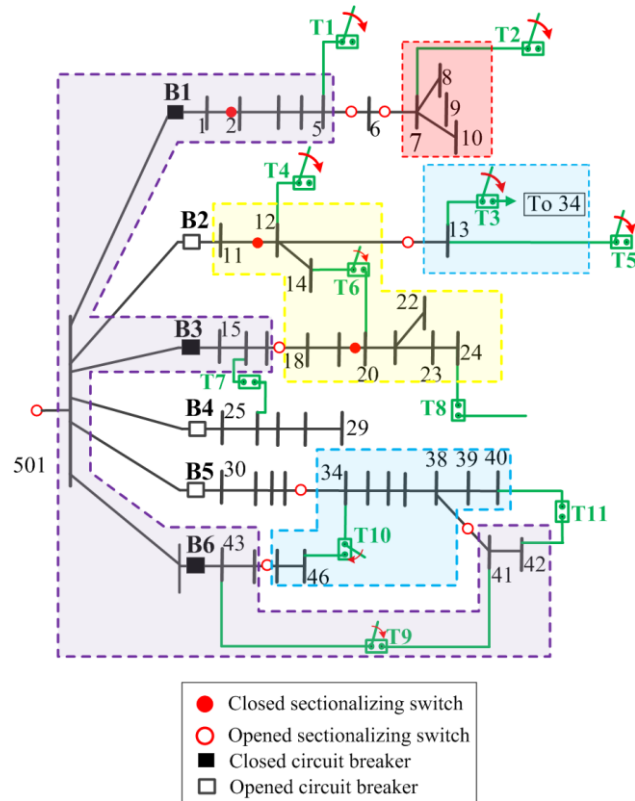
Fig. 2-7. The restoration strategy found using the proposed approach in scenario 6a.
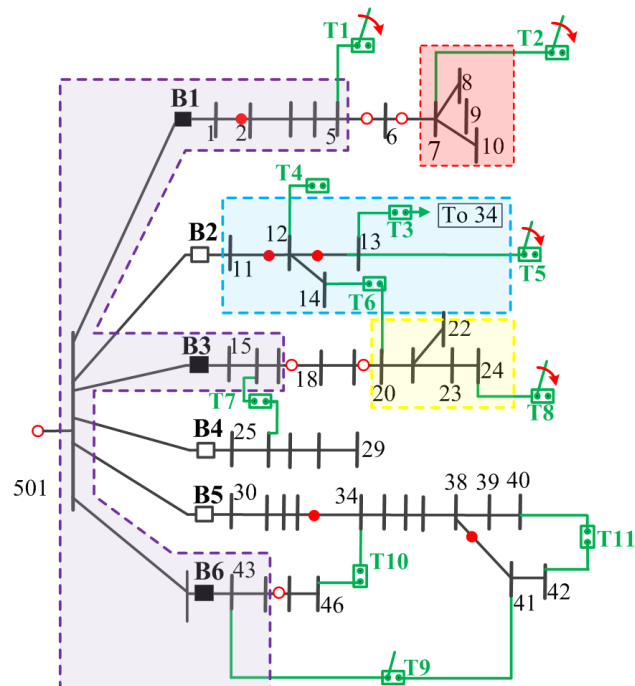
Fig. 2-8. The restoration strategy found using the heuristic approach proposed in [60] in scenario 6b.

- Tier_n: tie-switches, switch pairs and feeders that are incident to Tier_(n-1)

- I_M: spare capacity of a tie-switch. The spare capacity of a tie-switch T_i is defined as the minimum current margin over all the lines in the path from tie-switch T_i and the substation.

In the following, we provide the results obtained at each stage of the algorithm proposed in [60] under test scenario 6b.

- Stage1. The list of available tie-switches (referred to as Tier_1 tie-switches in [60]) in the ascending order according to their spare capacity (I_M) is $\{T2, T5, T4, T1, T8\}$.

- Stage2. Since no tie-switch with I_M larger than the total unsupplied loads exist, we select only the first tie-switch (T2) and proceed to step3.

- Step3: In this step, two procedures presented in [60] are followed to sequentially operate switch pairs. According to the first procedure, additional Tier_1 switch pairs are selected to restore the entire off-outage area. In this regard, 56 different configurations were tested. However, a feasible solution plan restoring the whole off-outage area has not been found. Therefore, we undergo the second procedure. This procedure aims at restoring indirectly the off-outage area by transferring loads from one Tier_1 feeder to an additional higher Tier feeder and therefore releasing its spare capacity. In this regard, 16 solutions were tested but no additional switching actions was found to be added.

- Step4: since we could not still find a feasible solution restoring the whole off-outage area, in this step, we try to find the best partial restoration solution restoring as much priority loads as possible. Following the procedure presented in [60], we open the combination of sectionalizing switches shedding the minimum amount of total load to relieve the voltage constraint violation. In this regard, the switches with only non-priority downstream loads are considered first. In this stage, we tested 14 more different possibilities and the following switching operations are found to be added:
  - Close T1 and open circuit breakers B4 and B5, and open switches 5-6, 17-18, and 44-45
  - Close T2 and open switch 6-7
  - Close T5 and open breaker B2
  - Close T8 and open switch 19-20

The obtained configuration is depicted in Fig. 2-8. The detailed results obtained with this heuristic strategy is given in Table 2-2 under scenario 6. The reliability objective values (F^{re})

Table 2-3. Checking technical constraints for restoration solutions in case of different fault scenarios.

Scenario	Fault location	Min. voltage (p.u.)	Min. current margin (p.u.)
1	Line 1-2	0.923 p.u. at node 2	3.81 p.u. on line 49
2a	Line 1-2	0.918 p.u. at node 2	1.97 p.u. on line 49
2b	Line 1-2	0.916 p.u. at node 2	2.08 p.u. on line 50
3	Line 1-2	0.919 p.u. at node 2	1.72 p.u. on line 77
4a	Line 16-17	0.925 p.u. at node 18	3.50 p.u. on line 12
4b	Line 16-17	0.922 p.u. at node 18	3.17 p.u. on line 78
5a	Bus 601	0.917 p.u. at node 30	2.33 p.u. on line 48
5b	Bus 602	0.917 p.u. at node 9	4.34 p.u. on line 11
6a	Bus 601	0.919 p.u. at node 40	1.03 p.u. on line 71
6b	Bus 601	0.930 p.u. at node 20	2.75 p.u. on line 47

obtained from the heuristic approach (scenario 6b) and the mathematical programming approach (scenario 6a), indicate that the restoration solution obtained from the heuristic algorithm is very far from the global optimal solution. It is because in the proposed mathematical formulation, all the possible combination of switching operations are considered implicitly and evaluated according to the technical constraints and objective terms. For this reason, the computation time of this heuristic restoration algorithm is less referring to the proposed MISOCP-based restoration strategy. However, the computation burden of algorithms proposed by heuristic methodologies will be higher when voltage regulation devices such as CBs, OLTCs, and SVRs are incorporated into the restoration problem.

In order to validate the technical feasibility (i.e. voltage and current limits) of the obtained solutions for each test scenario studied above, voltage and current profiles in the reduced network after applying each restoration solution are derived. The required power flow simulations are made using Matlab/MATPOWER toolbox. The selected representative information obtained out of these profiles is given in Table 2-3. This representative information includes the minimum nodal voltage magnitude and the minimum line current margin over, respectively, all the nodes and lines of the reduced network and over all the time steps of the restorative period. As it can be seen, the minimum voltage value and the current margin are all above the limits. Therefore, these results confirm the feasibility of the obtained solution for all the test scenarios. For the

normal operation of the network (before any fault occurrence), the minimum voltage magnitude and current margin over the entire network and throughout the whole considered day are 0.93 p.u. at node 9, and 2.08 p.u. in line 30, respectively.

2.8   Conclusion and summary

The first contribution of this chapter is developing a basis for the restoration problem formulation. This formulation will be used then in the next chapters for modeling specific aspects of the restoration problem in active distribution networks.

In this chapter, first, the restoration problem is defined according to the globally-approved fault management procedure in distribution networks. In this regard, different technical and practical considerations of the restoration problem are introduced. Section 2.5 is assigned to the mathematical formulation of the restoration problem in distribution networks. In this section, first, the general model of the restoration problem is developed. This general model includes a novel formulation of the reconfiguration problem. With respect to the existing ones in the literature, this novel formulation models the isolated areas of the network that are left without any supply. These isolated areas pertains to partial restoration scenarios where the free capacity of the network is not enough to restore the whole off-outage area. Following that, in subsection 2.5.2, a convex relaxation method for the OPF problem is applied into the proposed restoration problem ensuring that the electrical constraints will be all respected during the whole restorative period.

In Section 2.6, voltage control modeling is integrated into the restoration problem. The aim is to find, among other decision variables, the optimal setting of voltage regulation devices such that the voltage profile will be improved and therefore, more loads can be restored. Three types of voltage regulation devices are considered in this chapter, namely, I) OLTCs, II) SVRs, and III) CBs. In order to find the optimal set point of these voltage regulation devices in the reconfigured network, it is essential to consider the voltage dependency of the active/reactive load consumptions. For this aim, the voltage-dependent model of the loads is integrated into the developed optimization problem using a linear approximation formulation. The overall restoration problem is finally formulated in the form of a MISOCP optimization model.

The proposed restoration model is successfully tested on a real 83-bus distribution network in six test cases. The first test case illustrates the capability of the proposed strategy in providing

partial restoration solutions with isolated areas. In this test case, it is assumed that none of the voltage regulation devices is controllable. Then, an OLTC, a SVR, and a CB are integrated into the optimization problem gradually one by one through test scenarios 2, 3, and 4, respectively. In these scenarios, it is shown how the integration of these voltage regulation devices could improve the quality of the restoration solution. Test scenario 5 studies the restoration problem in case of a large off-outage area. The results shows that the proposed optimization algorithm can find an optimal and feasible solution within a reasonable time even for large-scale outages in distribution networks. Finally, in scenario 6, we illustrated the efficiency and superiority of the mathematical formulation proposed for the restoration problem with respect to a heuristic algorithm. The results indicate that the quality of the solution obtained from the heuristic algorithm is very poor with respect to the one obtained from the proposed optimization problem.

3 Service Restoration in DG-Integrated Distribution Networks

Chapter Highlights:

The main goal of this chapter is to modify the restoration strategy proposed in chapter 2 such that it is applicable also for active distribution networks. For this aim, first, we propose a novel restoration strategy for active distribution networks called "multi-step restoration". This strategy is introduced as a compromise between the *static* and *dynamic* approaches, which already exist in the literature. Then, we formulate the proposed restoration strategy as a MISOCP optimization problem. The start-up requirements of grid-connected DGs, including the energization of their hosting nodes and their start-up durations are accurately modeled and integrated into the derived formulation.

Afterwards, the power flow formulation is integrated into the developed formulation of the restoration problem. The aim is to ensure the feasibility of the obtained solution concerning the technical constraints (e.g. voltage and current limits). In this regard, a recently published method for the exact and convex relaxation of the AC-OPF formulation is incorporated making the restoration problem robust particularly in the case of high DG penetration.

Related Publication:

H. Sekhavatmanesh and R. Cherkaoui, "A Multi-Step Reconfiguration Model for Active Distribution Network Restoration Integrating the DG Start-Up Sequences," *IEEE Transactions on Sustainable Energy*, pp. 1–1, 2020, doi: 10.1109/TSTE.2020.2980890.

H. Sekhavatmanesh, M. Nick, M. Paolone, and R. Cherkaoui, "Service Restoration in DG-Integrated Distribution Networks Using an Exact Convex OPF Model," in *Power Systems Computation Conference (PSCC)*, Dublin, 2018, pp. 1–7, doi: 10.23919/PSCC.2018.8442963.

3.1 Chapter Organization

The motivation of proposing this chapter is presented in section 2.2. Section 3.3 is devoted to the restoration strategy in active distribution networks. In this regard, first, a literature review on the existing strategies of the restoration service is presented. Then, a proposed multi-step restoration strategy is introduced and formulated in subsections 3.3.2 and 3.3.3, respectively. Section 3.4 focuses on the integration of the power flow formulation into the restoration problem for active distribution networks. In this regard, first, a literature review on the existing formulations of the OPF problem is provided. Then, in subsection 3.4.2, the power flow equations are integrated into the developed restoration problem using a Relaxed Optimal Power Flow (R-OPF) formulation. This R-OPF formulation is updated in section 3.4.3 to an exact formulation named Augmented Relaxed Optimal Power Flow (AR-OPF). Section 3.5 provides three test studies verifying the main contributions of this chapter. The conclusion and summary of this chapter are provided in section 3.6.

3.2 Motivation

In chapter 2, the restoration problem was formulated integrating different elements of a passive distribution network. In recent years, the highly increasing penetration of DGs has changed the face of distribution networks from passive to active networks. This movement has affected many aspects of the distribution network operation such as monitoring, control and protection schemes [4]. In this context, the restoration strategy is not an exception. Therefore, the restoration of distribution systems is a timely topic that deserves to be revisited while integrating the DGs.

From one side, the ever-increasing penetration of DGs in distribution networks suggests to enable their potentials in better fulfilling the restoration objective. From the other side, the integration of DGs brings significant challenges into the restoration problem in distribution networks from both strategical and formulation point-of-views.

Regarding the strategical challenges, the restoration problem should address the requirements imposed by the start-up process of disconnected DGs. From the formulation point of view, it should be ensured that the relaxation used for the power flow formulation will be still exact in presence of high penetration of DGs. These strategical and formulation concerns are addressed in sections 3.3, and 3.4, respectively. Thanks to the proposed solutions in this chapter, we are

able to integrate the optimal dispatch of DGs into the restoration problem. In this regard, we make the most efficient use of DG capacities in improving the quality of the restoration solution.

3.3 The restoration strategy in ADNs

When a fault occurs in a radial distribution network, once it is isolated, the area downstream to the fault place (*off-outage area*) remains unsupplied even in presence of DGs in that area. The restoration problem aims at supplying the maximum loads in this off-outage area using a minimum number of switching operations. In this respect, the off-outage area will be restored through healthy feeders that can be directly connected to it through normally-open (tie) switches. These feeders and switches are called *available feeders* (Feeder-b in Fig. 1-1) and *available tie-switches* (T3 in Fig. 1-1), respectively. In order to maintain the radiality of the network configuration, some of the normally-closed (sectionalizing) switches should be open. The disconnected DGs are re-energized once their nodes are restored. They re-inject power into the network and support the available feeders to better procure the restoration objectives. The resulting new configuration of the network remains for a so-called *restorative period* starting from the fault isolation instant until the time when the faulted element is repaired. After the restorative period, the original configuration of the network will be restored.
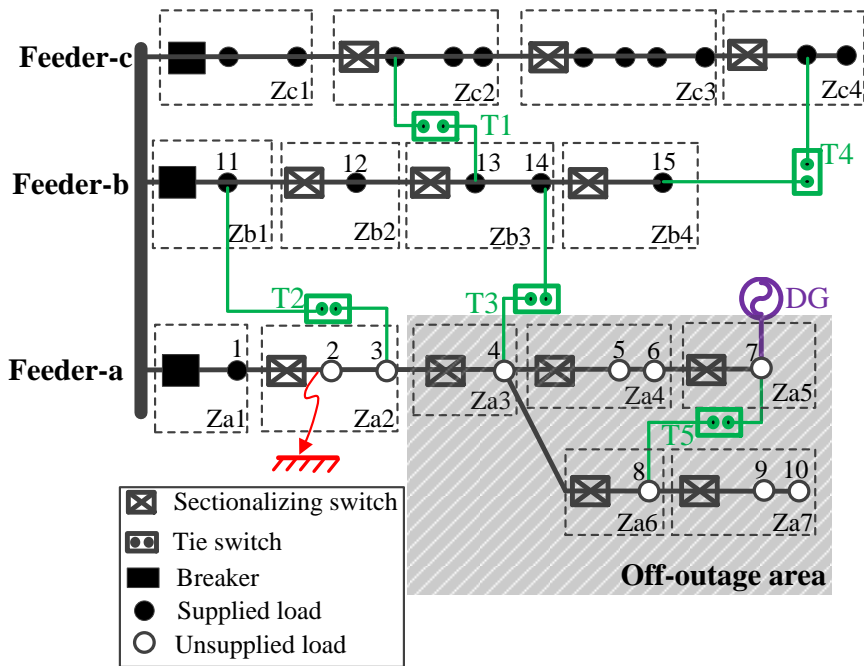
Fig. 3-1. A simple distribution network under fault conditions

3.3.1 State-of-the-art of the restoration strategies in ADNs

The restoration process in passive distribution networks counts only on the load transfer from the off-outage are to the healthy feeders using only switching operation. Today, in ADNs, new, fast and efficient restoration strategies can be developed incorporating also the set point modifications of DGs in the restoration strategies. In this regard, there are many studies in the literature on DG-aided service restoration. They propose to set up *intentional DG-island systems* [61] using different methodologies. Each of them supplies locally a group of nodes during the restorative period. The authors in [2, 3] use a clustering strategy to partition the off-outage area into self-sufficient DG-island systems. The sizes of the clusters are determined using a rolling-horizon optimization method with the aim of supplying a maximum of loads with minimum operational DG costs. However, these costs are not of interest for the restoration service. The DG-island systems proposed in [4–6] are set up for the restoration service by searching for feasible supply routes in the network graph considering each DG as a possible power source candidate. In these studies, heuristic approaches guided by expert-based ruled are used to find the suitable DG-island system regarding the targeted restoration objectives.

All the above-mentioned studies consider different DG operational requirements while setting up those islanding systems. These requirements are, among others, DG black start capability, generation capacity limits, and load pickup capability. However, according to [61], when an *intentional DG-island system* is planned, other requirements in addition to the ones related to the DG itself must be also considered. These requirements concern among others the protection equipment and settings, voltage regulation equipment, and proper operation of loads in the DG-island system. These requirements are all neglected in the above-mentioned studies. Consequently, in the proposed restoration strategy, all the DGs are assumed to be operated in the grid-connected mode only. Thus, the restoration solution will be compatible with respect to all the currently used operation standards.

According to the common practices in electrical utilities, it is desirable to provide a unique configuration that is valid regarding the load and generation profiles along the entire restorative period. This so-called *static approach* cannot handle dynamic processes that exist during the service restoration. Among these dynamic processes is the DG start-up process, which is neglected in the DG-aided restoration strategies proposed in the literature [26], [66]. This practical concern will be defined and discussed in details in section 3.3.2.

In order to account for a time-dependent process in the reconfiguration problem, the papers in the literature propose another approach, which is called *dynamic approach*. In the dynamic reconfiguration approaches, the topology of the network continually changes specifically in response to the variation of loads and intermittent resources. For instance, the authors in [67] and [68] propose intraday dynamic reconfiguration models with the aim of minimizing daily running costs, and minimizing DG power curtailments, respectively. However, the network configuration should not change frequently during the restorative period. The reason is to avoid many interruptions to the customers by transient switching disturbances especially in the restored part of the network that can be already pushed to the edge of its capabilities. Finally, we can conclude that the dynamic reconfiguration approach is also inappropriate for the restoration problem studied in this chapter.

As mentioned in chapter 2, the reconfiguration problem is, by nature, an NP-hard combinatorial optimization problem. This computational complexity is even higher in the case of using dynamic approaches, since these approaches need to integrate many binary variables indicating the switching operations at every time step. In order to relax the computation burden of the dynamic reconfiguration problems, papers [11] and [12] present methodologies to partition the time window of the optimization problem in clusters with similar load levels. The configuration for each cluster remains unchanged. Therefore, the number of required binary variables is reduced and the computation burden is significantly relaxed.

However, this clustering approach is not applicable if we plan to account for the DG start-up process. As it will be explained in section 3.3.2, regarding the restoration problem studied in this chapter, the time window (i.e. restorative period) should decompose in clusters at the time instants when the disconnected DGs are energized. These time instants are not pre-determined parameters like those of the variability of load and generations which are the only time-dependent processes studied in [11] and [12].

The authors in [71] propose to solve sequentially the reconfiguration problem for each time step (hour) of the day (successive single period optimization problems). Prior to each time step, an updated forecasting time horizon is considered which is obtained using stochastic model predictive control. In this respect, the dynamic reconfiguration problem is transformed into a series of static reconfiguration problems at different time steps. The weakness of this strategy is that the solutions at a given time step are not influenced by the future decisions during the rest

of the optimization process. Therefore, this approach cannot be applied to solve multi-period restoration problems (such as the one studied in this chapter), where the feasible and optimal solution at one time step depends on the solution of the problem in the previous and next steps.

In what follows, it is aimed to address the aforementioned weaknesses of static and dynamic reconfiguration approaches in handling time-dependent processes existing in the restoration problem. In this regard, a *multi-step* restoration strategy is proposed and formulated such that it can be solved using mathematical programming method. In specific, this formulation accounts for the requirements of the DG start-up process that might affect the restoration solution.

3.3.2 Proposed multi-step restoration strategy

In this section, it is aimed to propose a novel restoration strategy complying with the DG start-up requirements. This process accounts only for DGs that are in the off-outage area. We assume that the DGs outside the off-outage area are connected and ready to produce at the beginning of the restorative period. As already mentioned, the DGs inside the off-outage area should be automatically disconnected following the fault [61]. In order to enable these DGs to re-inject power into the network, they should go under a specific process called DG start-up process. The requirements of this DG start-up process that are impacting the restoration solution are defined in two-folds: I) energization of the DG hosting node, and II) start-up duration of the DG. Since in this chapter the DGs are assumed to operate only in grid-connected mode, at the beginning of the restoration, the disconnected DGs need a configuration that provides them feasible path(s) from the healthy part of the grid. Once the hosting node of the DG is energized, a sequence of actions is carried out to enable the DG to inject power. These actions take a period called *DG start-up duration*. They involve among others the response time of the DG primary source and the time for launching auxiliary control systems [72]. The detailed procedure of the DG start-up is not dealt with in this chapter. Only the two requirements mentioned above (I and II) are considered and formulated in section 3.3.3.3.

While the DG is still not ready to inject power, some parts of the off-outage area might need to be left unrestored. Once the DG is ready to produce, a new configuration might be needed in order to supply, if possible, those unrestored areas/loads thanks to a more efficient support of the DG. As an example, consider the faulted network shown in Fig. 1-1. In the first reconfiguration step shown in Fig. 3-2.a, the DG hosting node is energized by closing tie-switch T3. Since the DG does not inject power in this step, loads 6, 8, 9, and 10 cannot be restored while respecting
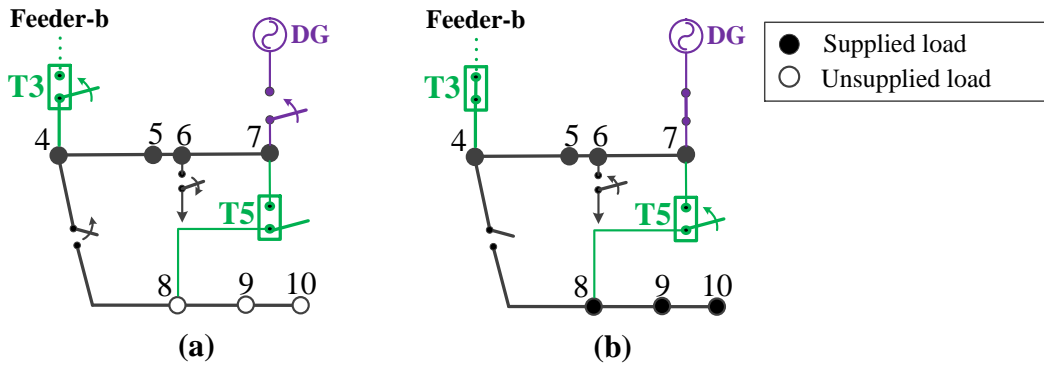
Fig. 3-2. Two reconfiguration steps of the restoration strategy in case of the fault in the test system of Fig. 1-1. a) step1, b) step 2.[5]

the network security constraints. In Fig. 3-2.b, the DG is ready to inject power in the grid-connected mode and supports feeder-b in supplying the loads. Therefore, tie-switch T5 and load breaker 6 are closed to supply the loads that were left unrestored in the first reconfiguration step.

Therefore, throughout the restoration process, the off-outage area changes its configurations through a certain sequence of switching called *network reconfiguration steps* (or simply *steps*). In this regard, a multi-step reconfiguration algorithm is proposed in this chapter as a compromise between static and dynamic approaches. Unlike the static approaches, the proposed algorithm allows the configuration of the network to change in some steps in order to handle the DG start-up process. However, unlike the dynamic reconfiguration approaches, the number of reconfiguration steps are limited to a predefined value.

This value is determined according to the policies or experience of distribution system operators. More number of stages helps to better procure the restoration objectives. However, as already said in section 3.3.1, it may cause more switching disturbances to the restored network. The number of steps should be at maximum equal to the number of DGs plus one. Actually, as soon as all the DGs restored are ready to produce no further reconfiguration is allowed.

As illustrated in the previous example, during the DG start-up process, it might be possible that all the nodes of the network cannot be energized since the DG is not still ready to produce (see Fig. 3-2.a). This scenario is already defined in chapter 2 as *partial restoration*. In this regard, we proposed in chapter 2 a novel model for the network reconfiguration that is accounting for partial restoration scenarios. However, using this formulation could violate the radiality

---

[5] Every node is equipped with a load breaker. Fig. 3-2 shows only those load breakers that should be operated.

constraint in cases where DGs exist in the off-outage area. This infeasibility is discussed and addressed in section 3.3.3.

3.3.3 Formulation of the multi-step restoration problem

In this section, a mathematical formulation is provided for the multi-step reconfiguration problem in the form of a mixed-integer convex optimization problem. The main decision variables of the proposed optimization problem are I) the line switching actions at each reconfiguration step, II) the load switching actions during the whole restorative period, and II) the active/reactive power dispatch of DGs during the whole restorative period. Since the network configuration is fixed between deploying each two successive steps, instead of indexing binary switching variables Y_{ij} with each single time step t, they will be indexed with reconfiguration steps s. In this way, the number of binary decision variables and therefore the computation burden of the problem decreases drastically.

Minimize:
$$F^{obj} = w_{re}.F^{re} + w_{sw}.F^{sw} + w_{op}.F^{op} \tag{3-1}$$

$$F^{re} = \sum_t \sum_{i \in N} D_i.\left(1 - L_{i,t}\right).P_{i,t}^D \tag{3-2}$$

$$F^{sw} = \sum_s \left(\sum_{ij \in W_{tie}^S} Y_{ij,s}.\lambda_{ij} + \sum_{ij \in W_{sec}^S} S_{ij,s}.\lambda_{ij} \right) \tag{3-3}$$

$$F^{Op} = \sum_t \sum_{(i,j) \in W} r_{ij}.F_{ij,t} \tag{3-4}$$

Subject to:

$$0 \leq Z_{ij,s} \leq 1 \qquad \forall ij \in W^S, \forall s \tag{3-5}$$

$$Z_{ij,s} = Y_{ij,s} \ , \ Z_{ji,s} = 0 \qquad \forall ij \in W_{ava}^S, \forall s \tag{3-6}$$

$$Z_{ij,s} + Z_{ji,s} = Y_{ij,s} \qquad \forall ij \in W^S, \forall s \tag{3-7}$$

$$\begin{cases} X_{i,s} = \sum_{j:(i,j) \in W^*} Z_{ji,s} \leq 1, & i \in N^* \\ X_{i,s} = 1, & i \in N \backslash N^* \end{cases} \tag{3-8}$$

$$X_{ij,s} = \begin{cases} \sum_{k \in Z^*} (A_{ij,k}.X_{k,s}) & : ij \in W^* \backslash W^S \\ Y_{ij,s}, & : ij \in W^S \\ 1, & : ij \in W \backslash W^* \end{cases} \qquad \forall s \tag{3-9}$$

$$0 \leq Y_{ij,s} \leq M.F_{ij,s} \qquad\qquad \forall ij \in W^S, \forall s \quad (3\text{-}10)$$

$$0 \leq \Psi_{ij,s} \leq M.Z_{ij,s}$$

$$0 \leq \Psi_{ji,s} \leq M.Z_{ji,s} \qquad\qquad \forall ij \in W^S, \forall s \quad (3\text{-}11)$$

$$\sum_{\forall j^*:(j^*,i)\in W} (\Psi_{j^*i,s}) = \sum_{\forall j^*:(i,j^*)\in W} (\Psi_{ij^*,s}) + X_{i,s} \qquad \forall i \in Z^*, \forall s \quad (3\text{-}12)$$

$$\sum_{\forall (i,j)\in W_{ava}^S} \Psi_{ij,s} = \sum_{\forall i\in Z^*} X_{i,s} \qquad\qquad \forall s \quad (3\text{-}13)$$

$$\begin{cases} (1 - Y_{ij,s}) + X_{i,s} - 1 \leq S_{ij,s} \leq 1 \\ (1 - Y_{ij,s}) + X_{j,s} - 1 \leq S_{ij,s} \leq 1 \\ 0 \leq S_{ij,s} \end{cases} \qquad \forall ij \in W_{sec}^S, \forall s \quad (3\text{-}14)$$

Time mapping constraints

Load Pick-up constraints

DG constraints

OPF constraints

The objective function of the restoration problem (F^{obj}) is formulated in (3-1) , which consists of reliability (F^{re}), switching (F^{sw}) and operational (F^{op}) terms, in decreasing order of priority. This hierarchical priority is enabled using $\epsilon-constraint$ method [53]. As formulated in (2.2), the reliability term expresses the total energy of loads that cannot be restored during the restorative period, while accounting for the load importance factors. The second priority term minimizes the total operation time of line switches including tie switches and sectionalizing switches, which are respectively formulated in the two sub-terms of (3-3). Since tie switches are normally-open, they are operated when they are energized ($Y_{ij} = 1$). In the case of the sectionalizing switches, their operation has to be determined using auxiliary variables $S_{ij,s}$, and the constraints (3-14) that are explained later on.

Unlike the first two objective terms, the third term has a very small weight (W_{op}) in the objective function. As expressed in (2.4), the operational term aims to minimize the total active power losses in the restored network. This term is included in the objective function just to ensure the exactness of the obtained solution regarding the relaxed power flow formulation. It should be noted that the weighting factors are applied on the normalized terms of the expressions defined

in (2.2) and (2.4). It should be noted that the weighting factors in (3-1) are applied on the normalized terms of the expressions defined in (2.2)-(2.4).

The network configuration is modeled using constraints (2.5)-(3-13), where M is a large multiplier. At each reconfiguration step s, the energization status of line ij which is equipped with a switch is identified by a binary variable $Y_{ij,s}$ and its orientation with respect to a virtual source node is determined by continuous variables $Z_{ij,s}$ and $Z_{ji,s}$. This virtual source node is defined as a node in the healthy feeder that is connected to an available tie-switch (ex. node 14 in Fig. 1-1). If the line is oriented from node i to node j, variable $Z_{ij,s}$ will be 1 and $Z_{ji,s}$ will be zero and if the line is oriented from node j to node i variable $Z_{ji,s}$ will be one and $Z_{ij,s}$ will be zero.

For cases with no DG in the off-outage area, an empirical discussion is provided in chapter 2, showing that the constraint set (3-5)-(2.9) ensures a radial configuration. However, in cases with DG, this approach could lead to an isolated loop where the loads are supplied in an islanded way using an existing DG in that loop [73]. In order to avoid this, we propose a new formulation for the radiality constraints based on the virtual commodity flow approach proposed in [55]. Compared to [55], the number of the auxiliary variables and the computation burden of the developed formulation in this paper are less. According to this developed formulation, to each line ij with switch in the off-outage area, two continuous flow variables Ψ_{ij} and Ψ_{ji} are assigned. They are associated with the binary variables Z_{ij} and Z_{ji}, respectively. The flow Ψ_{ij} or Ψ_{ji} is positive if it is travelling in the same direction as the orientation of the line carrying this flow. As formulated in (3-11), for each line ij with switch, at most one of the variables $\Psi_{ij,s}$ and $\Psi_{ji,s}$ gets a nonzero value depending on the line orientation that is identified with the variables $Z_{ij,s}$ and $Z_{ji,s}$. Constraint (3-12) formulates the flow[6] balance equation for each zone[7] i, assuming that each zone consumes a flow value equal to one. Finally, (3-13) implies that the total flows provided by all the available tie-switches as virtual sources must be equal to the total number of energized zones. In Fig. 3-3, the flow values are indicated for each line with switch. As it can be seen in this example, there is one tie-switch with the flow value of 5 that is energizing 5 zones. It should be mentioned that in order to respect (3-11)-(3-13), the lines that are constituting an

---

[6] It is meant directional flow with regard to the graph theory and should be distinguished with the electrical flow term used in the OPF formulation

[7] In this chapter, a zone is referring to each segment of the feeder that is surrounded by two or more sectionalizing switches (Fig. 1-1).
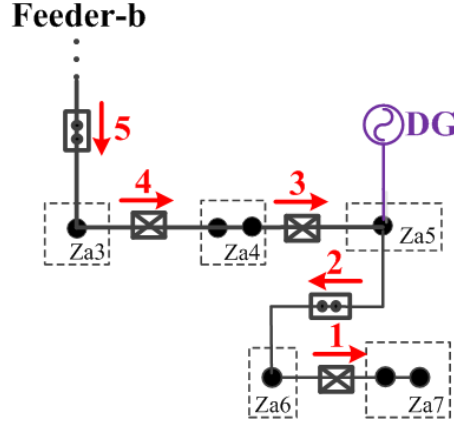
Fig. 3-3. The auxiliary flow variables in the test network of Fig. 3-2.b.

isolated loop can get only zero flow values. It means that the nodes of this isolated loop will not be energized. Regarding this discussion and the one provided in Chapter 2, it can be concluded that (3-5)-(2.9) ensure a radial configuration without creating isolated loops supplied by DGs in islanded mode.

The operation of sectionalizing switches is formulated in (3-14). Unlike tie-switches, for sectionalizing switches, energization status does not necessarily imply that they should be operated or not. At a given step s, the sectionalizing switch on line ij must be operated (opened) ($S_{ij,s} = 1$) only if it is de-energized ($Y_{ij,s} = 0$) and at least one of its ending buses are energized ($X_{i,s} = 1$ or $X_{j,s} = 1$). According to (3-14), for the other sectionalizing switches, $S_{ij,s}$ is free to get any value between 0 and 1. However, since the sum of S_{ij} variables is minimized according to (3-3), S_{ij} for these switches will be zero, meaning that they should not be opened. Time mapping, load pick up and DG constraints are presented in the following three subsections, whereas OPF constraints are formulated in section 3.4.

3.3.3.1   **Time mapping Constraints**

As mentioned earlier, in order to reduce the number of binary decision variables, reconfiguration variables are indexed with each reconfiguration step. Now in order to ensure that the operational security constraints are met, the temporal dependency of the reconfiguration variables should be correlated with the ones of the OPF variables. For this aim and since OPF variables are indexed with each time slot, each step is mapped to the time slots, during which its corresponding configuration is under operation. This is determined using variable $K_{t,s}$ under the constraints formulated in (3-15). Being of SOS1-type, constraint (3-15.a) ensures that for each

time slot t, variable $K_{t,s}$ is 1 only for one reconfiguration step s and is 0 for the rest. In other words, time slot t can be assigned only to one step according to the following condition:

$$if\ T_s \le\ t <\ T_{s+1}\ holds, then\ K_{t,s} = 1\ must\ hold$$

This conditional constraint is equivalent to the following expression:

$$(T_s >\ t)\ \ or\ \ (t \ge\ T_{s+1})\ \ or\ \ (K_{t,s} = 1)\ \ must\ hold$$

It means among the three constraints given above, only one must hold. Since $K_{t,s}$ is a binary variable, one can conclude that the first two constraints could hold only when $K_{t,s} = 0$ holds. This expression is formulated in (3-15.b-c). According to (3-15.b), $T_s >\ t$ could hold only when $K_{t,s} = 0$, and according to (3-15.c) $t \ge\ T_{s+1}$ could hold only when $K_{t,s} = 0$.

$$\begin{cases} \displaystyle\sum_{s^*\in N_s} K_{t,s^*} = 1, \quad : SOS1 \\ T_s - M(1 - K_{t,s}) \le t \\ t \le T_{s+1} + M(1 - K_{t,s}) \end{cases} \qquad \forall t,s \qquad \begin{matrix}(3\text{-}15.a)\\ (3\text{-}15.b)\\ (3\text{-}15.c)\end{matrix}$$

$$\sum_{ij\in W_{tie}^S} Y_{ij,s}.\lambda_{ij} + \sum_{ij\in W_{sec}^S} S_{ij,s}.\lambda_{ij} + T_{s-1} \le T_s \qquad \forall s \qquad (3\text{-}16)$$

Constraint (3-16) determines the time instant of each reconfiguration step. The network undergoes the configuration at step $s - 1$ starting from T_{s-1} until T_s, assuming that $T_0 = 0$. This duration must be larger than the time needed to deploy the switching operation at step s. Since at a given step s, the switching actions are deployed in a successive way, their deployment times are summed up in (3-16) resulting in the switching operation time of step s. λ_{ij} is pre-determined according to the average time that is taken to operate switch ij. This average time for the case of manually-controlled switches depends among others on the distance from the switch location to the operation center.

3.3.3.2 Load Pick-Up Constraints

Regarding the partial restoration scenarios, along with the possibility to setup isolated areas, the loads that are equipped with a breaker at their nodes could be shed to respect the security constraints particularly at the early stages of the network reconfiguration. If feasible, it is scheduled to pick-up these loads during the rest of the restorative period. In this regard, at each time slot t belonging to reconfiguration step s ($K_{t,s} = 1$), a decision is made with binary variable

$L_{i,t}$ in (3-17) for a given energized node ($X_{i,s} = 1$), indicating if its load will be supplied or rejected (1/0). It is assumed that once a given load in the off-outage area is restored at a given time, no further interruption is permitted during the subsequent time slots of the restorative period. This constraint is formulated in (3-18).

$$L_{i,t} \leq X_{i,s} + 1 - K_{s,t} \qquad\qquad \forall i \in N^*, \forall t, s \qquad (3\text{-}17)$$

$$\begin{cases} 0 \leq L_{i,t-1} \leq L_{i,t} \leq 1, & \forall i \in N^*, \forall t \\ L_{i,t} = 1, & \forall i \in N \backslash N^*, \forall t \end{cases} \qquad (3\text{-}18)$$

3.3.3.3 DG Constraints

In this chapter, we consider dispatchable DGs operating only in grid-connected control mode. In this regard, the disconnected DGs first need a configuration that energize their hosting nodes. Constraint (3-19) is forcing the active-/reactive power injection of DGs at time t to be zero if the hosting node is not energized according to the network configuration at time t. According to the developed formulation in section 3.3.3.1, the discrete reconfiguration variables at each step ($X_{i,s}, X_{ij,s}$) are linked to the electrical state variables at each time using auxiliary variables $K_{t,s}$. As formulated in (3-19), the DG can inject active and reactive power at time t only if its hosting node is energized ($X_{i,s} = 1$) according to the network configuration step s that is under operation at that time ($K_{t,s} = 1$). It is worth to note that the configurations at other steps s^* ($K_{t,s^*} = 0$) have no impact on the power injection of the DG at time t.

As mentioned in section 2.2 and formulated in (3-20), for a given DG in the off-outage area, once its hosting node is energized ($K_{s,t} = 1, X_{i,s} = 1$), it still cannot inject power before it is fully restarted ($K_{s,t-\Delta_i} = 0$). This restart process is assumed to take Δ_i time steps.

The apparent power injection of DGs is limited by the cone constraint of (3-21). In this chapter, it is assumed that the reservoir (e.g. gas tank or diesel tank) supplying the DG primary resource has a finite energy capacity during the restorative period. The availability of energy stored at the reservoir of each DG at time t is ensured according to (3-22).

$$\begin{cases} 0 \leq P_{i,t}^{inj} \leq M(X_{i,s} + 1 - K_{s,t}) & \forall i \in \Omega_{DG}, \forall t, s \qquad (3\text{-}19) \\ -(X_{i,s} + 1 - K_{s,t}) \leq Q_{i,t}^{inj} \leq M(X_{i,s} + 1 - K_{s,t}) \end{cases}$$

$$\begin{cases} 0 \leq P_{i,t}^{inj} \leq P_{i,max}^{inj}(2 - X_{i,s} - K_{s,t} + K_{s,t-\Delta_i}) \\ Q_{i,min}^{inj}(2 - X_{i,s} - K_{s,t} + K_{s,t-\Delta_i}) \leq Q_{i,t}^{inj} \leq Q_{i,max}^{inj}(2 - X_{i,s} - K_{s,t} + K_{s,t-\Delta_i}) \end{cases} \qquad (3\text{-}20)$$

$$\forall i \in \Omega_{DG}, \forall t > \Delta_i, \forall s$$

$$\left\|\begin{matrix} P_{i,t}^{inj} \\ Q_{i,t}^{inj} \end{matrix}\right\|_2 \leq S_{i,max}^{inj} \qquad\qquad \forall i \in \Omega_{DG}, \forall t, s \qquad (3\text{-}21)$$

$$E_{i,t} = E_{i,t-1} - P_{i,t}^{inj}\Delta t \geq 0 \qquad\qquad \forall\, i \in \Omega_{DG}\,, \forall t, s \qquad (3\text{-}22)$$

3.4 Optimal power flow in the restoration of active distribution networks

OPF is a known challenging optimization problem. It has been the main building block for the formulation of many control, operation, and planning problems in power systems. AC-OPF formulation should be integrated also to the restoration problem in order to ensure the feasibility of the obtained solution concerning the technical constraints such as voltage and current limits.

3.4.1 State-of-the-art of the methodologies for integrating network security constraints into the restoration problem

The OPF is a known challenging optimization problem. It has been the main building block for the formulation of many control, operation, and planning problems in power systems. In this respect, an AC-OPF should be integrated into the restoration problem in order to check the feasibility of the obtained solution concerning the technical constraints such as voltage and current limits. Due to the power flow formulation, the restoration problem is inherently a non-linear NP-hard problem and, consequently, its solution is challenging. In order to deal with the non-polynomial hardness of such an OPF-based optimization problem, some researchers applied meta-heuristic methods as the solution approach. Among these methods are Genetic Algorithm [74], Particle Swarm Optimization [75], Ant Colony [57], and Tabu Search [9] (see [9] for a comprehensive technical review). As mentioned in chapter 2, these methods are in general time-consuming and fail to give even a feasible solution in a reasonable time complying with online operation requirements. Therefore, heuristic approaches based on expert systems are proposed for the restoration problem to achieve a near-optimal solution in a short time. In addition to the weaknesses mentioned for heuristic approaches in chapter 2, in these methods, the feasibility of the solution concerning the technical constraints (ex., voltage and current limits) is either ignored [30] or checked after finding the restoration solution by a load flow simulation. Indeed, if the

solution does not satisfy the security constraints (e.g. voltage and current limits), it is removed from the search space and the search process is repeated to find a new restoration solution [28]. Some papers sort the possible combinations of loads that can be restored and check their technical feasibilities progressively [29]. All these approaches can be very time consuming or lead to a solution very far from the optimal one.

The main drawback of the existing literature related to the restoration techniques in ADNs is associated with the appropriate integration of the OPF formulation with regard to its non-convexities. The mathematical programming started to be an option for solving the restoration problem shortly after that some convex relaxation methods were proposed for the OPF problem. The authors of [76]-[77] used semidefinite programming (SDP) relaxation in order to solve it for radial unbalanced grids. Regarding the grid unbalancing, a distributed optimization technique is developed in [78] based on the Alternating Direction Method of Multipliers (ADMM). In this thesis, we assume that the distribution network is operated in a radial and balanced fashion. In this respect, relaxation methods are proposed in the literature for the OPF problem in the form of either Mixed-Integer Quadratic Constraint Programming (MIQCP) [25], [79] or Mixed-Integer Second-Order Cone Programming (MISOCP) model [26], [80], [81].

However, these relaxed formulations of the OPF might lead to technically infeasible solutions due to the inexactness of the optimal solution [82]. It is shown in [83] that using appropriate and more conservative constraints for the lines' ampacity limits and nodal voltage-magnitude limits ensure, under mild conditions, the exactness of the optimal solution. In this respect, we have employed the exact convex OPF model proposed in [83], where the lines' transverse-parameter as well as the network static operational constraints (lines ampacity limits and nodal voltage magnitudes) are appropriately included. This non-trivial coupling results in an exact optimization model for the restoration service in the form of a MISOCP problem. The dispatchable DGs in the off-outage area and available feeders are incorporated in the restoration process and their optimal set point during the restorative period is derived.

3.4.2   Formulation of the R-OPF in the restoration problem

In the following, a relaxed formulation of the OPF problem that is proposed in [26] is integrated into the restoration problem. Among others, the line transverse elements of the distribution cables are modeled in this formulation.
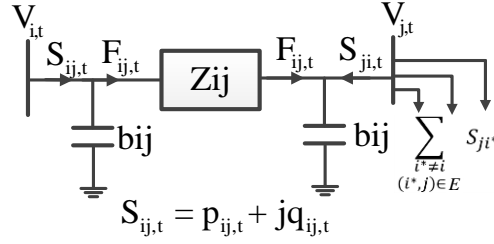
Fig. 3-4. Classical two-port Π model of a distribution cable adopted for the formulation of the OPF relaxed constraints.

In this regard and in order to introduce a part of the nomenclature, the Π model of a distribution cable is shown in Fig. 3-4.

$$0 \leq F_{ij,t} \leq f_{ij}^{max\,2}(X_{ij,s}+1-K_{s,t}) \qquad \forall ij \in W, \forall t, s \qquad (3\text{-}23)$$

$$v^{min\,2}(X_{i,s}-1+K_{s,t}) \leq V_{i,t} \leq v^{max\,2}(X_{i,s}+1-K_{s,t}) \qquad \forall i \in N, \forall t, s \qquad (3\text{-}24)$$

$$\begin{cases} -M(X_{ij,s}+1-K_{s,t}) \leq p_{ij,t} \leq M.(X_{ij,s}+1-K_{s,t}) \\ -M(X_{ij,s}+1-K_{s,t}) \leq q_{ij,t} \leq M.(X_{ij,s}+1-K_{s,t}) \end{cases} \qquad \forall ij \in W, \forall t, s \qquad (3\text{-}25)$$

$$-M.(2-X_{ij,s}-K_{s,t}) \leq V_{i,t}-V_{j,t}-2\big(r_{ij}.p_{ij,t}+x_{ij}.(q_{ij,t}+V_{i,t}b_{ij})\big)$$
$$\leq M.(2-X_{ij,s}-K_{s,t})$$
$$\forall(i,j) \in W, \forall t, s \qquad (3\text{-}26)$$

$$p_{ij,t} = (\sum_{\substack{i^*\neq i \\ i^*j \in W}} p_{ji^*,t})+r_{ij}.F_{ij,t}+L_{i,t}.P_{j,t}^D - P_{j,t}^{Sub} - P_{j,t}^{inj} \qquad \forall ij \in W, \forall t, s \qquad (3\text{-}27)$$

$$q_{ij,t} = (\sum_{\substack{i^*\neq i \\ i^*j \in W}} q_{ji^*,t})+x_{ij}.F_{ij,t}-j(V_{i,t}+V_{j,t})b_{ij}+L_{i,t}.Q_{j,t}^D - P_{j,t}^{Sub} - Q_{j,t}^{inj}$$
$$\forall ij \in W, \forall t, . \qquad (3\text{-}28)$$

$$F_{ij,t} \geq \frac{|p_{ij,t}+jq_{ij,t}+jV_{i,t}b_{ij,t}|^2}{V_{i,t}} \qquad \forall ij \in W, \forall t, s \qquad (3\text{-}29)$$

According to the developed formulation in section 3.3.3.1, the discrete variables of the multi-step reconfiguration problem $(X_{i,s}, X_{ij,s})$ are linked to the operational variables of the OPF problem using variable $K_{t,s}$. Therefore, the operational variables at time t follow the network

configuration step s that is under operation at that time ($K_{t,s} = 1$). It is worth to note that the configurations at other steps s^* ($K_{t,s^*} = 0$) have no impact on the OPF variables at time t.

Constraints (3-23) and (3-25) enforce, respectively, current and active/reactive power flows to be zero for each de-energized line ($X_{ij,s} = 0$, $K_{s,t} = 1$). The squared voltage magnitude is set to zero in (3-24), for de-energized nodes ($X_{i,s} = 0$, $K_{s,t} = 1$), and kept within the feasible region for energized nodes ($X_{i,s} = 1$, $K_{s,t} = 1$). Constraint (3-26) expresses the nodal voltage equations only for the energized lines ($X_{ij,s} = 1$, $K_{s,t} = 1$). The active and reactive power balance equations at the ending node of each line are formulated in (3-27) and (3-28), respectively.

Constraint (3-29) is the relaxed version of the current flow equation in each line as proposed in [26]. If the optimal solution obtained from the R-OPF formulation, given above, satisfies the original constraint (i.e. the equality condition in (3-29)), we say that the solution of R-OPF is exact. It is usually the case when there is not huge reverse power flow in the network caused by DG power injection. In case of networks with high DG penetration, it may often occur that the solution of R-OPF is inexact, i.e. it does not satisfy the equality condition in (3-29). In particular, this may happen when either one of the nodal voltage upper-bounds or/and line ampacity limits is/are binding.

3.4.3 Formulation of the AR-OPF in the restoration problem

In order to address the problem of inexactness associated with the R-OPF, it is enhanced with a formulation proposed in [83], called Augmented Relaxed Optimal Power Flow (AR-OPF). In this regard, the formulation given in (3-23)-(3-29) will be modified and extended according to the following considerations:

- Constraints (3-30)-(3-37) are added to the set of OPF constraints.
- Constraints (3-23) and (3-24) are replaced with constraints (3-38)-(3-42)
- For the sake of brevity, in what follows, the active power flow ($p_{ij,t}$) and reactive power flow ($q_{ij,t}$) in line ij are merged and represented using the complex power flow in line ij denoted by $S_{ij,t} = p_{ij,t} + jq_{ij,t}$.

The authors of [83] propose to use some auxiliary variables ($\bar{F}, \hat{S}, \bar{S}, \hat{V}$) to ensure the feasibility of the AR-OPF solution. These auxiliary variables include $\bar{F}$, $\hat{S} = \hat{p}_{ij,t} + j\hat{q}_{ij,t}$, and $\bar{S} = \bar{p}_{ij,t} + j\bar{q}_{ij,t}$ for the lines and $\hat{V}$ for the buses of the network as defined in (3-30)-(3-35). $\hat{S}$ and $\hat{V}$

represent the lower bound and upper bound on S and V, respectively and are adapted from DistFlow equations [84]. $\bar{S}$ and $\bar{F}$ are the upper bounds on S and F, respectively (see [83] for the proof of these statements). These auxiliary variables are subject to the following constraints.

$$0 \leq \bar{F}_{ij,t} \leq M.(X_{ij,s}+1-K_{s,t}) \qquad \forall ij \in W, \forall t, s \qquad (3\text{-}30)$$

$$0 \leq |\hat{S}_{ij,t}| \leq M.(X_{ij,s}+1-K_{s,t}) \qquad \forall ij \in W, \forall t, s \qquad (3\text{-}31)$$

$$0 \leq |\bar{S}_{ij,t}| \leq M.(X_{ij,s}+1-K_{s,t}) \qquad \forall ij \in W, \forall t, s \qquad (3\text{-}32)$$

$$\hat{S}_{ij,t} = \sum_{\substack{i^*\neq i \\ (i^*,j)\in W}} \hat{S}_{ji^*,t} - j(\hat{V}_{i,t} + \hat{V}_{j,t})b_{ij} - S_{i,t} \qquad \forall ij \in W, \forall t, s \qquad (3\text{-}33)$$

$$-M.\left(2 - X_{ij,s} - K_{s,t}\right) \leq \hat{V}_{i,t} - \hat{V}_{j,t} - 2\Re\left(z_{ij}^*(\hat{S}_{ij,t} + j\hat{V}_{i,t}b_{ij})\right) \leq M.\left(2 - X_{ij,s} - K_{s,t}\right)$$
$$\forall (i,j) \in W, \forall t, s \qquad (3\text{-}34)$$

$$\bar{S}_{ij,t} = \sum_{\substack{i^*\neq i \\ (i^*,j)\in W}} \bar{S}_{ji^*,t} + z_{ij}.\bar{F}_{ij,t} - j(V_{i,t} + V_{j,t})b_{ij} - S_{i,t} \qquad \forall ij \in W, \forall t, s \qquad (3\text{-}35)$$

$$\bar{F}_{ij,t}V_{j,t} \geq |max\{|\hat{p}_{ji,t}|, |\bar{p}_{ji,t}|\}|^2 + (max\{|\hat{q}_{ji,t} - j\hat{V}_{j,t}b_{ij}|, |\bar{q}_{ji,t} - V_{j,t}b_{ij}|\})^2$$
$$\forall ij \in W, \forall t, s \qquad (3\text{-}36)$$

$$\bar{F}_{ij,t}V_{i,t} \geq |max\{|\hat{p}_{ij,t}|, |\bar{p}_{ij,t}|\}|^2 + (max\{|\hat{q}_{ij,t} + j\hat{V}_{i,t}b_{ij}|, |\bar{q}_{ij,t} + V_{i,t}b_{ij}|\})^2$$
$$\forall ij \in W, \forall t, s \qquad (3\text{-}37)$$

Constraints (3-30)-(3-32) enforce, respectively, the auxiliary variables $\bar{F}$, $\hat{S}$, and $\bar{S}$ to be zero for each de-energized line ($X_{ij,s} = 0$, $K_{s,t} = 1$). The power flow balance and the nodal voltage equation of the DistFlow formulation are given in (3-33) and (3-34), respectively. The nodal voltage equation is imposed by (3-34) only for energized lines ($X_{ij,s} = 1$, $K_{s,t} = 1$). The power flow balance equation in terms of the auxiliary variables $\bar{F}$ and $\bar{S}$ is formulated in (3-35). Constraints (3-36) and (3-37) define the relaxed version of the current flow equation for the auxiliary variable $\bar{F}$ as proposed in [83].

The grid static security constraints are composed by: (i) the nodal voltage magnitudes and (ii) lines ampacity limit constraints. These two set of constraints, which were given in the R-OPF formulation using (3-23) and (3-24), respectively, should be replaced with the following formulation (for further details see [13]). The rest of formula given for R-OPF should be used without any change for AR-OPF.

$$v^{min^2}(X_{i,s} - 1 + K_{s,t}) \leq V_{i,t} \qquad\qquad \forall i \in N, \forall t, s \quad (3\text{-}38)$$

$$\hat{V}_{i,t} \leq v^{max^2}(X_{i,s} + 1 - K_{s,t}) \qquad\qquad \forall i \in N, \forall t, s \quad (3\text{-}39)$$

$$0 \leq F_{ij,t} \leq M.(X_{ij,s} + 1 - K_{s,t}) \qquad\qquad \forall ij \in W, \forall t, s \quad (3\text{-}40)$$

$$\left| \left| \max\{|\hat{P}_{ji,t}|, |\bar{P}_{ji,t}|\} \right| + j \max\{|\hat{Q}_{ji,t}|, |\bar{Q}_{ji,t}|\} \right|^2 \leq V_{j,t} f_{ij}^{max^2}$$
$$\forall ij \in W, \forall t, s \quad (3\text{-}41)$$

$$\left| \left| \max\{|\hat{P}_{ij,t}|, |\bar{P}_{ij,t}|\} \right| + j \max\{|\hat{Q}_{ij,t}|, |\bar{Q}_{ij,t}|\} \right|^2 \leq V_{i,t} f_{ij}^{max^2}$$
$$\forall ij \in W, \forall t, s \quad (3\text{-}42)$$

As formulated in (3-39), the maximum voltage limit is imposed on $\hat{V}_{i,t}$, which is the upper bound of $V_{i,t}$. The line ampacity limit is imposed on the maximum of absolute values of $\bar{P}_{ij,t}$ (resp. $\bar{Q}_{ij,t}$) and $\hat{P}_{ij,t}$ (resp. $\hat{Q}_{ij,t}$), as given in (3-41) and (3-42). It is proved in [83] that $\bar{P}_{ij,t}$ (resp. $\bar{Q}_{ij,t}$) and $\hat{P}_{ij,t}$ (resp. $\hat{Q}_{ij,t}$) are upper and lower bound of $P_{ij,t}$ (resp. $Q_{ij,t}$), respectively. The value of M used in (3-40) should be sufficiently larger than $f_{ij}^{max^2}$.

It should be noted that the new set of constraints (3-38)-(3-42) in AR-OPF is a bit more conservative than the corresponding constraints (3-23) and (3-24) that were given for the R-OPF. AR-OPF constraints shrink the feasible solution space of the original OPF problem. However, the removed space covers an operation zone close to the nodal voltage and line ampacity limits. This area is not a desirable operating region for the network operators. The exactness of the AR-OPF is discussed and proved in [83].

The overall multi-step restoration problem is obtained by integrating the AR-OPF formulation into the constraints of the optimization model formulated in section 3.3.3. As given in the following the overall restoration problem is in the form of a MISOCP optimization problem:

Minimize: $F^{obj} = w_{re}.F^{re} + w_{sw}.F^{sw} + w_{op}.F^{op}$

with: (2.2), (3-3), (2.4)

subject to:

multi-step switching constraints:	(3-15), (3-16)
Load pick-up constraints:	(3-17), (3-18)
DG constraints:	(3-19)-(3-22)
AR-OPF constraints:	(3-25)-(3-42)

3.5 Numerical analysis

The contributions of this chapter are tested using two medium voltage networks shown in Fig. 3-5 and Fig. 3-6. In test scenarios 1 and 2, the proposed multi-step restoration strategy is implemented and the results are compared with the results obtained from the state-of-the-art methodologies. In these scenarios, the test network shown in Fig. 3-5 will be used. Test scenario 3 validates the functionality of the proposed restoration model particularly when a high penetration of DGs is integrated into the distribution network. For this scenario, the test network shown in Fig. 3-6 will be used.

The test network shown in Fig. 3-5 is introduced in chapter 2, section 2.7. This network is modified in this chapter such that we can test the main proposed contributions. In this regard, four dispatchable DGs at nodes 7, 39, 59, and 80 and two non-dispatchable DGs at nodes 28 and 45 are added to the network. The active/apparent power capacities of DGs installed on nodes 7, 39, and 80 are equal to 2.8MW/3MVA, whereas the capacities of the DG at node 59 are equal to 0.8MW/1.0MVA. The start-up duration of these dispatchable DGs is assumed to be 30 minutes
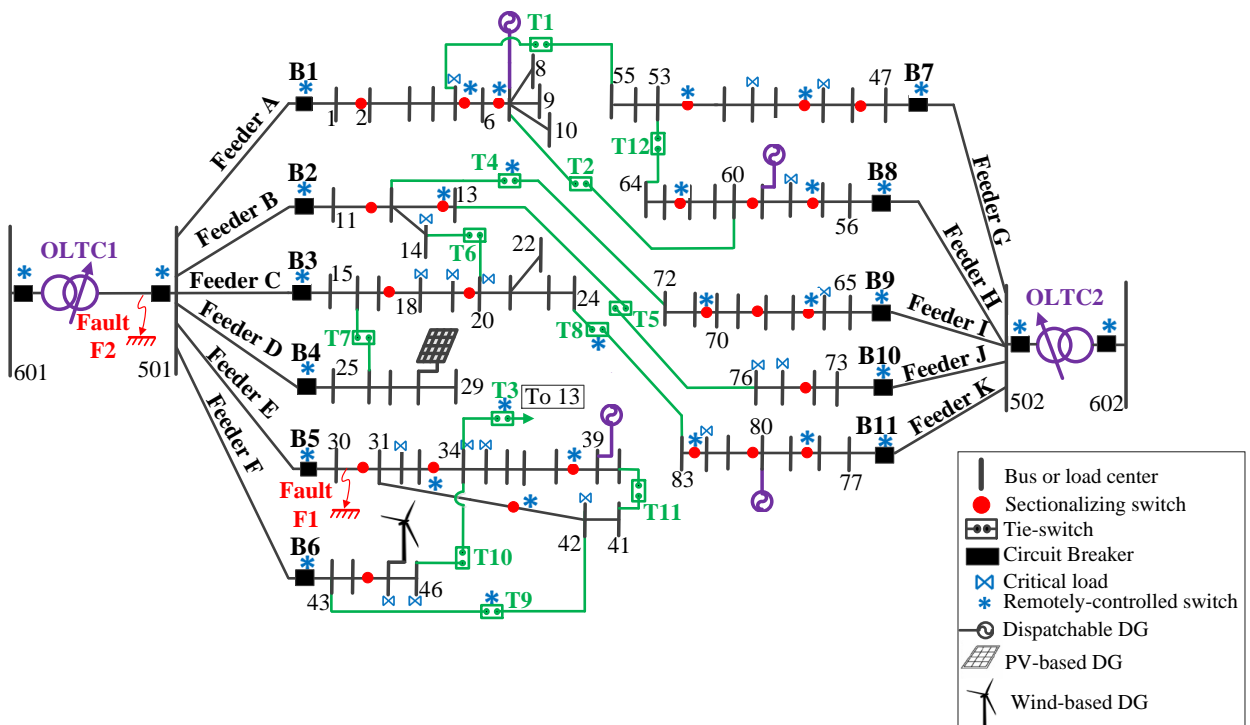
Fig. 3-5. Distribution network adapted from [58] to test the proposed multi-step restoration model under test scenarios 1 and 2.

for each [72]. The non-dispatchable DGs include a PV and a Wind generator at nodes 28 and 45, respectively. These intermittent DGs are modeled as voltage-independent power injection units with zero reactive power components. In this chapter, the forecasted active power generation of PV- and Wind-based DGs are derived from the real data reported in [85] and [86], respectively.

The second test system shown in Fig. 3-6 is introduced in [87] and will be used in test scenario 3. This test system is a 11kV distribution network with 2 substations, 4 feeders, 70 nodes, and 76 branches (incl. tie-branches). The system data is given in [87]. The majority of nodes along feeders 1-4 in Fig. 3-6 are assigned, respectively, to industrial, rural, residential, and commercial load types. There is also 10-30% of public light loads considered at each node. The hourly profile for each of these load patterns is given in [58]. One dispatchable DG with a capacity of 0.6 MW
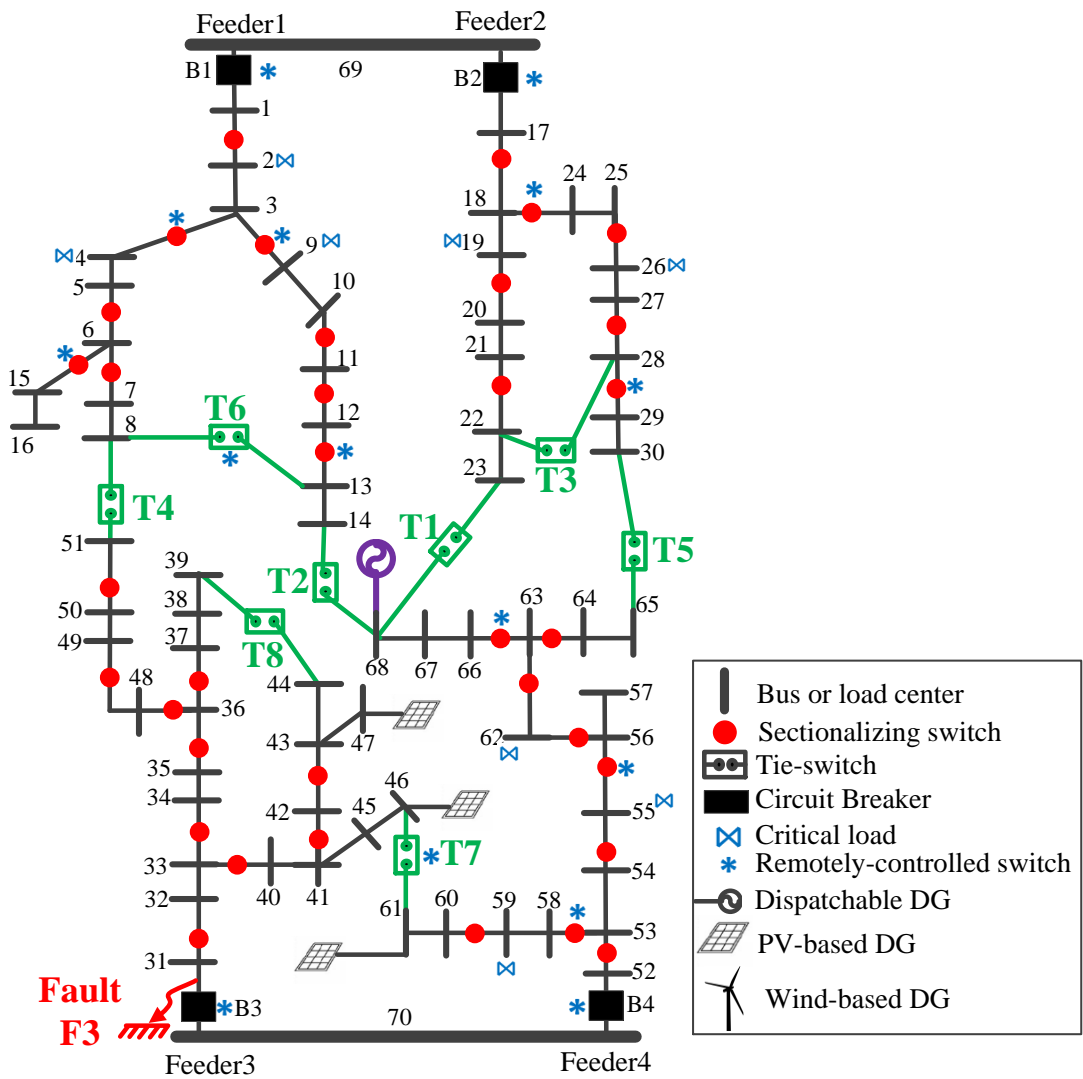
Fig. 3-6. Distribution network adapted from [87] to verify the integration of DGs into the proposed restoration problem using test scenarios 3 and 4.

is installed on bus 68. The set point of this DG is determined by DNO one day ahead, which might be subject to further tuning during the operation (for example, in case of network reconfiguration). The other type of DGs are PV-based DGs installed within LV networks at nodes 46, 47, and 61 with capacities of 0.6, 0.6 and 0.8 MW, respectively. The PV generation forecast profiles are obtained from [86].

For both test networks, the base power and energy values are set to 1MW and 1 MWh, respectively. According to ANSI C84.1 standard, the minimum and maximum voltage limits for the restorative period (as an emergency situation) are relaxed, respectively, to 0.917 and 1.05 p.u. [52]. The voltage set point at each substation node is assumed to be fixed at 1.05 p.u. It is assumed that each node of the networks shown in Fig. 3-6 and Fig. 3-5 is equipped with a load breaker. The manually-controlled line switches are labeled with '*', while the rest together with all the load breakers are remotely-controlled. It is assumed that the time needed for the operation of each manually controlled and remotely-controlled switch is 30 and 0.5 minutes, respectively. The critical loads, that are shown with '⋈' in Fig. 3-5, have priority factors equal to 100 while the priority factors of the other loads are equal to 1. The restorative period is assumed from 9:00 to 15:00. The time resolution of this study is chosen to be 15 minutes.

The algorithm is implemented on a PC with an Intel(R) Xeon(R) CPU and 6 GB RAM; and solved in Matlab/Yalmip environment, using Gurobi solver. Branch-and-Bound method is used to handle the developed mixed-integer optimization problem. The solver will not terminate until the gap between the lower and upper bounds is either less than 1e-10 (absolute gap limit) or less than 1e-4 (relative gap limit) times the absolute value of the upper bound. Therefore, it can be said that the global optimality of the solution is up to a good accuracy certified.

3.5.1.1 Scenario 1: comparison of multi-step reconfiguration with static and dynamic approaches

In this scenario, the restoration strategy is found in case of fault F1 shown in Fig. 3-5. In this regard, first, the developed multi-step restoration strategy is tested in scenario 1a, where the complete service restoration is deployed through two reconfiguration steps. The switching operations at each step are reported in Table 3-1 according to the order they should be deployed. The sketch of the timing of the restoration plan is shown in Fig. 3-7.a. Following Fault F1, the dispatchable DG at node 39 is disconnected. In order to energize this DG as soon as possible, its hosting node is energized after the first step, relying only on the remotely controlled switches.
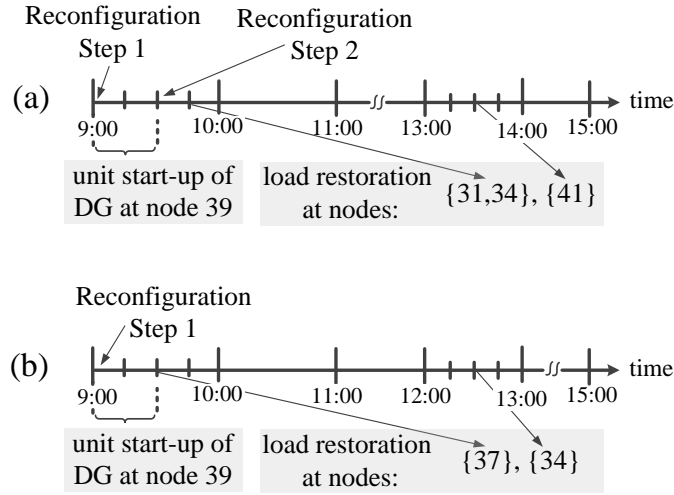
Fig. 3-7. The sketch of the timing of the restoration plan a) in scenario 1 using multi-step reconfiguration method, b) scenario 1 using static reconfiguration method.

As it can be seen in Fig. 3-7.a, the loads at buses 31 and 34 can be restored only after $t = 09{:}30\ A.M.$, when the DG starts to inject power.

In the next step, the dynamic reconfiguration method is applied to the simulation scenario 1. In this regard, it is assumed that the configuration of the network can be changed after each 30 minutes (two time steps). Therefore, binary switching variables Y_{ij} are indexed with each of these considered time steps. The obtained restoration solution is the same as the results of the multi-step reconfiguration method reported in Table 3-1. This is due to the large weight of the reliability term in the objective function. However, the computation time with dynamic approach is equal to 24.11 minutes which is significantly longer than the one obtained with the multi-step reconfiguration approach. This shows that using the proposed multi-step reconfiguration method, the computational burden of the dynamic formulation is relieved without compromising the quality of the solution.

In the next step, the test case of the scenario 1 is studied again using static reconfiguration method. According to this method, we consider only a single reconfiguration step. As the results of Table 3-1 shows, compared with the two-step reconfiguration, having a single reconfiguration step degrades significantly the quality of the restoration solution in terms of the reliability objective value (F^{re}). The sequence of DG starting and load pickup is shown in Fig. 3-7.b. As it can be seen, the load at node 31 that was detached at the beginning of the restoration strategy (see Table 3-1) cannot be picked up having only one reconfiguration step.

Table 3-1. Optimal restoration results in case of fault scenario 1.

Methodology	Step Number	Switching actions	F^{sw} (min)	F^{re} (p.u.)	Computation time (min)	Min. voltage (p.u.)	Max. voltage (p.u.)	Min. current margin (p.u.)
multi-step reconfiguration method	Step1	I. Open load breakers {31,34,41} and switch 33-34 II. Close {T3,T9}	3	8.3	1.16	0.9570 p.u. at node 38	1.05 p.u. at node 39	0.5192 p.u. on line 501-43
	Step2	II. Close T11 III. Open switch 38-39	30.5					
static reconfiguration method	Step1	I. Open switch 31-42 and load breakers {31,34,37} II. Close {T3,T9}	3	14.63	0.68	0.9375 p.u. at node 38	1.05 p.u. at node 501	0.0062 p.u. on line 11-12

In order to validate the feasibility of the obtained solution regarding the security constraints, the real values of voltage and current profiles are derived using post power flow simulations running for the obtained new configurations of the network during the whole restorative period. These power flow simulations are made using Matlab/MATPOWER toolbox. The representative numerical results are given in Table 3-1.

3.5.1.2 **Scenario 2: a large off-outage area**

In this scenario, the distribution network shown in Fig. 3-5 is considered, where fault F2 occurs on substation 601. Once this fault is isolated, all the feeders connected to substation 601 will be unsupplied. The scalability of the proposed multi-step formulation in comparison with the dynamic formulation is better understood in this scenario with such a huge outage area. The dynamic formulation in this scenario ends up with 1521 binary variables. The available computing facilities cannot solve this complex optimization problem and it failed to provide even a single feasible solution. However, with the proposed multi-step formulation, the number of binary variables is reduced to 396 variables. As reported in Table 3-2, the optimal solution is obtained with the same computing facilities in 10.46 minutes only. It shows that the proposed formulation can be applied efficiently to large-scale outages in distribution networks. The numerical results of Table 3-2 related to the voltage and current profiles are obtained using

Table 3-2. Optimal restoration results in case of fault scenario 2.

Scenario	Step number	Switching actions	F^{sw} (min)	F^{re} (p.u.)	Computation time (min)	Min. voltage (p.u.)	Max. voltage (p.u.)	Min. current margin (p.u.)
2	Step1	I. Open feeder breakers{B3,B4,B5,B6}, switch 12-13 ,and load breakers{3,4,6,7,9,10,12,20} II. Close {T4,T8}	7.5	664.98	10.46	0.9219 p.u. at node 46	1.05 p.u. at node 59	2.82 p.u. on line 502-65
	Step2	I. Open switch 31-42 and load breakers {13,31,33,34,35,36,37,38,41, 42,44} II. Close {T3,T9}, feeder breaker B6,and switch12-13	8					

posteriori power flow simulations in the same way as explained for scenario 1. These results validate the feasibility of the obtained solution regarding the security constraints.

As reported in Table 3-2, the reliability objective value is equal to 664.98 p.u. This value increases to 967 p.u. if only a single reconfiguration step is allowed. This shows that the proposed multi-step reconfiguration problem improves the quality of the restoration problem with respect to the static approaches especially in cases with large off-outage area. The switching operations of each reconfiguration step are reported in Table 3-2 and the timing sketch of this restoration plan is shown in Fig. 3-8. As mentioned in section 3.3.2, the timing of reconfiguration steps is optimized according to the optimal sequence of DG starting and load variation.

The switching operations and the resulting configuration of each step are depicted in Fig. 3-9. Under the configuration at step 1, the parts in the out-of-service area that are coloured with purple and blue are restored through available tie-switches T4 and T8, respectively. Nodes 7 and 39 that are hosting unsupplied DG are energized at steps 1 and 2, respectively. However, due to the DG energization time constants, both of these DGs start to inject power only when the network is
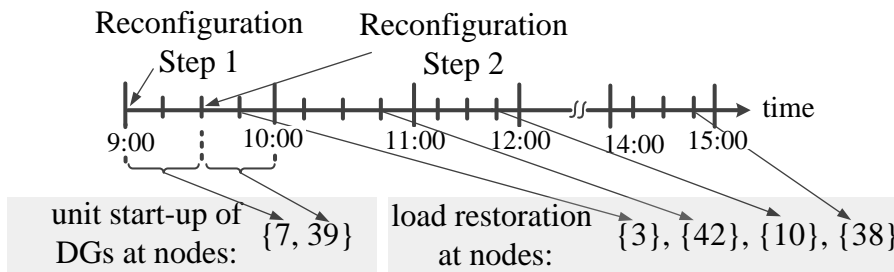
Fig. 3-8. The sketch of the timing of the restoration plan in scenario 2.
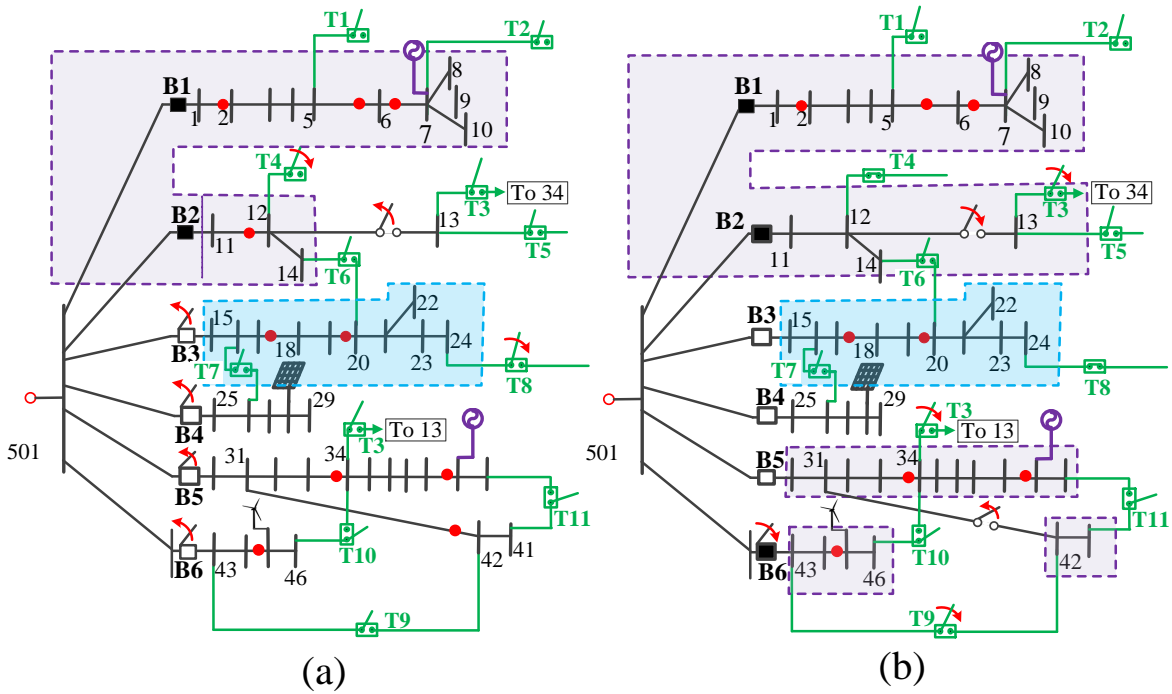
Fig. 3-9. The optimal reconfiguration scheme of test scenario 2 at a) step 1 and b) step2.

operated under the configuration at step 2. Therefore, during this time period, some of the unrestored loads can be picked up as illustrated in Fig. 3-9.b. However, feeder D is still left isolated without any supply until the end of the restorative period. As mentioned in section 3.3.2, the possibility to have such a partial restoration solution is missing in the literature, while respecting the radiality in presence of DGs.
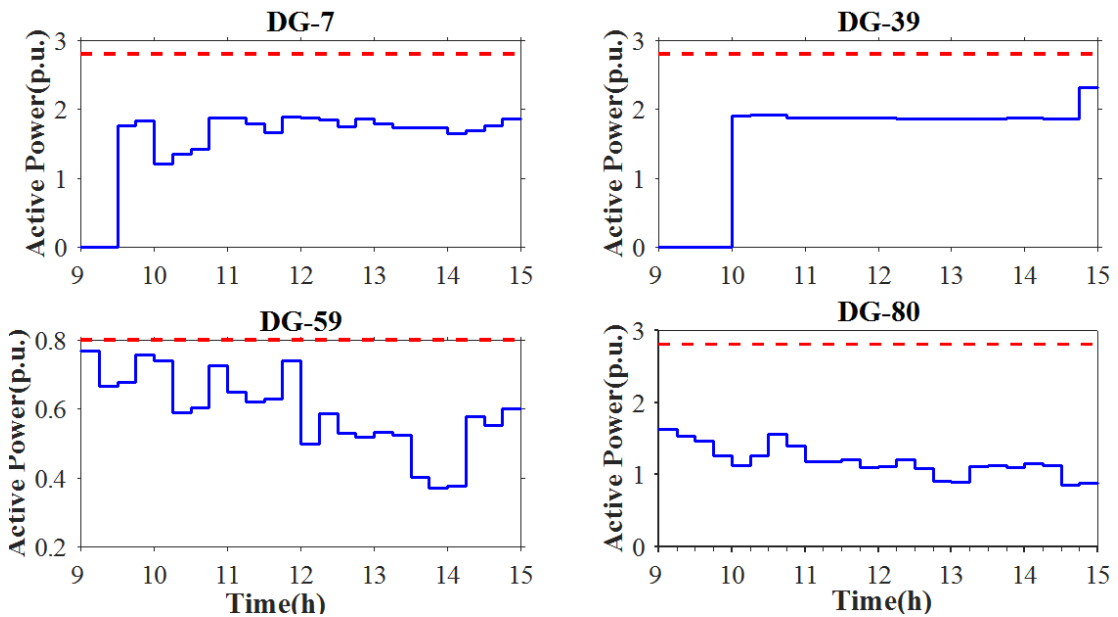
Fig. 3-10. The active power dispatch of DGs and their limits in test scenario 2.
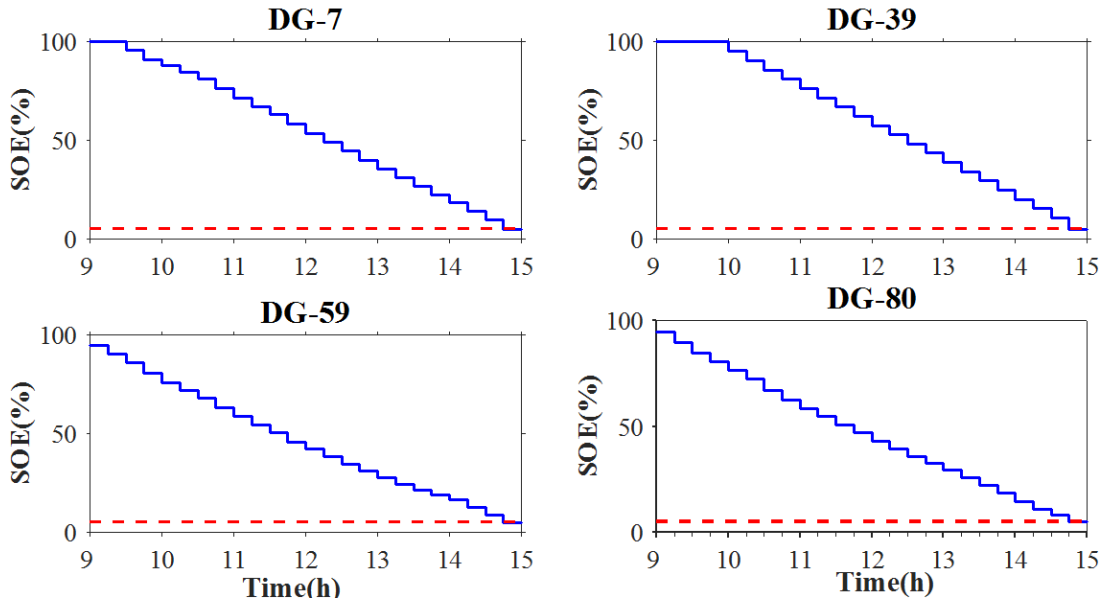
Fig. 3-11. The state of energy (SOE) of DGs and their limits in test scenario 2.

Fig. 3-10 shows the optimal DG set points according to the restoration solution. It is illustrated in Fig. 3-10 and Fig. 3-11, how the DGs contribute to the proposed restoration strategy within their power and energy capacity envelopes, respectively. As it can be seen, although nodes 7 and 39 are energized, respectively, at times 9:00 and 9:30, their hosted DGs start to inject power, respectively, from times 9:30 and 10:00 on. Fig. 3-11 shows that the State of Energy (SEO) at the end of the restorative period is above the minimum limit with a small margin. These results show that the network and DGs are operated within the safe region but very close to the limits in order to benefit at best of their capacities for the load restoration.

3.5.1.3 Scenario 3: Comparison of AR-OPF with R-OPF

In scenario 3, the distribution network shown in Fig. 3-6 is considered while fault F3 occurs. A single reconfiguration step is assumed for this scenario. In case of fault F3, switch 31-32 and breaker B3 are left open to isolate the fault. If R-OPF is used to formulate network security constraints, the solution is to restore the whole off-outage area by opening the switch on line 50-51 and close tie-switches T4 and T7 (see Table 3-3). For the obtained new configuration of the network, we run posteriori power flow simulations in order to obtain the real values of voltage and current profiles during the restorative period. The representative numerical results are reported in Table 3-3. As it can be seen, the obtained optimization solution is infeasible regarding the technical constraints (upper voltage limit violation). The voltage and current profiles in the

network at t=1:00 P.M., that are derived from the optimization problem are shown in Fig. 3-12. The voltage and current profiles obtained using posteriori power flow simulations are also shown

Table 3-3. Numerical results in case of fault F2

Scenario	Sequence of switching	Min. voltage (p.u.)	Max. voltage (p.u.)	Min. current margin (A)	CPU running time (s)
FaultF2_ Inexact OPF	I. Open switch 50-51 II. Close T4 and T7	0.940 p.u. at node 50 at t=20:00	1.068 p.u. at node 47 at t=13:00	17.75A in line 53-58 at t=20:00	11.6
FaultF2_ Exact OPF	I. Open load breaker at bus 46 II. Close T7	0.924 p.u. at node 51 at t=18:00	1.050 p.u. at nodes 69, 70 all the times	3.5A in line 53-58 at t=20:00	31.7
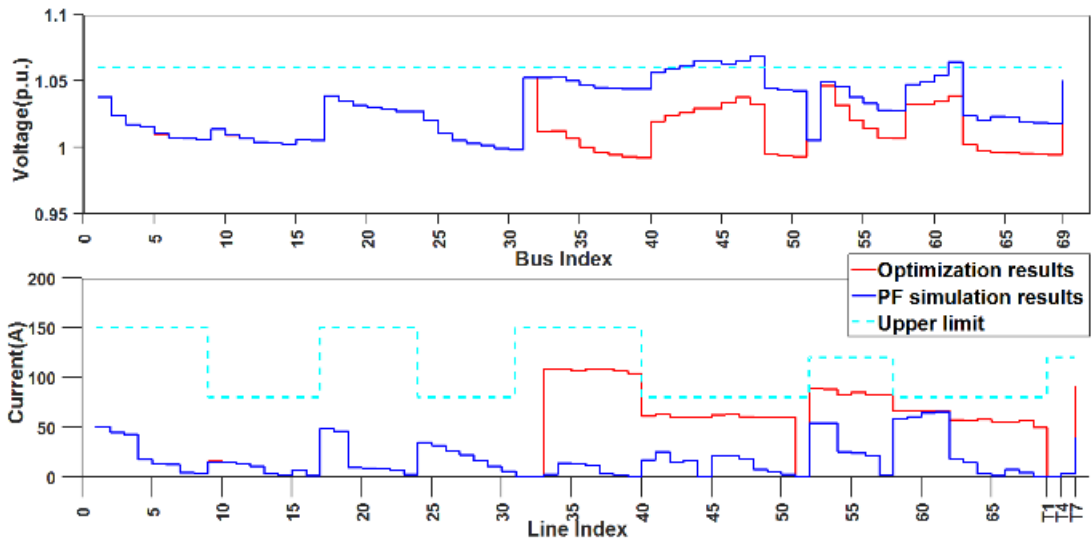
Fig. 3-12. The voltage and current profiles at t=13:00 P.M. in the new network configuration derived from the general relaxed OPF formulation and the power flow simulation.

in Fig. 3-12. As it can be seen, the line currents and voltage magnitudes resulting from the optimization problem become inexact in the off-outage area and Feeder-4 that is mainly restoring the off-outage area. The reason is that the reverse power flow injected by intermittent DGs at nodes 46, 47, and 61 causes the upper voltage limit to be binding and, consequently, leading to an inexact solution.

Now, if the modified OPF relaxation method is used, the results are according to the last row of Table 3-3. As it can be seen, the LV network at node 49 (including the connected DG) is rejected to limit the reverse power flow at the substation node. As validated by a posteriori power

flow simulation reported in Table 3-3, this solution is feasible regarding the technical constraints (voltage and current limits) all over the network during the restorative period. The voltage and
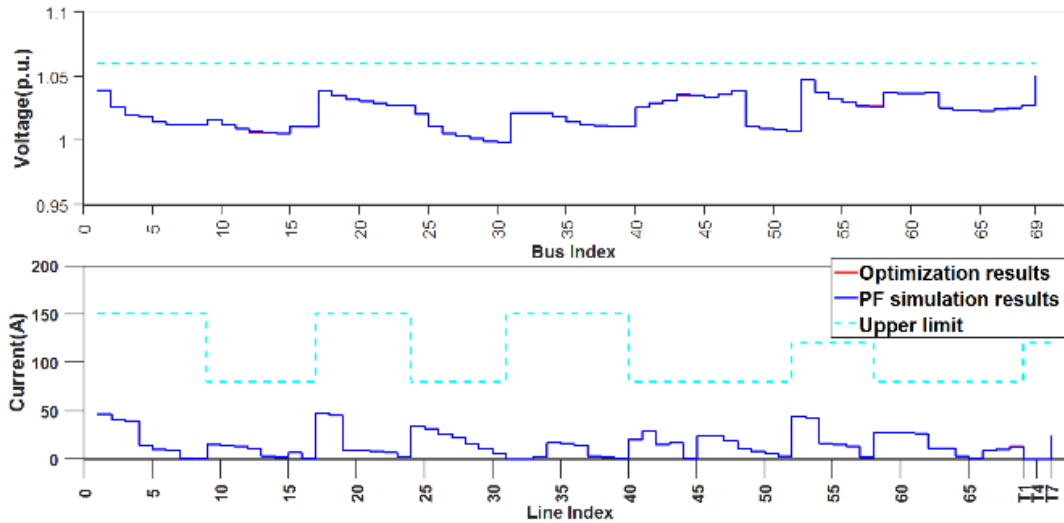
Fig. 3-13. The voltage and current profiles at t=13:00 P.M. in the new network configuration derived from the modified OPF formulation and the power flow simulation

current profiles at t=1:00 P.M. (when the voltage violates the upper limit with the inexact restoration solution) using the modified OPF formulation and the posteriori power flow simulation are shown in Fig. 3-13. As it can be seen, the profiles are matching the exact results derived from the power flow simulation.

3.6 Conclusion and summary

The aim of this chapter is to modify the restoration strategy presented in chapter 2 such that it can be applied for active distribution networks. From one hand, the restoration problem as formulated in chapter 2 cannot handle some of the requirements concerning the start-up process of disconnected DGs. These requirements include the energization of DG hosting node and the time duration of the DG start-up process. From the other hand, as shown in [83], the relaxed OPF formulation used in chapter 2 fails to be exact in the case of networks with high DG penetrations. Therefore, the restoration strategy as defined and formulated for passive distribution networks cannot be applied for active distribution networks. In this regard, the main motivation of this chapter is to propose a new restoration I) strategy and II) formulation such that the optimal dispatch of DGs can be integrated into the restoration problem considering specific DG characteristics.

In this chapter, first, a multi-step strategy is proposed for the restoration problem as a compromise between the static and dynamic approaches, which already exist in the literature. Then, this model is formulated as a MISOCP optimization problem. The start-up requirements of grid-connected DGs are accurately modeled and integrated into the proposed formulation for the restoration problem. In this regard, the radiality constraints would be respected in presence of DGs while accounting for partial restoration scenarios.

The second section of this chapter is assigned to the formulation of the security constraints (e.g. voltage and current limits) in the restoration of active distribution networks. This formulation should be integrated into the restoration problem in order to ensure the feasibility of the obtained solution concerning the technical constraints such as voltage and current limits. In this regard, a recently published method for exact convex formulation of the OPF problem is incorporated making the restoration problem robust particularly in the case of high DG penetrations.

In order to illustrate different features of the developed optimization model, it is successfully tested with two test distribution networks through three test scenarios. In the first scenario, the proposed multi-step restoration formulation is tested in case of a distribution network with a small off-outage area. Then the static and dynamic approaches are implemented on the same case study. The comparison of results confirms the superiority of the proposed multi-step restoration model with respect to the static and dynamic approaches in terms of the solution quality and computation time.

The second scenario illustrates the functionality of the proposed restoration formulation in solving large-scale optimization problems. In this regard, the optimal restoration plan is derived within a reasonable computation time in case of a fault scenario with a huge off-outage area. Finally, scenario 3 verifies the exactness of the obtained solution with reference to the relaxation that is used in the power flow formulation. In this regard, it is illustrated that the general relaxation method presented in chapter 2 fails to be exact in presence of high DG penetrations.

In summary, this chapter presents a mathematical formulation for the restoration problem complying with the DG integration requirements. However, the application of the proposed multi-step reconfiguration problem is not limited to consider only the starting process of DGs in the service restoration. This formulation is applicable when it is desired to consider the effect of

any time-dependent process existing in active distribution networks on the solution of the restoration problem.

4 A Novel Solution Algorithm for the Restoration Problem in Distribution Networks

Chapter Highlights:

We aim in this chapter to propose a solution strategy making the multi-period restoration problem tractable for analytical solvers in case of a grid of realistic size. The link between the line switching variables and the power flow model inhibits the use of classical Benders algorithm in decomposing the restoration problem. Therefore, we present a modification to the combinatorial Benders method so that it can be used for the multi-period restoration problem. According to the proposed modifications, in the outer level, the master problem solves an optimization problem in the form of Mixed-Integer Linear Programming (MILP) including line switching variables and load pickup variables. In the inner level, the value of line switching variables are fixed to the ones obtained from the master problem and the load pickup variables are optimized subject to the relaxed AC power flow constraints. The resulting sub problem is in the form of a MISOCP. This problem is broken down into several independent problems with smaller sizes. It makes the sub problem tractable in case of large-scale distribution networks. The solution of the sub problem is used to augment the feasibility or optimality cuts of the master problem. This algorithm is repeated through successive iterations until a solution with a desired level of optimality is obtained. The results indicate that the proposed decomposition algorithm provides, within a short time (after a few iterations), a restoration solution with a quality that is close to the proven optimality, when it can be exhibited.

4.1 Chapter Organization

The first part of the chapter illustrates the motivation of presenting this chapter according to the context of the whole thesis. Section 4.3 is devoted to the literature review on the existing solution approaches for the restoration problem. The standard combinatorial Benders method is reviewed in section 4.4. This method is the basis for the proposed decomposition strategy that is presented in section 4.5. In this section, first, the formulation of the multi-period restoration problem is reviewed and presented in the form of an integrated formulation. Then, the Modified Combinatorial Bender (MCB) method is described and applied to the restoration problem. Section 4.6 provides three test studies verifying the superiority of the proposed decomposition approach with respect to the integrated approach. Finally, section 4.7 concludes the chapter with final remarks concerning the main contributions presented in this chapter.

4.2 Motivation

In the previous chapters, we derived, first, a mathematical formulation for the restoration problem in passive distribution networks. This model was then augmented step-by-step by the model of different control facilities in active distribution networks. The integration of these actions results in a more efficient restoration solution. However, this leads to a huge and intractable optimization problem, especially in case of a grid of realistic size. From the other hand, the restoration problem corresponds to an emergency situation in the operation of distribution networks. Under these emergency conditions, it is required to provide a feasible and good-enough solution in a reasonable time complying with standards regarding customer interruption limits. In this regard, a solution approach is needed that makes the restoration formulation tractable for analytical solvers in case of a grid of realistic size in a multi-period optimization problem.

The restoration problem is, by nature, a mixed integer and non-linear optimization problem, respectively, due to the switching decisions and the AC power flow formulation. The link between these two parts involves logical implications that can be modelled using big-M coefficients. The presence of these coefficients makes the functionality of the branch-and-bound method in solving mixed-integer problems very poor in terms of computation burden. Moreover, this link inhibits the use of classical Benders algorithm in decomposing the problem, since the resulting cuts will still depend on the big-M coefficients. In this chapter, a novel decomposition approach is proposed for solving the restoration problem named **M**odified **C**ombinatorial

Benders (MCB). In this regard, the restoration problem is decomposed into master and sub problems, where line switching variables and the relaxed AC power flow model are handled separately. These master and sub problems are solved through successive iterations.

4.3   State-of-the-art of the solution approaches for the restoration problem

As mentioned in chapter 2, the mathematical programming started to be an option for solving the restoration problem shortly after that some convex relaxation methods were proposed for the OPF problem. The convexity of these power flow formulations allows finding a solution with proven optimality up to the desired accuracy. However, the computation burden of the resulting optimization problem could be intractable depending on the dimension of the distribution network. This drawback inhibits the use of mathematical programming methods to tackle the restoration problem as a multi-period and/or multi-scenario optimization problem.

In order to address this problem, different studies proposed decomposition methods. Some of them account for the uncertainty of load demands and DG injections using stochastic or robust optimization [5], [62], [88]–[90]. They proposed decomposition algorithms where the innermost problem is assigned to find the worst realization of uncertain parameters given a fixed radial configuration. In the uppermost level, the deterministic restoration problem is solved while fixing the uncertain parameters to their worst-case realizations found in the inner level problem. For solving this decomposed restoration problem, different solution approaches have been applied. Among the most important ones are stochastic rolling-horizon optimization method [62], Information Gap Decision Theory [5], and column-and-constraint generation algorithm [89], [90].

The restoration strategy should consider the time-varying loads in order to provide a unique configuration valid throughout the whole restorative period. Actually, none of the above-mentioned papers accounts for the time-varying loads. If those decomposition algorithms are used for solving a such multi-period optimization problem, the deterministic restoration problem in the uppermost level will be computationally intractable. In this regard, papers [69], [70], [91] propose to partition the time window of the optimization problem in clusters with similar load levels. Then, the reconfiguration problem is solved sequentially for each cluster of time instants. The weakness of this strategy is that the solution at a given sequence is not influenced by the

future sequences during the rest of the optimization process. Therefore, this approach cannot be applied to solve multi-period restoration problems (such as the one studied in this chapter), where the feasible and optimal solution at one time step depends on the solution of the problem in the previous and next steps.

In order to relax the computation burden of the multi-period restoration problems, the authors in [92] propose to solve the problem in two stages. In the first stage, the new network configuration is determined using a heuristic approach. The set of loads to be restored and the outputs of energy sources are determined in the second stage while fixing the network topology to the one obtained in the first stage. The optimization problems in the first and second stages, which are referred as reconfiguration problem and load pickup problem, respectively, are mutually interdependent. The decoupling of these two problems as proposed in [92] could lead either to no feasible solution or to a solution very far the optimal one.

Another approach that is widely employed in the literature for relaxing the computation burden of the multi-period restoration problem is to use linear load flow formulation instead of the original and non-linear formulation [88], [91], [93]. Since in the restoration strategy, the reconfigured network could be operated very close to its capacity envelop, applying the linear load flow model may result in an infeasible solution regarding the network security constraints (e.g. voltage and current limits).

In order to address all the afore-mentioned weaknesses, we propose a modification to the combinatorial Benders method so that it can be used for the multi-period restoration problem while considering case studies of realistic size. Combinatorial Benders method was firstly proposed by Hooker for solving optimization problems which include conditional constraints [94]. This method has been used in many different applications such as in circuit verification problems [95], map labeling problem [96] and asymmetric travelling salesman problem [97]. Compared with the state-of-the-art, the major contributions presented in this chapter are the following:

- A novel decomposition approach is proposed for the restoration problem while considering inter-temporal constraints (e.g. varying loads) and control actions (e.g. DG power set points). The original problem is in the form of a multi-period, mixed integer, and non-linear optimization problem. Thanks to the proposed decomposition approach, the restoration

problem is made tractable for analytical solvers in case of a grid of realistic size in a multi-period optimization problem.

• The standard combinatorial Benders method is augmented with new cuts identifying binary variable combinations that are either infeasible or non-optimal. In this regard, the proposed cuts distil the search space of the optimization problem at a given iteration into a smaller subset that includes the global optimal solution. Therefore, compared with the standard combinatorial Benders, the proposed MCB approach converges in less number of iterations.

• A convex AC-power flow formulation is integrated into the decomposed formulation proposed for the restoration problem in order to accurately model the electrical operational constraints (e.g. voltage and current limits).

4.4 Standard combinatorial benders method

Combinatorial Benders method was originally proposed in [97] to solve optimization problems in the form of MIP which involve conditional constraints. Let P be a MIP problem with the following structure:

$$P := \min_{Y,\phi} e^T Y \tag{4-1.a}$$

Subject to:

$$AY \geq a \tag{4-1.b}$$

$$if \quad \eta_\sigma(Y) = 1 \quad then \quad D_\sigma \phi \geq c_\sigma, \qquad \forall \sigma = 1,2,\dots,\sigma_{max} \tag{4-1.c}$$

$$B\phi \geq b \tag{4-1.d}$$

where, Y [1] and ϕ are vectors of binary and continuous variables, respectively. The other notations used in (4-1) are matrices (the ones in capital letter) or vectors (the ones in small letter) of parameters.

As expressed in (4-1.a), the continuous variables ϕ do not contribute to the objective function. They are only used to add feasibility properties to the solution space of the Y variables. This role of the continuous variables ϕ is amended into the optimization problem using (4-1.c) in the form conditional constraints. They mean that if a certain condition on Y variables holds ($\eta_\sigma(Y) = 1$), a constraint on ϕ variables is added to the optimization problem.

---

[1] In this chapter, all the capital letter represent matrix of parameters, except Y and L, which are vectors of binary variables as they were represented in previous chapters.

The usual way for modelling such conditional constraints is to use the famous big-M method. This method is formulated in (4-1.e), where a large positive coefficient M is introduced in order to activate/deactivate a given conditional constraint.

$$D_\sigma \phi \geq c_\sigma - M(1 - \eta_\sigma(y)), \qquad \forall \sigma = 1,2,\ldots,\sigma_{max} \qquad \text{(4-1.e)}$$

Although ϕ variables are just artificial variables, we face a large optimization problem to solve, involving both Y and ϕ variables. Moreover, due to the presence of the big-M coefficients, the relaxation of the resulting MIP model using branch-and-bound method is typically very poor. In principle, the solution space in terms of Y variables is only marginally affected by ϕ variables using the conditional constraint (4-1.c). However, when we apply the branch-and-bound method, the analytical solver at each decision branch should handle the burden of all additional constraints and variables in (4-1.d) and (4-1.e), although they are effective only in the case where the logical expression $\eta_\sigma(Y)$ is equal to 1.

A general and very usual approach to cope with non-tractable optimization problems is to use the Benders' decomposition method [5]. However, the Bender's cuts are weak for such MIP models and they still depend on the big-M values. Actually, the classical Benders' approach can only improve the computation time of an optimization problem. It cannot improve the quality of the final solution.

The main idea behind developing the combinatorial Benders method was to remove the model dependency on the big-M coefficients. According to this method, the optimization problem P given in (4-1) is decomposed into a master and a sub problem, which are solved through successive iterations.

4.4.1 Master problem

In (4-2.a) - (4-2.c), the master problem at iteration q ($\mathbb{M}^{(q)}$) is formulated the same as the original problem P while removing the continuous variables ϕ and associated constraints (4-1.c) and (4-1.d). Instead, it includes *Combinatorial Benders' (CB) cuts* expressed in (4-2.c). Thanks to these CB cuts, we work in the master problem only on the space of binary variables Y. In this sense, the master problem is in the form of an Integer Linear Programming (ILP).

$$\mathbb{M}^{(q)} := \min_{Y} e^T Y \qquad \text{(4-2.a)}$$

Subject to:

$$AY \geq a \tag{4-2.b}$$

$$\sum_{\sigma \in \Upsilon^{(k)}:\eta_\sigma(Y^{(k)})=1} (1 - \eta_\sigma(Y)) \geq 1 \qquad \forall k = 1, \dots, q-1 \tag{4-2.c}$$

where, $\Upsilon^{(k)} \subset \{1,2,\dots,\sigma_{max}\}$ induces a *Minimal Infeasible Subset (MIS)* of indices σ used in the conditional constraint (4-1.c). Corresponding to a given value of binary variables $Y^{(k)}$, MIS denotes an irreducible subset of activated constraints in (4-1.c) that lead to no feasible solution for the continuous variable ϕ. In other words, the following subsystem[1] of the original optimization problem P has no feasible solution for variables ϕ.

$$\begin{cases} D_\sigma \phi \geq c_\sigma, & \forall \sigma \in \Upsilon^{(k)} \\ B\phi \geq b \end{cases}$$

In this regard, the binary variable combinations that activate all the constraints included in the above subsystem will result in an infeasible solution. In other words, if the value of $\eta_\sigma(Y)$ is equal to 1 for all the indices $\sigma \in \Upsilon^{(k)}$, then Y is an infeasible solution. Such infeasible binary variable combinations are removed from the solution space using CB cuts given in (4-2.c). In this regard, the developed CB cuts provide "combinatorial" information on the feasible binary variable combinations that can be "distilled" from the solution space of the original MIP model.

4.4.2 Sub problem

According to the combinatorial Benders algorithm, first, we solve the master problem (4-2.a)-(4-2.c). If this problem is infeasible, then we can conclude that the original problem P is also infeasible. Otherwise, let $Y^{(q)}$ be an optimal solution of the master Problem at the current iteration q. The next step is to solve the sub problem $\mathbb{S}(Y^{(q)})$ as formulated in the following:

$$\mathbb{S}(Y^{(q)}) := \min_{\phi,\alpha_\sigma} \sum_{\sigma=1}^{\sigma_{max}} \alpha_\sigma \tag{4-3.a}$$

Subject to:

$$D_\sigma \phi + \alpha_\sigma \geq c_\sigma - M(1 - \eta_\sigma(Y^{(q)})) \qquad \forall \sigma = 1,2,\dots,\sigma_{max} \tag{4-3.b}$$

$$\alpha_\sigma \geq 0 \qquad \forall \sigma = 1,2,\dots,\sigma_{max} \tag{4-3.c}$$

$$B\phi \geq b \tag{4-3.c}$$

---

[1] This term of "subsystem" will be referred as the "sub problem" in the continue of this chapter.

The sub problem evaluates the feasibility of the obtained solution $Y^{(q)}$ in terms of the constraints on the continuous variables ϕ, i.e. (4-1.c) and (4-1.d). This feasibility is evaluated in (4-3.b) adding auxiliary and positive variables α_σ to the conditional constraints of the original problem (4-1.e). If the solution obtained from the master problem $Y^{(q)}$ is a feasible solution for the original problem P, then the optimal objective function of the sub problem $\mathbb{S}(Y^{(q)})$ equals to zero. In this case, $Y^{(q)}$ is obviously the optimal solution of P. Otherwise, if $\mathbb{S}(Y^{(q)})$ leads to a non-zero objective function, it means that the solution of the master problem $Y^{(q)}$ is an infeasible solution for the original problem P. In this case, the CB cut formulated in (4-2.c) will be added to the master problem for the next iterations to remove the corresponding set of infeasible binary variables from the solution space. In order to construct the CB cuts, we should look for one or more MISs ($\Upsilon^{(k)}$) corresponding to a given infeasible solution $Y^{(q)}$.
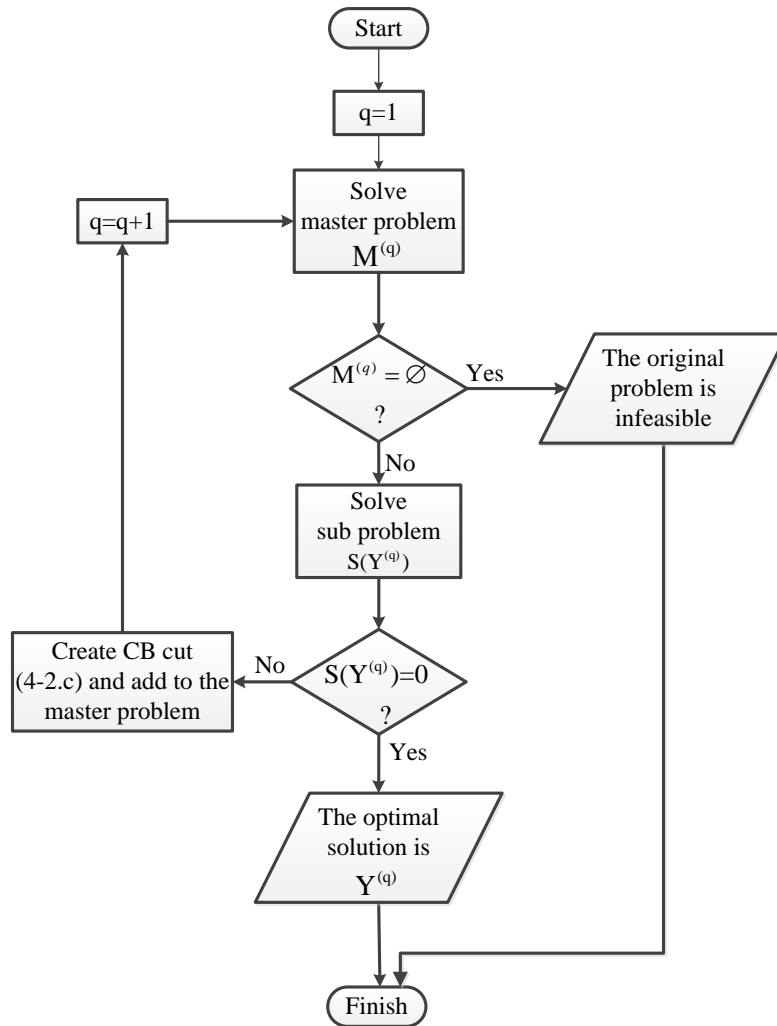
Fig. 4-1. The flowchart of the combinatorial Benders algorithm

Iterating the procedure of solving the master and sub problems, as explained above, produces an exact solution method in the same spirit as the classical Benders' decomposition method. This approach automatically produces a sequence of CB cuts, which try to shape the feasible solution space of the binary variables Y in a purely combinatorial fashion. Each CB cut acts as a tool to distill more and more the feasible solution space from the original one. As it can be noticed, thanks to the proposed technique, the role of the big-M coefficients in solving the MIP model vanishes. The algorithm of the combinatorial benders algorithm is described in the flowchart shown in Fig. 4-1.

4.5 Modified Combinatorial Benders (MCB) applied to the multi-period restoration problem

In this section, we present a modified version of the combinatorial benders method explained in section 4.4 so that it can be used for the multi-period restoration problem. In this regard, first we review the mathematical formulation of the restoration problem in distribution networks.

4.5.1 Integrated model of the restoration problem

After a failure in a radial distribution network, once the fault is isolated, the area downstream to the fault place remains unsupplied. This area is called *off-outage area*. The aim of the restoration operation is to restore the maximum energy of loads within this off-outage area while minimizing the total switching operation time [4]. In order to achieve this goal in passive distribution networks, the only possible action is to transfer the unsupplied loads to the healthy neighboring feeders (Fig. 4-2.). This reconfiguration is deployed through changing the status of normally-closed (*sectionalizing*) and normally-open (*tie*) switches. The resulting new configuration of the network remains for a so-called *restorative period* that starts from the fault
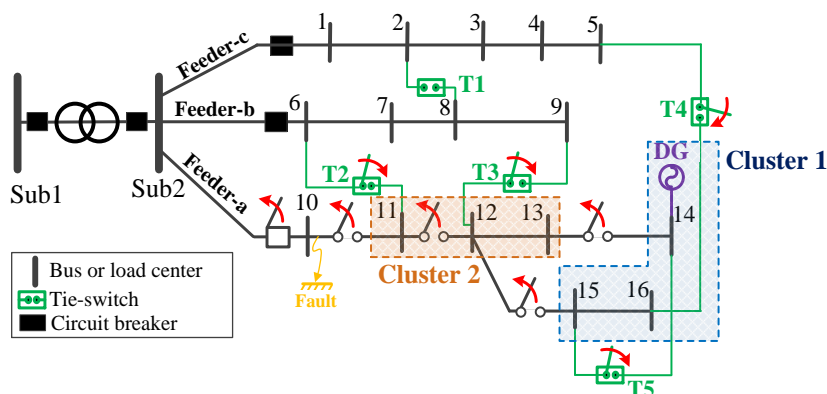
Fig. 4-2. A simple distribution network under post fault conditions.

isolation instant until the time when the faulted element is repaired.

The restoration problem encompasses three groups of decision variables namely, I) the binary variables Y_{ij} represent the energization status of line switch ij, II) the binary variables $L_{i,t}$ account for the status of the load at node i at time t, III) and the continuous variables $P_{i,t}^{DG}/Q_{i,t}^{DG}$ are associated to the active/reactive power set points of DG at node i at time t. The targeted restoration strategy is a multi-period optimization problem in the sense that the decision for the load pickup and DG power set points varies with time. The line switching variables (Y_{ij}) do not vary with time, since it is aimed to provide a single new network configuration for the whole restorative period.

$$\text{Minimize:} \qquad F^{obj} = W_{re}.F^{re} + W_{sw}.F^{sw} + W_{op}.F^{op} \qquad (4\text{-}4.a)$$

Where:

$$\begin{cases} F^{re} = \sum_{t} \sum_{i \in N} D_i.\left(1 - L_{i,t}\right).P_{i,t}^{D} \\[2mm] F^{sw} = \sum_{(i,j) \in W_{tie}^{S}} Y_{ij}.\lambda_{ij} + \sum_{(i,j) \in W_{sec}^{S}} (1 - Y_{ij}).\lambda_{ij} \\[2mm] F^{op} = \sum_{t} \sum_{(i,j) \in W} r_{ij}.F_{ij,t} \end{cases}$$

subject to:

$$\begin{cases} 0 \le Z_{ij} \le 1 & \forall(i,j) \in W^{S} \\ Z_{ij} + Z_{ji} = Y_{ij}, & \forall(i,j) \in W^{S} \\ Z_{ij} = Y_{ij}, Z_{ji} = 0, & \forall(i,j) \in W_{ava}^{S} \end{cases} \qquad (4\text{-}4.b)$$

$$\begin{cases} X_i = \sum_{j:(i,j) \in W^{*}} Z_{ji} \le 1, & \forall i \in N^{*} \\ X_i = 1, & \forall i \in N \backslash N^{*} \end{cases} \qquad (4\text{-}4.c)$$

$$\begin{cases} L_{i,t} \le N_i, & \forall i \in N^{*}, \forall t \\ L_{i,t} = 1, & \forall i \in N \backslash N^{*}, \forall t \end{cases} \qquad (4\text{-}4.d)$$

$$0 \le L_{i,t-1} \le L_{i,t} \le 1 \qquad \qquad \forall i \in N \backslash N^{*}, \forall t \quad (4\text{-}4.e)$$

$$-M.\left(1 - Y_{ij}\right) \le V_{i,t} - V_{j,t} - 2\left(r_{ij}.p_{ij,t} + x_{ij}.q_{ij,t}\right) \le M.\left(1 - Y_{ij}\right)$$

$$\forall ij \in W, \forall t \qquad (4\text{-}4.f)$$

$$
\begin{cases}
p_{ij,t} = \left(\sum_{\substack{i^* \neq i \\ (i^*,j) \in W}} p_{ji^*,t} \right) + r_{ij}. F_{ij,t} + L_{i,t}. P^D_{j,t} - P^{inj}_{j,t} \\[2em]
q_{ij,t} = \left(\sum_{\substack{i^* \neq i \\ (i^*,j) \in W}} q_{ji^*,t} \right) + x_{ij}. F_{ij,t} + L_{i,t}. Q^D_{j,t} - Q^{inj}_{j,t}
\end{cases}
\qquad \forall ij \in W, \forall t \qquad (4\text{-}4.\text{g})
$$

$$
\left\| \begin{matrix} 2p_{ij,t} \\ 2q_{ij,t} \\ F_{ij,t} - V_{i,t} \end{matrix} \right\|_2 \leq F_{ij,t} + V_{i,t} \qquad\qquad \forall (i,j) \in W, \forall t \qquad (4\text{-}4.\text{h})
$$

$$
\begin{cases}
0 \leq P^{inj}_{i,t} \leq P^{inj}_{i,max} \\[0.8em]
\left\| \begin{matrix} P^{inj}_{i,t} \\ Q^{inj}_{i,t} \end{matrix} \right\|_2 \leq S^{inj}_{i,max}
\end{cases}
\qquad\qquad \forall i \in \Omega_{DG} \cap N, \forall t \qquad (4\text{-}4.\text{i})
$$

$$
\begin{cases}
0 \leq F_{ij,t} \leq Y_{ij}. f^{max2}_{ij} \\
-M. Y_{ij} \leq p_{ij,t} \leq M. Y_{ij} \\
-M. Y_{ij} \leq q_{ij,t} \leq M. Y_{ij}
\end{cases}
\qquad\qquad \forall ij \in W, \forall t \qquad (4\text{-}4.\text{j})
$$

$$
v^{min2}. X_i \leq V_{i,t} \leq v^{max2}. X_i \qquad\qquad \forall i \in N, \forall t \qquad (4\text{-}4.\text{k})
$$

The objective function (4-4.a) tends to minimize the weighted total costs associated with the reliability (F^{re}), switching (F^{sw}), and operational (F^{op}) objectives, in decreasing order of priority. This hierarchical priority is enabled using $\epsilon-constraint$ method [53]. The reliability cost is the total energy not supplied of the loads, while accounting for their importance factors. The switching cost is formulated as the summation of two sub terms associated with the total operation time of tie-switches and sectionalizing switches, respectively. Finally, the least priority objective term is the operational term formulated as the total active power loss. As the formulation of the restoration problem is not the focus of this chapter, only a very brief description of constraints (4-4) will be provided in the following. The readers are recommended to go through chapter 2 for detailed explanation.

Constraints (4-4.b) and (4-4.c) model the reconfiguration problem ensuring the radial topology of the network. Constraints (4-4.d)-(4-4.e) formulate the load pickup problem. For an energized node i in the off-outage area ($X_i = 1$), a decision is made in (4-4.d) with binary variable $L_{i,t}$, indicating if its load is restored at time t or rejected (1/0). As formulated in (4-4.e), it is assumed that once a given load is restored at a given time, no further interruption is permitted during the subsequent time slots of the restorative period. The electrical constraints are presented in (4-4.f)-(4-4.i) using a relaxed power flow formulation [26]. The aim of this part is to dispatch the

active/reactive power set points of DGs, while respecting all the security constraints in the reconfigured network. The line switching variables are linked to the AC power flow formulation in (4-4.j) and (4-4.k) using variables Y_{ij} and X_i, respectively. These links inhibit the use of classical Benders algorithm in decomposing the problem because the resulting cuts will still depend on the big-M coefficients used in (4-4.j) and (4-4.k).

In the subsequent discussion, it is aimed to present a tractable approach for solving the restoration problem in a multi-period optimization environment. In this respect, the following compact form of the restoration model will be used to represent the above extensive formulation.

$$P := \min_{L,Y,\phi,u} \sum_{i \in N^*} f_i(1 - L_i) + \sum_{ij \in W^*} e_{ij} Y_{ij} + \sum_{ij \in W} d_{ij} \phi_{ij} \tag{4-5.a}$$

subject to:

$$\mathbb{C}_1(L, Y) \neq \emptyset \tag{4-5.b}$$

$$\mathbb{C}_2(L, Y, \phi, u) \neq \emptyset \tag{4-5.c}$$

where:

$$\tag{4-6.a}$$

$$\mathbb{C}_1(L,Y) := \begin{cases} Y \in \Gamma \\ AL \geq a \\ BY + CL \geq b \end{cases} \tag{4-6.b}$$

$$\tag{4-6.c}$$

$$\mathbb{C}_2(L,Y,\phi,u) := \begin{cases} if \quad \eta_\sigma(Y) = 1 \quad then \quad D_\sigma \phi \geq c_\sigma, & \forall \sigma = 1,2,\ldots,\sigma_{max} \quad (4\text{-}7.a) \\ E\phi = JL - Fu & (4\text{-}7.b) \\ \|G\phi_{ij}\| \leq g^T \phi_{ij}, & \forall ij \in W & (4\text{-}7.c) \\ \|Hu_i\| \leq h_i, & \forall i \in \Omega_{DG} & (4\text{-}7.d) \end{cases}$$

where, Y and L are vectors of binary variables indicating, respectively, line switching variables (Y_{ij}) and load pickup variables ($L_{i,t}$). Continuous variables are represented by vectors u and ϕ, which refer, respectively, to the DG power set point variables ($P_{i,t}^{DG}/Q_{i,t}^{DG}$), and the rest of state variables related to the optimal power flow formulation at each time t (such as $V_{i,t}, F_{ij,t}, \ldots$).

The three terms of (4-1.a) represent, respectively, the reliability, switching, and operational objective terms formulated in (4-4.a). $\mathbb{C}_1$ is expressed in (4-6) as the set of constraints only on the binary variables (L and Y). In (4-6.a), Γ is the set of radial network configurations described by (4-4.b) and (4-4.c). Constraint (4-6.b) accounts for (4-4.e) as the load pickup formulation.

Constraint (4-6.c) represents (4-4.d) as the link between reconfiguration and load pickup problems.

As given in (4-7), $\mathbb{C}_2$ represents the power flow formulation, which are linked to the binary variables (L and Y). This link is expressed in (4-7.a) in the form of conditional constraints, which are linearized using big-M formulation as formulated in (4-4.j) and (4-4.k). They mean that if a certain condition on Y variables holds ($\eta_\sigma(Y) = 1$), a constraint on ϕ variables is added to the optimization problem[1]. Equation (4-7.b) accounts for the voltage equation and the power balance equation given in (4-4.f) and (4-4.g), respectively. Equations (4-7.c) and (4-7.d) represent second-order constraints associated with the current flow equation (4-4.h), and DG apparent power capacity limit (4-4.i). In (4-7.d), h_i refers to the apparent power capacity of the DG at node i. The other notations used in (4-1),(4-6) and (4-7) are matrices (the ones in capital letter) or vectors (the ones in small letter) of parameters.

4.5.2 Master Problem

In this section, MCB as a novel decomposition approach is proposed for the restoration problem. In this regard, the line switching variables and the AC power flow formulation are decomposed into master and sub problems, which are solved through successive iterations. In the outer level of the proposed decomposition strategy, the master problem is solved. The master problem is the same as the original problem P while removing the AC power flow formulation ($\mathbb{C}_2$). However, the electrical constraints (e.g. voltage and current limits) are not completely disregarded as they are represented by DistFlow formulation ($\overline{\mathbb{C}_2}$).

$$\mathbb{M}^{(q)} := \min_{L,Y,\phi,u} \sum_{i \in N^*} f_i(1 - L_i) + \sum_{ij \in W^*} e_{ij} Y_{ij} \tag{4-8.a}$$

Subject to:

$$\mathbb{C}_1(L, Y) \neq \emptyset \tag{4-8.b}$$

$$\overline{\mathbb{C}_2}(L, Y, \phi, u) \neq \emptyset \tag{4-8.c}$$

$$\begin{cases} \sum_{i \in \varphi(v, Y^{(k)})} f_i(1 - L_i) \geq \mathbb{S}_v(Y^{(k)}) & : Y \in \Psi(v, Y^{(k)}), \mathbb{S}_v(Y^{(k)}) \neq \emptyset \\ Y \notin \Psi(v, Y^{(k)}) & : \mathbb{S}_v(Y^{(k)}) = \emptyset \end{cases}$$

[1] For example, if line ij is energized ($Y_{ij} = 1$), then the current flow in this line must be less than its ampacity limit ($F_{ij,t} \leq f_{ij}^{max2}$).

$$\forall v = 1, 2, \ldots, v_{max}(k), k = 1, \ldots, q - 1 \quad \text{(4-8.d)}$$

where:

$$\overline{\mathbb{C}_2}(L, Y, \phi, u) := \begin{cases} if \quad \eta_\sigma(Y) = 1 \quad then \quad D_\sigma \phi \geq c_\sigma, \quad \forall \sigma = 1, 2, \ldots, \sigma_{max} & \text{(4-9.a)} \\ E\phi = JL - Fu & \text{(4-9.b)} \\ \bar{G}^T \phi_{ij} \leq \bar{s}_{ij}, & \forall ij \in \Omega_{Sub} & \text{(4-9.c)} \\ \bar{H}^T u_i \leq \bar{h}_i, & \forall i \in \Omega_{DG} & \text{(4-9.d)} \end{cases}$$

$\overline{\mathbb{C}_2}$ is formulated in (4-9) as the set of linear DistFlow constraints linked to the binary variables. Constraints (4-9.c) and (4-9.d) are the linearized formulation of line ampacity and DG apparent power capacity limits, where $\bar{s}_{ij}$ and $\bar{h}_{ij}$ induce relaxed line ampacity limit and DG apparent power limit, respectively. The relaxed line ampacity limits $\bar{s}_{ij}$ are derived according to the strategy explained in section 4.5.3. This linearization technique is according to the technique presented in [89]. The detailed formulation of the DistFlow constraints is given in [84].

Two sets of constraints (4-8.d) are denominated as optimality cuts and feasibility cuts, respectively. These constraints represent the modified version of the Combinatorial Benders cuts introduced in [98]. The main idea behind this modification is to have recourse functions providing information not only on the feasibility of each solution but also on its optimality. As explained in section 4.4, according to the standard combinatorial Benders method, all the binary variables must be set as the complicating variables. The optimal value of these variables are found by the master problem and the sub problem just evaluates the feasibility of the solution. In case that the solution is identified by the sub problem as an infeasible solution, a cut will be added to the master problem for the next iterations to remove the corresponding set of infeasible binary variables from the solution space. In the proposed modified version, only a subset of binary variables is fixed in the sub problem and defined as the complicating variables. The other binary variables that are not fixed in the sub problem are called floating variables. In the formulation provided in (4-8) Y and L represent, respectively, complicating and floating variables. In the case where the solution of the master problem at iteration k ($Y^{(k)}$) leads to no feasible solution in the sub problem, the feasibility cuts are augmented by the second constraint of (4-8.d). If the sub problem at iteration k is feasible, its optimal solution $\mathbb{S}_v(Y^{(k)})$ is used to augment the optimality cuts according to the first constraint of (4-8.d). The constraints given in

(4-8.d) are non-convex and need to be linearized. This linearization together with the formulation of $\Psi(v, Y^{(k)})$ is provided in section 4.5.4.

$$LB^{(q)} = \mathbb{M}^{(q)} \tag{4-10}$$

As given in (4-10), the master problem $\mathbb{M}^{(q)}$ formulated in (4-8.c) provides a lower bound for the original optimization problem P expressed in (4-1). Actually, unlike in the case of AC power flow formulation in the sub problem, we incorporate electrical constraints into the master problem in a conservative fashion using DistFlow formulation. Therefore, the feasible region of $\mathbb{M}^{(q)}$ under DistFlow constraints is relaxed in comparison to the feasible region of P under AC power flow constraints.

4.5.3 Sub Problem

Once the optimal configuration is found in the master problem, the next step is to find the optimal load pickup solution, if any, for the obtained configuration subject to the AC power flow constraints. When we fix the network configuration, the topology of the off-outage area will be partitioned accordingly into several clusters. A cluster is defined as a collection of nodes and lines in the off-outage area that are supplied by only one available feeder. $\varphi(v, Y^{(k)})$ determines the index of nodes that are in cluster v. $\Psi(v, Y^{(k)})$ denotes a set of configurations which provide the same optimal load pickup solutions for the nodes in cluster v. The formulation of Ψ, optimality cuts and feasibility cuts are provided in section 4.5.4.

Consider the simple network of Fig. 4-2 as an example. The switching operations shown in this figure are assumed to represent the optimal solution found in the master problem. Under the resulting configuration, the off-outage area is partitioned in two clusters. First cluster includes nodes 14, 15 and 16 that are restored from feeder-c through tie-switch T4. The second cluster includes nodes 11, 12 and 13 that is supplied from feeder-b through tie-switches T2 and T3.

As shown in Fig. 4-2., there is no path between two nodes belonging to two different clusters except through the slack bus. We assume that the slack buses are effectively fixing the voltage set point at the top of each feeder (bus "Sub2" in Fig. 4-2.). Under this assumption, it can be said that the change of loading in one cluster (change of L variables) does not change any state variable outside that cluster except the current at the substation transformer (between buses "Sub1" and "Sub2" in Fig. 4-2.). If the ampacity limit of this substation is binding, then the optimal load pickup solution in one cluster could depend on the loading in other clusters. In order

to avoid making such a link, we should make sure that the master problem gives a network configuration under which the ampacity constraint at the substation line is not binding.

This is ensured putting a conservative ampacity limit ($\bar{s}_{ij}$) in (4-9.c), representing the substation line ampacity limit in the DistFlow formulation of the master problem. In order to find a proper $\bar{s}_{ij}$, once the master problem is solved, the current flow in the substation line is found using a power flow simulation for the obtained solution of the master problem. If this current ($\sqrt{F_{ij}}$) is beyond its ampacity limit (f_{ij}^{max}), the presumed value of $\bar{s}_{ij}$ will be modified according to the following rule:

$$\bar{s}_{ij}^{k+1} = \bar{s}_{ij}^{k} + \rho(f_{ij}^{max} - \sqrt{F_{ij}}) \tag{4-11}$$

where ρ is a penalty coefficient that must be set to a value between 0 and 1.

Using the above-mentioned strategy, the optimal values of load pickup variables in one cluster will be independent from the status of loads in the other clusters. Therefore, we solve a separate sub problem for each individual cluster. The aim is to break the computation burden of the inner level problem into several problems, which can be handled using different cores in parallel. The following MISOCP formulation models the sub problem for cluster v at iteration q, given network configuration $Y^{(q)}$.

$$\mathbb{S}_v(Y^{(q)}) := \min_{L,\phi,u} \sum_{i \in \varphi(v,Y^{(q)})} f_i(1 - L_i) + \sum_{ij \in \mathbb{E}(v,Y^{(q)})} d_{ij}\phi_{ij} \tag{4-12.a}$$

Subject to:

$$\mathbb{C}_1(L, Y^{(q)}) \neq \emptyset \tag{4-12.b}$$

$$\mathbb{C}_2(L, Y^{(q)}, \phi, u) \neq \emptyset \tag{4-12.c}$$

where, $\mathbb{E}$ denotes the index of lines within cluster v.

It should be noted that the sub problem $\mathbb{S}_v(Y^{(q)})$ incorporates only those variables that are related to the lines and nodes in cluster v. The main objective function in the sub problem is the minimization of the total energy not supplied in cluster v as formulated in (4-4.a). Since the complicating variables Y are fixed, the big-M coefficients used in (4-7.a) do not appear in the sub problem which is relaxing again the computation burden of the inner level problem with respect to the original optimization problem P given in (4-1).

$$UB^{(q)} = \sum_{v=1}^{v_{max}} \mathbb{S}_v(Y^{(q)}) \tag{4-13}$$

According to (4-13), the summation of optimal objective values $\mathbb{S}_v(Y^{(q)})$, associated with all the clusters, induce an upper bound $UB^{(q)}$ for the reliability optimal solution in the original optimization problem P (4-1). The optimal solution of the sub problem $\mathbb{S}_v(Y^{(q)})$ is also used to augment the feasibility cuts of the master problem as formulated in the first constraint of (4-8.d). In case that there is no feasible solution for the sub problem, a feasibility cut is generated and added to the master problem as formulated in the second constraint of (4-8.d).

4.5.4   Generating the optimality and feasibility cuts

At a given iteration k, if the sub problem $\mathbb{S}_v(Y^{(k)})$ has a solution, say $L^{(k)}$, then clearly, $L = L^{(k)}$ is the optimal solution of P if $Y=Y^{(k)}$. We look for Ψ as a set of Y-solutions, such that if we solve the sub problem while fixing Y variable to any point Y' in this set, no better solution than $L^{(k)}$ can be found. It means that for any $Y' \in \Psi$, $\mathbb{S}_v(Y') \geq \mathbb{S}_v(Y^{(k)})$. This constraint is formulated in the first expression of (4-8.d) and denominated as an optimality cut.

If the sub problem $\mathbb{S}_v(Y^{(k)})$ at iteration k is infeasible, then Ψ is defined as a set of Y-solutions, such that if Y variable is fixed to any other point Y' in this set, the sub problem will be still infeasible. In other words, in order to break the infeasibility, variable Y should take values outside the set of Ψ. This constraint is formulated in the second expression of (4-8.d) and referred as the feasibility cut.

Note that $\Psi(v, Y^{(k)})$ is associated with a given master problem solution $Y^{(k)}$ and also with a cluster v. Also note that the solution of the master problem, say $Y^{(k)}$, represents the network configuration and the solution of sub problem, say $L^{(k)}$, is the value of load pickup variables in cluster v. According to the definition of the optimality and feasibility cuts, in order to derive Ψ, we should find network configurations Y' that lead to no better reliability solutions in cluster v, with respect to $\mathbb{S}_v(Y^{(k)})$. The optimal solution of load pickup variables within cluster v will not improve under configuration Y' with respect to the optimal values under configuration Y if the following conditions hold:

a)   All the nodes in cluster v that were connected to each other under configuration Y (identified by $\varphi(v, Y^{(k)})$), are still connected to each other under configuration Y'.

b) The injection nodes that were supplying the nodes in cluster v under configuration Y are the same as those under configuration Y'.

Consider the test system of Fig. 4-2, as an example. As mentioned earlier, nodes 14, 15 and 16 are in the first cluster that is supplied by feeder-c through tie-switch T4 and by DG at node 5 through tie-switch T5. Tie-switches T4 and T5 are named as source lines. Source lines of cluster v are defined as the lines at the border of cluster v that are injecting active or-/and reactive power to the cluster. Considering the example shown in Fig. 4-2, assume that all the nodes in the first cluster should be restored except node 16, according to the solution of the sub problem $\mathbb{S}_v(Y^{(k)})$. Now, by changing the configuration, it is obvious that the load at node 16 still cannot be restored if a) nodes 14, 15 and 16 are still connected to each other and if b) these nodes are supplied through the same source lines (tie-switches T4 and T5).

According to two conditions mentioned above, the set $\Psi(v, Y^{(k)})$ is expressed as in (4-14).

$$\Psi(v, Y^{(k)}) = \{Y | \exists v' \le v_{max}(Y) :$$

$$\varphi(v, Y^{(k)}) \subseteq \varphi(v', Y), \mathbb{E}_s(v', Y) \subseteq \mathbb{E}_s(v, Y^{(k)})\} \qquad (4\text{-}14)$$

where, $\mathbb{E}_s$ represent the index of source lines that are injecting power to cluster v.

In order to preserve the linearity of the optimality and feasibility cuts in terms of Y variables, the two constraints expressed in (4-14) are reformulated in (4-15) and (4-16).

$$\sum_{ij \in \mathbb{E}(v, Y^{k)})} Y_{ij} = |\varphi(v, Y^{(k)})| - 1 \qquad (4\text{-}15)$$

$$Y_{ij} \le Y_{ij}^{(k)} \quad : \quad \forall ij \in \mathbb{E}_s(v, y^{(k)}) \qquad (4\text{-}16)$$

The connectivity condition mentioned in condition a) is formulated in (4-15). This constraint enforces that the number of closed lines in a given cluster v is equal to the total number of nodes in cluster v minus one. This is the tree condition for cluster v. The tree condition ensures the network connectivity if it is radial [99]. This radiality condition is ensured for a given cluster v using (4-8.b). Constraint (4-16) formulates condition b) that is mentioned above. This constraint ensures that the resource line ij of cluster v that was open under configuration $Y^{(k)}$ will stay open under any configuration $Y \in \Psi(v, y^{(k)})$.

According to the derived formulations for the set of $\Psi(v, Y^{(k)})$, the feasibility cut that was given in the second constraint of (4-8.d) is re-formulated in the following.

$$\sum_{ij\in\mathbb{E}(v,y^{k)})} Y_{ij} \leq |\varphi(v,Y^{(k)})| - 2 \tag{4-17}$$

$$\sum_{ij\in\mathbb{E}(v,Y^{(k)})} Y_{ij} \geq 1 + \sum_{ij\in\mathbb{E}(v,Y^{(k)})} Y_{ij}^{(k)} \tag{4-18}$$

where, at least one of the conditions (4-17*)* or (4-18*)* must hold.

This *either-or* constraint cannot be integrated into a convex model. Since in a convex optimization problem, all the constraints must hold. In order to integrate this either-or constraint into a convex optimization problem, binary variable θ is introduced subject to the following constraints:

$$\sum_{ij\in\mathbb{E}(v,y^{k)})} Y_{ij} \leq \left(|\varphi(v,Y^{(k)})| - 2\right) + M.\theta \tag{4-19}$$

$$M.(1 - \theta_1) + \sum_{ij\in\mathbb{E}(v,Y^{(k)})} Y_{ij} \geq 1 + \sum_{ij\in\mathbb{E}(v,Y^{(k)})} Y_{ij}^{(k)} \tag{4-20}$$

where, M is a positive and sufficiently-large number.

The auxiliary variable θ_1 determines which of the two constraints (4-17) and (4-18) must hold. According to (4-19), if $\theta_1 = 0$, (4-17) is imposed and (4-18) is relaxed. When $\theta_1 = 1$, the situation is reversed. In both cases, one of the constraints is forced to be satisfied while the other constraint may also hold.

Regarding the optimality cut, the first expression given in (4-8.d) can be translated into the following:

If constraint (4-15) and constraint (4-16) are satisfied,
then
$$\sum_{i\in\varphi(v,Y^{(k)})} f_i(1 - L_i) \geq \mathbb{S}_v\left(Y^{(k)}\right)$$
must be satisfied.

Therefore, the optimality cut is in the form of a conditional constraint. Let *"A implies B"* denote a conditional constraint, where A and B are logical expressions. This is logically equivalent to state that (*A and* $\sim$ *B)* is false, where $\sim B$ refers to the complement of *B*. The negation of (*A and* $\sim$ *B)* is equivalent to ($\sim$*A or B)*.

According to this explanation, the above-formulated conditional constraint associate with the optimality cuts is logically equivalent to the following expression:

either expression $\sim$*(4-15), or expression* $\sim$*(4-16),* *or*

$$\sum_{i\in\varphi(v,Y^{(k)})} f_i(1 - L_i) \geq \mathbb{S}_v\left(Y^{(k)}\right)$$

must hold.

It is worth to note that expressions (4-17) and (4-18) are the complements of (4-15) and (4-16), respectively. The complement of (4-16) means that at least one line $ij \in \mathbb{E}(v, Y^{(k)})$ exists such that $Y_{ij} \geq Y_{ij}^{(k)} + 1$. This expression is according to the formulation of (4-18). In this regard, the conditional constraint associated with the optimality cuts can be expressed as follows:

either expression (4-16), or expression (4-17), *or*

$$\sum_{i\in\varphi(v,Y^{(k)})} f_i(1 - L_i) \geq \mathbb{S}_v\left(Y^{(k)}\right)$$

must hold.

For the integration of this constraint into the convex optimization model, the algorithm already explained for the either-or constraints is used. As a result, the optimality cut is re-formulated as presented in the following:

$$\sum_{ij\in\mathbb{E}(v,y^{k})} Y_{ij} \leq \left(\left|\varphi\left(v, Y^{(k)}\right)\right| - 2\right) + M.\theta_2 \tag{4-21}$$

$$M.\theta_3 + \sum_{ij\in\mathbb{E}(v,Y^{(k)})} Y_{ij} \geq 1 + \sum_{ij\in\mathbb{E}(v,Y^{(k)})} Y_{ij}^{(k)} \tag{4-22}$$

$$M.(2 - \theta_2 - \theta_3) + \sum_{i\in\varphi(v,Y^{(k)})} f_i(1 - L_i) \geq \mathbb{S}_v\left(Y^{(k)}\right) \tag{4-23}$$

$$\begin{cases} \theta_2, \theta_3 \in \{0,1\} \\ \theta_2 + \theta_3 \geq 1 \end{cases} \tag{4-24}$$

where, M is a positive and sufficiently-large number.

θ_2 and θ_3 are two binary auxiliary variables, which determine which of the three constraints (4-17), (4-18), and $\sum f_i(1 - L_i) \geq \mathbb{S}_v\left(Y^{(k)}\right)$ must hold. According to (4-21), if $\theta_2 = 0$, then (4-17) is imposed. In this state, two other constraints are relaxed, since (4-24) forces θ_2 to be equal to 1. In the same way, if $\theta_2 = 0$, then (4-18) is imposed and two other constraints are

relaxed. Finally, if $\theta_2 = \theta_3 = 1$, then $\sum f_i(1 - L_i) \geq \mathbb{S}_v(Y^{(k)})$ is imposed, while (4-17) are (4-18) are relaxed.

To summarize, the overall developed formulation of the master problem is in the form of a MIL optimization problem. It is structured as follows:

$$\mathbb{M}^{(q)} := \min_{L,Y,\phi,u} \sum_{i \in N^*} f_i(1 - L_i) + \sum_{ij \in W^*} e_{ij} Y_{ij}$$

Subject to:

Network reconfiguration constraints:	(4-8.b)
Linear DistFlow constraints:	(4-8.c)
Feasibility Cuts:	(4-19), (4-20)
Optimality Cuts:	(4-21)-(4-24)

4.5.5 Modified Combinatorial Benders Algorithm

The proposed decomposition approach for solving the distribution network restoration problem is described as follows:

1- Initialize iteration number ($q \leftarrow 1$), lower bound ($LB \leftarrow 0$), upper bound ($UB \leftarrow +\infty$), and set the convergence tolerance ($\varepsilon > 0$).

2- Solve the master problem to get the optimal network configuration $Y^{(q)}$. Update the lower bound (LB $\leftarrow$ max(LB, LB$^{(q)}$)), where LB$^{(q)}$is given in (4-10).

3- Solve the sub problem for the obtained configuration $Y^{(q)}$ and for each cluster v.

    a. If the optimization problem is feasible, find the optimal load pickup variables L$^{(q)}$ and augment the optimality cuts according to the first constraint of (4-8.d). Update the upper bound (UB $\leftarrow$ min(UB, UB$^{(q)}$)), where UB$^{(q)}$is given in (4-13).

    b. If the optimization problem leads to no feasible solution, augment the feasibility cuts according to the second constraint of (4-8.d).

4- Check for convergence :

    a. If $UB - LB \leq \varepsilon_{opt}$ or if the computation time is larger than ε_{time}, then terminate the algorithm and propose the best UB solution found so far as the solution of the problem.

  b. Else, update the iteration number ($q \leftarrow q + 1$), and return to step 2.

While the iterations of the proposed algorithm are evolving, the original solution space is gradually reduced by removing more combinations of binary variables. This is realized in a conservative way using the proposed optimality and feasibility cuts. Therefore, using the MCB approach, we might not be able to converge to the global optimal solution. However, as it will be illustrated in section 4.6.1, when the MCB algorithm converges, the best solution visited so far is close to the global optimal solution, when it can be exhibited.

In order to end up with a tractable solution methodology in case of grids with realistic sizes, two stopping criteria are defined in the above-mentioned algorithm. According to this algorithm, we continue the running of iterations until the difference between the lower bound solution (LB) and the upper bound solution (UB) is lower than a threshold (ε_{opt}). In addition, we impose an additional threshold on the computation time (ε_{time}). In this regard, if the computation time is more than a threshold value, then the algorithm is stopped. The values of these thresholds (ε_{opt} and ε_{time}) are determined based on the experience of DSO.

4.6 Numerical results and discussion

In order to illustrate different features of the proposed solution algorithm for the restoration problem, two medium voltage networks shown in Fig. 4-3, and Fig. 4-4 are used. In this section, we study three test scenarios. Scenarios I and II are applied on the test network of Fig. 4-3, whereas for scenarios III, the test network of Fig. 4-4 is used.

The test network shown in Fig. 4-3 is introduced in chapter 2, section 2.7. The second test system shown in Fig. 4-4 is introduced in chapter 3, section 3.5. These test networks are modified in this chapter adding two types of DGs, namely, dispatchable and non-dispatchable DGs. The dispatchable DGs, such as the diesel generators, are controlled to deliver the active and reactive power references that are set by DNO ahead of their operation. We consider also non-dispatchable DGs such as PV and wind generators, which are modeled as voltage-independent active power injection units with zero reactive power components.

In the test network of Fig. 4-3, three dispatchable DGs on nodes 7, 39, and 80 have 2.8MW active and 3.0MVA apparent power capacities, while the DG on node 59 has 0.8MW active and 1.0MVA apparent power capacities. The non-dispatchable DGs in this test network include a PV
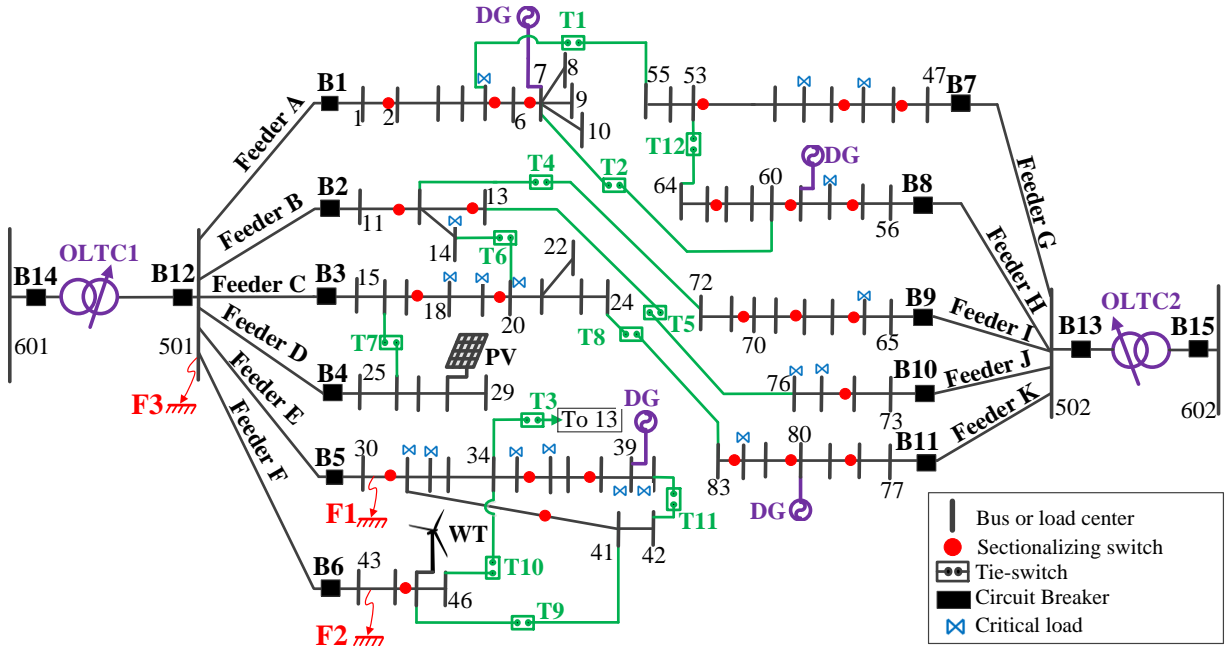
Fig. 4-3. The test distribution network for test scenarios I and II [57]

at node 28 and a Wind turbine at nodes 45, with capacities of 0.6 and 0.8 MW, respectively. In the test network of Fig. 4-4, one dispatchable DG with a capacity of 0.6 MW is installed on bus 68. In this test network, there exist three PV-based DGs at nodes 46, 47, and 61 with capacities of 0.6, 0.6 and 0.8 MW, respectively. The forecast power injections of PV- and Wind-based DGs are derived from the real data reported in [85] and [86], respectively.

The base power and energy values are assumed to 1MW, and 1MWh, respectively. The minimum and maximum voltage magnitude limits are set, respectively, to 0.917 and 1.05 p.u [52]. The hourly profiles for different types of load patterns that are used in the both test networks are given in [58]. In both test networks, it is assumed that each node is equipped with a load breaker. All the line switches are assumed manually-controlled, whereas the load breakers are all assumed remotely-controlled. The time needed for the operation of each manually controlled and remotely-controlled switch are assumed 30 and 0.5 minutes, respectively. It is assumed that the critical loads that are shown with '⋈'. in Fig. 4-3 and Fig. 4-4, have the priority factors equal to 100 while the priority factors of other loads are equal to 1.

In order to show the functionality of the proposed decomposition approach, the restoration problem in case of each case study is solved using two approaches: I) the Integrated Analytical Optimization (IAO) method, and II) the Modified Combinatorial Benders (MCB) decomposition
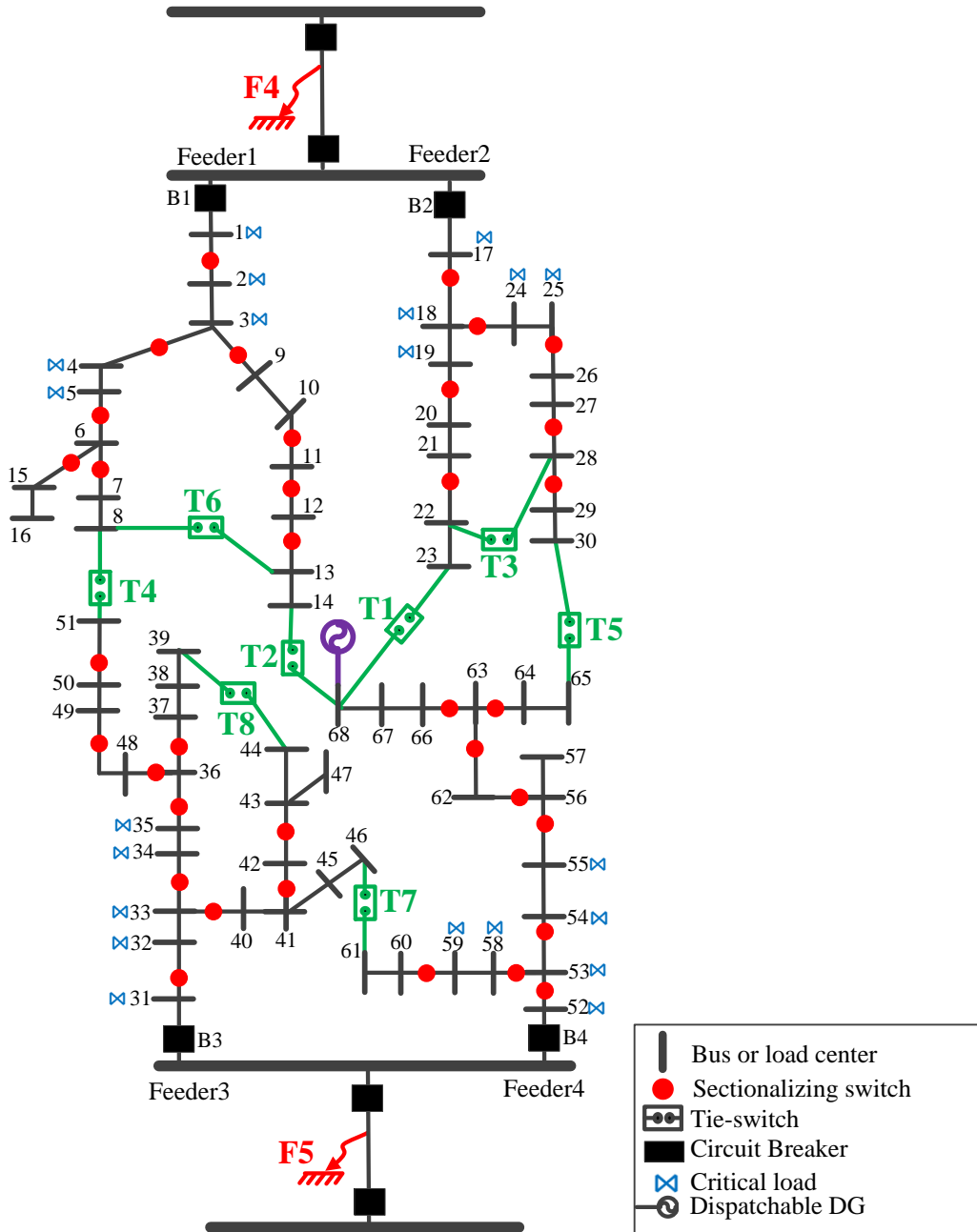
Fig. 4-4. The test network for test scenario III.

method proposed in section 4.5. According to the IAO approach, the integrated optimization problem (4-4) is solved in one shot using an analytical solver. For this aim, the Branch-and-Bound method is used to relax the integrality constraints of the original optimization problem in an iterative way. In this regard, the best integer (valid) solution that is found at any step in the algorithm is called *incumbent* solution. The objective value of this incumbent is an upper bound for the optimal solution of the original minimization problem. At any step through the Branch-and-Bound search algorithm, there is also a lower bound, called the *best-bound* solution. This

bound is obtained by taking the minimum of the optimal objective values of all the solutions obtained so far including the infeasible ones regarding the integrality constraints. The difference between the current upper and lower bounds is known as the *optimality gap.* It is said that the IAO approach converges to the optimality-proven solution, when the optimality gap is less than a desired accuracy. This accuracy is tuned in this study as 1e-10.

The comparison of MCB and IAO methods is made, applying both methods on the same PC with an Intel(R) Xeon(R) CPU and 6 GB RAM, coded in Matlab/Yalmip environment and solved using Gurobi Optimizer 8.0. The restoration problem for all the case studies is considered as a multi-period optimization problem. The restorative period is assumed from 9:00 Am until 20:00 PM. The time step resolution is chosen to be 1 hour. We assume that the optimality threshold (ε_{opt}) and the computation time threshold (ε_{time}) are set to 0.01 p.u. and 2 minutes, respectively.

4.6.1 Scenario I: a small-scale off-outage area

In scenario I, the restoration problem is solved for the test network shown in Fig. 4-3, where two faults occur at the same time on lines 30-31 (fault F1) and 43-44 (fault F2). These two faults are isolated by opening line switches {B5, 30-31} and {B6, 44-45}, respectively. The resulting off-outage area includes feeder E except node {30} and feeder F except nodes {43 and 44}. The restoration solution obtained from IAO and MCB approaches are reported in Table 4-1. In order to deploy this solution on the network, first, the "Reconfiguration Actions" must be implemented. The "Load Pickup Actions" are deployed throughout the subsequent instants of the restorative period according to the schedule given in Table 4-1. Along with these results, Table 4-1 provides the optimal values of different objective terms and the computation time.

The reliability objective term (F^{re}) is used to compare the quality of solutions provided by MCB and IAO methods[1]. In this regard, the *quality margin* of a restoration solution is defined as the difference of its reliability objective value with respect to the global optimal value of the reliability objective term. As reported in Table 4-1, the solution provided by the proposed MCB approach is 13.75% far from the global optimal solution, provided by IAO method.

The lower- and upper-bounds of the reliability objective term obtained using IAO and MCB approaches are plotted along their computation times in Fig. 4-5. In this regard, the lower and

---

[1] Since F^{re} has the largest weighting factor in the objective function, comparing the quality of the solution based on the overall objective value leads to the same result.

Table 4-1. Comparison of restoration results obtained using IAO and MCB methods in scenarios I and II.

Scenario	Solution Method	Reconfiguration Actions	Load Pickup Actions	F^{re}(p.u.)	F^{sw} (min)	Computation time (s)
I (faults F1 and F2)	IAO	I. Open switch 37-38 and load breakers {33,34,37,41,42}, and close T11 II. Close T3	-	88	92.5	2.12
	MCB	I. Open switch 35-36 and load breakers {33,34,37,38,41,42}, and close T11 II. Close T3	-	100.1	93	5.68
II (fault F3)	IAO	I. Open switches {1-2,33-34,31-41} and load breakers{2,3,4,5,6,12,13, 14,35,36,37,38,39,40,41}, and close{T3,T11} II. Close{T1,T4}	III. Close load breaker 37 at t=12 IV. Close load breaker 13 at t=19	5.97e3	219	385.3
	MCB	I. Open switches {5-6,11-12,31-41} and load breakers{1,3,12,14,15,17 ,19,20,22,25,26,27,28,29, 30,31,32,34,35,36,38,43, 44,46}, and close{T3,T7,T10} II.Close{T1,T2,T5,T8}	III. Close load breakers {3,22,25,29} at t=19 IV. Close load breaker 13 at t=20	4.13e3	313.8	45

upper bounds of the MCB algorithm refer to the solutions provided, respectively, by the master and sub problems at each iteration. Whereas, for the IAO approach, each lower and upper bound correspond, respectively, to the best-bound and incumbent solutions found at a given iteration. It should be noted that in both methods only the upper bound solutions provide feasible solutions. As illustrated in Fig. 4-5, the best solution of test scenario I using the MCB algorithm is found at iteration 2 after 5.68 seconds.

4.6.2 Scenario II: large-scale off-outage area in case of fault F3

In this scenario, the restoration problem is studied in case of fault F3 at substation 501 in the test network of Fig. 4-3. The off-outage area includes the whole feeders A, B, C, D, E, and F. In this case, the optimization problem P consists of 529 binary variables including 23 reconfiguration variables (Y) and 506 load pickup variables (L). As reported in Table 4-1, the quality of the solution provided by the MCB method is 30.82% better than the one obtained with
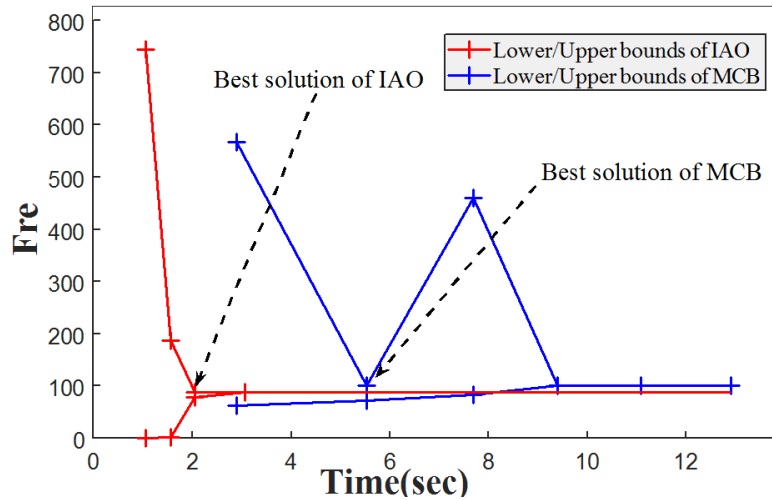
Fig. 4-5. The progress of the obtained solution using IAO and the MCB algorithms in scenario I.
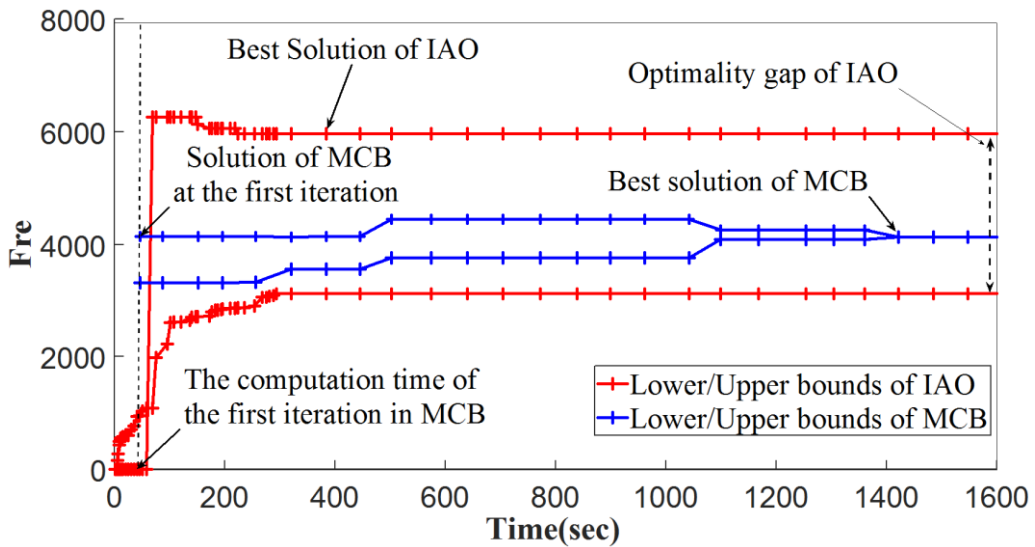
Fig. 4-6. The progress of the obtained solution using IAO and the MCB algorithms in scenario II.

IAO method. In this scenario, IAO approach could not converge to a proven optimality solution. In this regard, the computation time that is given in Table 4-1 for IAO approach corresponds to the earliest time when IAO provides its best solution.

In scenario II, the computation time threshold is met and we have to stop after the iteration number 2. However, for the sake of illustration goals, we let the iterations to continue until the LB and UB solutions converge. The results are shown in Fig. 4-6. This figure shows the same type of information as illustrated in Fig. 4-5 but for test scenario II. As it can be seen, the quality of the best-found solution of the MCB method after 2 minutes is only 0.05% far from the quality of the final solution found after the convergence. The functionality of the IAO approach for

solving scenario II is also illustrated in Fig. 4-6. As it can be seen, the optimality gap could not be reduced below 18% in IAO approach.

4.6.3 Scenario III: large-scale off-outage area in case of F4 and F5

In order to further illustrate the performance of the proposed restoration algorithm, it is tested considering additional fault case studies. These are faults F4 and F5 in the test network of Fig. 4-4, which are considered through two separated test scenarios, namely scenarios III.a and III.b, respectively. In case of fault F4, feeders 1 and 2 are in the off-outage area, whereas in case of fault F5, the off-outage area includes feeders 3 and 4. The restoration problem contains 24 binary variables Y and 186 binary variables L in case of scenario III.a; and 27 binary variables Y and 234 binary variables L in case of scenario III.b.

The IAO approach fails to present even a single feasible restoration solution for scenarios III.a and III.b. The progress of the MCB algorithm in solving the restoration problem for these scenarios is depicted in Fig. 4-7. The numerical results corresponding to the best solution obtained until the convergence of the MCB algorithm are given in Table 4-2. It can be seen that it takes only 21 and 48 seconds for the MCB to find these best solutions in case of scenarios III.a and III.b, respectively.
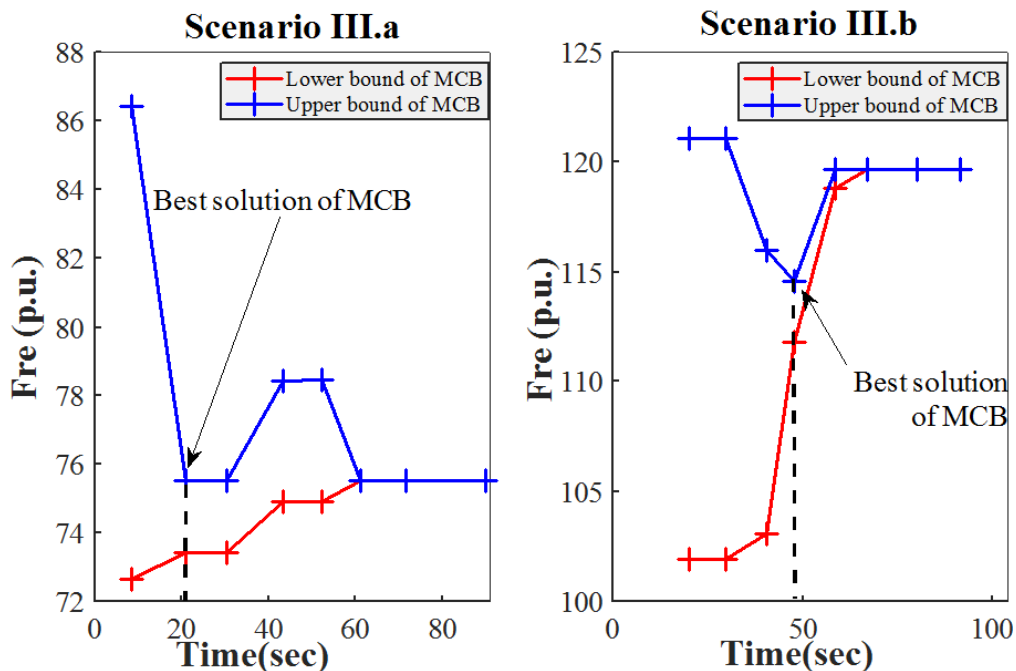
Fig. 4-7. The progress of the obtained solution using MCB in scenarios III.a and III.b.

Table 4-2. Numerical results of test scenario III.

Scenario	Solution Method	Reconfiguration Actions	Load Pickup Actions	F^{re} (p.u.)	F^{sw} (min)	Computation time (s)
III.a (fault F4)	MCB	I. Open switches {5-6,11-12,25-26,27-28,28-29} and load breakers{1,3,5,19,24,25} II.Close{T1,T4}	III. Close load breakers {5,25}at 12:00 P.M.	75.5	334	61.12
III.b (fault F5)	MCB	I. Open switches {31-32,33-40,41-42,42-43,59-60,63-64} and load breakers{32,33,34,35,52,53,54,55,58} II.Close{T1,T4}	III. Close load breakers {35,58}at 12:00 P.M.	114.6	245.5	65.76

4.6.4 Discussion

The functionality of the proposed MCB with respect to the IAO method should be discussed separately for small scale-outage-areas such as in scenario I, and for large scale-outage-areas such as scenarios II and III. For small–scale problems, the IAO method provides the optimality proven solutions within a short time. As mentioned in section 4.5.4, the proposed MCB algorithm does not necessarily provide the global optimal solution (as for IAO). However, as shown in scenario I, the quality of its solution is not far from the global optimal solution.

The main advantage of the MCB method with respect to IAO method lies in large-scale optimization problems. Scenarios II and III illustrate this advantage. Actually, IAO approach could fail to converge to a proven optimality solution or even to provide a first feasible solution. As shown in scenario II, the best optimality gap obtained using IAO approach is significant and it means that the quality of the best feasible solution is poor. On the other hand, the MCB method found, within a very short time, a good-enough solution. There is no any unique and standard measure defining a good-enough restoration. However, it is obvious that the 0.05% quality margin that is obtained after the initial iterations of the MCB algorithm in scenario II is acceptable and enough. In general, the IAO approach assigns the whole computational effort to finding the proven global optimality solution. If possible, this will be obtained for large-scale restoration problems after a long computation time. Whereas, the MCB method provides a good-

Table 4-3. Checking network security constraints for restoration solution obtained in different test cases

Scenario	Fault	Min. voltage Margin (p.u.)	Min. current margin (A)
I	F1 & F2	0.0236 p.u. at node 31 at time 11:00 A.M.	9.716 A in line 84-11 at time 11:00 A.M.
II	F3	0.0014 p.u. at node 29 at time 20:00 P.M.	12.82 A in line 85-47 at time 18:00 P.M.
III.a	F4	0.0013 p.u. at node 25 at time 14:00 P.M.	27.05 A in line 36-48 at time 13:00 P.M.
III.b	F5	0.0029 p.u. at node 31 at time 14:00 P.M.	19.04 A in line 67-68 at time 14:00 P.M.

enough solution at the first iterations thanks to the optimality cuts presented in section 4.5.2. Then, through the subsequent iterations, it tries to improve the quality of the solution gradually. This characteristic is essential for the restoration problem, where an appropriate decision should be made in a very short time.

In order to check the network security constraints for each scenario, the obtained restoration solution is deployed on the model of the corresponding test network implemented in Matlab environment. The voltage and current profiles along the time are derived using power flow simulations in Matlab/MATPOWER toolbox. Table 4-3 gives the representative numerical results out of these profiles for each scenario. These results include the minimum nodal voltage magnitude and minimum line current margins over, respectively, all the nodes and lines of the networks and over all the time steps during the restorative period. These results show that the network security constraints are all respected and therefore confirm the feasibility of the obtained solutions. Moreover, it can be seen that according to each restoration solution, the network is operated very close to its capacity envelop (especially in terms of the minimum voltage limit). This illustrates that within the safe region of the network operation, the most possible loads are restored for each scenario.

According to the proposed MCB algorithm, while the iterations are evolving, more feasibility and/or optimality cuts are added to the master problem. This leads to a lower bound solution profile, which is monotonically increasing. However, as it can be seen in Fig. 4-5, Fig. 4-6, and Fig. 4-7, unlike the classical Benders decomposition algorithm, the upper-bound solution obtained from the MCB algorithm (the sub-problem solution) is not monotonically decreasing with the iteration number.

Actually, the formulation of the optimality cuts in the classical Benders algorithm includes the optimal values of dual variables. These values provide the sensitivity of the objective function with respect to the complicating variables (which are Y variables in our case). It means that the optimality cuts in classical Benders algorithm provide marginal information about the optimality of the solution obtained at each iteration. In this regard, at each iteration of the classical benders algorithm, we move in direction toward the global optimal solution. Therefore, we can make sure that the quality of the sub-problem solution at each iteration is better with respect to the ones in the previous iterations.

Now, in the developed MCB algorithm, the cuts provide combinatorial information about the binary variable combinations that are either infeasible (the second expression of (4-8.d)) or non-optimal (the first expression of (4-8.d)). In this regard, the proposed cuts at a given iteration only distil the search space of the optimization problem into a smaller subset. It means that at each iteration of the proposed MCB method, instead of moving toward the global optimal solution, we shrink the search space around the global optimal solution. Therefore, there is no guarantee that the quality of the sub-problem solution at a given iteration will be improved with respect to all the previous iterations.

4.6.5   Comparison with other mathematical programming methods

In this section, it is aimed to show the efficiency and superiority of the MCB with respect to the two mathematical programming methods proposed in [91] and [92]. In the first step, the MCB results in scenario II are compared with the results obtained from a mathematical formulation proposed in [91] for the restoration strategy.

In [91], the electrical constraints are integrated into the restoration problem using DistFlow formulation. In this regard, the multi-period restoration problem is formulated in [91] as a mixed-integer linear programming model. According to this formulation, the resulting topology of the network (i.e. line switching variables y_{ij}) could change at each time step.

In order to make a fair comparison, we force the line switching variables in [91] to not change with time, as suggested in the proposed MCB methodology. With this modification, the formulation of [91] is implemented in Yalmip/Matlab and solved using Gurobi for the test case of scenario II. The obtained numerical results are reported in the first row of Table 4-4 (Method of [91]_try1).The comparison of the F^{re} value in Table 4-4 with F^{re} values reported in Table 4-1 for scenario II shows that the quality of the solution obtained using the method of [91] in

Table 4-4. Numerical restoration results obtained using the method of [91] in scenario II (fault F3 in the test network of Fig. 4-3).

Solution Method	Reconfiguration Actions	Load Pickup Actions	F^{re} (p.u.)	F^{sw} (min)	Computation time (s)
Method of [91]_try1	I. Open switches {5-6,12-13 ,38-39,44-45} and load breakers {12,14,17,19,26,27,28,29,31 ,32,34,35,36,37,38,41 ,46}, and close {T3,T7,T10,T11} II. Close {T1,T2,T4,T5,T8}	III. Close load breaker 38 at 12:00 P.M. IV. Close load breakers {2,14,29} at 18:00 P.M. V. Close load breakers {35,36} at 19:00 P.M.	3.32e3	1.11e3	28.04
Method of [91]_try2	I. Open switch 33-34 and load breakers {2,3,4,11,12,14,16,17,19,20, 21,26,27,28,29,31,32,33,34, 35,36,37,38,40,41,42,44,46} , and close {T3,T7,T9,T11} II. Close {T2,T4, T8}	III. Close load breakers {21,27,37} at 18:00 P.M. IV. Close load breakers {38,40} at 19:00 P.M.	6.32e3	1.23e3	18.82

try1 is better than the solution qualities of IAO and MCB approaches. However, since the DistFlow constraints are used in [91] instead of the AC power flow constraints, the obtained solution is infeasible regarding the minimum voltage limit. Fig. 4-8 confirms this infeasibility illustrating the results of a post power flow simulation for the obtained restoration solution. These results include the voltage magnitude profiles at different nodes and at different time steps during the restorative period. As it is shown, the lower voltage limit at some buses is violated at some time steps. The DistFlow approximation fails to guarantee the electrical constraints, since the network is operated close to its capacity envelop (i.e. current or/and voltage limits) during the restorative period.

In case where voltage and/or line power constraints are violated, it is suggested in [91] to impose conservative limits on the DistFlow constraints. In this regard, we replace the original lower voltage limit (0.917 p.u.) to 0.970 p.u. This is the smallest value for the lower voltage limit in the DistFlow constraints that can guarantee the feasibility of the solution of scenario II.

Adding these conservative constraints, the restoration formulation of [91] is applied in try2 to solve the restoration problem in case of scenario II. The obtained results are shown in the second
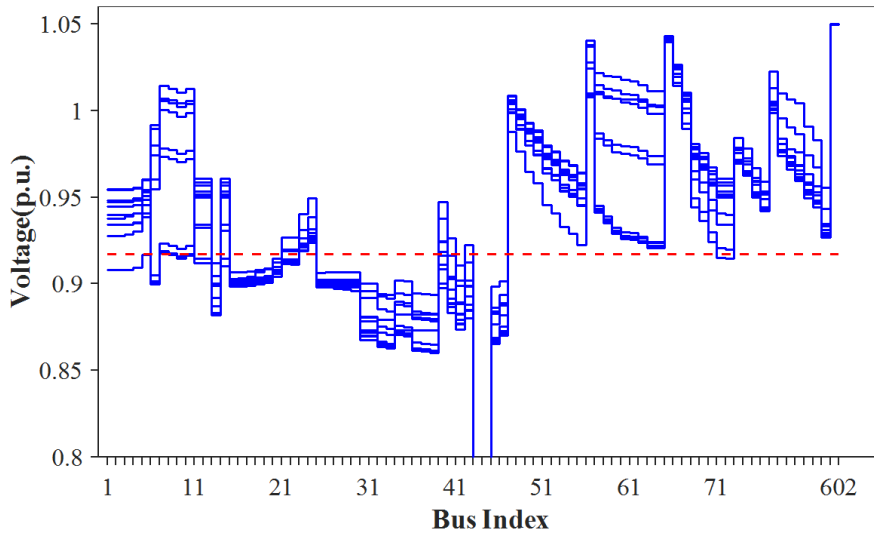
Fig. 4-8. The voltage magnitude profile at different times steps during the restorative period (blue lines) and lower voltage limit (red dotted line) according to the solution obtained from the method of [91]_try1 in scenario II (nodes 43 and 44 are left without any supply according to the results of Table 4-4).

row of Table IV (Method of [91]_try2). This solution is feasible concerning all the electrical constraints. However, as it can be seen, the quality of the obtained solution (in terms of F_{re}) is 52.74% lower than the solution quality of the proposed MCB method reported in Table 4-1.

This comparison clearly illustrates that it is not robust to simplify the AC power flow constraints in the restoration problem formulation with the corresponding DistFlow constraints. From the other hand, as the comparison of computation times related to the IAO and the method of [91] shows, the incorporation of AC power flow constraints increases the computation burden drastically. In order to make the restoration problem tractable in case of grids of realistic sizes while integrating the AC power flow constraints, the MCB method is proposed in this chapter as a decomposition solution approach.

In the next step, the proposed MCB methodology is compared with the restoration methodology presented in [92]. First of all, it should be mentioned that the methodology of [92] is particularly suitable for unbalanced networks and in case of extreme fault cases, where there is no access to the upper grid for the network restoration (referred as islanded network restoration). In this section, the comparison is conducted considering only assumptions made in this thesis (see Chapter 1). It means that we focus on balanced distribution networks and we do not consider the islanded restoration of the distribution network. For this comparison, it is assumed that a fault occurs at the top point of feeder A (fault F6) in the test network of Fig. 4-3.

Table 4-5. Numerical restoration results in case of fault F6 in the test network of Fig. 4-3.

Solution Method	Switching Actions		F^{re} (p.u.)	F^{sw} (min)	Computation time (s)
MCB Method	I. Open switch 3-4 II. Close T2		4.4	60	4.04
Method of [92]	Step1	I. Open switch 6-7 II. Close {T1,T2}	1.65e3	150	1.14
	Step2	Open load breakers {4,6}			

This fault is isolated by opening the feeder breaker B1 and the switch on line 1-2. All the parameters of this test case are similar to the ones of scenario I and scenario II except that all the nodes are not equipped with load breakers. In this case study, it is assumed that only critical loads that are shown with '⋈' can be detached from their nodes. It means that among all the nodes in the off-outage area, only nodes 4 and 6 are equipped with load breakers.

In order to make a fair comparison, we assume that load status variables (α_i) will not change with time, as proposed by the authors of [92]. With this modification, we apply the developed MCB formulation on this test case. The numerical results are reported in Table 4-5. According to this solution, since the switch on line 3-4 is opened, the nodes 2 and 3 are left without any supply.

The restoration methodology of [92] is explained in section 4.3. As mentioned, the authors of [92] propose to solve the restoration problem in two steps. In the first step, a heuristic approach is applied to find a suitable post-restoration topology for the network. This heuristic approach chooses a radial network configuration with the minimal diameter. The diameter of a tree is defined as the longest distance among all pairs of nodes in the network. The distance between a pair of nodes refers to the total impedance of lines on the shortest path between the two nodes. Applying this heuristic strategy to the test network of Fig. 4-3 in case of fault F6 results in the post-restoration configuration shown in Fig. 4-9.

According to the restoration algorithm presented in [92], in the second stage, the status of load breakers and the outputs of sources are determined while fixing the network topology to the one
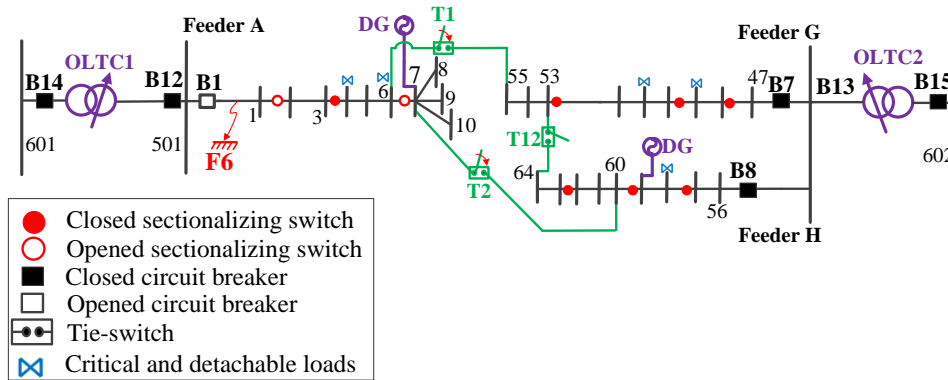
Fig. 4-9. The post-restoration configuration obtained in the first stage of the algorithm presented in [92].

obtained in the first stage. The resulting optimization problem is solved in [92] using a relaxed semi-definite programming methodology. But in this chapter, we solve this same optimization problem using Gurobi solver, which adopts the branch-and-bound method to handle integrality constraints. The optimal solution is to open all the load breakers in the off-outage area (i.e. at nodes 4 and 6). This leads to a reliability objective term equal to 1.65e3. The comparison of F_{re} values given in Table 4-4 shows that the quality of the solution obtained from the method of [92] is very far from the solution quality of the MCB method.

It should be noted that if there were no load breaker in the off-outage area (no detachable loads), there would be no feasible solution for the optimization problem in the second stage of the algorithm presented in [92]. These numerical results clearly highlights the limits of [92] mentioned in section 4.3.

4.7 Conclusion and summary

The restoration problem is an NP-hard combinatorial optimization problem including three interdependent parts, namely, I) the network reconfiguration, II) the load pickup, and III) the electrical safe operation of the network. This results in a huge and intractable problem especially considering a grid of realistic size in a multi-period problem. The link between the line switching variables (part I) and the power flow formulation (part III) involves conditional constraints modelled through big-M coefficients. The presence of these coefficients makes the relaxation of the mixed-integer problem using branch-and-bound method very poor in terms of computation burden. Moreover, this link inhibits the use of classical Benders algorithm in decomposing the problem because the resulting cuts will still depend on the big-M coefficients. In this regard, the

main motivation of this chapter was to relax the computation burden of the restoration problem while removing the model dependency on the big-M coefficients.

In this chapter, a two-stage decomposition approach was proposed named Modified Combinatorial Benders algorithm. This novel decomposition approach is based on the combinatorial Benders method that was firstly proposed by Hooker for solving optimization problems which include conditional constraints [94, p.]. This approach was briefly reviewed in section 4.4. Then, in section 4.5, we presented a modification to the combinatorial Benders method so that it can be used for the multi-period restoration problem. According to the proposed modifications, in the outer level, the master problem solves a Mixed-Integer Linear optimization problem including the reconfiguration and the load pickup problems. In the inner level, the value of line switching variables are fixed to the ones obtained from the master problem and the load pickup variables are optimized subject to the AC power flow constraints. The resulting sub problem is in the form of a MISOCP problem. This problem is then broken down into several independent problems with smaller sizes. It makes the sub problem tractable in case of large-scale distribution networks. The solution of the sub problem is used to augment the feasibility or optimality cuts of the master problem. This algorithm is repeated through successive iterations until a solution with a desired level of optimality is obtained.

The superiority of the proposed decomposition approach with respect to the integrated approach was illustrated using three test cases on two different test distribution networks. In scenario I, a small-scale restoration problem was studied. In this test case, the fault impacts only two feeders and therefore the restoration problem can be solved using the Integrated Analytical Optimization (IAO) method. For this small–scale case study, the IAO method finds the optimality proven solution within a short time. However, the proposed MCB algorithm provides a solution close (not equal) to the global optimal solution. Actually, the main advantage of the MCB method lies in large-scale optimization problems. In this regard, test scenario II was studied, where the fault impacts a large area of the distribution network. It was shown that the quality of the best feasible solution that is obtained by IAO in this scenario is very poor with respect to the one obtained using MCB method. In scenarios III, two other large-scale restoration scenarios were studied using a different test study. It was illustrated that in both of these scenarios, the MCB method provides, within a very short time, a good-enough solution. However, the IAO method fails in both test scenarios to find even a single feasible solution.

In summary, this chapter presented a two-stage mathemaical formulation for the restoration problem named Modified Combinatorial Benders algorithm. Compared with the state-of-the-art methods,

i.   The proposed decomposition approach makes the restoration problem tractable for analytical solvers in case of a grid of realistic size in a multi-period optimization problem,

ii.   Thanks to the new formulation proposed for the cuts, we can identify binary variable combinations that are either infeasible or non-optimal. In this regard, in the proposed MCB algorithm, we remove, at a given iteration, a larger area of the solution space compared to the standard combinatorial Benders.

iii.   A convex AC-power flow formulation is integrated into the decomposed formulation proposed for the restoration problem in order to accurately model the electrical operational constraints (e.g. voltage and current limits).

5 Optimal Load Restoration in Active Distribution Networks Complying with Starting Transients of Induction Motors

<u>**Chapter Highlights:**</u>

The large and reactive current driven by an induction motor during its acceleration period can impose high risks both in the motor side and in the network side. In this chapter, we aim to find the optimal restoration solution in active distribution networks, while accounting for the starting transients of induction motor loads. For this aim, a mathematical and convex model is derived representing the starting transients of an induction motor in a semi-static fashion. This model is then integrated into a load restoration problem aiming to find the optimal energization sequence of different loads (static and motor loads). In this optimization problem, we present a novel and convex model of the converter-interfaced DGs working in constant current mode following voltage sag induced by motor load starting. Using this model, we derive the optimal current set points of these DGs such that the DGs support the electrical constraints in an optimal fashion during motor acceleration period. The developed optimization problem includes also a convex model of the autotransformer that is used for the starting of a given induction motor. Therefore, the optimal tap setting of this autotransformer is also derived from the proposed optimization problem. Integrating the AC power flow formulation into the developed optimization problem guarantees that the starting transients of motor loads will not violate the transient operational limits imposed by different protection devices in the distribution network. In this chapter, we validate the feasibility of the optimization results in terms of these transient operational limits using I) off-line time-domain simulations, and II) a Power Hardware-In-the-Loop experiment.

<u>**Related Publication:**</u>

<u>H. Sekhavatmanesh</u>, J. Rodrigues, C. L. Moreira, and J. A. P. Lopes, R. Cherkaoui, "A convex model for induction motor starting transients imbedded in an OPF-based optimization problem," to be presented at the *PSCC2020*, Porto, Portugal, p. 7.

<u>H. Sekhavatmanesh</u>, J. Rodrigues, C. L. Moreira, and J. A. P. Lopes, R. Cherkaoui, "Optimal Load Restoration in Active Distribution Networks Complying with Starting Transients of Induction Motors," under third round of review in IEEE Transactions on Smart Grids.

5.1 Chapter Organization

In the first part, we illustrate the related motivation of presenting this chapter according to the global context of the thesis. In section 4.3, we define the problem and we clarify the approach that will be taken through the chapter for dealing with this problem. Section 5.4 is devoted to the review of the existing studies on motor starting transients. The proposed semi-static model for representing the motor starting transient is provided in section 5.5. This model is used in section 5.6 to formulate the load restoration problem accounting for the starting transient of induction motors. In this section, first, the overall optimization problem formulation is presented. Then, the formulation of the transient load powers, the formulation of the AC power flow, the model of converter-interfaced DGs working in constant current mode, the model of auto-transformer used for the starting of induction motors, and the formulation of transient constraints are presented in separated sub sections. Section 5.7 evaluates the functionality of the developed optimization problem in case of a large-scale test study and under three simulation scenarios. The feasibility and accuracy of the optimization results are validated in section 5.8 using I) off-line time-domain simulations, and II) a Power Hardware-In-the-Loop experiment. Finally, section 5.10 concludes the chapter with final remarks concerning the main contributions presented in this chapter.

5.2 Motivation

Large horsepower and high-speed squirrel-cage induction motor have been used for more than a century as industrial drives for compressors, pumps, fans, or blowers. These motor loads play an essential and critical role in most of industrial facilities such as in petrochemical installations [100]. Therefore, re-energization of these loads, following a failure in the distribution network, has a huge priority for distribution network operators.

When a secondary substation is restored, especially when it supplies a lot of motor loads, a large and reactive current might be driven during a transient period. Due to this inrush current, the re-acceleration of motor loads can impose high stresses both on the network and on the motor itself. In order to enable soft starting of induction motors, variable-speed drives have been largely used in recent years. In spite of significant developments made in these drives, they are only used if the costs of additional equipment can be justified. Large induction motors, especially in the past, were connected either directly or through an autotransformer to the grid. Special care and

attention are required for the starting of these large industrial loads in a network that was undergoing through switching actions following an outage. In such a reconfigured network, the Thevenin's impedance seen from the motor terminals is usually larger in comparison to the one in the normal configuration of the grid. Therefore, the optimal restoration plan obtained from the steady-state analysis presented in previous chapters cannot guarantee that the transient operational constraints (e.g. voltage-dip and over-current transient acceptability limits) are not violated. In all the previous chapters, the restoration problem was formulated using the steady-state model of different elements in an active distribution networks including loads, generation units, and voltage regulation devices. In this regard, the operational security constraints such as voltage and current limits were accounted for in steady state only.

The motivation of presenting this chapter is to modify the load restoration sequence obtained from those steady-state analyses in the most optimal way such that the transient constraints are respected during the motor acceleration period. The objective is to minimize the total energy of loads that cannot be restored according to the modified load restoration sequence.

5.3 Problem Statement

Among different load types in a distribution network, the re-energization of motor loads needs special attention. The large current driven by an induction motor during its acceleration period can impose high risks both I) in the motor side and II) in the network side [22].

Regarding the motor side constraints, the electrical torque generated by the motor should be larger than the mechanical load torque in order to accelerate the load. The large inrush current at the starting can make an extreme voltage drop at the motor node and ultimately a reduction in the electromagnetic torque. This may result in either the motor stall or a prolonged acceleration. This longer acceleration time causes more heat to be generated in the rotor bars and stator windings. This heat makes stresses on these parts and may impact the motor life. Besides these electrical effects, the sudden loading of the induction motor increases the wear on the mechanical load. The starting torque could reach to 600% of the locked rotor torque [101]. This transient torque may cause even a catastrophic failure if the load cannot handle this shock. These risks are more sensible for "heavy start duty loads". This term refers to the motor loads that may have in addition to a high moment of inertia, a high starting load torque such as large turbo compressors and blowers [101].

The starting of large induction motors could also put high strains on the distribution network. The high inrush current driven by a large induction motor may cause to trip I) the over-current relays protecting the transformers at the feeder substations or/and II) the under-voltage relays protecting the critical loads and DGs. In the latter case, if the motor starting causes the disconnection of a DG or any other voltage compensator unit, then a chain reaction might be followed leading to the voltage instability at least in one part of the distribution network. These effects are more significant when an induction motor starts under "*weak network*" conditions. Weak network conditions are characterized with a limited reactive power generation capacity or/and with large Thevenin's impedance between the motor terminals and the slack bus.

In order to reduce these risks, different starting methods are used for the large induction motors. These methods include Wye-Delta, part winding, and reduced voltage either by autotransformer or by an adjustable variable-speed drive. Although variable-speed drives have been significantly developed in recent years, they have been used for large industrial induction motors only if the costs of additional equipment could be justified. Therefore, the large industrial motors (over 25 horsepower) and especially the old-fashioned ones are connected either directly or through an autotransformer to the grid. These approaches are referred as the Direct On-Line (DOL) starting and the autotransformer starting, respectively.

As it will be discussed in the next section, different methodologies are presented in the literature for the dynamic analysis of the induction motor starting. These approaches are not suitable for decision-making problems, especially for problems with huge and complex solution spaces. In this chapter, we aim to provide an optimization model that represents the transient electrical states of an active distribution network during the motor acceleration period. This model is used to find the optimal energization sequence of different loads (static and motor loads) following a fault in an active distribution network.

When a fault occurs in a distribution network, once it is isolated, the area downstream to the fault place remains unsupplied which is called the "*off-outage area*". This area is re-energized by the healthy neighboring feeders using switching operations. This new configuration remains for a so-called "*restorative period*" until the faulted element is repaired. During this period, it is aimed to restore the loads in the most optimal sequence such that the total energy not supplied is minimized. In this regard, the network security constraints must be respected especially in case

of starting large motor loads. The problem of finding the optimal load energization sequence given a new network configuration is referred as the "*load restoration problem*".

Due to the difficulties of integrating the transient constraints related to the motor load starting in the full restoration problem formulation, a two-stage approach is exploited.

In the first stage, we solve the restoration problem according to the formulation presented in the previous chapters. This restoration problem contains the model of passive and active elements only in steady-state conditions. Solving this optimization problem provides I) the optimal configuration of the network (line switching variables) and II) the optimal load restoration sequences during the restorative period. This stage of analysis is referred in this chapter as the *steady-state analysis*.

In the second stage, which is studied in this chapter, we take the restoration solution obtained from the first stage and we modify it concerning the transient constraints during the motor acceleration period. In this stage, we modify only the obtained load restoration sequence, while considering the starting transients of induction motors, which were neglected in the first stage. It means that the line switching variables are fixed to the ones obtained from the steady-state analysis. We assume that considering the starting transients of motor loads does not affect the optimal network configuration that was obtained from the steady-state analysis. In this second stage, we just change the energization sequence of the loads in the most optimal way such that the transient constraints are respected in case of starting of each induction motor in the off-outage area. The main objective is to minimize the resulting increase of energy not supplied referring to its value obtained from the steady-state analysis.

Apart from the load energization sequence, another decision variable that is considered to support the network security constraints during the motor acceleration period is the control of converter-interfaced generation units. In this chapter, we consider only dispatchable generation units including DGs, storage systems, and/or static synchronous compensators that are interfaced with the grid via full-bridge power converters. In this regard, the term of DG is used in this chapter to refer to all these generation units. The re-energization of the DGs after the fault is accounted for in the steady-state analysis. In the optimization problem studied in this chapter, it is assumed that the DGs are already connected to the grid and they work in *normal state*. It means

that the DG converter controls the active and reactive power injections (or active power and voltage) following pre-determined set points.

When a motor load starts, the voltage at the DG hosting node drops. This voltage drop is detected at the DG hosting node and launches the proposed voltage support control scheme, referred in this chapter as *current saturation mode*. In this mode, instead of the active and reactive powers, the injection current of the DG is controlled. This control mode is achieved through already existing LVRT strategies in the converter interface while assuming that their current set points can be modified. In this regard, we should derive a convex model of the converter control in the current saturation mode. This model should be integrated into the optimization problem in order to obtain the optimal values of the current set points in case of starting each of the motor loads during the restorative period.

In addition to the load energization sequence and dispatch of DGs, we should determine the optimal tap setting of the autotransformer that is used for the starting of the induction motor. According to the autotransformer starting approach, an autotransformer and a changeover switch are put in series with the terminals of the motor. This autotransformer usually reduces the applied voltage to the motor by 65% to 80%. When the motor attains 80% of normal speed, the changeover switch takes out the autotransformer from the circuit. Therefore, the full line voltage is applied to the motor terminals. The aim of applying the reduced voltage to the motor during its acceleration period is to lower the starting current, power loss, and radiated heat in the induction motor. Moreover, with this reduced voltage, the mechanical vibration and noise levels will be reduced during the acceleration period. However, reducing the voltage causes the starting torque to reduce and therefore the acceleration time to lengthen. Therefore, great care should be taken to find the optimal trade-off for the tap setting of the autotransformer. In order to obtain this optimal tap setting, a mathematical and convex model of the autotransformer should be derived and incorporated into the optimization problem.

In summary, the main decision variables in the proposed load restoration problem are three folds, namely, I) the energization sequence of different loads during the restorative time, II) the optimal tap setting of the autotransformer that is used for the starting of the induction motor, and II) the optimal active and reactive current injections by dispatchable DGs. In this regard, convex optimization models are derived for the autotransformer tap setting and for the DG set points in

the current saturation mode. These mathematical models together with the proposed semi-static model of the induction motor are integrated into a relaxed power flow formulation in a convex fashion. In this regard, the above-mentioned three control actions are set to provide the optimal support to the network security constraints during the motor acceleration period.

5.4 State-of-the-art on the dynamic analysis of the motor starting

The analysis of motor acceleration transients has been studied in the literature in the context of many power system applications. In this regard, some papers study the reacceleration of motor loads following a complete-blackout in the context of different stages of the power system restoration [102]–[104]. The first stage is studied in [102] and [103]. In these papers, the optimal sequence of starting large induction motors is derived during the startup process of a power plant using black-start generation units and microgrids, respectively. In the second stage of the power system restoration, the network skeleton is rebuilt through successive switching steps. In this stage, in order to stabilize the system frequency and the voltage magnitude, certain loads must be energized. Since the motor starting currents involve large inductive components, special care and attention is required for the starting of large industrial loads during the early stage of line energizations [103]. The last stage of the power system restoration is load pickup. In this stage, in order to avoid under frequency deviations or extreme voltage dips, the loads should be picked up in multiple steps. In this regard, the maximum restorable load that a high-voltage substation can pick up at one shot is evaluated in [104].

Another situation where starting of the induction motor should be given a special attention is in low-voltage networks. In this regard, the authors of [72], [105], [106] evaluate the effects of the motor starting on the frequency stability and on the voltage stability in low-inertia and islanded microgrids. There are also studies in the literature which focus on the re-acceleration scheme of motor drives in a grid-connected industrial facility such as a petro-chemical installation following an outage [100], [107]. In these studies, first, the critical motors are categorized into groups mainly based on their function in the production process of the factory. Then, these groups of motor loads are scheduled to be restored in successive time steps while minimizing the total interruption time of the production process.

Apart from the permanent fault situations, there are papers evaluating the behavior of induction motors in other situations such as in voltage sags [108] and in short interruptions [109]. The main

reason for difficult reacceleration of induction motors in these situations is the system hot-load pickup. This term refers to the recovery of the whole system at one shot following a short interruption of power supply. The authors in [109] determine the optimal place and setting of protection relays in the network while accounting for the interaction between the system hot load pick-up and motor loads reacceleration.

In all the papers mentioned above, the behavior of the induction motor is evaluated using only time-domain simulations. However, if these approaches are used for decision-making problems, different combination of decision variables should be tested, separately. This approach would be very time-consuming for the problems with huge and complex solution spaces. For such problems, it is needed to formulate the motor starting dynamics in an analytical way such that it can be integrated to an optimization problem.

Such mathematical approaches are proposed in [110]–[113]. The authors of [110] developed nonlinear differential-algebraic formulations to estimate the voltage dip during the motor acceleration period. This voltage dip is predicted in [111] using neural network for an induction motor with a certain kVA capacity installed on a bus with a certain short circuit capacity. The developed formulations are all nonlinear and non-convex. Therefore, they cannot be integrated into convex optimization problems. The presented formulation in [112] is incorporated into a maximum restorable load problem and solved iteratively using a heuristic approach. This approach is applicable only in the case of simple problems involving only one decision variable. The authors in [113] presented a quadratic optimization problem for the minimization of the voltage deviation with respect to the nominal value in case of the induction motor starting. In that paper, the motor reactive power during the acceleration period is approximated to a simple algebraic function of the terminal voltage magnitude. This simplified model does not account for the motor starting transients in an accurate way. In consequence, it cannot evaluate correctly the feasibility of the motor starting with respect to the network security constraints.

An important control action that can support the network security constraints during the acceleration period of large motor loads is the dispatch of converter-interfaced DGs. In this regard, different strategies are proposed in the literature for the control of the DG converter in current saturation mode. Most of these studies consider the operation of the DG under fault conditions. Each of them aims at specific objectives such as enhancing the quality of the injected

current [114], reduction of the dc-voltage ripple [115], supporting frequency dips [116], or supporting voltage dips [117]–[122]. In the following, we provide a detail review of those papers aiming at the support of voltage dips in the network.

The authors of [118] propose a strategy for controlling the DG active power injection during unbalanced grid faults. However, the reactive power injection of the DG and its role in the network voltage support is disregarded. On the other hand, the authors of [116], [119], [120] focus only on the reactive power control of DGs under grid faults. These strategies work well just for transmission grids. In distribution networks, where the ratio of R/X of lines is large, both the active and reactive power injections play significant roles in the voltage support.

This peculiarity is addressed in [20] and [21] by considering the characteristics of the distribution line impedances in setting the DG active and reactive power injections during voltage drops. The authors of [121] aim to support the voltage dip only at the DG hosting node, whereas the authors of [122] focus on the node with the most voltage drop during the fault condition. Since both of these control methodologies are aimed to support the nodal voltage constraint only at a single node, the network is simplified using its Thevenin's equivalent seen from the target node. In this chapter, we aim to support all the network security limits during the motor acceleration period. Therefore, the detailed AC-OPF formulations with the detailed model of the network is used to determine the optimal active and reactive current injections.

In this chapter, a mathematical optimization model is derived for the load restoration problem, while accounting for the starting transients of induction motors. Compared with the state-of-the-art algorithms proposed so far for the restoration problem, the major contributions of the developed load restoration problem are the following:

- The proposed load restoration problem incorporates a convex semi-static model of induction motor loads representing their starting transients.

- A convex model is derived for the converter-interfaced DGs working in constant current mode following voltage sags induced by motor load starting. This model is integrated into the optimal load restoration problem in order to obtain the optimal current set points of these DGs. Using these set points, the DGs support the electrical constraints in an optimal fashion during the motor acceleration period.
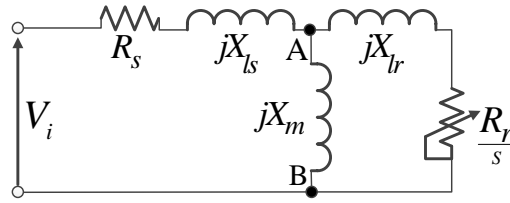
Fig. 5-1. The equivalent circuit of the induction motor.

- The developed optimization problem includes a convex model of the autotransformer that is used for the starting of the induction motor. Therefore, the optimal tap setting of this autotransformer is derived from the proposed optimization problem.

- The transient operational limits imposed by under-voltage and over-current protection devices are integrated into the developed optimization problem. The aim is to guarantee that the starting transients of motor loads will not trigger the protection devices that exist in the distribution network.

5.5 Modelling of the induction motor starting

In this section, a semi-static model is proposed for the starting transient of induction motors such that it can be integrated into the power flow formulation in a convex fashion. The aim is to formulate the operational security constraints in the whole distribution network during the motor acceleration period. Fig. 5-1 shows the equivalent circuit of the induction motor, neglecting the dynamics of rotor fluxes. Using this equivalent circuit, the electrical torque of the induction motor (T^{ele}) is formulated in the following as a function of the rotor slip:

$$T_{k,m}^{ele} = \frac{R_r V_{th}/S_{k,m}}{\left(R_r/S_{k,m} + R_{th}\right)^2 + (X_{lr} + X_{th})^2} \tag{5-1}$$

where:

$V_{th} = \frac{V_i X_m^2}{R_s^2 + \left(X_{ls}^2 + X_m^2\right)}$

$R_{th} = \frac{R_s X_m^2}{R_s^2 + \left(X_{ls}^2 + X_m^2\right)}$

$X_{th} = \frac{R_s^2 X_m + X_{ls} X_m (X_{ls} + X_m)}{R_s^2 + \left(X_{ls}^2 + X_m^2\right)}$

V_i is the square of the stator voltage. S is the motor slip. R_s and X_{ls} represent the resistance and reactance of the stator. R_r and X_{lr} are the resistance and reactance of the rotor. X_m is the
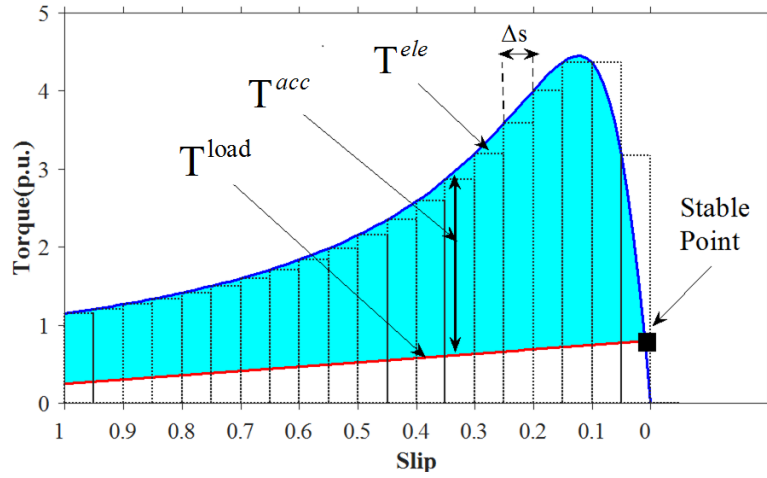
Fig. 5-2. The discretized electrical, mechanical, and accelerating torques of the induction motor

magnetization reactance. V_{th}, R_{th} and X_{th} are the Thevenin's voltage square, resistance and reactance seen from the rotor terminals (AB in Fig. 5-1), respectively.

Fig. 5-2 shows the typical electrical torque-slip curve of the induction motor assuming that the motor terminal voltage is fixed. The load torque (T^{load}) refers to the summation of the mechanical torque on the shaft (T^{mec}) and the friction and windage torque ($Kd_m(1 - S_{k,m})$). In Fig. 5-2, it is assumed that the mechanical load has a linear torque-speed characteristic. The difference between the electrical and load torques is named the acceleration torque and referred as T^{acc} in Fig. 5-2.

When starting, the slip is unity and then it decreases gradually to a stable point where it is close to zero and the speed is close to the synchronous speed. As it can be seen in Fig. 5-2, the electromagnetic torque is a non-linear function of the motor slip. In order to build a convex model of the induction motor starting, we divide the slip range between standstill ($s = 1$) and the stable point into K_{max} fixed steps with equal length of Δs. In this regard, the slip value during each step k is assumed fixed and equal to its value $S_{k,m}$ at the beginning of the step interval k, which is considered as a parameter. Other discretizing approaches could be applied such as assuming the average value of torque during each interval as the value of $S_{k,m}$. The approach taken in this thesis is rather conservative referring to the transient constraints related to the starting of induction motor loads. In this chapter, the terminology of *slip step* (or shortly *step*[12])

---

[12] [12] These slip steps (k) should not be confused with time steps (t), which refer to low-resolution intervals within the whole restorative period.

refers to each of these discretized intervals within the transient acceleration period of each energized motor load. As discussed in Appendix 5.11.1, the step length Δs should be small enough depending on the total inertia of the induction motor.

Given the slip value $S_{k,m}$ as a parameter, the electrical torque of the induction motor at node m and at each step k can be obtained using (5-1) as a linear function of the square of voltage terminal (V_i), which is a state variable in the branch flow model of the AC power flow formulation. The next step is to derive the time duration of a given step k indicated by $\Delta t_{k,m}$. The inverse of this time length is obtained using the dynamic motion equation given in (5-2).

$$\frac{1}{\Delta t_{k,m}} = \frac{1}{2H_m.\Delta S_m}\left(T_{k,m}^{ele} - T_{k,m}^{mec} - Kd_m\left(1 - S_{k,m}\right)\right) \tag{5-2}$$

$$\tilde{t}_{k,m} = \sum_{k^*=1}^{k} \widetilde{\Delta t}_{k^*,m} \tag{5-3}$$

Since the acceleration torque during each step is fixed, the time derivative of the slip is represented by $\frac{\Delta S}{\Delta t}$. In order to derive Δt_k, the piece-wise linear approximation method is used as explained in Appendix 5.11.1. In this regard, we use (5-15)-(5-18), replacing x and $f(x)$ with $\frac{1}{\Delta t_{k,m}}$ and $\Delta t_{k,m}$, respectively. Therefore, $\widetilde{\Delta t}_{k,m}$ is obtained in a linear way as an approximation for $\Delta t_{k,m}$.

In (5-3), we obtain an approximation for the acceleration time of the motor at node m until step k ($\tilde{t}_{k,m}$) by adding the approximated time lengths of all previous steps to step k ($\widetilde{\Delta t}_{k,m}$). The obtained variable $\tilde{t}_{k,m}$ will be used in section 5.6.5 to derive the transient voltage and current limits.

During each single step, since the slip and therefore all the parameters of the motor equivalent circuit shown in Fig. 5-1 are fixed, the electrical state variables can be represented in the phasor domain. The aim of the next section is to obtain the values of these state variables for a given step k and in the whole distribution network using a relaxed formulation of the AC power flow equations. In the developed semi-static model, we neglect the DC term imbedded in the starting current of the induction motor. This assumption is justified because of the low X/R ratio in distribution networks. Therefore, the DC term of the starting current disappears shortly.

5.6 Load Restoration Problem Formulation

In this section, the load restoration problem is presented as an example to show how the proposed semi-static model of the motor starting could be integrated into the power flow formulation. As mentioned in section 5.3, in the second stage of the restoration problem, which is studied in this section, the line switching variables are fixed to the ones obtained from the steady-state analysis. In this regard, we aim to modify only the load restoration sequence obtained from the steady-state analysis, while considering the starting dynamics of induction motors, which were neglected in the first stage. The main objective is to minimize the resulting increase of energy not supplied referring to its value obtained from the steady-state analysis.

The main decision variables of the proposed optimization problem are three folds, namely, I) the energization sequence of different loads during the time ($L_{i,t}$), II) the optimal tap setting of the autotransformer that is used for the starting of the induction motor (Δr_m), and III) the optimal active/reactive current injections from dispatchable DGs ($Fp_{i,m}^{DG}/Fq_{i,m}^{DG}$). The optimization problem is formulated in the following in the form of a MISOCP. In the first stage (steady-state analysis), it includes the power flow formulation for each time step t during the restorative period. However, in the second stage (studied in this chapter), the optimization problem includes the power flow formulation for each step k in the acceleration period of each motor load m in the off-outage area.

In this chapter, it is assumed that only one motor load can be started at time and only once the starting transient of any other motor disappeared. As suggested in [100], the motor loads in an industrial plant are categorized into groups mainly based on their functional processes. These groups of motor loads are considered to be restored in successive time steps with certain intervals. Only the motor loads that are in the same group are restored simultaneously. In this regard, a given motor load in the proposed optimization problem can represent a group of motor loads in the LV network. The dynamic parameters of this aggregated motor load are specified according to the strategy given in [106].

According to the assumption mentioned above, to each motor load in the off-outage area a specific set of steps k ($k \in \{1,2,..,k_{max}\}$) is assigned. Therefore, all the electrical state variables are indexed with k and m. The constraints involving these indices should hold for all the steps and all the motors in the off-outage area.

$$\text{Minimize:} \qquad F^{obj} = W_{re}.F^{re} + W_{op}.F^{op} \tag{5-4}$$

$$F^{re} = \sum_{i \in N} \sum_{t \in T} D_i.\left(L_{i,t}^0 - L_{i,t}\right).P_{i,t}^0 \tag{5-5}$$

$$F^{Op} = \sum_{m \in N_m^*} \sum_{k=1}^{k_{max}} \sum_{ij \in W} r_{ij}.F_{ij,k,m} \tag{5-6}$$

Subject to:

$$\begin{cases} L_{i,t} \le L_{i,t}^0 \ , \ L_{i,t} \le L_{i,t+1} \ : \qquad i \in N^* \\ \qquad\qquad L_{i,t} = 1 \qquad\qquad : \qquad i \in N\backslash N^* \end{cases} \qquad \forall t \in T \tag{5-7}$$

$$\textbf{\textit{Load Modeling}} \tag{5-8}$$

$$\textbf{\textit{AC power flow formulation}} \tag{5-9}$$

$$\textbf{\textit{DG Modeling}} \tag{5-10}$$

$$\textbf{\textit{Autotransformer Modeling}} \tag{5-11}$$

$$\textbf{\textit{Transient Constraints}} \tag{5-12}$$

The objective function (F^{obj}) is formulated in (5-4) as the weighted sum of the reliability (F^{re}) and operational (F^{op}) objective terms. As mentioned earlier, the main objective is to minimize the unsupplied energy of loads due to the shifting in their energization times, which is referred in this chapter as the reliability objective term. This energy is calculated in (5-5) summing the power of all the loads that are not restored ($L_{i,t} = 0$), whereas they were commanded to be restored according to the steady state analysis ($L_{i,t}^0 = 1$).

Consider the assumed optimization results shown in Fig. 5-3 as an example. These results concern the energization status of the load at node i during the restorative period obtained from the steady-state analysis ($L_{i,t}^0$) and from the analysis in the second stage ($L_{i,t}$). The time shifting of the load energization is shown in Fig. 5-3 as Δt. The energy of the load at node i during this time period Δt is added to the reliability objective function (F^{re}).

It should be noted that according to (5-7), the load at node i and time t remains unrestored ($L_{i,t} = 0$) if it is commended to be so according to the results of the steady-state analysis ($L_{i,t}^0 = 0$). Moreover, once a load is restored ($L_{i,t} = 1$), it remains supplied during the rest of the restorative period ($L_{i,t+1} = 1$). The loads outside the off-outage area remains always supplied.
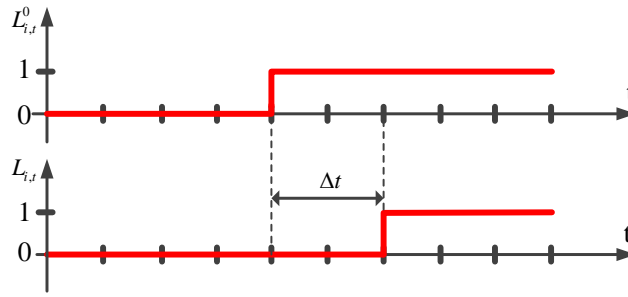
Fig. 5-3. An example of optimization results concerning the energization status of the load at node i.

Unlike the reliability term, the operational term has a very small weighting coefficient. This term is expressed in (5-6) as the total active line power losses in the distribution network. This term is included in the objective function just to satisfy the exactness condition stated in [123] for the relaxed AC power flow formulation.

5.6.1 Load Modeling

As already explained, in the second stage of the restoration problem, we consider the network security constraints only for the acceleration period of each motor load instead of covering the whole restorative period. In this regard, first, we have to find the time instant when a given motor is started. The expression $L_{m,t} - L_{m,t-1}$ is equal to one for time t when motor load m is started and equal to zero for all the other times. This expression is used in (5-8.a) and (5-8.b) in order to extract respectively, $P_{i,m}^0$ and $Q_{i,m}^0$, as the nominal active and reactive powers of the load at node i when the motor m is started. At this time t, if the load at node i is not restored ($L_{i,t} = 0$), then $P_{i,m}^0$ and $Q_{i,m}^0$ are equal to zero. The product of binary variables in (5-8.a) and (5-8.b) introduces non-linear terms. These terms are linearized according to the reformulation technique proposed in [54].

$$P_{i,m}^0 = \sum_{t \in T} P_{i,t}^0 . L_{i,t} . \left(L_{m,t} - L_{m,t-1} \right) \qquad \forall i \in N, \forall m \in N_m \qquad (5\text{-}8.a)$$

$$Q_{i,m}^0 = \sum_{t \in T} Q_{i,t}^0 . L_{i,t} . \left(L_{m,t} - L_{m,t-1} \right) \qquad \forall i \in N, \forall m \in N_m \qquad (5\text{-}8.b)$$

In the following, we use $P_{i,m}^0$ and $Q_{i,m}^0$ to formulate the active and reactive power consumptions of different type of loads. We start with the static loads. The active and reactive power of the static load at node i and at step k, during the acceleration period of motor load m are expressed

in (5-8.c) and (5-8.d), respectively. Assuming that $V_{i,k,m}$ is close to $1\ p.u$, the model is linearized using the binomial approximation approach as proposed in [99]. The products of the binary variables $L_{i,t}$ (in the formulation of $P_{i,m}^0$ and $Q_{i,m}^0$) and the positive continuous variable $V_{i,k,m}$ introduce non-linear terms in (5-8.c) and (5-8.d). In order to preserve the linearity, these terms are re-formulated as given in Appendix 5.11.3.

$$P_{i,k,m}^D = P_{i,m}^0\left(1 + (V_{i,k,m} - 1)\right)^{kp_i/2} \approx P_{i,m}^0\left(1 + \frac{kp_i}{2}\left(V_{i,k,m} - 1\right)\right) \qquad \begin{array}{l}\forall i \in N_s, \\ ,\forall k, \forall m \in N_m\end{array} \qquad \text{(5-8.c)}$$

$$Q_{i,k,m}^D = Q_{i,m}^0\left(1 + (V_{i,k,m} - 1)\right)^{kq_i/2} \approx Q_{i,m}^0\left(1 + \frac{kq_i}{2}\left(V_{i,k,m} - 1\right)\right) \qquad \begin{array}{l}\forall i \in N_s, \\ ,\forall k, \forall m \in N_m\end{array} \qquad \text{(5-8.d)}$$

Now, we move to the formulation of the motor load powers. The active and reactive power of the motor load at node i and at step k, in case of the motor load starting at node m are expressed in the following. For the motor load that is starting ($i = m$), (5-8.e) and (5-8.g) express the active and reactive power consumptions according to the equivalent circuit shown in Fig. 5-1. The other motor loads ($i \neq m$) that are already energized are modeled in (5-8.f) and (5-8.h) as PQ constant loads in case of the motor load starting at node m.

$$P_{i,k,m}^D = \begin{cases} U_{i,k,m}\left(\dfrac{R_{k,m}^{th}}{R_{k,m}^{th\ 2} + X_{k,m}^{th\ 2}}\right) & : i = m \\[4mm] P_{i,m}^0 & : i \neq m \end{cases} \qquad \forall i, m \in N_m, \forall k \qquad \begin{array}{l}\text{(5-8.e)}\\[3mm]\text{(5-8.f)}\end{array}$$

$$Q_{i,k,m}^D = \begin{cases} U_{i,k,m}\left(\dfrac{X_{k,m}^{th}}{R_{k,m}^{th\ 2} + X_{k,m}^{th\ 2}}\right) & : i = m \\[4mm] Q_{i,m}^0 & : i \neq m \end{cases} \qquad \forall i, m \in N_m, \forall k \qquad \begin{array}{l}\text{(5-8.g)}\\[3mm]\text{(5-8.h)}\end{array}$$

where, $R_{k,m}^{th}$ and $X_{k,m}^{th}$ represent the Thevenin's equivalent resistance and reactance seen from the terminals of motor m at a given step k, respectively. The value of these Thevenin's equivalent impedances depend on the slip value at each step k.

5.6.2 AC power flow formulation

Constraints (5-9.a)-(5-9.d) represent the second-order cone relaxation of the branch flow model proposed in [26] for each step k in the acceleration period of each motor load m. The aim is to extract the electrical state variables (i.e. voltage, current, and power flow variables). These

variables are needed for the optimal control of the converter-interfaced generation units and for checking the transient constraints as it will be discussed in sections 5.6.3 and 5.6.5, respectively.

$$V_{j,k,m} = V_{i,k,m} - 2\left(r_{ij}.p_{ij,k,m} + x_{ij}.q_{ij,k,m}\right) + F_{ij,k,m}(r_{ij}^2 + x_{ij}^2) \qquad \begin{array}{l} \forall ij \in W, \\ \forall m \in N_m, \forall k \end{array} \qquad (5\text{-}9.a)$$

$$p_{ij,k,m} = \sum_{i^* \neq i} p_{ji^*,k,m} + r_{ij}.F_{ij,k,m} + P_{j,k,m}^D - P_{j,k,m}^{Sub} - P_{j,k,m}^{DG} \qquad \begin{array}{l} \forall ij \in W, \\ \forall m \in N_m, \forall k \end{array} \qquad (5\text{-}9.b)$$

$$q_{ij,k,m} = \sum_{i^* \neq i} q_{ji^*,k,m} + x_{ij}.F_{ij,k,m} + Q_{j,k,m}^D - Q_{j,k,m}^{Sub} - Q_{j,k,m}^{DG} \qquad \begin{array}{l} \forall ij \in W, \\ \forall m \in N_m, \forall k \end{array} \qquad (5\text{-}9.c)$$

$$0 \leq U_{i,k,m} \leq v_{max}^2 \qquad \forall i \in N, \forall m \in N_m, \forall k \quad (5\text{-}9.e)$$

$$F_{ij,k,m} \geq \frac{p_{ij,k,m}^2 + Q_{ij,k,m}^2}{U_{i,k,m}} \qquad \forall ij \in W, \forall m \in N_m, \forall k \quad (5\text{-}9.d)$$

Constraint (5-9.a) expresses the nodal voltage equation as given in [26]. The last term in the right hand side of (5-9.a) is usually neglected, since it is much smaller than the other terms. Constraints (5-9.b) and (5-9.c), respectively, concern with the active and reactive power balances at both extremities of each line. The first term in the right hand side of (5-9.b) and (5-9.c), represent, respectively, the sum of active and reactive power flows in lines that are connected to bus j except the line ij. According to these two equations, the power flow from bus i to bus j is equal to the sum of power flows in the other lines connected to bus j plus the net injection power at bus j and the power losses in line ij. Constraint (5-9.e) imposes the maximum voltage limit at the nodes of the network. Constraint (5-9.d) is the relaxed version of the current flow equation in each line according to [26]. This constraint is implemented in the form of the following second order cone constraint.

$$\left\| \begin{array}{c} 2p_{ij,k,m} \\ 2q_{ij,k,m} \\ F_{ij,k,m} - U_{i,k,m} \end{array} \right\|_2 \leq F_{ij,k,m} + U_{i,k,m} \qquad \forall ij \in W, \forall m \in N_m, \forall k$$

5.6.3 Converter control of generation units

In the *current saturation mode*, the injection current of the DG is controlled. According to the following formulation, we compute the optimal values of current set points in case of starting each of the motor loads during the restorative period.

$$Fp_{i,m}^{DG} + Fq_{i,m}^{DG} = f_{max,i}^{DG}{}^{2} \tag{5-10.a}$$

$$P_{i,k,m}^{DG}{}^{2} \le Fp_{i,m}^{DG} \cdot U_{i,k,m} \tag{5-10.b}$$

$$Q_{i,k,m}^{DG}{}^{2} \le Fq_{i,m}^{DG} \cdot U_{i,k,m} \tag{5-10.c}$$

The magnitude of the current injection by the DG converter at node i is forced in (5-10.a) to be equal to its maximum current limit ($f_{max,i}^{DG}$). Constraints (5-10.b) and (5-10.c) derive the square of the active and reactive current components, respectively. These constraints are relaxed versions of the original formulations that are equalities instead of inequalities. The aim is to build a convex model of the DG control in current saturation mode. These relaxations are exact according to the discussion provided in Appendix 5.11.4. Constraints (5-10.b) and (5-10.c) are implemented in the form of second order cone constraints as expressed in the following:

$$\left\| \begin{matrix} 2P_{i,k,m}^{DG} \\ Fp_{i,m}^{DG} - V_{i,k,m} \end{matrix} \right\|_{2} \le Fp_{i,m}^{DG} + V_{i,k,m}$$

$$\left\| \begin{matrix} 2Q_{i,k,m}^{DG} \\ Fq_{i,m}^{DG} - V_{i,k,m} \end{matrix} \right\|_{2} \le Fq_{i,m}^{DG} + V_{i,k,m}$$

5.6.4 Autotransformer tap setting

In what follows, the autotransformer that is used for the starting of a given induction motor is modeled and incorporated into the optimization problem. The tap position of the autotransformer will be set according to the obtained optimal solution before starting the motor.

Fig. 5-4 shows the equivalent circuit of an autotransformer, where Z_p and Z_s denote the impedances at the primary and secondary sides, respectively. $S_{i'j'}$ is the apparent power flowing from the auxiliary node i' to the auxiliary node j'. Based on this equivalent circuit, the constraints related to each autotransformer installed at the terminals of motor m are formulated as follows:

$$V_{j,k,m} = V_{i,k,m} \cdot (1 + \sigma_m \cdot \Delta r_m)^2 \tag{5-11.a}$$

$$V_{j,k,m} \approx V_{i,k,m} \cdot (1 + 2\sigma_m \cdot \Delta r_m) \tag{5-11.b}$$

where, σ is the ratio change between two consecutive taps of the autotransformer. Assuming that the turn ratio of the autotransformer is close to 1, the non-linear term in (5-11.a) is linearized in (5-11.b) using the binomial approximation. The product of the integer variable Δr_m and the
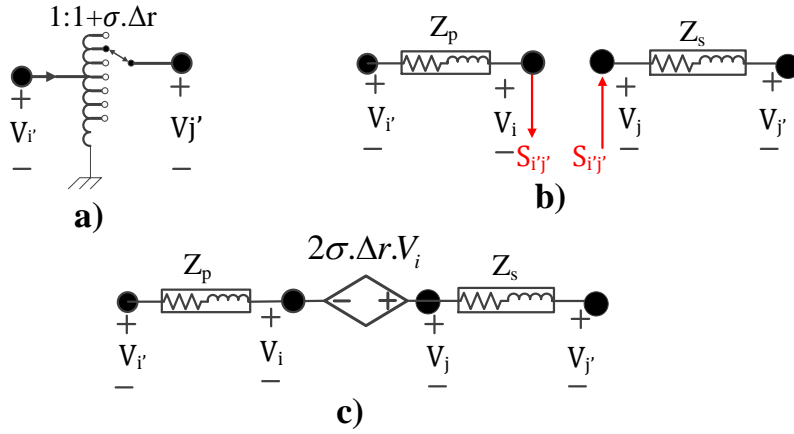
Fig. 5-4. Modelling of the autotransformer. a) schematic, b) standard equivalent circuit, c) linearized model.

positive continuous variable $V_{i,k,m}$ makes a non-linear term. This non-linear term is reformulated according to the linearization strategy given in [99]. For this aim, first the integer variable Δr_m should be expressed as the weighted sum of auxiliary binary variables. Then, the product of each of these auxiliary binary variables and the positive continuous variable $V_{i,k,m}$ is linearized using the approach given in Appendix 5.11.3.

Finally, Fig. 5-4.c shows how the derived model in (5-11.b) together with the primary and secondary impedances of the autotransformer are incorporated into the AC-power flow equations.

5.6.5 Transient Constraints

In this section, transient constraints are expressed regarding the safe starting of the induction motor in a distribution network.

$$T_{k,m}^{ele} \geq T_{k,m}^{mec} + Kd_m\big(1 - S_{k,m}\big) \tag{5-12.a}$$

$$\tilde{V}_{k,m}^{min} \leq V_{i,k,m} \qquad \forall i \in N_p \tag{5-12.b}$$

$$F_{ij,k,m} \leq \tilde{F}_{ij,k,m}^{max} \qquad \forall ij \in W_p \tag{5-12.c}$$

In order to avoid the induction motor to stall, (5-12.a) enforces the electrical torque to be larger than or equal to the load torque. For a given slip $S_{k,m}$, the electrical torque of the motor m is obtained using (5-1) and the mechanical load torque is determined according to the torque-speed curve of the mechanical load. This curve is assumed to be given for a specific load on the shaft.
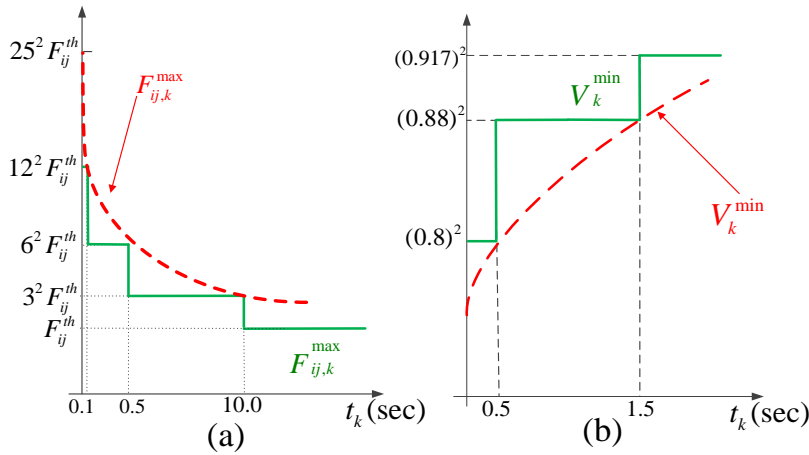
Fig. 5-5. Typical protection curve of a) over-current and b) under-voltage relays used in this study

The tripping of the under voltage relays and the over-current relays is avoided, adding (5-12.b) and (5-12.c) for every step k of the starting of each motor load at node m. Fig. 5-5 shows the typical protection curves reported in [5] and [10]. These curves represent the values of the under-voltage ($V_{k,m}^{min}$) and over-current ($F_{ij,k,m}^{max}$) limits as functions of the acceleration time ($\tilde{t}_{k,m}$), which was formulated in (5-3).

For the sake of preserving the linearity in terms of variable $\tilde{t}_{k,m}$, V_k^{min} and $F_{ij,k}^{max}$ are approximated by $\tilde{V}_k^{min}$ and $\tilde{F}_{ij,k}^{max}$, respectively, according to the piecewise linear approximation method explained in Appendix 5.11.1. In this regard, for obtaining $\tilde{V}_k^{min}$, we add (5-15)-(5-18) to the set of constraints, replacing x and $f(x)$ with $\tilde{t}_{k,m}$ and V_k^{min}, respectively. For deriving $\tilde{F}_{ij,k}^{max}$, we augment the set of constraints by (5-15)-(5-18), replacing x and $f(x)$ with $\tilde{t}_{k,m}$ and $F_{ij,k}^{max}$, respectively.

5.7 Numerical Results

In this section, the functionality of the proposed optimization model is evaluated using a test distribution network shown in Fig. 5-6. This test network is introduced in chapter 2, section 2.7.

Except the motor loads that are indicated in Fig. 5-6, the rest of loads are assumed as static loads. The nameplate power ratings of the induction motors at nodes {13}, {20, 29}, and {41} are equal to 805, 435, and 80.5 horsepower, respectively. The parameters of the equivalent circuit (see Fig. 5-1) of these motor loads are adopted from the real data given in [100]. The static loads are assumed to be of constant-impedance type. Therefore, their voltage sensitivity coefficients
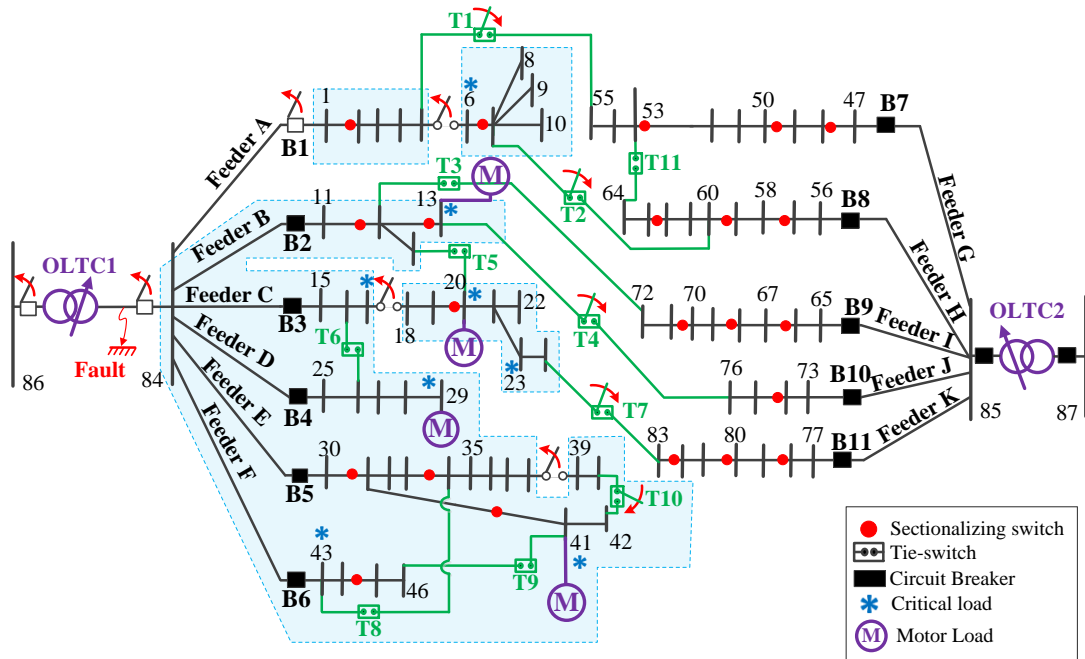
Fig. 5-6. The test distribution network under the post-fault configuration.

are set to $K_p = 2$ and $K_q = 2$. It is assumed that each node in the network shown in Fig. 5-6 is equipped with a load breaker. The load variation data along time is according to the practical data reported in [57]. In Fig. 5-6, the critical loads are identified with '*'. The priority factor (D_i) of these loads is equal to 10 and for the other loads is equal to 1.

It is assumed that a fault occurs on the substation 86-84 shown in Fig. 5-6. The faulted substation is isolated by opening its nearest breakers at both sides. The restorative period is assumed from 17:00 P.M. to 03:00 A.M [4]. As mentioned in section 5.3, in order to obtain the optimal restoration strategy, first, the steady-state analysis is performed according to [99]. The reconfiguration results are shown in Fig. 5-6. The areas in the off-outage area that are colored with red, green, blue, and yellow are energized through closing tie-switches T1, T2, T4, and T7. The optimal load restoration sequence obtained from the steady-state analysis is depicted on a time axes in Fig. 5-7.a.

Then, the proposed optimization problem in this chapter is solved in order to shift the energization instants of certain loads to account for the starting dynamics of the motor loads. In this regard, three sets of simulation scenarios are studied. The algorithm is implemented on a PC with an Intel(R) Xeon(R) CPU and 6 GB RAM; and solved in Matlab/Yalmip environment, using Gurobi solver. Branch-and-Bound method is used to handle the developed mixed-integer
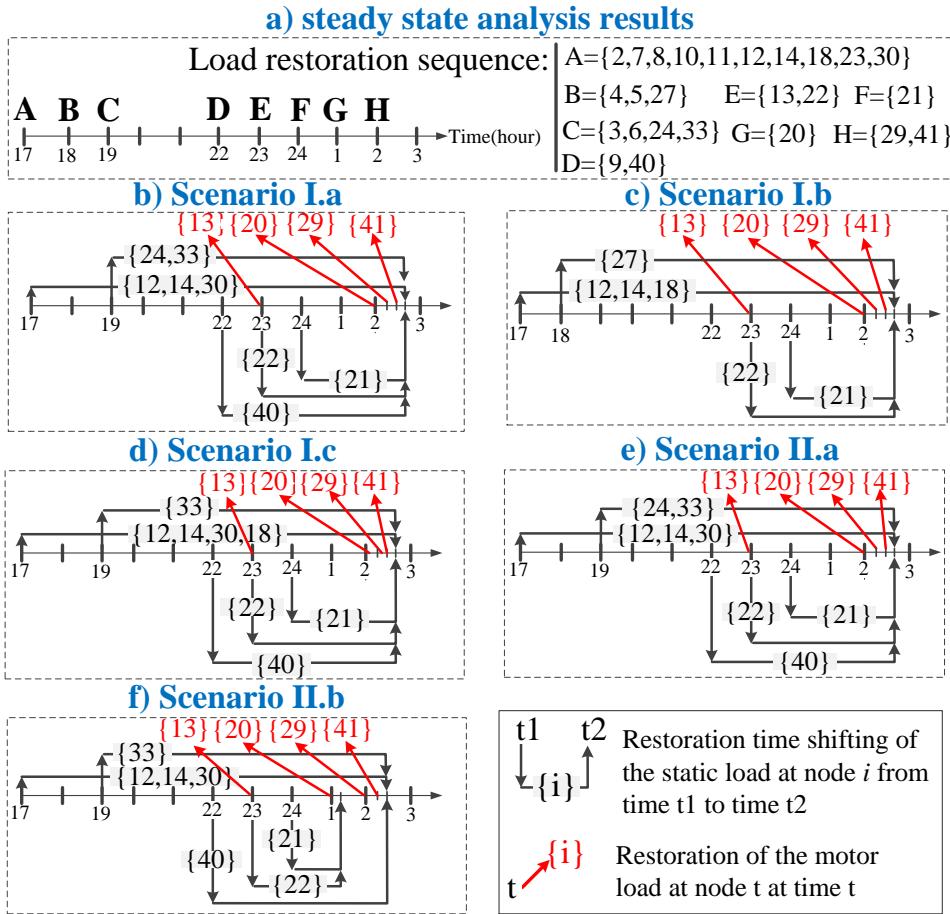
Fig. 5-7. The optimal load energization sequences.

optimization problem. The base power and energy values are set to 1MW and 1 MWh, respectively. The slip step size (Δs) is assumed to 0.05 p.u.

5.7.1 Simulation scenario I: linear load torque

The first set of simulation scenarios are studied assuming that the mechanical loads of all the motor loads have linear torque-speed characteristics. The magnitude of the nominal mechanical torques (at the synchronous speed) are equal to 0.4, 0.3, and 0.05 p.u. for the loads at nodes {13}, {20, 29}, and {41}.

Scenario I.a is defined assuming the critical and sensitive loads are set according to the default conditions shown in Fig. 5-6. The optimization problem is solved and the resulting optimal decisions are shown in Fig. 5-7.b. This figure shows the loads whose energization times should be shifted with reference to the results obtained from the steady-state analysis (see Fig. 5-7.a). The time resolution of this study is chosen to be 1 hour. As it can be seen in Fig. 5-7, the motor

loads are energized in sequential steps with sufficient time intervals such that the starting transients of different motors do not overlap [100].

This shifting of the load energization times causes 29.7 p.u. additional energy not supplied (while considering the priority factors D_i). This simulation scenario includes a large-scale off-outage area and 4 unsupplied motor loads resulting in 134 binary and 24282 continuous variables. However, the solution for such a large study case is found just in 12.28 s.

In order to see the effects of the critical loads on the optimal results, scenario I.b is studied. In this scenario, the loads at nodes {24, 30, 33, 40} are considered as additional critical loads. The optimal results obtained for the load restoration sequence is depicted in Fig. 5-7.c. Compared to the results of scenario I.a (see Fig. 5-7.b), it can be seen that the energization times of the new critical loads are not postponed in scenario I.b. The reliability objective value is obtained equal to 29.95 p.u. The computation time is 11.64 s.

In the next step, scenario 1.c is defined such that node 18 is added to the protected nodes. The rest of the simulation conditions are the same as in scenario I.a. The results in Fig. 5-7.d shows that the restoration of the load at node 18 is shifted to the time when all the motor loads are already energized. The reason is that the under voltage limit at node 18 (during the motor acceleration period) cannot be respected without shifting the energization of many of other loads. This decision leads to increase the reliability objective value from 29.07 p.u. in scenario I.a to 29.87 p.u. The computation time in scenario I.c is 11.69 s.

5.7.2 Scenario II: fixed load torque

In scenario II.a, it is assumed that the mechanical load on the shaft of the induction motor at node 20 has a fixed torque-speed characteristic equal to 0.06 p.u. The rest of the simulation conditions are the same as in scenario I.a. According to the results shown in Fig. 5-7.e, for the safe starting of the motor load at node 20, the same amount of loads should be shifted with respect to the ones in scenario I.a, although the mechanical load power in this scenario is so much less than the one in scenario I.a. The reason is that under a fixed-torque mechanical load, the induction motor can accelerate only if the starting torque (electrical torque at the standstill, s=1) is larger than the mechanical torque. In order to generate this starting torque, the voltage at the motor terminal should be large enough. This is obtained by shifting the energization of loads in

the off-outage area, which results in a reliability objective value equal to 29.07 p.u.. The computation time is 16.98 second.

In Scenario II.b, the test case of the scenario II.a is studied while assuming an autotransformer at the terminals of the motor load at node 20. It is located in series between node 20 and the induction motor terminals during its acceleration period. Once the motor reaches to 80% of its nominal speed, this autotransformer is taken out from the circuit and the motor is directly connected to the grid [124]. This autotransformer enables $\pm 20\%$ voltage regulation range in 5 steps ($\sigma = 10\%, n = 4$). According to the results shown in Fig. 5-7.f, with the optimal setting of the autotransformer, there is no need any more to shift the energization time of loads at nodes $\{20, 24\}$.

The optimal setting of the autotransformer is obtained with the tap position equal to -1. It means that the autotransformer reduces the voltage at motor terminals, which in turn reduces the starting current magnitude of the induction motor. Therefore, the magnitudes of the line voltage drops are reduced. In this regard, this optimal tap setting improves the quality of the restoration solution by increasing the margins of the nodal voltage magnitudes with respect to the transient under-voltage limits. The optimal value of the reliability objective is 25.175 p.u. and the computation time is 14.57 second. It will be validated in the next section that all the transient operational limits are respected with the obtained restoration solutions. Among all the constraints, the voltage magnitude at the accelerating motor node has a very narrow margin with respect to the transient minimum voltage limit.

5.7.3 Scenario III: DG control in current saturation mode

Scenario III is defined, where a fault occurs on line 84-30. Fig. 5-8 shows the part of the network that is affected by the post-fault configuration. As it can be seen, the only motor load in this part of the network is at node 41.
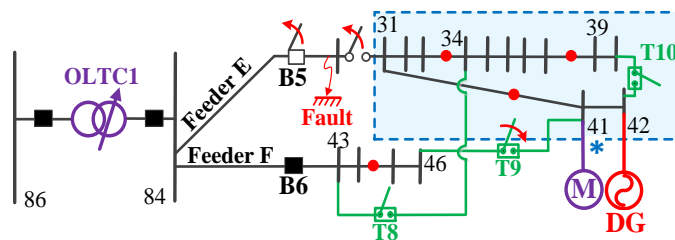

Fig. 5-8. Part of the test distribution network under the post-fault configuration in simulation scenario III.

Table 5-1. The parameters of the induction motor at INESC TEC.

Size (W)	$R_1(\Omega)$	$X_1(\Omega)$	$R_2(\Omega)$	$X_2(\Omega)$	$X_m(\Omega)$	H(sec)
4000	1.44	2.56	1.37	2.56	56.17	0.198

The parameters of this induction motor are given in Table 5-1. The mechanical load torque on the shaft of the induction motor changes linearly with speed and equals to 2.2 N.m. at the synchronous speed. There is also a DG at node 42, with the ampacity limit equal to 3.65 A. These parameters are according to the parameters of the physical induction motor and DG in the test setup at INESC TEC[13].

The proposed optimization problem is solved in case of this simulation scenario. The optimal load restoration sequence is to energize the static loads at nodes {32,35,36,37} together with the motor load at node {41} at the beginning of the restorative period (at 17:00 P.M). Once the transients of the motor starting disappear (at 17:15 P.M.), we will restore the loads at nodes {31,33,39,40}. The control of the DG converter at node 42 enters to the saturation mode during the motor acceleration period. The optimal active and reactive components of the converter current references are obtained as 2.106 A and 2.970 A, respectively.
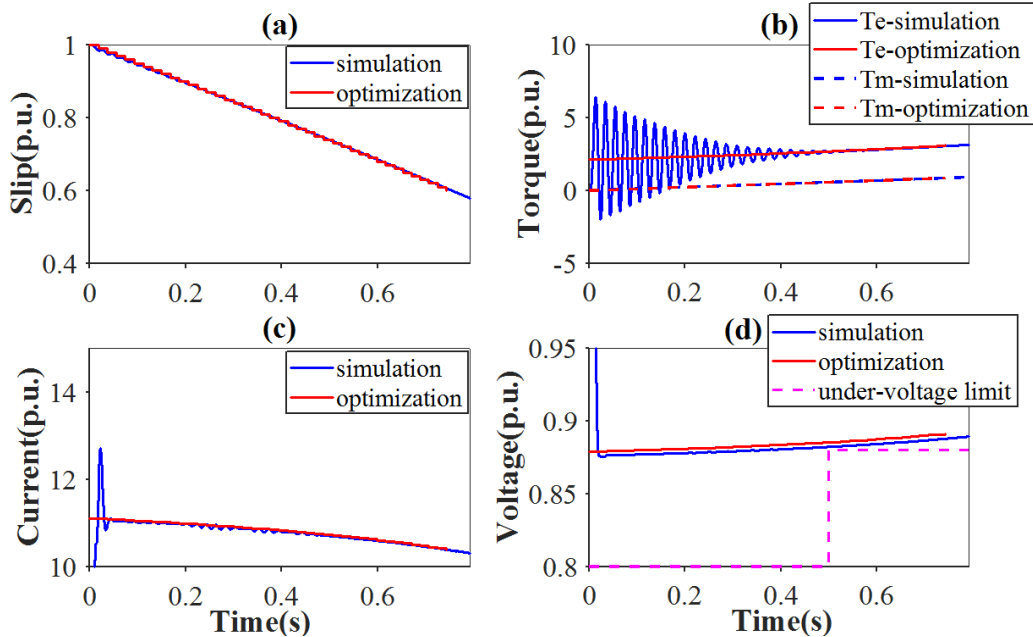
Fig. 5-9. Simulation results for scenario III. a) slip, b) electrical and mechanical torques, c) motor starting current, d) voltage at node 41.

---

[13] Institute for systems and computer engineering, technology and science (INESC TEC) is an institution in Porto, Portugal operating at the interface of the academic and business worlds.
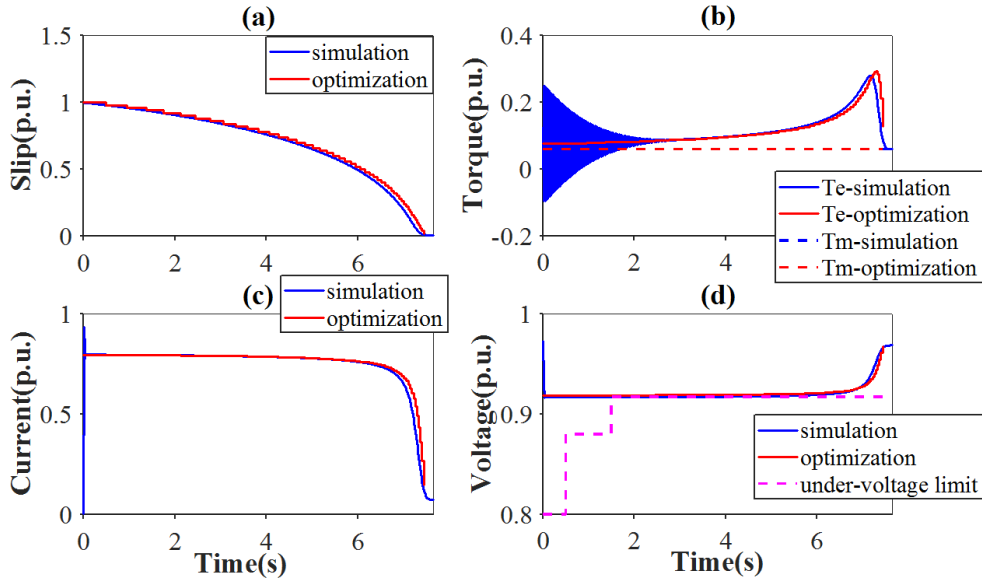
Fig. 5-10. Simulation results for scenario II.b. a) slip, b) electrical and mechanical torques, c) motor starting current, d) voltage at node 20.

5.8 Feasibility Validation Results

This section is aimed to validate the solution feasibility of the proposed semi-static optimization model using an off-line simulation and a physical test experiment. It will be illustrated that the dynamics of the induction motor starting are represented into the optimization problem with a sufficient degree of accuracy. For this aim, the results obtained from scenario III and given in section IV.C are applied on the distribution network shown in Fig. 5-8.

5.8.1 Time-domain simulation results

In this section, an off-line model of the distribution network shown in Fig. 5-8 is built in Matlab/Simulink. The motor loads and static loads are represented by the Simulink model of the induction motor, and the impedance loads, respectively. The DG is modeled with a controllable dynamic load. First, we apply the obtained optimization results of scenario III on the off-line simulation model and then we start the motor. Fig. 5-9 shows the simulation results. In this figure, the electrical state profiles obtained from the optimization problem are compared with the ones obtained from the time-domain simulation. As it can be seen, the proposed semi-static optimization model does not represent the initial overshoot transients of the motor inrush current. As mentioned in section 5.5, in deriving the semi-static model, we neglect the DC term in the motor starting current. Disregarding these very fast transients, Fig. 5-9 shows that the proposed

semi-static model represents accurately the behavior of electrical state variables during the motor acceleration at the motor and network sides.

In a similar fashion, the optimal results obtained from scenario II.b are tested using a time-domain simulation in Matlab/Simulink. The results at t=01:00, when the motor load at node 20 is started (see Fig. 5-7.f), are provided in Fig. 5-10. These results validate the feasibility of the optimal setting that was found in scenario II for the tap position of the auto-transformer.

5.8.2 Experimental test

As the next step of the validation study, a Power Hardware In the Loop (PHIL) experiment is performed. The test setup is implemented as shown in Fig. 5-11 in the smart grid laboratory at INESC TEC [125]. The block diagram of the laboratory test setup is depicted in Fig. 5-12. This PHIL test setup consists of three main parts. I) The first part includes the Matlab/Simulink network model of the whole network shown in Fig. 5-8 except the nodes 41 and 42. This model is compiled, and then executed by a Real-Time Simulator, namely OPAL-RT OP5600. II) The second part includes the Power Amplifier which magnifies the motor voltage signal received from the Real-Time Simulator. In this test setup TriPhase PM15 is used as the power amplifier
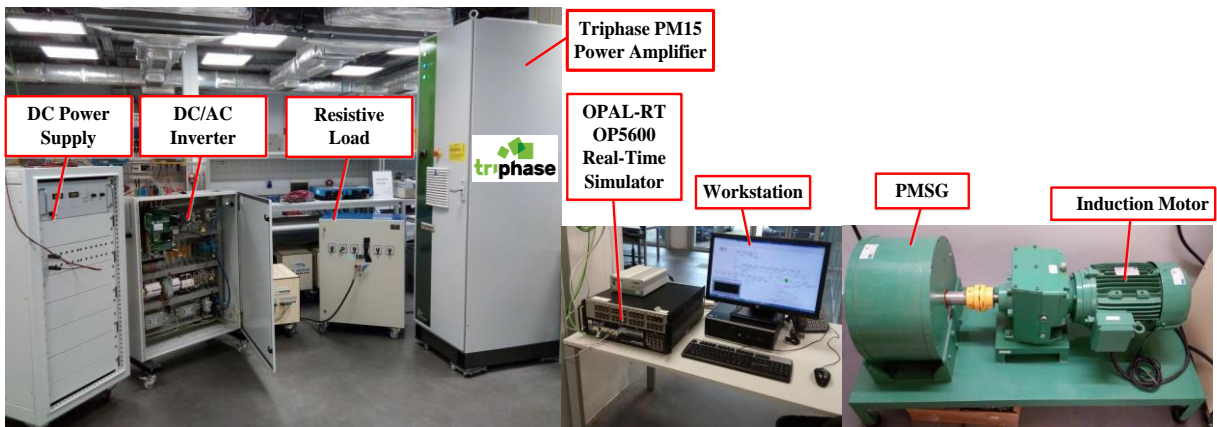

Fig. 5-11. The experimental PHIL test setup in the smart grid laboratory at INESC TEC.
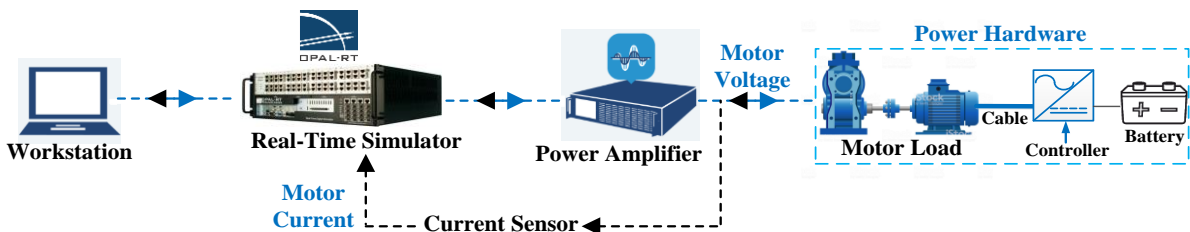
Fig. 5-12. Block diagram of the PHIL test setup.

with the nominal voltage equals to 400V. It can tolerate up to 30A of peak current per phase. In order to respect this ampacity limit during the motor acceleration period, the base power and voltage of the test network are reduced to 320 VA and 150 V, respectively. III) The third part of the PHIL test setup is the physical hardware, including the motor load at node 41 and the DG at node 42 that are connected through a co-axial cable. In order to emulate a mechanical load with a linear torque-speed characteristic, the induction motor is loaded with a permanent magnet synchronous generator connected to a resistive load. The DG is emulated using an AC-DC inverter that is supplied by a DC power supply and controlled in current saturation mode.

We start the induction motor and measure the voltages at the motor terminals during the motor acceleration period. As shown in Fig. 5-13, the voltage amplitude is always above the transient under-voltage limit. It verifies that the under-voltage relay installed at the motor terminals will not trip in case of starting the motor load.
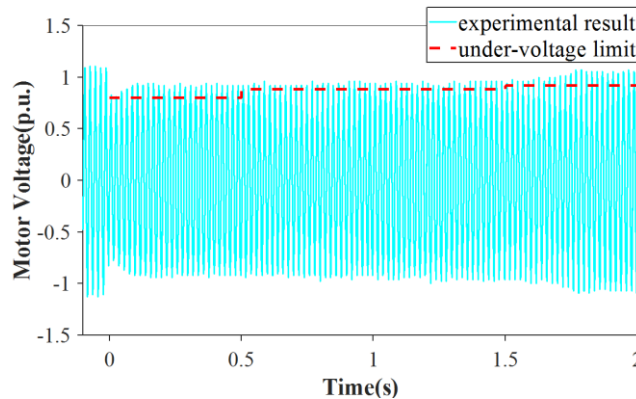
Fig. 5-13. The voltage magnitude measured at the motor terminals during its acceleration period.
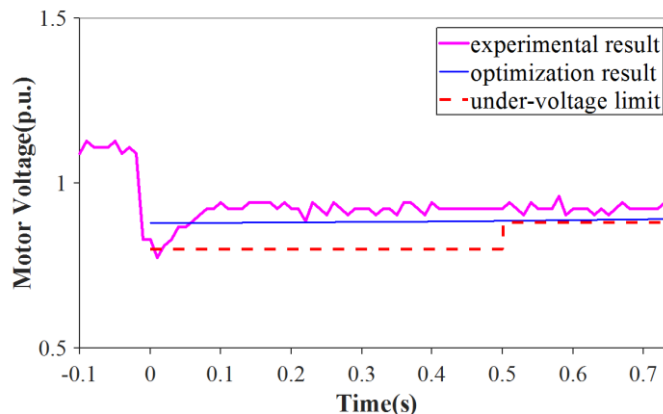
Fig. 5-14. The voltage at the motor terminal during its acceleration period obtained from the experiment and from the optimization model.

In Fig. 5-14, the RMS value of the voltage measured at the motor terminal during the experiment is compared with the voltage profile obtained from the proposed semi-static model. Fig. 5-14 shows that except at the first instants after the motor energization, the results of the semi-static model are sufficiently accurate with respect to the experimental results. At the first instants following the motor starting, the voltage at the motor terminal experiences a voltage dip that cannot be represented using the semi-static model. This voltage dip is caused by the DC term in the motor inrush current, which is neglected in deriving the semi-static model. As it can be seen in Fig. 5-14, this transient voltage dip disappears very fast and does not affect the feasibility of the solution with respect to the transient under-voltage limit.

Fig. 5-15 shows the voltage, current, and power measured at the terminals of the DG during the motor acceleration period. The active and reactive components of the DG current are almost controlled to the reference values, which are obtained in section 5.7.3 as 2.106 A and 2.97 A, respectively. Fig. 5-15 validates that the DG is working in current constant mode during the period that the DG experiences the voltage dip at its terminals due to the inrush starting current of the motor.

5.9 Sensitivity Analysis

When it comes to the practical application of a strategy in the operational management of a distribution network, it is important to undergo a sensitivity analysis. In this regard, the
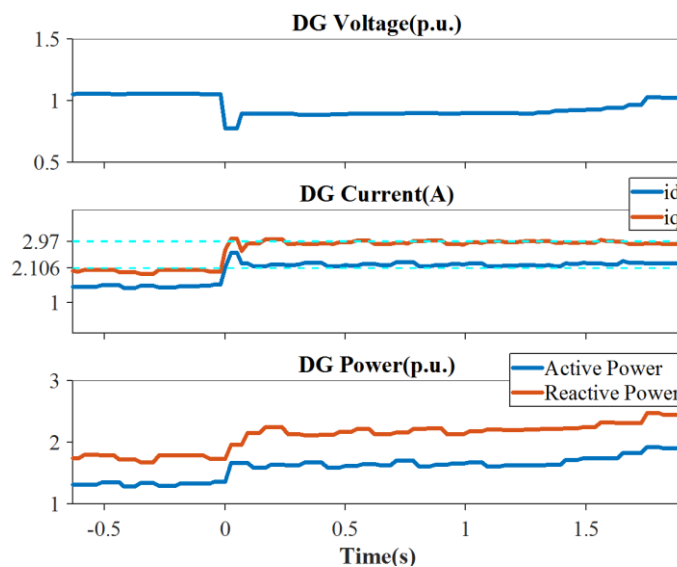

Fig. 5-15. The measured voltage, current and power of the DG during the motor acceleration period in the PHIL test experiment.

sensitivity of the restoration solution obtained from the proposed optimization problem is evaluated with respect to the changes in the DG capacity and to the changes in the line impedances.

In the first step, we assess the effect of changing the DG capacities on the optimal restoration plan. For this aim, scenario III is considered as the reference case study. The optimal solution obtained in case of this scenario was reported in section 5.7.3, which is given again in Table 5-2. Two new case studies are considered, where all the DG capacity parameters increase by 10% and decrease by 10% with respect to their default values, defined in scenario III. The results of the first stage optimization problem (steady-state analysis) in case of these new case studies are the same as the solution obtained in the first stage in case of scenario III. The reason is that the over voltage limit at the DG hosting node is binding and it does not let the DG to inject more power in steady state. However, the second stage optimization problem leads to different solutions in case of these new case studies. The numerical results given in Table 5-2 show that with 10% increase in the DG ampacity limit, the optimal value of the objective function decreases by 15.38%, and with 10% decrease in the DG ampacity limit, the optimal value of the

Table 5-2. The sensitivity of the optimal solution of the second stage of the restoration problem to the changes in the DG capacities

Case Studies	DG capacity			Optimal load restoration sequence	i_d (A)	i_q (A)	ENS (p.u)
	P_{max}^{DG} ($p.u$)	S_{max}^{DG} ($p.u$)	f_{max}^{DG} (A)				
Scenario III	2.8	3.0	3.65	- Restore loads {32,35,36,37,40, 41} at 17:00 P.M - Restore loads {31,33,39,40} at 17:15 P.M	2.11	2.970	3.90
10% increase in DG capacities	3.08	3.3	4.02	- Restore loads {32,33,35,37,40, 41} at 17:00 P.M - Restore loads {31,36,39} at 17:15 P.M	2.47	3.16	3.3
10% decrease in DG capacities	2.52	2.7	3.29	- Restore loads {32,35,37,41} at 17:00 P.M - Restore loads {31,33,36,39,40} at 17:15 P.M	1.80	2.74	4.79

objective function increases by 22.832%.

In the second step, the results regarding the sensitivity analysis of the restoration solution with respect to the estimation errors in the line impedances are presented. First, the impact of these estimation errors on the feasibility of the obtained restoration solution in terms of the network security constraints is studied. In this regard, Scenario III is considered again as the reference case study. Four new case studies are defined, where it is assumed that the impedances of all the lines in the network equally have 10% overestimation errors, 5% overestimation errors, 5% underestimation errors and 10% underestimation errors. In Scenario III, the restoration solution was obtained from the optimization problem with the default estimated line impedances. Now, the goal is to evaluate the feasibility of this restoration solution under the assumptions given in each of these new case studies. In this regard, the off-line time-domain simulation is used and the obtained restoration solution is applied on the off-line model of the distribution network, where line impedances are equal to the assumed values in each case study.

Since the minimum-security margin in case of starting the motor load in scenario III is associated with the transient under-voltage limit at the motor hosting node, the feasibility of the restoration solution is assessed illustrating only the voltage magnitude at this node. Fig. 5-16 shows the simulation results under each case study. As it can be seen in Fig. 5-16, the
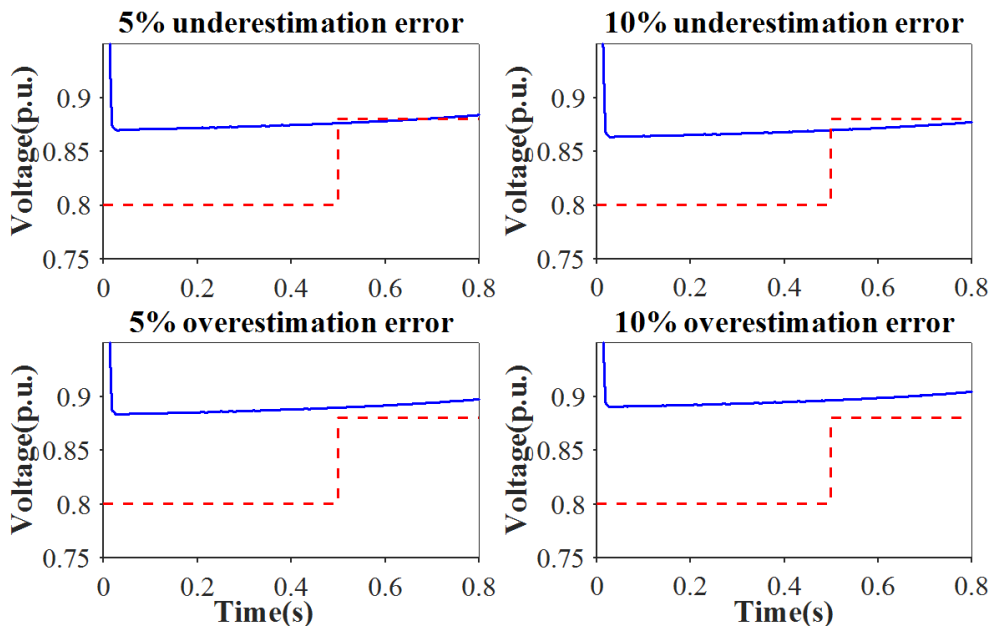

Fig. 5-16. Simulation results for the feasibility of the obtained restoration solution in scenario III, under different levels of estimation errors for the line impedances. The blue curve is the voltage magnitude at the motor hosting following starting the motor and the red line is the transient under-voltage limits.

Table 5-3. The Sensitivity of the optimal restoration solution with respect to the line impedances

Case Studies	Optimal load restoration sequence	ENS (p.u.)
Scenario III	- Restore loads {32,35,36,37,40,41} at 17:00 P.M - Restore loads {31,33,39,40} at 17:15 P.M	3.90
5% decrease in line	- Restore loads {32,33,35,36,37,41} at 17:00 P.M - Restore loads {31,39,40} at 17:15 P.M	2.41
10% decrease in line	- Restore loads {31,32,35,36,37,41} at 17:00 P.M - Restore loads {33,39,40} at 17:15 P.M	1.52

underestimated line impedances lead to a decrease in the nodal voltage margin with respect to the transient under voltage limit. By 5% underestimation error, the solution is still feasible, whereas by 10% underestimation error, the solution is not any more feasible.

Fig. 5-16 illustrates that the overestimation of line impedances causes the security margin of the obtained restoration solution to increase with respect to the reference case study. Therefore, for providing a robust restoration solution against estimation errors in the line impedances, we should overestimate the values of these line impedances.

However, by this overestimation, the quality of the obtained restoration solution is defected (in terms of the value of F^{ENS} objective term). Table 5-3 shows the optimization results, where the line impedances are equal to the default values and where these values are decreased equally by 5% and by 10%. The numerical results of Table 5-3 show that by 5% and 10% overestimation in the line impedances, we lose the quality of the restoration solution by 38.21% and 61.03%, respectively.

5.10 Conclusion and Summary

The optimal restoration plan obtained from the steady-state analysis cannot guarantee that the transient network security constraints (e.g. voltage-dip and over-current transient acceptability limits) are respected during the acceleration period of large motor loads. Due to the large and reactive inrush currents driven by induction motor loads, the re-acceleration of these loads can

impose high stresses both on the network and on the motor itself. In this regard, we aimed in this chapter to modify the load restoration sequence obtained from the steady-state analysis in the most optimal way such that the transient constraints are respected during the motor acceleration period. The objective is to minimize the total energy of loads that cannot be restored according to the modified load restoration sequence.

In this chapter we presented a convex optimization model representing the starting transients of induction motors in a semi-static fashion. This model was integrated into a relaxed AC power flow formulation while preserving the convexity of the optimization model. The resulting optimization problem represents the transient electrical states of an active distribution network during the motor acceleration period. The transient operational limits imposed by under-voltage and over-current protection devices are integrated into the developed optimization problem. The aim is to guarantee that the starting transients of motor loads will not trigger the protection devices that exist in the distribution network.

A convex model is derived for the converter-interfaced DGs working in constant current mode following the voltage sags induced by motor load startings. By integrating this model into the optimal load restoration problem, we obtained the optimal current set points such that the DGs support the electrical constraints in case of the motor starting transients in an optimal fashion. In addition, the proposed optimization formulation includes a convex model for the optimal tap setting of the autotransformer that is used for the starting of the induction motors.

The functionality of the formulated optimization problem was evaluated using three simulation scenarios. The optimal load restoration sequences are obtained in scenarios I and II while considering the starting transients of induction motors under mechanical loads with linear and fixed torque-speed characteristics, respectively. The optimization problem for each of these simulation scenarios includes large-scale off-outage areas and four unsupplied motor loads. The short computation time reported for these case studies confirm that the proposed optimization problem can scale up to solve large-scale case studies. The effects of critical loads and also the effect of protected nodes on the optimization results were illustrated using simulation scenarios I.b and I.c, respectively. In scenario II.b, the model of the autotransformer is added to the optimization problem and the optimal setting for its tap position is obtained. It was shown that with the inclusion of the autotransformer, the quality of the obtained solution can be largely

improved. In scenario III, a different test case is studied in order to integrate the model of the DG into the optimization problem. The results of this test study provide the optimal set point for the current references of the DG converter for the starting of each induction motor.

The accuracy of the proposed semi-static model in providing feasible restoration solutions was shown using off-line simulation and experimental test studies. Regarding the experimental test, we implemented a Power Hardware In the Loop (PHIL) test setup while having the induction motor load and the DG as physical hardware. It was illustrated that all the transient constraints both in motor side and in the network side are respected during the acceleration period of the induction motor. In addition, we provided simulation results to show the superiority of the proposed DG control strategy with respect to the control strategies suggested by the existing grid codes during the transient voltage dips.

In summary, this chapter provides a semi-static and convex optimization model for the starting transients of an induction motor load. This optimization model can be applied in any decision-making problem that is facing operational bottlenecks imposed by the motor starting transients. The developed semi-static model is used in this chapter to solve the optimal load restoration problem in a distribution network. In this problem, the optimal energization sequence of different loads (static and motor loads) are obtained such that the total energy of loads that cannot be supplied is minimized.

5.11 Appendices

5.11.1 Slip Discretization

In this section, it is aimed to justify the assumption made in section 5.5 that the slip is fixed at each step. Equation (5-13) is the first-order approximation of the tailor expression for the motor slip as a function of time. This approximation is made for the time interval $[t_k, t_k + \Delta t_k]$, where t_k and Δt_k are the starting time and the time length of step k, respectively.

$$S_m(t) \approx S_{k,m} + \frac{dS_m}{dt}(t - t_k) \quad \forall t \in [t_k, t_k + \Delta t_k] \tag{5-13}$$

The time derivative of slip can be expressed according to the dynamic motion equation (5-14).

$$\frac{dS_m}{dt} = \frac{1}{2H_m}\left(T_m^{ele} - T_m^{mec} - Kd(1 - S_m)\right) \tag{5-14}$$

As it can be understood from (5-13), the time derivative of slip should be small enough in order to assume that the slip equals to $S_{k,m}$ during each step k. According to (5-14), it will be the case when the total inertia of the induction motor is large. This condition holds when we study the starting of large induction motors under mechanical loads with high moment of inertia or when we study an aggregated model of multiple induction motors. According to (5-13), for modeling low-inertia induction motors, we have to assume a greater number of slip steps so that the time length of each step k (Δt_k) will be small enough. Therefore, we can assume that the second expression in the right-hand side of (5-13) is almost zero and therefore the slip can be approximated to $S_{k,m}$ during the step k.

5.11.2 Piecewise Linear Approximation

Consider $f(x)$ as a continuous function with the domain of $[x_1, x_n]$. The concept of the piece-wise linear approximation introduced in [126] is shown in Fig. 5-17, where $\tilde{f}(x)$ denotes an approximation function for $f(x)$. We divide the domain of function f by n break-points $x_1, x_2, \ldots, x_n$. Between each two successive breaking points x_i and x_{i+1}, the function f is approximated with a straight line connecting the points x_i and x_{i+1}. In order to formulate this approximation method, we introduce n non-negative auxiliary variables λ_i under (5-15)-(5-18).

Assume a given point x between two breaking point x_i and x_{i+1}. The value of x is expressed in (5-15) in terms of the weighted sum of breaking points x_i and x_{i+1}, with λ_i and λ_{i+1} as the weighting coefficients. Using the same auxiliary variables, function $\tilde{f}(x)$ is formulated as in (5-16). The sum of all auxiliary variables λ_i should be one (5-17). Therefore, $\tilde{f}(x)$ consists of straight lines between successive breakpoints.
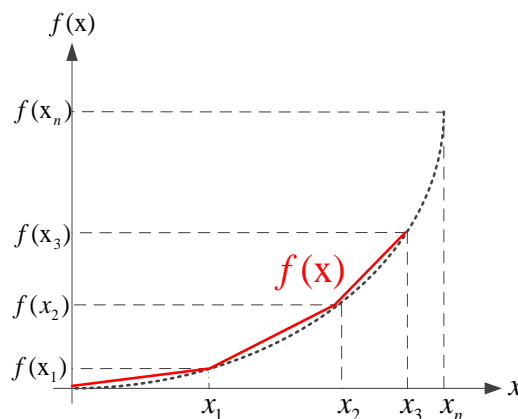
Fig. 5-17. Piece-wise linear approximation of an arbitrary continuous function $f(x)$

For the given point $x \in [x_i, x_{i+1}]$, all the auxiliary variables, except λ_i and λ_{i+1}, will be zero. Because as given in (5-18), variables λ are forced to respect the Special Ordered Set-2 (SOS2) constraint [56]. According to this constraint, out of all λ_i variables, at most two successive variables can be non-zero. Most of the commercial solvers have the feature to account for these types of constraints during the Branch-and-Bound search algorithm.

$$x = \sum_{i=1}^{n} \lambda_i x_i \tag{5-15}$$

$$\tilde{f}(x) = \sum_{i=1}^{n} \lambda_i f(x_i) \tag{5-16}$$

$$\sum_{i=1}^{n} \lambda_i = 1 \tag{5-17}$$

$$\lambda_i \geq 0 \;:\; SOS2 \tag{5-18}$$

We can increase the accuracy of this approximation using more number of breaking points (n). However, it leads to a greater number of auxiliary variables, which could increase the computation burden of the optimization problem.

5.11.3 Elimination of product of variables

In this section, a method is provided for the linearization of the constraints which incorporates a product of two variables. The product of two variables x_1 and x_2 can be replaced by one new variable y, subject to the constraints given in (5-19) and (5-20). The proof of this linearization is provided in [126]. It is assumed that x_1 is a binary variable and x_2 is a positive continuous variable, for which $0 \leq x_2 \leq u$ holds.

$$0 \leq y \leq u x_1 \tag{5-19}$$

$$x_2 - u(1 - x_1) \leq y \leq x_2 \tag{5-20}$$

5.11.4 Exactness of the relaxation used in the modeling of the DG control in the current saturation mode.

According to [123], it can be proved that the relaxation made in (5-10.b) and (5-10.c) will be exact under the following conditions:

I)   The maximum voltage limit at the DG hosting node is not binding during the acceleration period of the motor load.

II)   The line ampacity limits are not binding during the acceleration period of the induction motor.

III) The objective function strictly decreases with the square of active and reactive power injections of the DG ($P_{i,k,m}^{DG}{}^2$ and $Q_{i,k,m}^{DG}{}^2$).

Condition I holds, since the voltage at the DG node is already dropped due to the starting of the induction motor. Therefore, there is a large margin for the voltage at the DG node with respect to its maximum limit. Condition II is usually ensured during the planning phase of the distribution networks. For example, in industrial networks, the line ampacity limits are sufficiently larger than the starting current of induction motors.

Under these two conditions, the optimal value of the objective function (F_{re} in (5-4)) will be bounded only by the minimum voltage constraint. In this regard, during the acceleration period of an induction motor, the minimum voltage limit at the hosting node of the starting motor is the bottleneck constraint. Therefore, in order to restore more loads (to decrease the value of objective function F_{re}), the voltage at the motor node should increase. From the other hand, with the starting of the motor load (increasing of power absorption at the motor node), the voltage at the DG terminal decreases. It means that the sensitivity of the voltage at the DG node (V_{DG}) is positive with respect to the power injection at the motor node (P_m: negative of power absorption). Due to the symmetry of the grid admittance matrix, we can intuitively infer that the sensitivity of the voltage at the motor node (V_m) with respect to the power injection at the DG node (P_{DG}) is also positive. The mathematical proof of this expression is provided here below:

We make our analysis around the operation point corresponding to the first instants of the motor starting. The bus voltage at the motor node is affected by both active and reactive power injections at the DG node. However, for the sake of analysis, we may first keep the active power injection constant and evaluate the incremental relationship between Q and V. In this regard, we put $\Delta P = 0$ into the Newton Raphson formulation of the load flow equations given in (5-21). In the result, the $V - Q$ sensitivity is derived in (5-22) as a function of the reduced Jacobian matrix (J_R).

$$\begin{bmatrix} \Delta P_d \\ \Delta Q_d \end{bmatrix} = \begin{bmatrix} J_{P\theta} & J_{PV} \\ J_{Q\theta} & J_{QV} \end{bmatrix} \begin{bmatrix} \Delta\theta \\ \Delta V \end{bmatrix} \tag{5-21}$$

$$\Delta V = J_R^{-1} \Delta Q \tag{5-22}$$

where

$$J_R = [J_{QV} - J_{Q\theta} \, J_{P\theta}^{-1} \, J_{PV}] \tag{5-23}$$

ΔP_d, ΔQ_d, $\Delta \theta$ and ΔV are incremental changes in the bus real power output, bus reactive power out put, but voltage angle, and bus voltage magnitude, respectively. The reduced Jacobian matrix can be expressed in terms of its eigenvalues and eigenvectors according to (5-24).

$$J_R = \xi \Lambda \eta \tag{5-24}$$

where, ξ and η are the right and left eigenvector matrices of J_R, respectively. Λ is the diagonal eigenvalue matrix of J_R. Substituting of (5-24) into(5-22) gives;

$$\Delta V = \xi \Lambda^{-1} \eta \Delta Q \tag{5-25}$$

Finally, the sensitivity of the voltage at the DG hosting node (node i) to the power injection at the motor hosting node (node j) is derived as the following :

$$\Delta V_i = \sum_k \frac{\xi_{ik} \eta_{kj}}{\lambda_k} \Delta Q_j \tag{5-26}$$

where, each eigenvalue λ_k and the corresponding right and left eigenvectors (ξ_k and η_k, respectively) define the kth mode of the $Q - V$ response. We know that $\xi^{-1} = \eta$ and also we know that $\xi^{-1} = \xi^H$ if the consider only the first-order eigenvalues of J_R. Therefore, we can write:

$$\eta_{kj} = \xi_{kj}^{-1} = \xi_{jk}^* \tag{5-27}$$

$$\xi_{ik} = \eta_{ik}^{-1} = \eta_{ki}^* \tag{5-28}$$

Substituting (5-27) and (5-28) into (5-26) gives:

$$\frac{\Delta V_i}{\Delta Q_j} = \sum_k \frac{\eta_{ki}^* \xi_{jk}^*}{\lambda_k} = \sum_k \frac{\xi_{jk} \eta_{ki}}{\lambda_k} = \frac{\Delta V_j}{\Delta Q_i} \tag{5-29}$$

Since J_R is real, complex eigenvalues always occur in conjugate pairs, say $\lambda_{k_1} = \lambda_{K_2}^*$. Then, we can say that $\eta_{k_1 i} = \eta_{k_2 i}^*$ and $\xi_{jk_1} = \xi_{jk_2}^*$. Otherwise, if k is a real eigenvalue, we can conclude that η_{ki} and ξ_{jk} are also real. Therefore, we can rewrite (5-29) as the following:

151

$$\frac{\Delta V_i}{\Delta Q_j} = \sum_k \frac{\xi_{jk}\eta_{ki}}{\lambda_k} = \frac{\Delta V_j}{\Delta Q_i} \tag{5-30}$$

Since, at the starting of the induction motor ($\Delta Q_i > 0$), the voltage at the DG hosting node drops (ΔV_j), we can conclude that $\frac{\Delta V_j}{\Delta Q_i} < 0$. According to (5-30), we can conclude $\frac{\Delta V_i}{\Delta Q_j} < 0$. With the same argument, we can conclude that $\frac{\Delta V_i}{\Delta P_j} < 0$.

Therefore, if the DG power injection increases, the voltage at the motor load increases and therefore the total unrestored energy of loads (F_{re}: objective function) decreases. It means that condition III also holds according to the specific characteristics of the load restoration problem studied in chapter 5.

6 Conclusion

In this thesis, we propose an automatic service restoration strategy with specific reference to active distribution networks. In this respect, we present the following main contributions through the different chapters.

- Chapter2: Developing a mathematical optimization model for the restoration problem in passive distribution networks
- Chapter3: Integrating the re-energization and re-dispatch of DGs into the restoration problem for distribution networks
- Chapter4: Enhancing the tractability of the restoration problem formulation using a novel decomposition approach
- Chapter5: developing a convex optimization model for the starting transients of dynamic loads and integrating this model into the restoration problem

Chapter 2 presents a mathematical optimization model for the restoration problem in distribution networks. In this regard, first, we develop a linear formulation for the radiality constraints during the reconfiguration of passive distribution networks. Unlike the existing formulations in the literature, the proposed formulation covers real scenarios that could occur during the service restoration, such as partial restoration scenarios. This formulation is then augmented with the mathematical models of voltage regulation devices including I) On-Line Tap-Changing (OLTC) transformers, II) Step Voltage Regulators (SVRs), and III) Capacitor Banks (CBs). In this regard, the quality of the restoration solution is enhanced using the optimal

setting of these voltage regulation devices. In order to account for the voltage dependency of active and reactive load powers, their models are integrated into the optimization problem using a linear approximation method. Finally, different test studies are used to illustrate the effectiveness of the mathematical programming method in solving the proposed restoration problem formulation for passive distribution networks. This formulation is regarded as the basis of the contribution made in the next chapters.

Chapter 3 enables the potentials of DGs in better fulfilling the restoration objectives. For this aim, we present a new i) strategy and ii) formulation for the service restoration in DG-integrated distribution networks. i) Regarding the restoration strategy, we address the requirements imposed by the start-up process of disconnected DGs. In this regard, a "multi-step restoration" strategy is introduced as a compromise between the *static* and *dynamic* approaches which already exist in the literature. The start-up requirements of grid-connected DGs, including the energization of their hosting nodes and their start-up durations are accurately modeled in the proposed restoration strategy. ii) Regarding the restoration formulation, the developed restoration model in Chapter 2 is augmented with an exact power flow formulation called, Augmented Relaxed Optimal Power Flow (AR-OPF). The aim is to ensure the feasibility of the obtained restoration solution concerning the network security constraints (e.g. voltage and current limits). Unlike the other relaxation methods, the AR-OPF is exact even in presence of high DG penetrations in distribution networks. The overall restoration problem is in the form of a Mixed-Integer Second-Order Cone Programming (MISOCP) optimization problem. Therefore, it can be solved efficiently by the state-of-the-art commercial solvers for convex optimization problems. In order to illustrate different features of the developed optimization model, it is successfully tested with two test distribution networks through three test scenarios.

Chapter 4 proposes a novel solution strategy that makes the restoration problem formulated in previous chapters tractable for analytical solvers in case of a grid of realistic size. The link between the line switching variables and the power flow constraints inhibits the use of the classical Benders algorithm in decomposing the restoration problem. Therefore, we present a modification to the combinatorial Benders method so that it can be used for the multi-period restoration problem. According to the proposed modifications, the restoration problem is decomposed into master and sub problems, where line switching variables and the relaxed AC power flow formulation are handled separately. These master and sub problems are solved

through successive iterations. At each iteration, the solution of the sub problem is used to augment the constraints of the master problem with the proposed feasibility or optimality cuts. The numerical results indicate that the proposed decomposition algorithm provides, within a short time (after a few iterations), a restoration solution with a quality that is close to the proven optimality, when it can be exhibited.

Chapter 5 modifies the load restoration sequence obtained from the previous chapters such that the transient constraints are respected during the motor acceleration period. The large inrush current driven by induction motors during their acceleration period can impose high risks both in the motor side and in the network side. In this chapter, a mathematical and convex optimization model is derived for the induction motor loads representing their starting transients in a semi-static fashion. This model is then integrated into a load restoration problem aiming to find the optimal energization sequence of different loads (static and motor loads). In this optimization problem, we present a novel and convex model of the converter-interfaced DGs working in constant current mode following voltage sags induced by a motor load starting. Using this model, we derive the optimal current set points of these DGs such that the DGs support the transient network security constraints in an optimal fashion during motor acceleration period. The developed optimization problem includes also a convex model of the autotransformer that is used for the starting of a given induction motor. Therefore, the optimal tap setting of this autotransformer is also derived from the proposed optimization problem. Integrating the AC power flow formulation into the developed optimization problem guarantees that the starting transients of motor loads will not violate the transient operational limits imposed by different protection devices in the distribution network. In this chapter, we validate the feasibility of the optimization results in terms of these transient operational limits using I) off-line time-domain simulations, and II) a Power Hardware-In-the-Loop experiment.

Future Works

In the continuation of this work, the following topics are suggested for further studies. In this section, we provide insights about how to extend the restoration approach proposed in this thesis such that the untreated challenges mentioned in Chapter 1 will be addressed.

- Restoration of unbalanced grids:

In this thesis, the restoration problem is formulated for balanced distribution grids. The proposed formulation can be further developed to account for generic unbalanced grids. In this regard, a potential way is to use the well-known sequence transformation method. If we neglect the impact of non-transposed or partially transposed (asymmetrical) lines, the unbalanced grid is decomposed into three symmetrical and balanced three-phase circuits. Since the lines in MV distribution networks are relatively short and have small impedances, the impact of line asymmetry on the voltage unbalance may be ignored as it is negligible with respect to the impact of unbalanced load and generation [127].

In this regard, all the electrical state variables (not the switching variables) including voltage, current, and power flow variables are decomposed into three subsystems using well-known sequence transformation method. To each of these subsystems, we apply the relaxed-OPF formulation as given in Chapter3. Regarding the transformation of the voltage/current limits from phase domain to the sequence domain, we apply the methodology given in [81]. In this regard, we make a conservative assumption. We assume that the negative and zero sequence terms of voltage and current magnitudes are binding to their standard/normal limits. Therefore, the voltage and current limits associated with the positive sequence terms are derived a priori. Once the optimization problem is solved, we transform the obtained values of electrical state variables from sequence domain back into the phase domain.

- Cold Load Pick-Up (CLPU) effect

Load behavior during the restorative period might be different from that in the normal operation state. As mentioned in chapter 1, the loss of diversity of thermostatically controlled loads makes an increase in their consumption levels at the starting of the restorative period. This effect is called CLPU. A large number of papers studied the modeling of CLPU in case of faults in transmission networks [128]–[130]. These models cannot be directly applied for the distribution network restoration. In case of faults in transmission networks, all the loads are restored following a relatively long outage duration. However, for the faults in distribution networks, some of the unsupplied loads might be restored in a short time and experience a short outage duration, whereas the others experience relatively longer outage durations. The CLPU effect for a given load depends among others on its outage duration. Therefore, in case of faults in distribution networks, the extent of increase in the consumption level of a given unsupplied load cannot be estimated before solving the restoration problem. In other words, the load value

cannot be considered as a parameter in the restoration problem and it should be formulated as a function of the energization time instant.

In this regard, the first step, is to adopt a model for the CLPU that is suitable for the faults at the distribution level. In the second step, the developed model of CLPU should be integrated into the restoration problem. The excessive loading conditions restrict the simultaneous restoration of all the unsupplied loads due to the violation of network security constraints. In order to avoid these violations, the loads should be restored in sequential steps with sufficient time intervals. In this way, we let the additional consumption level of restored loads to decay and then we proceed with the restoration of other loads. However, such a step-wise restoration strategy makes it longer for the loads to be restored and thus affects the reliability of supply.

In chapter 3, we formulated a novel multi-step restoration strategy complying with the DG integration requirements. However, the application of the proposed strategy is not limited to the integration of the DG starting process into the service restoration. This formulation is applicable when it is desired to consider the effect of any time-dependent process existing in active distribution networks on the solution of the restoration problem. In this regard, CLPU can be integrated into the restoration problem using the developed multi-step reconfiguration method presented in chapter 3.

- Restoration of meshed distribution grids

As mentioned in section 1, in some cases, it is beneficial to operate the distribution network in a meshed topology, especially in case of high penetration of DGs [23]. With respect to the radial networks, meshed networks face more complex operational challenges. For example, the protection system that is designed for the radial operation of the network might be inadequate to cope with the increased short circuit level in meshed topologies. Moreover, the coordination of the protection relays needs to be redesigned for meshed networks. Regarding the restoration problem, meshed operation of the network impacts the problem formulation in particular refering to the AC power flow formulation. In this regard, a potential future work would be to modify the developed restoration formulation such that it can be applied for meshed distribution networks.

- Optimal restoration of distribution networks under uncertainty

Another possible future work would be to account for the uncertainties of the load and generation forecast data in the developed restoration problem. In general, for the inclusion of

uncertainties into the optimal operation of ADNs, the researchers use either stochastic optimization or robust optimization techniques. The key difference between these two methods is that the robust optimization provides a solution considering the worst case realization of the uncertain parameters, whereas the stochastic programming provides a solution with respect to probability of the considered uncertainty scenarios. The uncertainty parameters of each load and generation unit can be estimated using established mathematical methods in the field of stochastic analysis.

The author of this thesis has already applied stochastic programming method in the restoration problem. The aim is to account for the uncertainty of the demand and production profiles for loads and renewable (non-dispatchable) resources along the restorative period [131]. In this regard, first, the K-means method is used to cluster the input load and production data into some reduced number of fluctuation scenarios [87]. These scenarios are then integrated into the analytical formulation of the restoration problem, resulting in a multi-time multi-scenario optimization problem. It is illustrated using numerical results such that the optimal solution is obtained in a reasonable time thanks to the employed scenario reduction method.

- Integration of ESSs into the restoration problem

In chapter 3, we integrated the re-dispatch of DGs into the restoration problem in order to improve the quality of the resulting restoration solution. Other generation units that could contribute to the quality enhancement of the restoration solution are Energy Storage Systems (ESSs). The authors of [132] propose a convex optimization model for ESSs representing their specific operational constraints. A possible future work would be to integrate this model into the restoration problem developed in Chapter 3 in order to benefit from the advantages of ESSs in the most optimal fashion.

- Integration of DSM into the restoration problem

In this thesis, we modeled detachable loads in the restoration problem formulation. It means that if a given load is equipped with a load breaker, it could be either kept connected or detached from its node. A possible way to further develop this restoration problem formulation would be to consider load curtailment options, which are called Demand Side Management (DSM) techniques. DSM covers a wide spectrum of techniques, from simply improving energy efficiency using better materials to some smart energy pricing methodologies including

contribution incentives for certain consumption patterns. There are particular types of DSM techniques that are designed for the case of contingencies in the network (e.g. faults) [12]. The future work would be to model these DSM techniques according to their specific characteristics. Then, the developed model should be integrate into the restoration problem formulation.

- Stochastic behavior of protection systems

In practice, protection relays (e.g. under voltage or over-current relays) are not perfectly reliable [133]. They might not trip when required or they might trip when not required. A potential future work is to account for the probabilistic behavior of protection relays, in particular referring to the formulation developed in chapter 5. In this regard, the network security constraints cannot be modeled using hard constraints on the voltage and current variables, as formulated in this thesis. Instead, the probability of tripping a protection relay should be limited to a maximum value that is predefined according to the experience of DNO.

- Implementation of the restoration strategy in operational frameworks

Distribution network are operated either with centralized or decentralized operational frameworks. In centralized framework, the data related to the whole system is aggregated and processed in an operation center. This characteristic satisfies all the requirements for the successful implementation of the proposed restoration algorithm in a centralized operational framework. However, regarding the decentralized frameworks, it is not obvious how to implement the restoration strategy proposed in this thesis. Actually, the restoration problem is composed of interdependent decision variables related to the elements in different parts of the network. Therefore, the feasible and optimal solution of the restoration problem can be found only by a single decision-making entity. This entity should have a broad view of the network including the off-outage area and all the available neighboring feeders.

The author of this thesis published a journal and a conference paper proposing a multi-agent-based restoration strategy compatible with the decentralized control schemes in distribution networks [131], [134]. In this regard, an agent interaction mechanism is designed to build a reduced model of only those parts of the network that might significantly participate in the restoration process (reduced network). The developed decentralized algorithm for the restoration problem complies with the specific limitations of the distributed control agents regarding their computation and storage capabilities. Unlike most of the decentralized restoration strategies in

the literature, which use heuristic approaches, the proposed MAS-based strategy applies mathematical programming methodology to solve the restoration problem according to the formulation proposed in chapter 2. Therefore, it provides a global optimal solution (up to the desired accuracy) while accounting for the accurate modeling of network security constraints.

In a very next step, the author plans to illustrate the functionality of the proposed MAS-based restoration strategy while applying on JADE (Java Agent Development Framework) [135]. JADE is a software framework to facilitate the development of multi-agent applications in compliance with the FIPA (Foundation for Intelligent Physical Agents) specifications [136]. FIPA is an IEEE Computer Society standard organization, developed in 1996. It deploys agent-based technology and makes its standard compatible with other technologies. Unlike the object-oriented model of IEC 61850, the model defined by FIPA is service-oriented. In the TCP/IP models, there is only one application layer, while the FIPA model has multiple sub-application layers enabling multi-round interactions between the agents [135].

- Infrastructure Planning Complying with Service Restoration Requirements

In this thesis, we focus on the operational planning of the restoration problem in distribution networks. Another aspect of the restoration problem is related to its effect on the infrastructure planning. In this respect, the following question rises.

What would be the optimal number, size and location of DERs in an ADN such that the restoration process in case of fault can observes at best the required criteria?

Answering to this question assumes that DNO and DG owners are willing to cooperate in order to guaranty a reliable and secure system capable, among others, to be restored in an efficient way in case of any fault.

Regarding the problem of the infrastructure planning complying with service restoration, the literature is rather limited. According to a literature review on the infrastructure planning works analyzed so far, we can see that the presence of DGs and switching devices as restoration resource components in ADNs have not been considered simultaneously [137]–[141]. In this regard, the author of this thesis published a paper, where the optimization problem regarding the numbers, locations and sizes of these components is investigated [54].It is modelled in the form of a SOCP problem and solved to find a global optimal trade-off between service reliability and economical objectives while considering the overall network security constraints.

The foundation of the proposed investment planning is a two-stage clustering approach. For a fault occurring in a feeder of an active distribution system, the targeted restoration strategy consists of activating, in a first stage, clusters of nodes supplied each by a unique resource. This resource could be a DG or a tie-switch (tie-line) that provides power from a neighboring feeder. To reinforce the security of supply, in a second stage, each DG cluster is connected to a tie-switch cluster to form a so-called large cluster. The proposed clustering solution is unique and is supposed to be valid whatever the fault location.

In a very next step, the author plans to improve the proposed method in [54], increasing among others its flexibility. For instance, it would be desirable to provide each DG cluster with multiple choice of large cluster integration. This will be certainly helpful in case of an unexpected unavailability of a tie-switch resource during the operational planning stage.

Bibliography

[1] E. H. Allen, R. B. Stuart, and T. E. Wiedman, "No Light in August: Power System Restoration Following the 2003 North American Blackout," *IEEE Power and Energy Magazine*, vol. 12, no. 1, pp. 24–33, Jan. 2014, doi: 10.1109/MPE.2013.2285591.

[2] Y. Xue and S. Xiao, "Generalized congestion of power systems: insights from the massive blackouts in India," *J. Mod. Power Syst. Clean Energy*, vol. 1, no. 2, pp. 91–100, Sep. 2013, doi: 10.1007/s40565-013-0014-2.

[3] O. P. Veloza and F. Santamaria, "Analysis of major blackouts from 2003 to 2015: Classification of incidents and review of main causes," *The Electricity Journal*, vol. 29, no. 7, pp. 42–49, Sep. 2016, doi: 10.1016/j.tej.2016.08.006.

[4] S. Ćurčić, C. S. Özveren, L. Crowe, and P. K. L. Lo, "Electric power distribution network restoration: a survey of papers and a review of the restoration problem," *Electric Power Systems Research*, vol. 35, no. 2, pp. 73–86, Nov. 1995, doi: 10.1016/0378-7796(95)00991-4.

[5] K. Chen, W. Wu, B. Zhang, and H. Sun, "Robust Restoration Decision-Making Model for Distribution Networks Based on Information Gap Decision Theory," *IEEE Transactions on Smart Grid*, vol. 6, no. 2, pp. 587–597, Mar. 2015, doi: 10.1109/TSG.2014.2363100.

[6] "Report on Distribution and Transmission System Performance," OFFER-Office of Electricity Regulation, Birmingham, UK, 2001 2000.

[7] I. Konstantelos, S. Giannelos, and G. Strbac, "Strategic Valuation of Smart Grid Technology Options in Distribution Networks," *IEEE Transactions on Power Systems*, vol. 32, no. 2, pp. 1293–1303, Mar. 2017, doi: 10.1109/TPWRS.2016.2587999.

[8] L. F. Rocha, C. L. T. Borges, and G. N. Taranto, "Reliability Evaluation of Active Distribution Networks Including Islanding Dynamics," *IEEE Transactions on Power Systems*, vol. 32, no. 2, pp. 1545–1552, Mar. 2017, doi: 10.1109/TPWRS.2016.2585648.

[9] Y. Liu, R. Fan, and V. Terzija, "Power system restoration: a literature review from 2006 to 2016," *J. Mod. Power Syst. Clean Energy*, vol. 4, no. 3, pp. 332–341, Jul. 2016, doi: 10.1007/s40565-016-0219-2.

[10] F. Dorsemagen *et al.*, "Decentralized, integrated automation system for medium- and low-voltage grids," in *International ETG Congress 2015; Die Energiewende - Blueprints for the new energy age*, 2015, pp. 1–7.

[11] H. Guo, V. Levi, and M. Buhari, "Reliability assessment of smart distribution networks," in *2015 IEEE Innovative Smart Grid Technologies - Asia (ISGT ASIA)*, 2015, pp. 1–6, doi: 10.1109/ISGT-Asia.2015.7387037.

[12] P. Palensky and D. Dietrich, "Demand Side Management: Demand Response, Intelligent Energy Systems, and Smart Loads," *IEEE Transactions on Industrial Informatics*, vol. 7, no. 3, pp. 381–388, Aug. 2011, doi: 10.1109/TII.2011.2158841.

[13] S. Ćurčić, C. S. Özveren, L. Crowe, and P. K. L. Lo, "Electric power distribution network restoration: a survey of papers and a review of the restoration problem," *Electric Power Systems Research*, vol. 35, no. 2, pp. 73–86, Nov. 1995, doi: 10.1016/0378-7796(95)00991-4.

[14] T. S. Basso and R. DeBlasio, "IEEE 1547 series of standards: interconnection issues," *IEEE Transactions on Power Electronics*, vol. 19, no. 5, pp. 1159–1162, Sep. 2004, doi: 10.1109/TPEL.2004.834000.

[15] J. J. Ancona, "A framework for power system restoration following a major power failure," *IEEE Transactions on Power Systems*, vol. 10, no. 3, pp. 1480–1485, Aug. 1995, doi: 10.1109/59.466500.

[16] C. E. Ling, Y. W. Huang, H. L. Chow, and C. L. Huang, "A distribution system outage dispatch by data base method with real-time revision," *IEEE Transactions on Power Delivery*, vol. 4, no. 1, pp. 515–523, Jan. 1989, doi: 10.1109/61.19242.

[17] K. Hotta, H. Nomura, H. Takemoto, K. Suzuki, S. Nakamura, and S. Fukui, "Implementation of a real-time expert system for a restoration guide in a dispatching center," *IEEE Transactions on Power Systems*, vol. 5, no. 3, pp. 1032–1038, Aug. 1990, doi: 10.1109/59.65935.

[18] N. A. Latare, S. S. Bhat, and I. Srivastava, "Literature review of service restoration in distribution system," in *2017 Second International Conference on Electrical, Computer and Communication Technologies (ICECCT)*, 2017, pp. 1–6, doi: 10.1109/ICECCT.2017.8118035.

[19] Z. Li, Y. Bao, Y. Han, C. Guo, W. Wang, and Y. Xie, "Multi-objective distribution network reconfiguration based on system homogeneity," in *2015 IEEE PES Asia-Pacific Power and Energy Engineering Conference (APPEEC)*, 2015, pp. 1–5, doi: 10.1109/APPEEC.2015.7381004.

[20] C. Peng, L. Xu, X. Gong, H. Sun, and L. Pan, "Molecular Evolution Based Dynamic Reconfiguration of Distribution Networks With DGs Considering Three-Phase Balance and Switching Times," *IEEE Transactions on Industrial Informatics*, vol. 15, no. 4, pp. 1866–1876, Apr. 2019, doi: 10.1109/TII.2018.2866301.

[21] A. Azizivahed *et al.*, "Energy Management Strategy in Dynamic Distribution Network Reconfiguration considering Renewable Energy Resources and Storage," *IEEE Transactions on Sustainable Energy*, pp. 1–1, 2019, doi: 10.1109/TSTE.2019.2901429.

[22] H. Sekhavatmanesh, R. Cherkaoui, J. Rodrigues, C. L. Moreira, and J. A. P. Lopes, "A convex model for induction motor starting transients imbedded in an OPF-based optimization problem," presented at the PSCC2020, Porto, Portugal, p. 7.

[23] "Meshed Network - an overview | ScienceDirect Topics." [Online]. Available: https://www.sciencedirect.com/topics/engineering/meshed-network. [Accessed: 21-Jan-2020].

[24] A. P. S. Meliopoulos *et al.*, "Smart Grid Technologies for Autonomous Operation and Control," *IEEE Transactions on Smart Grid*, vol. 2, no. 1, pp. 1–10, Mar. 2011, doi: 10.1109/TSG.2010.2091656.

[25] K. Chen, W. Wu, B. Zhang, and H. Sun, "Security evaluation for distribution power system using improved MIQCP based restoration strategy," in *ISGT 2014*, 2014, pp. 1–6, doi: 10.1109/ISGT.2014.6816493.

[26] J. A. Taylor and F. S. Hover, "Convex Models of Distribution System Reconfiguration," *IEEE Transactions on Power Systems*, vol. 27, no. 3, pp. 1407–1413, Aug. 2012, doi: 10.1109/TPWRS.2012.2184307.

[27] Z. Wang and J. Wang, "Self-Healing Resilient Distribution Systems Based on Sectionalization Into Microgrids," *IEEE Trans. Power Syst.*, vol. 30, no. 6, pp. 3139–3149, Nov. 2015, doi: 10.1109/TPWRS.2015.2389753.

[28] J. B. Leite and J. R. S. Mantovani, "Development of a Self-Healing Strategy With Multiagent Systems for Distribution Networks," *IEEE Trans. Smart Grid*, vol. PP, no. 99, pp. 1–9, 2016, doi: 10.1109/TSG.2016.2518128.

[29] T. T. H. Pham, Y. Besanger, and N. Hadjsaid, "New Challenges in Power System Restoration With Large Scale of Dispersed Generation Insertion," *IEEE Trans. Power Syst.*, vol. 24, no. 1, pp. 398–406, Feb. 2009, doi: 10.1109/TPWRS.2008.2009477.

[30] Y. Xu and W. Liu, "Novel Multiagent Based Load Restoration Algorithm for Microgrids," *IEEE Transactions on Smart Grid*, vol. 2, no. 1, pp. 152–161, Mar. 2011, doi: 10.1109/TSG.2010.2099675.

[31] A. Botea, J. Rintanen, and D. Banerjee, "Optimal Reconfiguration for Supply Restoration With Informed A$^{ast\$}$ Search," *IEEE Transactions on Smart Grid*, vol. 3, no. 2, pp. 583–593, Jun. 2012, doi: 10.1109/TSG.2012.2184778.

[32] C. C. Liu, S. J. Lee, and S. S. Venkata, "An Expert System Operational Aid for Restoration and Loss Reduction of Distribution Systems," *IEEE Trans. Power Syst.; (United States)*, vol. 3:2, May 1988, doi: 10.1109/59.192914.

[33] T. Nagata, H. Sasaki, and R. Yokoyama, "Power system restoration by joint usage of expert system and mathematical programming approach," *IEEE Transactions on Power Systems*, vol. 10, no. 3, pp. 1473–1479, Aug. 1995, doi: 10.1109/59.466501.

[34] C.-M. Huang, "Multiobjective service restoration of distribution systems using fuzzy cause-effect networks," *IEEE Transactions on Power Systems*, vol. 18, no. 2, pp. 867–874, May 2003, doi: 10.1109/TPWRS.2003.811003.

[35] Y. T. Hsiao and C. Y. Chien, "Enhancement of restoration service in distribution systems using a combination fuzzy-GA method," *IEEE Transactions on Power Systems*, vol. 15, no. 4, pp. 1394–1400, Nov. 2000, doi: 10.1109/59.898118.

[36] W.-H. Chen, M.-S. Tsai, and H.-L. Kuo, "Distribution system restoration using the hybrid fuzzy-grey method," *IEEE Transactions on Power Systems*, vol. 20, no. 1, pp. 199–205, Feb. 2005, doi: 10.1109/TPWRS.2004.841234.

[37] S. Toune, H. Fudo, T. Genji, Y. Fukuyama, and Y. Nakanishi, "Comparative study of modern heuristic algorithms to service restoration in distribution systems," *IEEE Transactions on Power Delivery*, vol. 17, no. 1, pp. 173–181, Jan. 2002, doi: 10.1109/61.974205.

[38] W. van der Hoek and M. Wooldridge, "Chapter 24 Multi-Agent Systems," in *Foundations of Artificial Intelligence*, vol. 3, F. van Harmelen, V. Lifschitz, and B. Porter, Eds. Elsevier, 2008, pp. 887–928.

[39] Yu Liu, Yunhe Hou, Shunbo Lei, and Dong Wang, "A distribution network restoration decision support algorithm based on multi-agent system," in *2016 IEEE PES Asia-Pacific Power and Energy Engineering Conference (APPEEC)*, 2016, pp. 33–37, doi: 10.1109/APPEEC.2016.7779465.

[40] H. Liu, X. Chen, K. Yu, and Y. Hou, "The Control and Analysis of Self-Healing Urban Power Grid," *IEEE Transactions on Smart Grid*, vol. 3, no. 3, pp. 1119–1129, Sep. 2012, doi: 10.1109/TSG.2011.2167525.

[41] F. Ding and K. A. Loparo, "Hierarchical Decentralized Network Reconfiguration for Smart Distribution Systems—Part I: Problem Formulation and Algorithm Development," *IEEE Transactions on Power Systems*, vol. 30, no. 2, pp. 734–743, Mar. 2015, doi: 10.1109/TPWRS.2014.2337260.

[42] J. M. Solanki, S. Khushalani, and N. N. Schulz, "A Multi-Agent Solution to Distribution Systems Restoration," *IEEE Transactions on Power Systems*, vol. 22, no. 3, pp. 1026–1034, Aug. 2007, doi: 10.1109/TPWRS.2007.901280.

[43] R. F. Sampaio, L. S. Melo, R. P. S. Leão, G. C. Barroso, and J. R. Bezerra, "Automatic restoration system for power distribution networks based on multi-agent systems," *Transmission Distribution IET Generation*, vol. 11, no. 2, pp. 475–484, 2017, doi: 10.1049/iet-gtd.2016.1018.

[44] M.-S. Tsai and Y.-T. Pan, "Application of BDI-based intelligent multi-agent systems for distribution system service restoration planning," *Euro. Trans. Electr. Power*, vol. 21, no. 5, pp. 1783–1801, Jul. 2011, doi: 10.1002/etep.542.

[45] A. Sharma, D. Srinivasan, and A. Trivedi, "A Decentralized Multi-Agent Approach for Service Restoration in Uncertain Environment," *IEEE Transactions on Smart Grid*, vol. PP, no. 99, pp. 1–1, 2017, doi: 10.1109/TSG.2016.2631639.

[46] M. Eriksson, M. Armendariz, O. O. Vasilenko, A. Saleem, and L. Nordström, "Multiagent-Based Distribution Automation Solution for Self-Healing Grids," *IEEE Transactions on Industrial Electronics*, vol. 62, no. 4, pp. 2620–2628, Apr. 2015, doi: 10.1109/TIE.2014.2387098.

[47] A. Zidan and E. F. El-Saadany, "A Cooperative Multiagent Framework for Self-Healing Mechanisms in Distribution Systems," *IEEE Transactions on Smart Grid*, vol. 3, no. 3, pp. 1525–1539, Sep. 2012, doi: 10.1109/TSG.2012.2198247.

[48] M. J. Ghorbani, M. A. Choudhry, and A. Feliachi, "A Multiagent Design for Power Distribution Systems Automation," *IEEE Transactions on Smart Grid*, vol. 7, no. 1, pp. 329–339, Jan. 2016, doi: 10.1109/TSG.2015.2453884.

[49] P. L. Cavalcante *et al.*, "Centralized Self-Healing Scheme for Electrical Distribution Systems," *IEEE Transactions on Smart Grid*, vol. 7, no. 1, pp. 145–155, Jan. 2016, doi: 10.1109/TSG.2015.2454436.

[50] R. Romero, J. F. Franco, F. B. Leão, M. J. Rider, and E. S. de Souza, "A New Mathematical Model for the Restoration Problem in Balanced Radial Distribution Systems," *IEEE Transactions on Power Systems*, vol. 31, no. 2, pp. 1259–1268, Mar. 2016, doi: 10.1109/TPWRS.2015.2418160.

[51] N. C. Koutsoukis, P. A. Karafotis, P. S. Georgilakis, and N. D. Hatziargyriou, "Optimal service restoration of power distribution networks considering voltage regulation," in *2017 IEEE Manchester PowerTech*, 2017, pp. 1–6, doi: 10.1109/PTC.2017.7981110.

[52] National Electrical Manufacturers Association (NEMA). "Std, A. N. S. I. 'C84. 1-2011, American National Standard for Electric Power Systems and Equipment-Voltage Ratings (60 Hertz)." Rosslyn, Virginia, 2011.

[53] A. P. Wierzbicki, "A mathematical basis for satisficing decision making," *Mathematical Modelling*, vol. 3, no. 5, pp. 391–405, Jan. 1982, doi: 10.1016/0270-0255(82)90038-0.

[54] H. Sekhavatmanesh and R. Cherkaoui, "Optimal Infrastructure Planning of Active Distribution Networks Complying with Service Restoration Requirements," *IEEE*

Transactions on Smart Grid, vol. PP, no. 99, pp. 1–1, 2017, doi: 10.1109/TSG.2017.2716192.

[55] M. Lavorato, J. F. Franco, M. J. Rider, and R. Romero, "Imposing Radiality Constraints in Distribution System Optimization Problems," *IEEE Transactions on Power Systems*, vol. 27, no. 1, pp. 172–180, Feb. 2012, doi: 10.1109/TPWRS.2011.2161349.

[56] E. M. L. Beale and J. Tomlin, "Special facilities in a general mathematical programming system for nonconvex problems using ordered sets of variables," *Operational Research*, vol. 69, pp. 447–454, Jan. 1969.

[57] C.-T. Su, C.-F. Chang, and J.-P. Chiou, "Distribution network reconfiguration for loss reduction by ant colony search algorithm," *Electric Power Systems Research*, vol. 75, no. 2, pp. 190–199, Aug. 2005, doi: 10.1016/j.epsr.2005.03.002.

[58] E. Lopez, H. Opazo, L. Garcia, and P. Bastard, "Online reconfiguration considering variability demand: applications to real networks," *IEEE Transactions on Power Systems*, vol. 19, no. 1, pp. 549–553, Feb. 2004, doi: 10.1109/TPWRS.2003.821447.

[59] Y. Kumar, B. Das, and J. Sharma, "Multiobjective, Multiconstraint Service Restoration of Electric Power Distribution System With Priority Customers," *IEEE Transactions on Power Delivery*, vol. 23, no. 1, pp. 261–270, Jan. 2008, doi: 10.1109/TPWRD.2007.905412.

[60] K. N. Miu, H.-D. Chiang, and R. J. McNulty, "Multi-tier service restoration through network reconfiguration and capacitor control for large-scale radial distribution networks," *IEEE Transactions on Power Systems*, vol. 15, no. 3, pp. 1001–1007, Aug. 2000, doi: 10.1109/59.871725.

[61] T. S. Basso and R. DeBlasio, "IEEE 1547 series of standards: interconnection issues," *IEEE Transactions on Power Electronics*, vol. 19, no. 5, pp. 1159–1162, Sep. 2004, doi: 10.1109/TPEL.2004.834000.

[62] Z. Wang and J. Wang, "Self-Healing Resilient Distribution Systems Based on Sectionalization Into Microgrids," *IEEE Transactions on Power Systems*, vol. 30, no. 6, pp. 3139–3149, Nov. 2015, doi: 10.1109/TPWRS.2015.2389753.

[63] S. A. Arefifar, Y. A. R. I. Mohamed, and T. H. M. El-Fouly, "Supply-Adequacy-Based Optimal Construction of Microgrids in Smart Distribution Systems," *IEEE Transactions on Smart Grid*, vol. 3, no. 3, pp. 1491–1502, Sep. 2012, doi: 10.1109/TSG.2012.2198246.

[64] I. K. Song, W. W. Jung, J. Y. Kim, S. Y. Yun, J. H. Choi, and S. J. Ahn, "Operation Schemes of Smart Distribution Networks With Distributed Energy Resources for Loss Reduction and Service Restoration," *IEEE Transactions on Smart Grid*, vol. 4, no. 1, pp. 367–374, Mar. 2013, doi: 10.1109/TSG.2012.2233770.

[65] Y. Xu, C. C. Liu, K. Schneider, F. Tuffner, and D. Ton, "Microgrids for Service Restoration to Critical Load in a Resilient Distribution System," *IEEE Transactions on Smart Grid*, vol. PP, no. 99, pp. 1–1, 2016, doi: 10.1109/TSG.2016.2591531.

[66] G. Niu *et al.*, "A fast power service restoration method for distribution network with distributed generation," in *2017 IEEE Transportation Electrification Conference and Expo, Asia-Pacific (ITEC Asia-Pacific)*, 2017, pp. 1–6, doi: 10.1109/ITEC-AP.2017.8081038.

[67] X. Meng, L. Zhang, P. Cong, W. Tang, X. Zhang, and D. Yang, "Dynamic reconfiguration of distribution network considering scheduling of DG active power outputs," in *2014 International Conference on Power System Technology*, 2014, pp. 1433–1439, doi: 10.1109/POWERCON.2014.6993730.

[68] S. Lei, Y. Hou, F. Qiu, and J. Yan, "Identification of Critical Switches for Integrating Renewable Distributed Generation by Dynamic Network Reconfiguration," *IEEE*

Transactions on Sustainable Energy, vol. 9, no. 1, pp. 420–432, Jan. 2018, doi: 10.1109/TSTE.2017.2738014.

[69] G. Li and M. Peng, "Dynamic reconstruction of active distribution network with electric vehicles," in *2017 International Conference on Circuits, Devices and Systems (ICCDS)*, 2017, pp. 127–130, doi: 10.1109/ICCDS.2017.8120464.

[70] A. Asrari, S. Lotfifard, and M. Ansari, "Reconfiguration of Smart Distribution Systems With Time Varying Loads Using Parallel Computing," *IEEE Transactions on Smart Grid*, vol. 7, no. 6, pp. 2713–2723, Nov. 2016, doi: 10.1109/TSG.2016.2530713.

[71] M. Rahmani-Andebili, "Dynamic and adaptive reconfiguration of electrical distribution system including renewables applying stochastic model predictive control," *Transmission Distribution IET Generation*, vol. 11, no. 16, pp. 3912–3921, 2017, doi: 10.1049/iet-gtd.2016.1549.

[72] C. L. Moreira, F. O. Resende, and J. A. P. Lopes, "Using Low Voltage MicroGrids for Service Restoration," *IEEE Transactions on Power Systems*, vol. 22, no. 1, pp. 395–403, Feb. 2007, doi: 10.1109/TPWRS.2006.888989.

[73] H. Ahmadi and J. R. Martí, "Mathematical representation of radiality constraint in distribution system reconfiguration problem," *International Journal of Electrical Power & Energy Systems*, vol. 64, pp. 293–299, Jan. 2015, doi: 10.1016/j.ijepes.2014.06.076.

[74] H. D. de M. Braz and B. A. de Souza, "Distribution Network Reconfiguration Using Genetic Algorithms With Sequential Encoding: Subtractive and Additive Approaches," *IEEE Transactions on Power Systems*, vol. 26, no. 2, pp. 582–593, May 2011, doi: 10.1109/TPWRS.2010.2059051.

[75] Y. Fu and H. Chiang, "Toward Optimal Multiperiod Network Reconfiguration for Increasing the Hosting Capacity of Distribution Networks," *IEEE Transactions on Power Delivery*, vol. 33, no. 5, pp. 2294–2304, Oct. 2018, doi: 10.1109/TPWRD.2018.2801332.

[76] L. Gan, S. H. Low, "Convex relaxations and linear approximation for optimal power flow in multiphase radial networks," presented at the Power Systems Computation Conference, Wroclaw, Poland, 2014, p. 9.

[77] E. Dall'Anese, G. B. Giannakis, B. F. Wollenberg, "Optimization of unbalanced power distribution networks via semidefinite relaxation," presented at the North American Power Symposium (NAPS), Champaign, IL, USA, 2012, p. 6.

[78] E. Dall'Anese, H. Zhu, G. B. Giannakis, "Distributed Optimal Power Flow for Smart Microgrids," *IEEE Transactions on Smart Grid*, vol. 4, no. 3, pp. 1467–1475, Sep. 2013, doi: 10.1109/TSG.2013.2248175.

[79] N. C. Koutsoukis, D. O. Siagkas, P. S. Georgilakis, and N. D. Hatziargyriou, "Online Reconfiguration of Active Distribution Networks for Maximum Integration of Distributed Generation," *IEEE Transactions on Automation Science and Engineering*, vol. 14, no. 2, pp. 437–448, Apr. 2017, doi: 10.1109/TASE.2016.2628091.

[80] R. A. Jabr, R. Singh, and B. C. Pal, "Minimum Loss Network Reconfiguration Using Mixed-Integer Convex Programming," *IEEE Transactions on Power Systems*, vol. 27, no. 2, pp. 1106–1115, May 2012, doi: 10.1109/TPWRS.2011.2180406.

[81] M. Nick, R. Cherkaoui, J.-Y. L. Boudec, and M. Paolone, "An Exact Convex Formulation of the Optimal Power Flow in Radial Distribution Networks Including Transverse Components," *IEEE Transactions on Automatic Control*, vol. 63, no. 3, pp. 682–697, Mar. 2018, doi: 10.1109/TAC.2017.2722100.

[82] K. Christakou, D.-C. Tomozei, J.-Y. Le Boudec, and M. Paolone, "AC OPF in radial distribution networks − Part I: On the limits of the branch flow convexification and the

alternating direction method of multipliers," *Electric Power Systems Research*, vol. 143, no. Supplement C, pp. 438–450, Feb. 2017, doi: 10.1016/j.epsr.2016.07.030.

[83] M. Nick, R. Cherkaoui, J.-Y. L. Boudec, and M. Paolone, "An Exact Convex Formulation of Optimal Power Flow in Radial Distribution Networks Including Transverse Components," *arXiv:1605.01964 [math]*, May 2016.

[84] M. E. Baran and F. F. Wu, "Optimal capacitor placement on radial distribution systems," *IEEE Transactions on Power Delivery*, vol. 4, no. 1, pp. 725–734, Jan. 1989, doi: 10.1109/61.19265.

[85] [Online], "Home Energy," *http://homerenergy.com*, 15-Oct-2017. [Online]. Available: http://homerenergy.com.

[86] [Online], "Solar Irradiation Data (SODA)," *http://www.soda-is.com/eng/index.html*, 15-Oct-2017. [Online]. Available: http://www.soda-is.com/eng/index.html.

[87] D. Das, "Reconfiguration of distribution system using fuzzy multi-objective approach," *International Journal of Electrical Power & Energy Systems*, vol. 28, no. 5, pp. 331–338, Jun. 2006, doi: 10.1016/j.ijepes.2005.08.018.

[88] H. Haghighat and B. Zeng, "Distribution System Reconfiguration Under Uncertain Load and Renewable Generation," *IEEE Transactions on Power Systems*, vol. 31, no. 4, pp. 2666–2675, Jul. 2016, doi: 10.1109/TPWRS.2015.2481508.

[89] X. Chen, W. Wu, and B. Zhang, "Robust Restoration Method for Active Distribution Networks," *IEEE Transactions on Power Systems*, vol. 31, no. 5, pp. 4005–4015, Sep. 2016, doi: 10.1109/TPWRS.2015.2503426.

[90] C. Lee, C. Liu, S. Mehrotra, and Z. Bie, "Robust Distribution Network Reconfiguration," *IEEE Transactions on Smart Grid*, vol. 6, no. 2, pp. 836–842, Mar. 2015, doi: 10.1109/TSG.2014.2375160.

[91] B. Chen, C. Chen, J. Wang, and K. L. Butler-Purry, "Multi-Time Step Service Restoration for Advanced Distribution Systems and Microgrids," *IEEE Transactions on Smart Grid*, vol. 9, no. 6, pp. 6793–6805, Nov. 2018, doi: 10.1109/TSG.2017.2723798.

[92] Y. Wang *et al.*, "Coordinating Multiple Sources for Service Restoration to Enhance Resilience of Distribution Systems," *IEEE Transactions on Smart Grid*, vol. 10, no. 5, pp. 5781–5793, Sep. 2019, doi: 10.1109/TSG.2019.2891515.

[93] H. Ahmadi and J. R. Martí, "Distribution System Optimization Based on a Linear Power-Flow Formulation," *IEEE Transactions on Power Delivery*, vol. 30, no. 1, pp. 25–33, Feb. 2015, doi: 10.1109/TPWRD.2014.2300854.

[94] J. Hooker, *Logic-Based Methods for Optimization: Combining Optimization and Constraint Satisfaction*. John Wiley & Sons, 2011.

[95] J. N. Hooker and H. Yan, "Logic circuit verification by Benders decompo-sition," 1995.

[96] G. W. Klau and P. Mutzel, "Optimal labeling of point features in rectangular labeling models," *Math. Program., Ser. B*, vol. 94, no. 2, pp. 435–458, Jan. 2003, doi: 10.1007/s10107-002-0327-9.

[97] G. Codato and M. Fischetti, "Combinatorial Benders' Cuts for Mixed-Integer Linear Programming," *Operations Research*, vol. 54, pp. 756–766, 2006, doi: 10.1287/opre.1060.0286.

[98] J. N. Hooker, "A Hybrid Method for Planning and Scheduling," in *Principles and Practice of Constraint Programming – CP 2004*, 2004, pp. 305–316.

[99] H. Sekhavatmanesh and R. Cherkaoui, "Analytical Approach for Active Distribution Network Restoration Including Optimal Voltage Regulation," *IEEE Transactions on Power Systems*, pp. 1–1, 2018, doi: 10.1109/TPWRS.2018.2889241.

[100] G. S. Grewal, S. Pocsai, and M. M. Hakim, "Transient motor reacceleration study in an integrated petrochemical facility," *IEEE Transactions on Industry Applications*, vol. 35, no. 4, pp. 968–977, Jul. 1999, doi: 10.1109/28.777207.

[101] J. Larabee, B. Pellegrino, and B. Flick, "Induction motor starting methods and issues," in *Record of Conference Papers Industry Applications Society 52nd Annual Petroleum and Chemical Industry Conference*, 2005, pp. 217–222, doi: 10.1109/PCICON.2005.1524557.

[102] I. Beil, A. Allen, A. Tokombayev, and M. Hack, "Considerations when using utility-scale battery storage to black start a gas turbine generator," in *2017 IEEE Power Energy Society General Meeting*, 2017, pp. 1–5, doi: 10.1109/PESGM.2017.8274529.

[103] Z. Zhao and B. Ooi, "Feasibility of fast restoration of power systems by micro-grids," *Transmission Distribution IET Generation*, vol. 12, no. 1, pp. 126–132, 2018, doi: 10.1049/iet-gtd.2017.0323.

[104] H. Qu and Y. Liu, "Maximum restorable load for substation during power system restoration," in *2009 International Conference on Sustainable Power Generation and Supply*, 2009, pp. 1–4, doi: 10.1109/SUPERGEN.2009.5348350.

[105] D. Wu, H. Wu, and H. Dongt, "Influence of Induction Motor Starting on Microgrid," in *2018 IEEE PES Asia-Pacific Power and Energy Engineering Conference (APPEEC)*, 2018, pp. 376–381, doi: 10.1109/APPEEC.2018.8566305.

[106] F. K. Tuffner, K. P. Schneider, J. Hansen, and M. A. Elizondo, "Modeling Load Dynamics to Support Resiliency-Based Operations in Low-Inertia Microgrids," *IEEE Transactions on Smart Grid*, vol. 10, no. 3, pp. 2726–2737, May 2019, doi: 10.1109/TSG.2018.2809452.

[107] J. Bredthauer and N. Struck, "Starting of large medium voltage motors: design, protection, and safety aspects," *IEEE Transactions on Industry Applications*, vol. 31, no. 5, pp. 1167–1176, Sep. 1995, doi: 10.1109/28.464534.

[108] H. Zheng and C. L. DeMarco, "A New Dynamic Performance Model of Motor Stalling and FIDVR for Smart Grid Monitoring/Planning," *IEEE Transactions on Smart Grid*, vol. 7, no. 4, pp. 1989–1996, Jul. 2016, doi: 10.1109/TSG.2016.2548082.

[109] J. C. Gomez, M. M. Morcos, C. A. Reineri, and G. N. Campetelli, "Behavior of induction motor due to voltage sags and short interruptions," *IEEE Transactions on Power Delivery*, vol. 17, no. 2, pp. 434–440, Apr. 2002, doi: 10.1109/61.997914.

[110] F. G. Limbong, "The use of neural network (NN) to predict voltage drop during starting of medium voltage induction motor," in *2016 3rd International Conference on Information Technology, Computer, and Electrical Engineering (ICITACEE)*, 2016, pp. 156–160, doi: 10.1109/ICITACEE.2016.7892428.

[111] S. Hasan, K. M. Muttaqi, R. Bhattarai, and S. Kamalasadan, "A Coordinated Control Approach for Mitigation of Motor Starting Voltage Dip in Distribution Feeders," in *2018 IEEE Industry Applications Society Annual Meeting (IAS)*, 2018, pp. 1–6, doi: 10.1109/IAS.2018.8544554.

[112] H. Qu and Y. Liu, "Maximizing restorable load amount for specific substation during system restoration," *International Journal of Electrical Power & Energy Systems*, vol. 43, no. 1, pp. 1213–1220, Dec. 2012, doi: 10.1016/j.ijepes.2012.05.049.

[113] M. Falahi, K. L. Butler-Purry, and M. Ehsani, "Induction Motor Starting in Islanded Microgrids," *IEEE Transactions on Smart Grid*, vol. 4, no. 3, pp. 1323–1331, Sep. 2013, doi: 10.1109/TSG.2013.2271261.

[114] M. Castilla, J. Miret, J. L. Sosa, J. Matas, and L. G. d Vicuña, "Grid-Fault Control Scheme for Three-Phase Photovoltaic Inverters With Adjustable Power Quality

Characteristics," *IEEE Transactions on Power Electronics*, vol. 25, no. 12, pp. 2930–2940, Dec. 2010, doi: 10.1109/TPEL.2010.2070081.

[115] A. Moawwad, M. S. E. Moursi, and W. Xiao, "Advanced Fault Ride-Through Management Scheme for VSC-HVDC Connecting Offshore Wind Farms," *IEEE Transactions on Power Systems*, vol. 31, no. 6, pp. 4923–4934, Nov. 2016, doi: 10.1109/TPWRS.2016.2535389.

[116] L. Hadjidemetriou, P. Demetriou, and E. Kyriakides, "Investigation of different Fault Ride Through strategies for renewable energy sources," in *2015 IEEE Eindhoven PowerTech*, 2015, pp. 1–6, doi: 10.1109/PTC.2015.7232594.

[117] M. Castilla, J. Miret, A. Camacho, J. Matas, and L. G. de Vicuña, "Voltage Support Control Strategies for Static Synchronous Compensators Under Unbalanced Voltage Sags," *IEEE Transactions on Industrial Electronics*, vol. 61, no. 2, pp. 808–820, Feb. 2014, doi: 10.1109/TIE.2013.2257141.

[118] P. Rodriguez, A. V. Timbus, R. Teodorescu, M. Liserre, and F. Blaabjerg, "Flexible Active Power Control of Distributed Power Generation Systems During Grid Faults," *IEEE Transactions on Industrial Electronics*, vol. 54, no. 5, pp. 2583–2592, Oct. 2007, doi: 10.1109/TIE.2007.899914.

[119] Y. Yang, F. Blaabjerg, and H. Wang, "Low-Voltage Ride-Through of Single-Phase Transformerless Photovoltaic Inverters," *IEEE Transactions on Industry Applications*, vol. 50, no. 3, pp. 1942–1952, May 2014, doi: 10.1109/TIA.2013.2282966.

[120] J. Miret, A. Camacho, M. Castilla, L. G. de Vicuña, and J. Matas, "Control Scheme With Voltage Support Capability for Distributed Generation Inverters Under Voltage Sags," *IEEE Transactions on Power Electronics*, vol. 28, no. 11, pp. 5252–5262, Nov. 2013, doi: 10.1109/TPEL.2013.2246190.

[121] A. Camacho, M. Castilla, J. Miret, L. G. de Vicuña, and R. Guzman, "Positive and Negative Sequence Control Strategies to Maximize the Voltage Support in Resistive–Inductive Grids During Grid Faults," *IEEE Transactions on Power Electronics*, vol. 33, no. 6, pp. 5362–5373, Jun. 2018, doi: 10.1109/TPEL.2017.2732452.

[122] A. Camacho, M. Castilla, J. Miret, L. G. de Vicuña, and G. L. M. Andrés, "Control Strategy for Distribution Generation Inverters to Maximize the Voltage Support in the Lowest Phase During Voltage Sags," *IEEE Transactions on Industrial Electronics*, vol. 65, no. 3, pp. 2346–2355, Mar. 2018, doi: 10.1109/TIE.2017.2736486.

[123] L. Gan, N. Li, U. Topcu, and S. H. Low, "Exact Convex Relaxation of Optimal Power Flow in Radial Networks," *IEEE Transactions on Automatic Control*, vol. 60, no. 1, pp. 72–87, Jan. 2015, doi: 10.1109/TAC.2014.2332712.

[124] R. F. McElveen and M. K. Toney, "Starting high-inertia loads," *IEEE Transactions on Industry Applications*, vol. 37, no. 1, pp. 137–144, Jan. 2001, doi: 10.1109/28.903136.

[125] C. Gouveia *et al.*, "Experimental validation of smart distribution grids: Development of a microgrid and electric mobility laboratory," *International Journal of Electrical Power & Energy Systems*, vol. 78, pp. 765–775, Jun. 2016, doi: 10.1016/j.ijepes.2015.12.005.

[126] H. P. Williams, *Model Building in Mathematical Programming*. John Wiley & Sons, 2013.

[127] Z. Liu and J. V. Milanović, "Probabilistic Estimation of Voltage Unbalance in MV Distribution Networks With Unbalanced Load," *IEEE Transactions on Power Delivery*, vol. 30, no. 2, pp. 693–703, Apr. 2015, doi: 10.1109/TPWRD.2014.2322391.

[128] V. Kumar, R. K. H. C, I. Gupta, and H. O. Gupta, "DG Integrated Approach for Service Restoration Under Cold Load Pickup," *IEEE Transactions on Power Delivery*, vol. 25, no. 1, pp. 398–406, Jan. 2010, doi: 10.1109/TPWRD.2009.2033969.

[129]   V. Gupta and A. Pahwa, "A voltage drop-based approach to include cold load pickup in design of distribution systems," *IEEE Transactions on Power Systems*, vol. 19, no. 2, pp. 957–963, May 2004, doi: 10.1109/TPWRS.2003.821440.

[130]   K. N. Miu, H.-D. Chiang, B. Yuan, and G. Darling, "Fast service restoration for large-scale distribution systems with priority customers and constraints," *IEEE Transactions on Power Systems*, vol. 13, no. 3, pp. 789–795, Aug. 1998, doi: 10.1109/59.708643.

[131]   H. Sekhavatmanesh and R. Cherkaoui, "Distribution Network Restoration in a Multi-Agent Framework Using a Convex OPF model," *IEEE Transactions on Smart Grid*, vol. PP, no. 99, pp. 1–1, 2018, doi: 10.1109/TSG.2018.2805922.

[132]   M. Nick, "Exact Convex Modeling of the Optimal Power Flow for the Operation and Planning of Active Distribution Networks with Energy Storage Systems," *Infoscience*, 2016. [Online]. Available: https://infoscience.epfl.ch/record/218631. [Accessed: 21-Jan-2020].

[133]   Y. Damchi and J. Sadeh, "Considering failure probability for back-up relay in determination of the optimum routine test interval in protective system using Markov model," in *2009 IEEE Power Energy Society General Meeting*, 2009, pp. 1–5, doi: 10.1109/PES.2009.5275612.

[134]   H. Sekhavatmanesh, R. Cherkaoui, "A Multi-agent Based Analytical Approach for Service Restoration in Distribution Networks," presented at the POWERTECH, Manchester, 2017.

[135]   F. Bellifemine, A. Poggi, and G. Rimassa, "Developing Multi-agent Systems with JADE," in *Intelligent Agents VII Agent Theories Architectures and Languages*, 2001, pp. 89–103.

[136]   "The foundation for intelligent physical agents standards," *http://www. fi pa. org/*, 2015. [Online]. Available: http://www. fi pa. org/.

[137]   H. Ghoreishi, H. Afrakhte, and M. Jabbari ghadi, "Optimal placement of tie points and sectionalizers in radial distribution network in presence of DGs considering load significance," in *2013 Smart Grid Conference (SGC)*, 2013, pp. 160–165, doi: 10.1109/SGC.2013.6733787.

[138]   P. M. S. Carvalho, L. A. F. M. Ferreira, and A. J. C. da Silva, "A decomposition approach to optimal remote controlled switch allocation in distribution systems," *IEEE Transactions on Power Delivery*, vol. 20, no. 2, pp. 1031–1036, Apr. 2005, doi: 10.1109/TPWRD.2004.838470.

[139]   A. Moradi, M. Fotuhi-Firuzabad, and M. Rashidi-Nejad, "A Reliability Cost/Worth Approach to Determine Optimum Switching Placement in Distribution Systems," in *2005 IEEE/PES Transmission Distribution Conference Exposition: Asia and Pacific*, 2005, pp. 1–5, doi: 10.1109/TDC.2005.1547169.

[140]   Jen-Hao Teng and Chan-Nan Lu, "Feeder-switch relocation for customer interruption cost minimization," *IEEE Transactions on Power Delivery*, vol. 17, no. 1, pp. 254–259, Jan. 2002, doi: 10.1109/61.974215.

[141]   Chao-Shun Chen, Chia-Hung Lin, Hui-Jen Chuang, Chung-Sheng Li, Ming-Yang Huang, and Chia-Wen Huang, "Optimal placement of line switches for distribution automation systems using immune algorithm," *IEEE Transactions on Power Systems*, vol. 21, no. 3, pp. 1209–1217, Aug. 2006, doi: 10.1109/TPWRS.2006.876673.

Curriculum Vitae

Hossein SEKHAVATMANESH

Power System research group (SCI-STI-RC)
École Polytechnique Fédérale de Lausanne (EPFL)

Born in 22th July, 1991, Dezfool, Iran
Email: hossein.sekhavat@epfl.ch
LinkedIn:
https://www.linkedin.com/in/hossein-sekhavat/

Education

Feb.2016 – April.2020: PhD candidate in Electrical Power Engineering, École Polytechnique Fédérale de Lausanne (EPFL), Lausanne, Switzerland.
Thesis: Service restoration strategy in active distribution networks.

Sep.2013 - July.2015: M.Sc. in Electrical Power Engineering, GPA: 18.93 (of 20), Sharif University of Technology, Tehran, Iran.
Thesis: Power flow control and power quality enhancement in grid-connected microgrid with the back-to-back converter

Sep.2009 – Sep.2013: B.Sc. in Electrical Power Engineering, GPA: 19.00 (of 20), Amirkabir University of Technology (Tehran Polytechnic), Tehran, Iran.

Professional Experiences

Power System research group (PWRS**), EPFL, Lausanne, Switzerland**
Position: Research Assistant (Feb.2016 - April.2020)

Power Quality Laboratory, Sharif University of Technology, Tehran, Iran
Position: Research Assistant (Sep.2014 – July.2015)

Laboratory of Smart Grids and Electrical Vehicles, INESC**, Porto, Portugal**
Position: Visiting PhD Student (Spring 2019)

Tehran Urban and Suburban Railway Co (TUSRC**), Tehran, Iran**
Position: Project Engineer (Feb-Dec.2014)

Research Interests

- Power Network Operational Planning
- Distributed Generation Planning and Control
- Smart Grid
- Mathematical Programming Optimization Applied to Power Systems.

Language Skills

- Persian: Mother tongue
- English: Fluent (level C1, TOEFL IBT: 102/120)
- German: Intermediate (level B2)

List of Publications

Peer-reviewed scientific journals:

[J7]. Hossein Sekhavatmanesh, J. Rodrigues, C. L. Moreira, J. A. P. Lopes, and R. Cherkaoui, "Optimal Load Restoration in Active Distribution Networks Complying with Starting Transients of Induction Motors," *IEEE Transactions on Smart Grid*, pp. 1–1, 2020, doi: 10.1109/TSG.2020.2985783.

[J6]. Hossein Sekhavatmanesh, Rachid Cherkaoui, "A Novel Decomposition Solution Approach for the Restoration Problem in Distribution Networks," IEEE Transactions on Power Systems, pp. 1–1, 2020, doi: 10.1109/TPWRS.2020.2982502.

[J5]. Hossein Sekhavatmanesh and R. Cherkaoui, "A Multi-Step Reconfiguration Model for Active Distribution Network Restoration Integrating the DG Start-Up Sequences," *IEEE Transactions on Sustainable Energy*, pp. 1–1, 2020, doi: 10.1109/TSTE.2020.2980890.

[J4]. Hossein Sekhavatmanesh, J. Rodrigues, C. L. Moreira, J.A.P. Lopes, R. Cherkaoui, " A convex model for induction motor starting transients imbedded in an OPF-based optimization problem," to appear in Elsevier Power System Research (EPSR) Journal, 2020.

[J3]. Hossein Sekhavatmanesh and R. Cherkaoui, "Analytical Approach for Active Distribution Network Restoration Including Optimal Voltage Regulation," *IEEE Transactions on Power Systems*, pp. 1–1, 2018, doi: 10.1109/TPWRS.2018.2889241.

[J2]. Hossein Sekhavatmanesh and R. Cherkaoui, "Distribution Network Restoration in a Multi-Agent Framework Using a Convex OPF model," *IEEE Transactions on Smart Grid*, vol. PP, no. 99, pp. 1–1, 2018, doi: 10.1109/TSG.2018.2805922.

[J1]. Hossein Sekhavatmanesh and R. Cherkaoui, "Optimal Infrastructure Planning of Active Distribution Networks Complying with Service Restoration Requirements," *IEEE Transactions on Smart Grid*, vol. PP, no. 99, pp. 1–1, 2017, doi: 10.1109/TSG.2017.2716192.

Conferences:

[C3]. Hossein Sekhavatmanesh, M. Nick, M. Paolone, and R. Cherkaoui, "Service Restoration in DG-Integrated Distribution Networks Using an Exact Convex OPF Model," in *Power Systems Computation Conference (PSCC)*, Dublin, 2018, pp. 1–7, doi: 10.23919/PSCC.2018.8442963.

[C2]. Hossein Sekhavatmanesh and R. Cherkaoui, "A multi-agent based analytical approach for service restoration in distribution networks," in *IEEE PowerTech*, Manchester, 2017, pp. 1–6, doi: 10.1109/PTC.2017.7980877.

[C1]. Hossein Sekhavatmanesh, H. Mokhtari, M. Hamzeh, and A. Asbafkan, "Power and voltage control in a grid-connected microgrid system with a back-to-back converter," in *The 6th Power Electronics, Drive Systems Technologies Conference (PEDSTC)*, Tehran, 2015, pp. 468–473, doi: 10.1109/PEDSTC.2015.7093320.